Forschungszentrum Jülich
*in der Helmholtz-Gemeinschaft*

50 Jahre / Zukunft

# Biomacromolecules of Fossil Algae, Spores and Zooclasts from Selected Time Windows of Proterozoic to Mesozoic Age as Revealed by Pyrolysis-Gas Chromatography-Mass Spectrometry

## – A Biogeochemical Study –

Suryendu Dutta

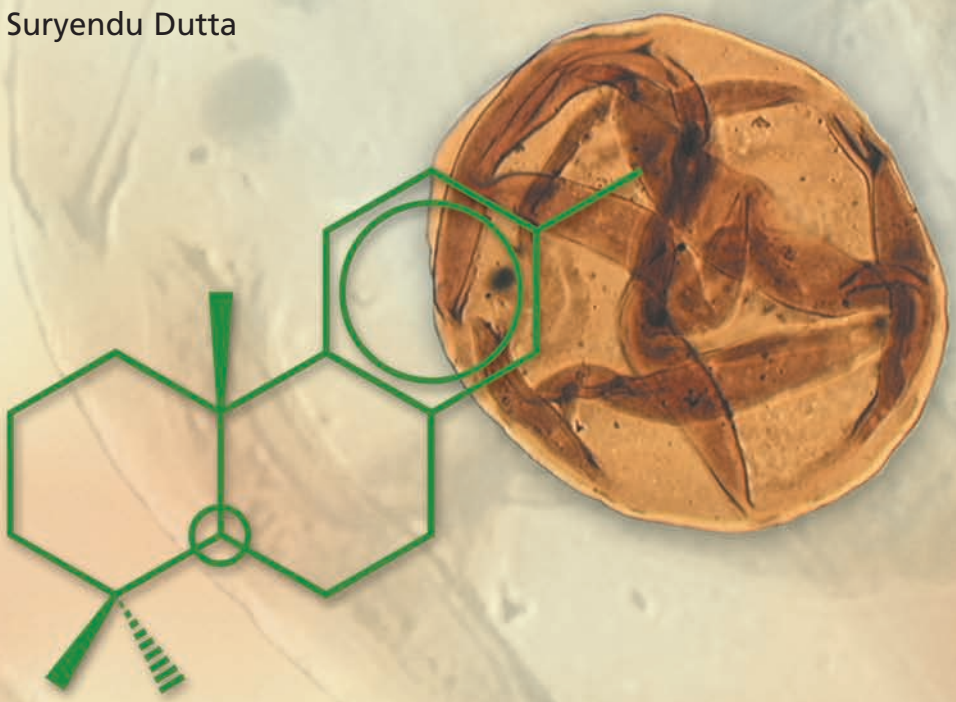

**Umwelt**
**Environment**

Schriften des Forschungszentrums Jülich
Reihe Umwelt/Environment Band/Volume 67

Forschungszentrum Jülich GmbH
Institut für Chemie und Dynamik der Geosphäre
Institut V: Sedimentäre Systeme (ICG-V)

# Biomacromolecules of Fossil Algae, Spores and Zooclasts from Selected Time Windows of Proterozoic to Mesozoic Age as Revealed by Pyrolysis-Gas Chromatography-Mass Spectrometry

## - A Biogeochemical Study -

Suryendu Dutta

Schriften des Forschungszentrums Jülich
Reihe Umwelt/Environment Band/Volume 67

ISSN 1433-5530 ISBN 3-89336-455-2

Bibliographic information published by the Deutsche Nationalbibliothek.
The Deutsche Nationalbibliothek lists this publication in the Deutsche Nationalbibliografie; detailed bibliographic data are available in the Internet at <http://dnb.d-nb.de>.

| | |
|---|---|
| Publisher and Distributor: | Forschungszentrum Jülich GmbH<br>Zentralbibliothek,Verlag<br>52425 Jülich<br>Phone +49 (0) 24 61 61-53 68 · Fax +49 (0) 24 61 61-61 03<br>e-mail: zb-publikation@fz-juelich.de<br>Internet: http://www.fz-juelich.de/zb |
| Cover Design: | Grafische Medien, Forschungszentrum Jülich GmbH |
| Printer: | Grafische Medien, Forschungszentrum Jülich GmbH |
| Copyright: | Forschungszentrum Jülich 2006 |

Schriften des Forschungszentrums Jülich
Reihe Umwelt / Environment Band / Volume 67

D 82 (Diss., RWTH Aachen, 2006)

ISSN 1433-5530
ISBN-10: 3-89336-455-2
ISBN-13: 978-3-89336-455-8

## ACKNOWLEDGEMENTS

This thesis was performed at the Institute for Chemistry and Dynamics of the Geosphere: Sedimentary Systems (ICG-V) at the Research Centre Jülich. First of all, I would like to express my gratitude to my supervisors Prof. Dr. Ralf Littke (RWTH Aachen University), Dr. Ulrich Mann (Research Centre Jülich) and Dr. Heinz Wilkes (GFZ Potsdam) for their support, many fruitful discussions and valuable contributions to this thesis.

I am grateful to Mr. Christoph Hartkopf-Fröder (Geological Survey of North Rhine-Westphalia, Krefeld) and Dr. Rainer Brocke (Research Centre Senckenberg, Frankfurt) for providing the kerogen fractions and taxonomic classification of palynomorphs. I have learnt many valuable aspects on palynology from them during my Ph.D. tenure. I wish to thank Dr. Paul Greenwood (University of Western Australia, Perth) for valuable discussions and suggestions on various aspects on pyrolysis results of my work. I am thankful to Dr. Rainer G. Schaefer (Research Centre Jülich) who provided many valuable ideas at the beginning of my Ph.D. work. Dr. S. Roberts (University of Southampton) is acknowledged for support with respect to micro-FTIR investigations. I am grateful to Prof. Dr. Santanu Banerjee (Indian Institute of Technology, Bombay) and Prof. Dr. Bernd-Dietrich Erdtmann (Technical University of Berlin) for introducing me to Precambrian palynomorphs.

This work would not have been completed without the cordial relationship with colleagues at ICG-V. I am particularly thankful to Dr. Oliver Kranendonck and Mr. Ulrich Herten. I always found them to discuss on scientific issues and ideas. Mr. Herten provided many supports throughout my Ph.D. tenure. For technical assistance, I would like to thank Mr. Ulrich Disko, Mr. Franz Leistner, Mr. Helmut Willsch, Mr. Karlheinz Nogai, Mr. Willi Benders, Ms. Anneliese Richter and Mr. Wolfgang Lüdtke. I have learnt many aspects on GC-MS from Mr. Disko during my stay at FZ Jülich. I am thankful to Dr. R. Woisch (GSG Mess-und Analysengeräte GmbH, Bruchsal) for supporting with some of the Py-GC-MS analyses. Many thanks to my colleague Dr. Wen-Jin Zhao.

German Research Foundation (DFG) and Research Centre Jülich are acknowledged for providing financial support.

Personally, I would like to thank my parents, my father for his support and my beloved mother for her endless love and great courage. There is no way to fully express my gratefulness to them.

## ABSTRACT

This study has revealed the molecular composition of extraordinarily well preserved palynomorphs (organic-walled microfossils) from selected time windows of Proterozoic to Mesozoic time. Sedimentary rock samples were collected from 11 localities: Hazro area (SE Turkey), Ruhr Basin (Germany), Weilerbach-Quierchied (Germany), Zwickau (Germany), Alstätte Embayment (German-Dutch border), Wülfrath (Germany), Gotland (Sweden), Oklahoma (USA), Virginia (USA), Rampura (India) and Tasmania (Australia). All samples are of low thermal maturity (Rock Eval $T_{max}$ 418°C ($R_c$~0.40) - 444°C ($R_c$~0.75)), except sediments from Suket Shale (Rampura, India). Palynomorphs which are taxonomically well assigned by project collaborators have been handpicked from the total organic residues. For the present investigations, various types of palynomorphs, for example, *Tasmanites*, *Leiosphaeridia*, chitinozoans, scolecodonts, various megaspores and *Chuaria circularis* have been selected. An approach combining microscopy, Micro-Fourier transform infrared (FTIR) spectroscopy and pyrolysis-gas chromatography-mass spectrometry (Py-GC-MS) has been applied.

***Tasmanites*** (thick-walled) and ***Leiosphaeridia*** (thin-walled) are assigned to prasinophycean green algae. Although, *Tasmanites* and *Leiosphaeridia* are morphologically distinct, their overall chemical compositions are similar. The pyrolysates from both thick-walled and thin-walled prasinophytes are dominated by a series of *n*-$C_{6-22}$ alkene/alkane doublets which are typical of pyrolysis products of algaenan, the microbiological resistant algal biopolymer. The pyrolysates of the *Tasmanites* from Tasmania (Upper Carboniferous/Lower Permian) show a normal tricyclic terpenoid product distribution, but no traces of tricyclic terpenoids have been detected from the pyrolysates of *Tasmanites* from Turkey (Dadas Formation, Upper Silurian/Lower Devonian) and USA (Arbuckle Mountains, Oklahoma, Upper Devonian/Lower Carboniferous and Chattanooga Shale, Upper Devonian, Virginia). However, the pyrolysates of *Leiosphaeridia* from Turkey show the presence of monounsaturated and diunsaturated tricyclic terpenes as well as monoaromatic tricyclic terpanes. Hence, the inherent source-biomarker relationship between the *Tasmanites* and tricyclic terpenoids does not always exist. Furthermore, tricyclic terpenoid pyrolysates of the *Leiosphaeridia* confirms that there are more than one biological source(s) of these biomarkers and they are not exclusively from or always diagnostic of *Tasmanites*.

**Chitinozoans** represent a group of flask-like, marine, organic-walled microfossils with uncertain biological affinity. Biomacromolecules of Chitinozoa (Dadas Formation, Upper Silurian, SE Turkey) of present investigation consist of both aliphatic and aromatic moieties. Aromatic pyrolysis products predominate over aliphatic pyrolysis products. Alkylbenzenes, alkylnaphthalenes, alkylphenols and alkylphenanthrenes are the major aromatic compounds found in the pyrolysates of Chitinozoa. A series of *n*-alkene/*n*-alkane doublets in the pyrolysates represents the aliphatic moiety. Micro-FTIR data are consistent with the pyrolytic studies emphasizing that biomacromolecules of the Chitinozoa investigated in the present study consist of both aromatic and aliphatic components. No pyrolysis products diagnostic of chitin have been detected in the present study. It is unlikely that the original macromolecules of Chitinozoa before fossilization were made of chitin related compounds. Chitinozoans belong to a group of rare marine fossils that have a substantial amount of 'lignin-like' macromolecular matter.

Both spectroscopic and pyrolytic investigations demonstrate that the sporopollenin of the fossil **megaspores** (from Cretaceous and Pennsylvanian sediments, Germany) consists of both aliphatic

and aromatic moieties. Alkylated benzenes and alkylphenols are the major aromatic compounds and a homologous series of *n*-alkene/*n*-alkane doublets are present in the pyrolysates of all the fossil sporopollenin. Acetophenone is present in the pyrolysates of megaspores of Cretaceous age, but is absent in the pyrolysates of other megaspores of Pennsylvanian age. The relative abundance of phenols compared to other compounds is higher in the Cretaceous megaspores than that of Pennsylvanian. It is suggested that oxygenated aromatic compounds were selectively degraded during burial and diagenesis with increasing thermal maturation and time. On the other hand, relative abundance of aliphatic moieties selectively increased during burial and diagenesis with increasing thermal maturation and time. The pyrolysates of *Paxillitriletes midas* contain the aromatic compounds like cadalene, retene, dehydroabietane, simonellite and ferruginol which are generally believed to be the biomarkers of coniferous resins. More investigations are needed to reveal the relationship between these biomarkers and sporopollenin.

**Scolecodonts** are fossilized jaws of polychaete annelids of the order Eunicida. The pyrolysates of the scolecodonts (Högklint Formation, Silurian, Gotland, Sweden) include aromatic hydrocarbons such as alkylbenzenes, alkylnaphthalenes and alkylphenols. The aliphatic hydrocarbons are represented by a homologous series of *n*-alkenes and *n*-alkanes. Except phenols, no compounds diagnostic of amino acid origin have been recognised, and it is concluded that amino acids which are commonly found in the extant polychaete jaws were degraded during diagenesis. Presence of predominant aromatic pyrolysates in scolecodonts may suggest that kerogen of marine origin enriched with zooclasts like scolecodonts can also yield aromatic pyrolysates which are typically attributed to type-III kerogen originating from terrestrial higher plants.

***Chuaria circularis*** from the Early Mesoproterozoic Suket Shale of the Vindhyan Supergroup (Central India) has been investigated for its morphology and chemical composition by using microscopy, spectroscopy and pyrolysis-gas chromatography. Morphology and microscopic investigations provide little clues on the specific biological affinity of *Chuaria* as numerous preservational artifacts seem to be incorporated. The predominance of *n*-aliphatic pyrolysates of *Chuaria circularis* suggests that the biomacromolecules of *C. circularis* are of aliphatic nature. Micro-FTIR data are consistent with the pyrolytic studies emphasizing that biomacromolecules of the *C. circularis* investigated in the present study consist of aliphatic moiety and supports its algal affinity. *Chuaria circularis* was probably a very early eukaryotic algae which appeared during Early Mesoproterozoic time in the area of the Indian Platform.

According to the biomacromolecular composition, the investigated organic-walled micro fossils can be grouped as follows:

- As demonstrated by abundant alkenes/alkanes in pyrolysates, only algae posses a wall consisting of highly aliphatic biomacromolecules.
- Megaspores, chitinozoans and scolecodonts consist of both aliphatic and aromatic moieties.

It is concluded that kerogen of marine origin can also yield aromatic compounds including phenols upon pyrolysis. Conversely, aromatic compounds generated upon pyrolysis of kerogen may not always be attributed to kerogen derived from terrestrial higher plants.

## KURZFASSUNG

In dieser Arbeit wurde die Molekularzusammensetzung von außergewöhnlich gut erhaltenen Palynomorphen (Mikrofossilien mit organischer Wandung) aus bestimmten Zeitabschnitten des Proterozoikums bis Mesozoikums ermittelt. Dazu sind Sedimentgesteinsproben aus 11 Lokalitäten im Gebiet von Hazro (SE-Türkei), dem Ruhr-Becken (Deutschland), Weilerbach-Quierchied (Deutschland), Zwickau (Deutschland), Alstätte-Bucht (deutsch-niederländischer Grenzbereich), Wülfrath (Deutschland), Gotland (Schweden), Oklahoma (USA), Virginia (USA), Rampura (Indien), Tasmanien (Australien) untersucht worden. Wenn man von der Formation des Suket Shale (Rampura, Indien) absieht, zeichnen sich all diese Proben durch eine geringe thermische Reife (Rock Eval $T_{max}$ 418°C) ($R_c$~0,40) – 444°C ($R_c$~0,75)) aus. Palynomorphen, deren taxonomische Zugehörigkeit von Projektmitarbeitern bestimmt wurde, wurden manuell aus den Gesamtrückständen des organischen Materials herausgepickt. Dazu sind verschiedene Arten von Palynomorphen wie zum Beispiel *Tasmanites*, *Leiosphaeridia*, Chitinozoen, Scolecodonten, diverse Megasporen und *Chuaria circularis* ausgewählt worden, die in einem Ansatz, der Methoden der Mikroskopie, Mikro-Fourier-Transformations-Infrarot (FTIR) Spektroskopie sowie Pyrolyse-Gaschromatographie-Massenspektrometrie (Py-GC-MS) kombiniert, untersucht wurden.

Die Grünalgen ***Tasmanites*** (dickwandig) und ***Leiosphaeridia*** (dünnwandig) werden den Prasinophyceen zugeordnet. Obwohl *Tasmanites* und *Leiosphaeridia* sich morphologisch unterscheiden, sind ihre chemischen Pauschalzusammensetzungen ähnlich. Die Produkte, die bei der Pyrolyse der dickwandigen als auch dünnwandigen Prasinophyten anfallen, werden von Alken/Alkan-Paaren der homologen Reihe *n*-$C_{6-22}$ bestimmt, die für die Pyrolyseprodukte von Algaenan, dem gegenüber mikrobiellem Abbau widerstandsfähigen Biopolymer der Algen, kennzeichnend sind. Die Pyrolyseprodukte der *Tasmanites* aus Tasmanien (Oberkarbon/Unteres Perm) geben in der Ausbeute der trizyklischen Terpenoide eine gewöhnliche Verteilung zu erkennen, während in den Pyrolyseprodukten der *Tasmanites* aus der Türkei (Dadas-Formation, Oberes Silur/Unterdevon) und den USA (Arbuckle Mountains, Oklahoma, Oberdevon/Unterkarbon und Chattanooga Shale, Oberdevon, Virginia) keine Spuren von trizyklischen Terpenoiden nachzuweisen waren. Allerdings sind in den Pyrolyseprodukten von *Leiosphaeridia* aus der Türkei einfach und doppelt ungesättigte trizyklische Terpene und auch monoaromatischen trizyklische Terpane nachzuweisen. Demnach ist die mutmaßliche Beziehung zwischen Ausgangsmaterial und Biomarker bei den *Tasmanites* und trizyklischen Terpenoiden nicht immer richtig. Darüber hinaus bestätigen die trizyklischen Terpenoide in den Pyrolyseprodukten von *Leiosphaeridia*, dass mehr als eine biologische Quelle für diese Biomarker existiert, und dass diese nicht ausschließlich von *Tasmanites* abstammen oder für diese Form charakteristisch sind.

**Chitinozoen** stellen eine Gruppe von flaschenartigen Mikrofossilien mit organischer Wandung aus dem marinen Bereich dar, deren biologische Zugehörigkeit ungewiss ist. Die Biomarkromoleküle der Chitinozoen (Dadas-Formation, Oberes Silur, SE-Türkei) setzen sich in der vorliegenden Untersuchung sowohl aus aliphatischen als auch aromatischen Bestandteilen zusammen. In den Pyrolyseprodukten herrschen die Aromaten gegenüber den Aliphaten vor. Alkylbenzole, Alkylnaphthaline, Alkylphenole und Alkylphenanthrene bilden den Hauptteil der aromatischen Verbindungen, die in den Pyrolyseprodukten der Chitinozoen anzutreffen sind. Eine Reihe von *n*-Alken/*n*-Alkan-Paaren bildet die Fraktion der Aliphaten in den

Pyrolyseprodukten. Daten aus der Mikro-FTIR sind mit den Pyrolyse-Untersuchungen insofern vereinbar, als dass sie klar zu erkennen geben, dass die Biomakromoleküle der im Rahmen dieser Studie untersuchten Chitinozoen sowohl aus aromatischen als auch aliphatischen Komponenten bestehen. In der vorliegenden Studie war kein Chitin in den Pyrolyseprodukten nachweisbar. Es ist unwahrscheinlich, dass die ursprünglichen Makromoleküle der Chitinozoen vor ihrer Fossilwerdung aus Komponenten aufgebaut waren, die mit Chitin verwandt sind. Chitinozoen zählen zu einer seltenen Gruppe von Fossilien aus dem marinen Bereich, deren organisches Material eine beachtliche Menge von „ligninartigen" Makromolekülen enthält.

Sowohl spektroskopische als auch pyrolytische Untersuchungen zeigen, dass das Sporopollenin der fossilen **Megasporen** (aus Sedimenten der Kreide und des Oberkarbons von Deutschland) sowohl aus aliphatischen als auch aromatischen Komponenten besteht. Alkylierte Benzole und Alkylphenole stellen die vorwiegenden aromatischen Komponenten dar und in den Pyrolyseprodukten des gesamten fossilen Sporopollenin ist eine homologe Reihe von *n*-Alken/*n*-Alkan-Paaren vertreten. Acetophenon kommt zwar in den Pyrolyseprodukten der Megasporen aus der Kreide vor, fehlt aber in den Pyrolyseprodukten der anderen Megasporen aus dem Oberkarbon. Der Relativanteil der Phenole gegenüber den übrigen Komponenten ist in den Proben aus der Kreide größer als in denjenigen aus dem Oberkarbon. Vermutlich wurden die sauerstoffreichen organischen Bestandteile mit Zunahme der thermischen Reife im Zuge der Einbettung und Diagenese selektiv abgebaut. Andererseits hat der Relativanteil der aliphatischen Bestandteile mit Zunahme der thermischen Reife im Zuge der Einbettung und Diagenese zugenommen. In den Pyrolyseprodukten von *Paxillitriletes midas* sind aromatische Verbindungen wie Cadalen, Reten, Dehydroabietane, Simonellite und Ferruginol enthalten, von denen man im allgemeinen annimmt, dass es sich um die Biomarker der Wachse von Koniferen handelt. Um die Beziehung zwischen diesen Biomarkern und dem Sporopollenin klarzustellen, sind weitere Untersuchungen erforderlich.

**Scolecodonten** sind die fossilen Kiefer von polychaeten Anneliden aus der Ordnung Eunicida. Zu den Hauptprodukten, die bei der Pyrolyse der Scolecodonten (Formation von Högklint, Silur, Gotland, Schweden) anfallen, zählen aromatische Kohlenwasserstoffe wie Alkylbenzole, Alkylnaphthaline, Alkylphenole. Die aliphatischen Kohlenwasserstoffe liegen in Form einer homologen Reihe aus *n*-Alken/*n*-Alkan-Paaren vor. Außer Phenolen sind keine Verbindungen entdeckt worden, deren Ursprung auf Aminosäuren zurückgeführt werden kann, so dass daraus zu schließen ist, dass Aminosäuren, die in den Kiefern der heute lebenden polychaeten Würmer vorkommen, während der Diagenese abgebaut wurden. Die Vorherrschaft von aromatischen Pyrolyseprodukten in den Scolecodonten könnte dafür sprechen, dass Kerogen marinen Ursprungs, in dem Zooklasten wie Scolecodonten angereichert sind, auch aromatische Pyrolyseprodukte liefern kann, die normalerweise dem Kerogentyp III vorbehalten sind, der auf höhere Pflanzen terrestrischer Herkunft zurückgeht.

***Chuaria circularis*** aus der Formation des Suket Shale (Vindhyan Supergruppe, Unteres Mesoproterozoikum, Zentral-Indien) ist unter Anwendung der Mikroskopie, Spektroskopie und Pyrolyse-Gaschromatographie nach ihrer Morphologie und chemischen Zusammensetzung untersucht worden. Mikroskopische Untersuchungen liefern kaum Hinweise zur spezifischen biologischen Zuordnung von *Chuaria*, weil diverse erhaltungsbedingte Artefakte darin verwickelt zu sein scheinen. Die Vorherrschaft von *n*-aliphatischen Verbindungen in den Pyrolyseprodukten von *Chuaria circularis* spricht dafür, dass die Biomakromoleküle von *C. circularis* aliphatischen Ursprungs sind. Daten aus Untersuchungen mittels Mikro-FTIR sind mit den

Pyrolyseergebnissen insofern vereinbar, dass die Biomakromoleküle der in dieser Studie untersuchten Form von *C. circularis* aus aliphatischen Komponenten bestehen und deren Zuordnung zu Algen bestätigt. *Chuaria circularis* war vermutlich eine sehr frühe eukaryotische Alge, die zur Zeit des Unteren Mesoproterozoikums im Bereich der Indischen Plattform in Erscheinung getreten ist.

Gemäß der Zusammensetzung der Biomakromoleküle lassen sich die untersuchten Mikrofossilien mit organischer Wandung wie folgt gruppieren:
- wie anhand der Anteile von Alken/Alkan-Paaren in den Pyrolyseprodukten zu erkennen ist, besitzen nur Algen eine Wand, die aus hochgradig aliphatischen Biomakromolekülen besteht.
- Megasporen, Chitinozoen und Scolecodonten setzen sich sowohl aus aliphatischen als auch aromatischen Bestandteilen zusammen.

Daraus ist zu schließen, dass die Pyrolyse von Kerogen marinen Ursprungs ebenfalls aromatische Verbindungen wie Phenole hervorbringen kann, oder umgekehrt: aromatische Verbindungen, die bei der Pyrolyse von Kerogen erzeugt werden, sind nicht immer auf Kerogen zurückzuführen, das von höheren Pflanzen terrestrischen Ursprungs stammt.

## CONTENTS

**Acknowledgments ……I**

**Abstract ……II**

**Kurzfassung ……IV**

**Contents ……VII**

**Figure captions ……XI**

**Plate captions ……XIV**

**Table captions ……XV**

**Abbreviation index ……XVI**

**Chapter 1: Introduction……1**

1.1. Motivation and objective ……1

1.2. Previous studies on organic–walled microfossils …… 2

1.2.1. Palynological investigations on Paleozoic organic–walled microfossils …… 2

1.2.2. Previous studies on organic geochemistry of organic–walled microfossils ……4

1.3. Samples …… 6

1.3.1. Sample preparation …… 7

1.4. Analytical methods ……7

1.4.1 Light and scanning electron microscopy ……9

1.4.2. Rock-Eval Pyrolysis …… 9

1.4.3. Pyrolysis-Gas Chromatography-Mass spectrometry ……10

1.4.4. Micro-Fourier transform infrared spectroscopy ……11

1.5. References ……12

**Chapter 2: Molecular Composition of Silurian/Devonian *Tasmanites* and *Leiosphaeridia* (Dadas Formation, SE Turkey)……17**

2.1. Introduction ……17

2.2. Samples and preparation ……19

2.3. Experimental …… 20

2.4. Results and discussion …… 22

2.4.1. Py-GC-MS analysis of *Tasmanites* ……...22

2.4.2. Py-GC-MS analysis of *Leiosphaeridia* ……..……...24

2.5. Conclusions ……..….. 31

2.6. References ……..…..33

**Chapter 3: Molecular composition of Upper Silurian Chitinozoa from the Dadas Formation, SE Turkey as revealed by spectroscopic and pyrolytic investigations…….37**

3.1. Introduction …… 37

3.2. Geological settings ……. 38

3.3. Experimental ……..……..40

3.3.1. Samples and preparation …….. 40

3.3.2. Micro-FTIR spectroscopy …….43

3.3.3. Curie point pyrolysis-gas chromatography-mass spectrometry ……... 43

3.3.4 GC-MS of rock extract ……...44

3.4. Results and discussion ……... 45

3.4.1. Micro-FTIR spectroscopy …… 45

3.4.2. Curie point pyrolysis-gas chromatography-mass spectrometry …….. 46

3.4.2.1. *n*-Alkenes/*n*-alkanes ……...…… 46

3.4.2.2. Aromatic compounds ……..47

3.4.2.3. Chitin derived compounds ……..56

3.5. Conclusions …… 57

3.6. References……..…….. 59

**Chapter 4: The molecular composition of sporopollenin from fossil megaspores as revealed by micro-FTIR and pyrolysis-GC-MS ……..…..63**

4.1. Introduction ……....63

4.2. Experimental …….. 64

4.2.1. Samples …….....64
4.2.2. Palynological preparation ……..….69
4.2.3. Micro-FTIR spectroscopy …….....70
4.2.4. Curie point pyrolysis-gas chromatograph-mass spectrometry ……..…..70
4.3. Results and discussion ……..….71
4.3.1 FTIR spectral characteristics of fossil sporopollenin ……..…..71
4.3.2 Curie point pyrolysis-gas chromatography-mass spectrometry ……..…..74
4.4. Conclusions ……..….82
4.5. References ……..…...84

**Chapter 5: Molecular composition of Silurian scolecodonts (Gotland, Sweden) as revealed by pyrolysis-GC-MS……..……..…89**

5.1. Introduction…….…….…. 89
5.2. Geological background……..…. 90
5.3. Experimental……..91
5.3.1. Sample preparation…….…….…91
5.3.2. Curie point pyrolysis-gas chromatography-mass spectrometry…….…….……92
5.4. Results and discussion……...92
5.5. Conclusions…….…..…98
5.6. References…….…....99

**Chapter 6: *Chuaria circularis* from the Early Mesoproterozoic Suket Shale, Vindhyan Supergroup, India: Insights from Microscopy, Spectroscopy and Pyrolysis-Gas Chromatography ……..……101**

6.1. Introduction …….……....101
6.2. Samples ……..…..102
6.3. Methods …….…..104
6.3.1. Microscopy…….…….....104
6.3.2. Pyrolysis-Gas Chromatography…….…104
6.3.3. Micro-FTIR…….....105
6.4. Systematic description …….....105
6.4.1. Discussion ……106
6.5. Colour ……109

6.6. Biostatistics ……110
6.7. Ultrastructure ……112
6.8. Reflectance studies ……....113
6.9. Molecular composition ……..……114
6.9.1. Pyrolysis-Gas Chromatograpy ……..…114
6.9.2. Micro-FTIR…….…...116
6.10. Age and geographical distribution ……..…..117
6.11. Conclusions ……..….119
6.12. References …….…...120

**Chapter 7: Summary and Perspective ……..….127**

**Appendix …….…....135**

## FIGURE CAPTIONS

**Fig. 1.1.** World map showing samples localities of the present study...……....6

**Fig. 1.2.** Flow chart depicting different analytical steps applied in this study ….....9

**Fig. 2.1.** Photomicrographs of palynomorphs. (a, b) *Tasmanites* from the Dadas Formation; (c, d) *Tasmanites* from Tasmania; (e, f) *Leiosphaeridia* from the Dadas Formation ……..…..21

**Fig. 2.2.** Total ion chromatogram resulting from Curie point pyrolysis-GC-MS of *Tasmanites* from the Dadas Formation, SE Turkey ……22

**Fig. 2.3.** Total ion chromatogram resulting from Curie point pyrolysis-GC-MS of *Tasmanites* from Tasmania, Australia ……..…23

**Fig. 2.4.** Total ion chromatogram resulting from Curie point pyrolysis-GC-MS of *Leiosphaeridia* from the Dadas Formation, SE Turkey ……...24

**Fig. 2.5.** Partial mass chromatograms at *m/z* 191 from the Curie point pyrolysis-GC-MS analysis of (a) *Tasmanites* from SE Turkey; (b) *Tasmanites* from Tasmania and (c) *Leiosphaeridia* from SE Turkey …….25

**Fig. 2.6.** Partial mass chromatograms from the Curie point pyrolysis-GC-MS analysis of *Leiosphaeridia* from SE Turkey at (a) *m/z* 242; (b) *m/z* 256; (c) *m/z* 260; (d) *m/z* 272; (e) *m/z* 274 ……27

**Fig. 2.7.** Partial mass chromatograms from the Curie point pyrolysis-GC-MS analysis of *Tasmanites* from Tasmania at (a) *m/z* 242; (b) *m/z* 256; (c) *m/z* 260; (d) *m/z* 272; (e) *m/z* 274 ……28

**Fig. 2.8.** Partial mass chromatograms from the Curie point pyrolysis-GC-MS analysis of *Tasmanites* from SE Turkey at (a) *m/z* 242; (b) *m/z* 256; (c) *m/z* 260; (d) *m/z* 272; (e) *m/z* 274 ……28

**Fig. 2.9.** Partial mass chromatograms (SIM analysis) from the pyroprobe pyrolysis-GC-MS analysis of Tasmanite oil shale at (a) *m/z* 242; (b) *m/z* 256; (c) *m/z* 260; (d) *m/z* 272; (e) *m/z* 274 ……29

**Fig. 2.10.** Partial mass chromatograms (SIM analysis) from the pyroprob pyrolysis-GC-MS analysis of *Tasmanites* from SE Turkey at (a) *m/z* 242; (b) *m/z* 256; (c) *m/z* 260; (d) *m/z* 272; (e) *m/z* 274 ……...29

**Fig. 3.1.** Stratigraphic column of the Fetlika-1 core between –110 m and –44 m (Dadas Formation ) around Hazro area, SE Turkey. Sample positions in the core are indicated by arrows ……..…39

**Fig. 3.2.** Total ion chromatogram resulting from Curie point pyrolysis-GC-MS (pyrolysis at 610ºC for 10s) of chitin standard from crab (*Cancer magister*) shells ……..…….……44

**Fig. 3.3.** A micro-FTIR spectrum of Chitinozoa. Assignments of absorption bands and vibration modes (δ=deformation; ν=stretching; s=symmetric; as=asymmetric) are indicated in parentheses ……..45

**Fig. 3.4.** Total ion chromatogram resulting from Curie point pyrolysis-GC-MS (pyrolysis at 610ºC for 10s) of (a) handpicked Chitinozoa from the Dadas Formation, SE Turkey; (b) total organic residues (size> 63 µm) ……..48

**Fig. 3.5.** Histograms showing relative abundance of various compound classes in the pyrolysates of handpicked chitinozoans and total kerogen from the Dadas Formation ……..49

**Fig. 3.6.** Mass chromatogram (*m/z* 57) of the 610°C Curie-point pyrolysates of (a) handpicked Chitinozoa; (b) total organic residues (size> 63 µm) ……..50

**Fig. 3.7.** Mass chromatogram (*m/z* 91+105+106+119+120+134) of the 610°C Curie-point pyrolysates of handpicked Chitinozoa ……..51

**Fig. 3.8.** Mass chromatogram (*m/z* 133+134) of aromatic hydrocarbon fraction from sediment extract at depth –92.30 m revealing typical distributions of aryl isoprenoids ……..52

**Fig. 3.9.** Mass chromatogram (*m/z* 128+142+156+170+184) of (a) the 610°C Curie-point pyrolysates of handpicked Chitinozoa and (b) host sediment extract showing the distribution of alkylnaphthalenes ……54

**Fig. 3.10.** Mass chromatogram (*m/z* 94+107+108+121+122) of the 610°C Curie-point pyrolysates of handpicked Chitinozoa ……..55

**Fig. 4.1.** (a) Map of Germany showing megaspore sample localities; (b) Stratigraphic position of the megaspore samples. …….……66

**Fig. 4.2.** Micro-FTIR spectra of megaspores from the Pennsylvanian (a) *Tuberculatisporites* sp.; (b) *Laevigatisporites reinschii*; (c) *Calamospora laevigata*……..……..72

**Fig. 4.3.** Micro-FTIR spectra of megaspores of Cretaceous age (a) *Dijkstraisporites helios*; (b) Megaspore concentrate; (c) *Paxillitriletes midas*……..……..…73

**Fig. 4.4.** Total ion chromatogram resulting from Curie point pyrolysis-GC-MS (pyrolysis at 610ºC for 10s) of (a) *Tuberculatisporites* sp.; (b) *Laevigatisporites reinschii*; (c) *Calamospora laevigata*……..…75

**Fig. 4.5.** Total ion chromatogram resulting from Curie point pyrolysis-GC-MS (pyrolysis at 610ºC for 10s) of (a) *Dijkstraisporites helios*; (b) Megaspore ……..……77

**Fig. 4.6.** Total ion chromatogram resulting from Curie point pyrolysis-GC-MS (pyrolysis at 610ºC for 10s) of megaspore *Paxillitriletes midas* ….……78

**Fig. 4.7.** Partial mass chromatograms resulting from Curie point pyrolysis-GC-MS (pyrolysis at

610ºC for 10s) of megaspore *Paxillitriletes midas*……..79
**Fig. 4.8.** Histograms showing relative abundance of various compound classes in the pyrolysates of megaspores …….81
**Fig. 5.1.** Map of Gotland showing different stratigraphical units and sample location (based on Hede, 1960) ……..91
**Fig. 5.2.** Scanning electron micrograph of a scolecodont from the Högklint Formation, Gotland, Sweden ……..92
**Fig. 5.3.** Reconstructed total ion chromatogram resulting from Curie point pyrolysis-GC-MS (pyrolysis at 610ºC for 10s) of (a) handpicked scolecodonts and (b) total organic residues (size> 20 μm) from the Högklint Formation, Gotland ……93
**Fig. 5.4.** Histograms showing relative abundance of various compound classes in the pyrolysates of (a) handpicked scolecodonts; (b) total kerogen from the Högklint Formation, Gotland, Sweden ……94
**Fig. 5.5.** Mass chromatogram (*m/z* 91+92+105+106+119+120) of the 610°C Curie-point pyrolysates of handpicked scolecodonts showing the distribution of alkylbenzenes …….96
**Fig. 5.6.** Mass chromatogram (*m/z* 128+142+156+170) of the 610°C Curie-point pyrolysates of handpicked scolecodonts showing the distribution of alkylnaphthalenes……..…96
**Fig. 5.7.** Mass chromatogram (*m/z* 94+107+108+121+122) of the 610°C Curie-point pyrolysates of handpicked scolecodonts showing the distribution of alkyphenols……..…..97
**Fig. 6.1.** Geological map of the Rampura area, Neemuch district, Madhya Pradesh (after Kumar, 2001) ……103
**Fig. 6.2.** Variation of colour with total "wall" thickness of *Chuaria circularis*, Suket Shale, Vindhyan Supergroup, India ……..…110
**Fig. 6.3.** Size histogram of *Chuaria circularis*, Suket Shale, Vindhyan Supergroup, India ……...111
**Fig. 6.4.** Scatter diagram for longer dimension plotted against shorter dimension for *Chuaria circularis*, Suket Shale, Vindhyan Supergroup, India……...…...111
**Fig. 6.5.** Composite histograms showing distribution of reflectance of *Chuaria* from (a) the Suket Shale, India; (b) the Visingsö Formation, Sweden; (c) the Liulaobei Formation, China ……...113
**Fig. 6.6.** Total ion chromatogram resulting from Pyrolysis-GC of *Chuaria circularis*, Suket Shale, Vindhyan Supergroup, India ……...…..115
**Fig. 6.7.** A micro-FTIR spectrum of *Chuaria circularis* from Suket Shale, India……..…117
**Fig. 6.8.** Distribution of the *Chuaria circularis* in a palaeogeographic reconstruction of Vendian age ……..…118

PLATE CAPTIONS

**Plate 1.1.** Light and scanning electron micrographs of various palynomorphs……..…3

**Plate 3.1.** Photomicrographs of chitinozoans from the Dadas Formation (Fetlika 1 borehole, Dadas Formation, SE Turkey, Upper Silurian)…….41

**Plate 4.1.** Light and Scanning electron micrographs of megaspores…….……...69

**Plate 6.1.** Photo micrographs of *Chuaria circularis* from the Early Mesoproterozoic Suket Shale, Vindhyan Supergroup, India……..…107

**Plate 6.1.** Scanning electron and transmission electron micrographs of *Chuaria circularis* from the Early Mesoproterozoic Suket Shale, Vindhyan Supergroup, India….....108

TABLE CAPTIONS

**Table 1.1.** Individual palynomorphs, location, stratigraphy and thermal maturity of their host rocks…..8

**Table 2.1.** Tricyclic terpenoids from pyrolysis-GC-MS analyses of *Tasmanites* and *Leiosphaeridia* ……..26

**Table 3.1.** Total organic carbon and Rock Eval data of Chitinozoa bearing sediments from the Dadas Formation, SE Turkey ……..……..…….....41

**Table 3.2.** Major alkylbenzenes identified in the pyrolysates of the handpicked Chitinozoa …….....53

**Table 3.3.** Major alkylnaphthalenes identified in the pyrolysates of the handpicked Chitinozoa ….....53

**Table 4.1.** Sample descriptions, bulk chemical and Rock-Eval data of the megaspore bearing host rock ……..67

**Table 4.2.** Aromatic products detected from Curie point pyrolysis of different megaspores of Carboniferous and the Cretaceous age……...…….…..……..80

**Table 5.1.** Total organic carbon and Rock Eval data of scolecodonts bearing sediments from the Högklint Formation ……..…...…...90

**Table 5.2.** Aromatic compounds found in the pyrolysates from scolecodonts and total kerogen ……..….....95

**Table 7.1.** Individual palynomorphs (hand picked), thermal maturity of their host rocks ($T_{max}$ from Rock Eval pyrolysis) and major, minor and specific biomarkers produced upon pyrolysis.……...…..…….…..…130

# ABBREVIATION INDEX

| | |
|---|---|
| ARO | Aromatic Hydrocarbon |
| FTIR | Fourier Transform Infrared Spectroscopy |
| GC | Gas Chromatography |
| HCl | Hydrochloric acid |
| HF | Hydrofluoric acid |
| HI | Hydrogen Index |
| *m/z* | Mass/Charge |
| MPLC | Medium Pressure Liquid Chromatography |
| OM | Organic Matter |
| OWM | Organic-Walled Microfossil |
| NSO | Nitrogen, Sulphur and Oxygen |
| PI | Production Index |
| Py-GC-MS | Pyrolysis-Gas Chromatography-Mass Spectrometry |
| $R_c$ | Equivalent Vitrinite Reflectance based on $T_{max}$ value |
| SAT | Saturated Hydrocarbon |
| $S_1$ | Volatile Hydrocarbon |
| $S_2$ | Hydrocarbons derived from the cracking of kerogen |
| S/D | Silurian/Devonian |
| SEM | Scanning Electron Microscope |
| TEM | Transmission Electron Microscope |
| $T_{max}$ | Temperature at which thermal cracking of releases the maximum amounts of hydrocarbons |
| TOC | Total Organic Carbon |

# CHAPTER-1

## Introduction

### 1.1. Motivation and objectives

A major part of the sedimentary organic material in the geosphere consists of insoluble macromolecular material termed kerogen. Ever since the 1800s, organic geochemists have been intrigued by the origin and nature of organic matter in the geologic record. Organic geochemical studies of organic matter have concentrated mainly on bulk characterization of kerogen in response to the needs of coal, oil and gas industries. Such investigations were based on a model for the formation of kerogen in sediments that involved random repolymerization and recondensation of lipids, sugars, amino acids or other moieties (Tissot and Welte, 1984). Only recently, an alternative concept has focused on the chemical and structural identification of specific organisms such as algae (Blokker, 2000; Versteegh and Blokker, 2004 and references therein), terrestrial plants (van Bergen et al., 1994; Mösle et al., 1998) and animal remains (Stankiewicz et al. 1997, 1998). This led to the development of a different model of kerogen formation involving the selective preservation (Tegelaar, 1989) or in situ polymerization (Stankiewicz et al., 2000) of chemically resistant biomacromolecules. However, most of the kerogen fractions consist of different groups of organic-walled microfossils (palynomorphs) and the chemical composition of the individual fossil group remains unclear until now. The investigations of biomacromolecules and their subsequent products from identifiable fossil remains can offer a wealth of information concerning the fundamentals of paleobiology, and these studies have considerable potential to understand the source-biomarker relationship and to resolve questions of organic matter diagenesis in sediments. Conventional extraction of lipid biomarker molecules can provide valuable information on early life (see for example Brocks et al., 2005), but correlation of biomarkers with specific microfossil taxa is difficult. Another major difficulty resides in the fact that very little is known about the chemical composition of various extant organic-walled micro organisms and their fossilized counterpart. Thus, the present study has two major objectives

- To document the chemical composition of pure concentrates (=handpicked), extraordinarily well preserved, organic-walled microfossils (OWM) from some selected time windows of Proterozoic to Mesozoic age and to classify them using a chemotaxonomic approach.
- To understand the source-biomarker relationship.

## 1.2. Previous studies on organic–walled microfossils

### *1.2.1. Palynological investigations on Paleozoic organic–walled microfossils*

Research of the spores/pollen of living plants commenced in the 17th century. N. Green in 1640 (see Bradbury, 1967) was the first to observe pollen grains under a microscope. Development of optical microscopy facilitated the spores/pollen research. Studies on fossil spores/pollen soon followed. In 1838, Goeppert had described and illustrated by line drawing fossil pollen. In 1884, Reinsch (cited in Servais and Wellman, 2004) had provided the first photograph of a fossil spore from the Carboniferous sediments. In 1916, Von Post (see Servais and Wellman, 2004) had published his classical work primarily on recent pollen and applying this to the Quaternary record of dispersed pollen. Raistrick (1934) used spore to correlate individual coal seams of the British Carboniferous. At this time, coal was the world's source of energy, and the coal industries supported palynological investigations. Soon after, the potential for palynology in the field of petroleum exploration was also realized. Thus, the study of organic-walled microfossils took off and was fuelled by industrial use.

Other than spore and pollen, acritarchs (see Plate 1.1c) are a significant source of paleobiological information. Acritarchs are thought to represent fossilized, organic-walled cysts of unicellular protist that can not be assigned to known groups of organisms. The group acritarchs (akritos = uncertain, mixed, confused, and arche = beginning, origin) was proposed by Evitt (1963). Prior to 1963, the acritarchs were part of a group of organic-walled microfossils labeled "hystrichospheres" by O. Wetzel in 1933 (see Jansonius and McGregor, 1996). Alfred Eisenack was the pioneer, who started research on Paleozoic microphytoplankton. He was the first to describe in detail "hystrichospheres" from erratics of the southern Baltic area. Another early pioneer was Geogres Defladre who started investigations on acritarchs from the French Silurian at the same time that Eisenack was working on acritarchs from the Baltic Ordovician and Silurian. Following Evitt's (1963) proposal, all acritarch workers adopted the concept that acritarchs are a polyphyletic grouping of organic-walled microfossils of varied but unknown biological affinities. Acriatarchs are biostratigraphically useful in areas where no other fossils occur (Servais and Wellman, 2004).

Alfred Eisenack started his research not only on the Paleozoic "hystrichospheres", he also reported several new microfossil groups from the erratic boulders of the Baltic Sea shore (Eisenack, 1930). The small bottle- to urn shaped organic-walled microfossils that were found together with acritarchs were assigned to a new group: the Chitinozoans. Chitinozoans (Plate 1.1e) represent a group of organic walled microfossils, occurring in Early Ordovician to at least Late Devonian marine sediments (Paris et al., 1999). They appear exclusively in marine

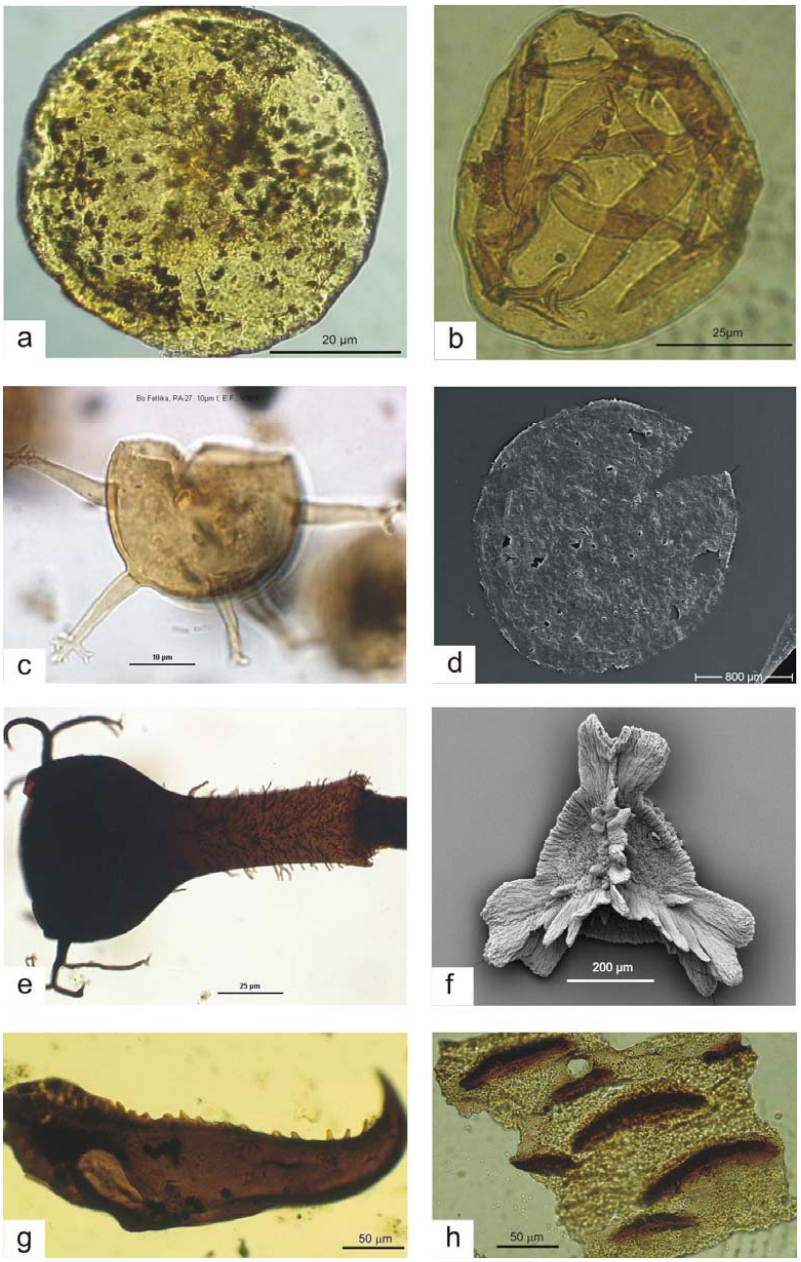


**Plate 1.1.** Light and scanning electron micrographs of various palynomorphs. (a) *Tasmanites* from Tasmania, Late Carboniferous/Early Permian, Australia; (b) *Leiosphaeridia* from the Dadas Formation, Late Silurian, SE Turkey; (c) Acritarch from the Dadas Formation, Late Silurian, SE Turkey; (d) *Chuaria circularis* from the Suket Shale, Mesoproterozoic, India; (e) Chitinozoa (*Ancyrochitina*) from the Dadas Formation, Late Silurian, SE Turkey; (f) Megaspore (*Paxillitriletes midas*) from the Kuhfeld Formation, Cretaceous, German-Dutch border; (g) Scolecodont from the Dadas Formation, Late Silurian, SE Turkey; (h) Cuticle of arthropod from the Dadas Formation, Late Silurian, SE Turkey [photo micrographs (c), (e), (g) courtesy of R. Brocke, and scanning electron micrograph (f) courtesy of C. Hartkopf-Fröder].

sediments and have variously been assigned to Protozoa (e.g., foraminifers, ciliates), various Metazoa (e.g., eggs of annelids, graptolites), algae or even fungi (see references in Miller, 1996). More recently, chitinozoans are assigned to ontogenetic vesicles ("eggs") of unknown soft-bodied organisms (Paris and Nõlvak, 1999). Chitinozoans are considered to be an extremely powerful biostratgraphical tool (Servais and Wellman, 2004). Recently, chitinozoans have been used to measure the thermal maturity of the host sediments by measuring the reflectance of their wall (Bertrand and Héroux, 1987; Tricker et al., 1992). Lécuyer and Paris (1997) used chitinozoans as a source of marine carbon for documenting the excursions of $\delta^{13}C$ during Early Ordovician to latest Devonian times.

Another organic-walled microfossil commonly found during palynological preparations are scolecodonts. Scolecodonts (Plate 1.1g) are the fossilized elements of the proboscidal armatures of polychaetous annelids (Szaniawski, 1996). The first report of scolecodonts was published by Eichwald (1854) who described a single specimen from the Silurian of Saaremaa Island, Baltic Sea. Subsequently, more detailed descriptions were provided by Hinde (1879). The fossil record extends at least back to the middle Cambrian (Conway-Moris, 1979). The stratigraphic use of scolecodonts is still not very significant, possibly due to our insufficient knowledge (Szaniawski, 1996). The majority of the Paleozoic taxa with scolecodonts are traditionally placed in the order Eunicida (Eriksson et al., 2004). Photo and scanning electron micrographs of various palynomorphs are shown in Plate 1.1.

*1.2.2. Previous studies on the organic geochemistry of organic–walled microfossils*

In 1968, Kjellstrom analysed some selected prasinophytes (e.g., *Leiosphaeridia, Tasmanites*) using Micro-FTIR and interpreted that these organic-walled micro fossils contained saturated fatty acid derivatives similar to those from spores and pollen grains. *Tasmanites* representing the only fossil member of the prasinophyta have been studied in detail by using pyrolytic (Philp et al., 1982, Greenwood et al., 2000) and spectroscopic (Hemesly et al., 1993) investigations and it has been suggested that the fossil walls consist of long chains of aliphatic saturated hydrocarbons. *Gloeocapsomorpha prisca* which constitutes the bulk organic matter of Middle Ordovician oil shales (kukersites) has been studied extensively. The building blocks of the resistant macromolecule present in the fossil remains of this organism are based on 5-*n*-alkyl-resorcinols with the alkyl side chain being mainly $C_{15}$, $C_{17}$, $C_{19}$ (Derenne et al., 1992; Blokker et al., 2001). Moldowan and Talyzina (1998) and Talyzina et al. (2000) detected dinoflagellate specific biomarkers, dinosteranes and 4α-methyl-24-ethylsteranes, in the pyrolysates of Early Cambrian acritarch concentrate and concluded that some acritarchs

are related to dinoflagellates and that evolution of dinoflagellates started at least as early as the Early Cambrian.

Arouri et al. (1999) investigated two Neoproterozoic acritarchs, *Multifronsphaeridium pelorium* and the informally identified Species A, by electron microscopy, micro-FTIR spectroscopy and pyrolytic studies and concluded that the macromolecular structure of these acritarchs consisted of short *n*-alkylpolymethylenic chains, probably linked via ether/ester bonds, with possibly a small aromatic content. In 2000, Arouri et al. analysed some more Neoproterozoic acritarchs (*Tanarium* sp., *Hocosphaeridium scaberfacium*, *Alicesphaeridium medusoidum*, *Chuaria circularis*, *Leiosphaeridia* sp., and *Tasmanites* sp.) by spectroscopic and pyrolytic methods. They concluded that little chemical data was obtained by micro-FTIR spectroscopy and py-GC-MS and this was indicative of a polyaromatic biomacromolecule of high recalcitrance. Moreover, they suggested that the Raman spectra showed a signal which could be interpreted as significant carbon ordering characteristic of polyaromatic structures. Foster et al. (2002) documented the wall chemistry of the microfossil *Reduviasporonites* which was believed to be a fungal spore occurring as spikes at the Permo-Triassic boundary at various locations. However, they suggested that this fossil was in fact algal in origin. Versteegh et al. (2004) analysed monotypic assemblage of fossil dinoflagellate from Eocene sediments of Pakistan. Their chemical analysis showed that macromolecles of those dinoflagellate were highly aliphatic consisting of etherlinked aliphatic carbon chains, notably with 16 and 18 carbon atoms and a predominantly $C_9$ mid chain functionality. They suggested that the microfossils had been formed post-mortem by oxidative polymerization of the fatty acids equivalents of the macromolecular building blocks, derived from cellular membranes and storage vesicles. Recently, Marshall et al. (2005) analysed a range of Neoproterozoic acritarchs (*Tanarium conoideum*, *Leiosphaeridia* sp.) and Mesoproterozoic acritarchs (*Leiosphaeridia jacutica*, *Satka squamifera*, *Shuiyousphaeridium macroreticulatum*) by micro-FTIR and micro-Raman spectroscopy. They concluded from infrared spectra that Neoproterozoic acritarch *Tanarium conoideum* contains a biopolymer consisting of long chained polymethylenic material which is consistent with algaenan, but that the Neoproterozoic acritarchs *Leiosphaeridia* sp. may contain a new class biopolymer containing significant aliphatic, branched aliphatic and saturated molecular constituents, different from those of algaenan, lignin, sporopollenin, or dinosporin. They also suggested that the biopolymer in the walls of Mesoproterozoic acritarchs consist predominantly of aromatic carbon, with some methylene chains, terminal methyl groups, and carbon-oxygenated functional groups.

Fossil spores are also of particular interest as they make up the maceral sporinite which is an important component of some coals. Previously, it was believed that sporopollenin (biopolymer of exine part of spore) was chemically similar to carotenoids (Brocks and Shaw, 1968; Shaw, 1971). This was based on studies on extant pollen and spores. However, later investigations suggested that carotenoids do not contribute to sporopollenins (Herminghaus et al., 1988; Wehling et al., 1989) and that their identification could be due to incomplete


**Figure 1.1.** World map showing sample localities of the present study. (1) Dadas Formation (Late Silurian/Early Devonian), Hazro area, SE Turkey; (2) Högklint Formation (Silurian), Gotland, Sweden ; (3) Kuhfeld Formation (Cretaceous), Alstätte Embayment, German-Dutch border, (4) Wülfrath (Cretaceous), Germany; (5) Weilerbach (Pennsylvanian), Germany; (6) Upper Horst Formation (Pennsylvanian), Ruhr Basin, Germany; (7) Zwickau Formation (Pennsylvanian), Zwickau, Germany; (8) Ebey dam section (Late Devonian/Early Carboniferous), Arbuckle Mountains, Oklahoma, USA; (9) Chattanooga Shale (Late Devonian), Virginia, USA; (10) Suket Shale (Early Mesoproterozoic), Rampura, India; (11) Tasmania (Late Carboniferous/Early Permian), Australia.

purification of sporopollenin isolates. More recent studies suggest that sporopollenins may have two different types of chemical structures. In one type the main building blocks are oxygenated aromatic compounds (e.g. Schenck et al., 1981; Wehling et al., 1989), while in the other, the main building blocks are aliphatic compounds (Guilford et al., 1988; Hayatsu et al., 1988; Stout 1993; Hemesly et al., 1996). For more detailed discussion please see chapter 4.

### 1.3. Samples

Sedimentary rock samples were collected from 11 localities (Fig. 1.1 and Table 1.1): Hazro area (SE Turkey), Ruhr Basin (Germany), Weilerbach-Quierchid (Germany), Zwickau (Germany), Alstätte Embayment (German-Dutch border), Wülfrath (Germany), Gotland

(Sweden), Oklahoma (USA), Virginia (USA), Rampura (India) and Tasmania (Australia). All palynomorphs are of low thermal maturity, except sediments from Suket Shale (Rampura, India). According to established conversion of $T_{max}$ to equivalent vitrinite reflectance, the $T_{max}$ values 418°C and 444°C refer to equivalent vitrinite reflectance ($R_c$) 0.40 and 0.75, respectively (after Bordenave et al., 1993). Samples from Hazro area, Ruhr Basin, Alstätte Embayment were collected from cores. The remaining samples were collected from outcrops. Detailed descriptions on samples and geological background have been provided in each chapter separately.

*1.3.1. Sample preparation*

Organic walled-microfossils were separated from rock matrix by normal palynological processing methods by using HF, HCl and water filtration and sieving. Kerogen separation from the rocks was done at Forschungsinstitut Senckenberg, Frankfurt, Germany (R. Brocke) and at Geologischer Dienst Nordrhein–Westfalen, Krefeld, Germany (C. Hartkopf-Fröder). No oxidising agents were used as they do alter the colour and chemical composition of the organic residues (Saxby, 1970). The organic residue has been separated into two fractions (10-63 μm and >63 μm). For each analysis, I have selectively handpicked about 300 to 500 individual microfossils from the larger fractions, under a stereomicroscope. In order to avoid any misinterpretations due to compositional mixing by signals from other microfossils, I have exclusively used handpicked palynomorphs which have taxonomically been well assigned. Prior to chemical investigations, these palynomorphs have been cleaned several times with dichloromethane to remove soluble organic matter. Detailed description of samples preparation is given in the respective chapter and the overall flow chart of the same is shown in Figure 1.2.

## 1.4. Analytical methods

An approach combing microscopy and various chemical methods may help to understand several important steps in the evolution of the early biosphere paleobiology and paleoecology. This approach has been applied in the present study to some extraordinarily well preserved palynomorphs collected from selected time windows of Proterozoic to Mesozoic age. The various chemical methods that are used to study the resistant biomacromolecules can be subdivided into non-destructive and destructive techniques. The non-destructive techniques

**Table 1.1.** Individual palynomorphs, location, stratigraphy and thermal maturity of their host rocks ($T_{max}$ from Rock Eval pyrolysis).

| Taxon | Locality | Stratigraphy | Age | $T_{max}$ [°C] |
|---|---|---|---|---|
| *Tasmanites* | Tasmania, Australia | | Late Carboniferous/ Early Permian | 444 |
| *Tasmanites* | Hazro area, SE Turkey | Dadas Formation | Late Silurian/ Early Devonian | 430 |
| *Tasmanites* | Oklahoma, USA | Ebey dam section, Arbuckle Mountain | Late Devonian/ Early Carboniferous | 424 |
| Cf. *Tasmanites* | Virginia, USA | Chattanooga Shale | Late Devonian | 439 |
| *Leiosphaeridia* | Hazro area, SE Turkey | Dadas Formation | Late Silurian/ Early Devonian | 430 |
| Cf. *Leiosphaeridia* | Virginia, USA | Chattanooga Shale | Late Devonian | 439 |
| Chitinozoa | Hazro area, SE Turkey | Dadas Formation | Late Silurian | 430 |
| *Calamospora laevigata* | Saarland, Germany | - | Pennsylvanian | 432 |
| *Laevigatisporites reinschii* | Ruhr Basin, Germany | Upper Horst Formation | Pennsylvanian | 437 |
| *Tuberculatisporites* | Zwickau, Germany | Zwickau Formation | Pennsylvanian | 429 |
| *Paxillitriletes midas* | Alstätte Embayment, German-Dutch border | Kuhfeld Formation | Cretaceous | 419 |
| Megaspores | Wülfrath, Germany | - | late Early to early Late Cretaceous | 422 |
| *Dijkstraisporites helios* | Wülfrath, Germany | - | late Early to early Late Cretaceous | 418 |
| Scolecodont | Gotland, Sweden | Högklint Formation | Silurian | 428 |
| *Chuaria circularis* | Rampura, India | Suket Shale, Vindhyan Supergroup | Early Mesoproterozoic | - |

include e.g. solid state $^{13}C$ NMR and FTIR, both of which are used to reveal information on various carbon environment presents. Pyrolysis and chemolysis are both destructive methods that can be used to reveal detailed molecular information about the specific building blocks. As both the destructive and non-destructive methods can yield biased results, a combination of these techniques has been applied in the present study, as this will provide greater insight into the composition of the biomacromolecules under investigation (van Bergen, 2004).

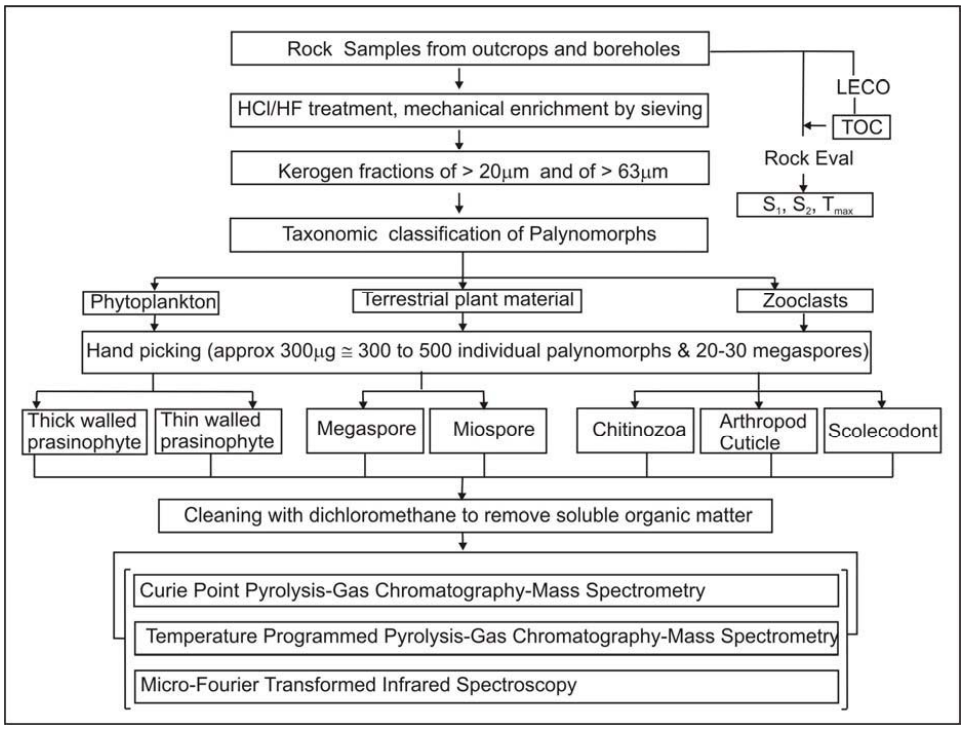


**Figure 1.2.** Flow chart depicting different analytical steps applied in this study.

*1.4.1. Light and scanning electron microscopy*

Transmitted light microscopy is commonly used to examine the morphology of the fossils mounted on glass slides, as well as for determining the diversity of the assemblages. Scanning electron microscopy (SEM) of microfossils permits us to study details of surface sculpture or ornaments or even the wall structure in fractured specimens. A detailed account on microscopic investigations of prasinophytes and chitinozoans (of present study) is being carried out by R. Brocke at Forschungsinstitut Senckenberg, Germany and of spores and scolecodonts by C. Hartkopf-Fröder at Geologischer Dienst Nordrhein-Westfalen, Krefeld, Germany.

*1.4.2. Rock-Eval Pyrolysis*

Rock Eval Pyrolysis is used to identify the type and maturity of kerogen. The data produced from a Rock Eval Pyrolysis are 1) the amount of free hydrocarbons; 2) the amount of hydrocarbons generated through thermal cracking of non-volatile organic matter; 3) the amount of $CO_2$ produced during pyrolysis of kerogen; and 4) the temperature at which the

maximum release of hydrocarbons from cracking of kerogen occurs during pyrolysis. $T_{max}$ is an indication of the stage of maturation of the organic matter.

For the present study, a first characterisation of finely disseminated organic material was performed using a Rock-Eval, Delsi II, pyrolyzer (Espitalié, 1977). Small amounts (~100 mg) of the powdered rock samples were pyrolysed with a specific time/temperature program in an inert helium atmosphere. The following temperature and time intervals correspond to the flame ionisation detected hydrocarbon amounts, expressed as $S_1$ and $S_2$ peaks, respectively:

$S_1$ – isothermal 300°C during 3 min.: volatilisation of soluble organic matter (liquid hydrocarbons)

$S_2$ – constant heating rate of 25°C/min from 300° up to 550°C: hydrocarbons derived solely from the cracking of the residual organic matter (kerogen)

In this study, the $CO_2$ content coming from the cracking of kerogen ($S_3$-peak) is not taken into consideration, because of the early decomposition of carbonate minerals below the $CO_2$ trapping temperature of 390°C, due to mineral matrix effects. This produces additional $CO_2$, which leads at least to overestimated oxygen indices (Katz, 1983). All values are means of double determinations and have been calibrated on an international standard distributed by the Institute Francaise du Pétrole (IFP 55000).

*1.4.3. Pyrolysis-gas chromatography-mass spectrometry*

The term “Pyrolysis” (Greek: pyros = fire and lyso = decompose) is in general the breaking apart of large molecules into smaller ones using only thermal energy. The way a large molecule behaves at elevated temperature is dependent on the relative strengths of the bonds which hold the molecule together. It is essential to recognise that a large molecule will break apart in a characteristic way, and that another sample of the same material heated to the same temperature will behave exactly the same way, making an analysis of the degradation products a reproducible way to study the original macromolecule.

The application of pyrolysis-gas chromatography-mass spectrometry (Py-GC-MS) provides an effective means of evaluating molecular preservation, especially for structural biopolymers in organic-walled fossils (van Bergen et al., 1993; 2004 and references therein). Using only minimal amounts of fossil material, the analysis of pyrolysis products allows for the inference of the original composition and structure of ancient macromolecules preserved in the specimens.

This analytical technique is being used from the 19$^{th}$ century when Williams (1862, see Tsuge, 1995) reported the formation of isoprene and dipentene during the heating of natural rubber. Various methods of analytical pyrolysis are used, and they are broadly described as

confined pyrolysis, which can be hydrous or anhydrous and flash pyrolysis which employs rapid heating of the samples, normally in an inert atmosphere. The products released upon flash pyrolysis can be collected separately (off-line) and studied using various separation and identification techniques. Alternatively, the pyrolysis products can be transferred directly (on-line) into a GC (Py-GC), or the source of a MS (Py-MS). Advances in analytical pyrolysis in the second half of the last century have closely paralleled the developments in GC and MS (see Tsuge, 1995). The use of flash pyrolysis increased dramatically with the introduction of the fused silica GC column. The crucial feature of flash pyrolysis is the need to achieve rapid and highly reproducible heating rates and final temperatures. Three main modes of heating are now employed: inductive (Curie-point), resistive (filament) and micro-furnace, the first two methods being the more widely used. The Curie-point method, in which a ferromagnetic sample holder is placed in a high-frequency induction coil, attracted the attention of many researchers in the field of analytical pyrolysis (Tsuge, 1995). Depending on the alloy of metal used, when it reaches a characteristic temperature (the Curie-point of that metal) no more current can be induced, so that the temperature stops at that point. With increasing temperature the permeability of ferromagnetic materials decreases. At the Curie-point temperature the relative permeability of the sample carrier falls suddenly and the status changes instantaneously from ferromagnetic to paramagnetic. The Curie-point device was first introduced in 1964 (Giacabbo and Simon, 1964 cited in Tsuge, 1995). In 1966, Simon and co-workers (cited in Tsuge, 1995) reported the first directly coupled Py-GC-MS system using a Curie-point pyrolyzer, a metal capillary column GC, and a rapid scanning MS. Curie-point pyrolysis-GC-MS is an especially valuable analytical tool in applications where sample amount is limited to microgram quantities of heterogeneous or polymeric substances often not amenable to analysis by conventional, wet- chemical methods (Stankiewicz et al., 1998). Experimental conditions of the pyrolytic studies have been specifically mentioned in of the each following chapters.

*1.4.4. Micro-Fourier transform infrared (FTIR) spectroscopy*

Infrared spectroscopy is the absorption measurement of different IR frequencies by a sample positioned in the path of an IR beam. The main goal of IR spectroscopic analysis is to determine the chemical functional groups in the sample. Different functional groups absorb characteristic frequencies of IR radiation. Micro-Fourier transform infrared (FTIR) spectroscopy has been used in the present study to analyse a single organic–walled micro fossil. Experimental conditions of infrared spectroscopic study have been specifically mentioned in the respective chapter.

**1.5. References**


Arouri, K., Greenwood, P F., Walter, M.R, 1999. A possible chlorophycean affinity of some Neoproterozoic acritarchs. Organic Geochemistry 30, 1323-1337.

Arouri, K., Greenwood, P F., Walter, M.R., 2000. Biological affinities of Neoproterozoic acritarchs from Australia: microscopic and chemical characterisation. Organic Geochemistry 31, 75-89.

van Bergen, P.F., Collinson, M.E., de Leeuw, J.W., 1993. Chemical composition and ultrastructure of fossil and extant salvinialean microspore massulae and megaspores. Grana Suppl. 1, 18-30.

van Bergen, P.F., Goñi, M., Collinson, M.E., Barrie, P.J., Sinninghe Damsté, J.S., de Leeuw, J.W., 1994. Chemical and microscopic characterization of outer seed coats of fossils and extant water plants. Geochimica et Cosmochima Acta 58, 3823-3844.

van Bergen, P.F., Blokker, P., Collinson, M.E., Sinninghe Damsté, J.P., de Leeuw, J.W., 2004. Structural biomacromolecules in plants: what can be learnt from the fossil records? In: Hemesly, A.R., Poole, I. (Eds.), Evolution of Plant Physiology, Elsevier, Amsterdam, pp. 133-154.

Bertrand, R., Héroux, Y., 1987. Chitinozoan, graptolite and scolecodont reflectance as an alternative to vitrinite and pyrobitumen reflectance in Ordovician and Silurian strata, Anticosti Island, Quebec, Canada. AAPG Bulletin 71, 951-957.

Blokker, P., 2000. Structural analysis of resistant polymers in extant algae and ancient sediments. Geologica Ultraiectina 193, pp. 145

Blokker, P., van Bergen, P.F., Pancost, R., Collinson, M.E., de Leeuw, J.W., Sinninghe Damsté, J.S., 2001. The chemical structure of *Gloeocapsomorpha prisca* microfossils: Implications for their origin. Geochimica et Cosmochima Acta 65, 885-900.

Bordenave, M.L., Espitalié, J., Leplat, P., Oudin, J.L., Vandenbrouke, M., 1993. Screening techniques for source rock evaluation. In: Bordenave, M.L. (Ed.), Applied petroleum geochemistry, pp. 217-278.

Bradbury, S., 1967. The evolution of the microscope; Pergamon Press, New York, pp. 375.

Brocks, J.J., Love, G.D., Summons, R.E., Knoll A.H., Logan G.A., Bowden, S.A., 2005. Biomarker evidence for green and purple sulfur bacteria in an intensely stratified Paleoproterozoic sea. Nature 437, 866-870.

Brocks, J., Shaw, G., 1968. Chemical structure of the exine of pollen walls and a new function for cartenoids in nature. Nature 219, 532-533.

Conway-Moris, S., 1979. Middle Cambrian polychaetes from the Burgess Shale of British Columbia. Philos. Trans. R. Soc. Lond. B 285, 227-274.

Derenne, S., Metzger, P., Largeau, C., Bergen, P.F.V., Gatellier, J.P., Sinninghe Damsté, J.S., de Leeuw, J.W., Berkaloff, C., 1992. Similar morphological and chemical variations of *Gloeocapsomorpha prisca* in Ordovician sediments and cultured *Botryococcus braunii* as a response to changes in salinity. Organic Geochemistry 19, 299-313.

Eichwald, E., 1854. Die Grauwackenschichten von Live- und Esthland. Bulletin de la Société Impériale des Naturalistes de Moscou 27, 1-11.

Eisenack, A., 1930. Neue Mikrofossilien des baltischens Silurs (Vorläufige Mitteilung). Die Naturwissenschaften 18, 180-181.

Erriksson, M.E., Bergman, C.F., Jeppsson, L., 2004. Silurian scolecodonts. Review of Palaeobotany and Palynology 131, 269-300.

Espitalié, J., Laporte, J.L., Madec, M., Marquis, F., Leplat, P., Paulet, J., Boutefeu, A., 1977. Méthode Rapide de Charactérisation des Roches Mères de leur Potentiel Pétrolier et de leur Degré d´Évolution. Revue de L´Insitut Francais du Pétrole 32, 23-42.

Evitt, W.R., 1963. A discussion and proposals concerning fossil dianoflagellates, hytrichospheres and acritarchs. Proceedings of the national Academy of Sciences 49, 158-164.

Foster, C.B., Stephenson, M.H., Marshall, C., Logan, G.A., Greenwood, P.F., 2002. A revision of *Reduviasporonites* Wilson 1962: description, illustration, comparison and biological affinities. Palynology 26, 35-58.

Greenwood, P.F., Arouri, K.R., George, S.C., 2000. Tricyclic terpenoid composition of *Tasmanites* kerogen as determined by pyrolysis GC-MS. Geochimica et Cosmochimica Acta 64, 1249-1263.

Guilford, W.J., Schneider, D.M., Labovitz, J., Opella, S. J., 1988. High resolution solid state $^{13}C$ NMR spectroscopy of sporopollenins from different plant taxa. Plant physiology 86, 134-136.

Hayatsu, R., Botto, R.E., Mc Beth, R.L., Scott, R.G., Winans R.E., 1988. Chemical alteration of a biological polymer "sporopollenin" during coalification: Origin, formation, and transformation of the coal maceral sporinite. Energy & Fuels 2, 843-847.

Hemesly, A.R., Barrie, P.J., Chaloner, W.G., Scott, A.C., 1993. The composition of sporopollenin and its use in living and fossil plant systematics. Grana Suppl. 1, 2-11.

Hemesly, A.R., Scott, A.C., Barrie, P.J., Chaloner, W.G., 1996. Studies of fossil and modern spore wall biomacromolecules using $^{13}C$ solid-state NMR. Annals of Botany 78, 83-94.

Herminghaus, S., Gubatz, S., Arendt, S., Wiermann, R., 1988. The occurrence of phenols as degradation products of natural sporopollenin – a comparison with 'synthetic sporopollenin'. Zeitscrift Naturforschung 43c, 491-500.

Hinde, G.J., 1879. On annelid jaws from the Cambro-Silurian, Silurian and Devonian Formation in Canada and from the Lower Carboniferous in Scotland. Quaterley Journal of the Geological Society of London 35, 370-389.

Jansonius, J., McGregor, D.C., 1996. Chapter 1. Introduction; In: Jansonius, J., McGregor, D.C. (Eds.), Palynology: principles and applications; American Association of Stratigraphic Palynologists Foundation, vol. 1, pp. 1-10.

Katz, B.J., 1983. Limitations of "Rock-Eval" pyrolysis for typing organic matter. Organic Geochemistry 4, 195-199.

Kjellstrom, G., 1968. Remarks on the chemistry and ultrastructure of the cell wall of some Paleozoic leiospheres. Geol. Foreningens Stockholm Forhandl. 90, 221-228.

Lécuyer, C., Paris, F., 1997. Variability of the $\delta^{13}C$ of lower Paleozoic palynomorphs: implications for the interpretation of ancient marine sediments. Chemical Geology 138, 161-170.

Marshall, C.P., Javaux, E.J., Knoll, A.H., Walter, M.R., 2005. Combined micro-Fourier transform infrared (FTIR) spectroscopy and micro-Raman spectroscopy of Proterozoic acritarchs: A new approach to Palaeobiology. Precambrian Research 138, 208-224.

Miller, M.A., 1996. Chitinozoa, In : Jansonius, J., McGregor, D.C., (Eds.), Palynology: principles and applications; American Association of Stratigraphic Palynologist Foundation. Vol. 1, pp. 307-336.

Moldowan, J.M., Talyzina, N.M., 1998. Biogeochemical evidences for dinoflagellate ancestors in the Early Cambrian. Science 281, 1168-1170.

Mösle, B., Collinson, M., Finch, P., Stankiewicz, B.A., Scott, A.C., Wilson, R., 1998. Factors influencing the preservation of plant cuticles: a comparison of morphology and chemical composition of modern and fossil examples. Organic Geochemistry 29, 1369-1380.

Paris, F., Grahn, Y., Nestor, V., Lakova, I., 1999. A revised chitinozoan classification. Journal of Paleontology 73, 549-570.

Paris, F., Nõlvak, J., 1999. Biological interpretation and palaeodiversity of a cryptic fossil group: the "chitinozoan animal". Geobios 32, 315-324.

Philp, R.P., Gilbert, T.D., Russell, N.J., 1982. Characterisation by pyrolysis-gas chromatography- mass spectrometry of the insoluble organic residues derived from the hydrogenation of *Tasmanites* sp. oil shale. Fuel 61, 221-226.

Raistrick, A., 1934. The correlation of coal-seams by microspore-contant: Part 1. The seams of Northumberland. Transactions of the federated Institution of Mining Engineers 88, 142-153, 259-264.

Saxby, J.D., 1970. Isolation of kerogen in sediments by chemical methods. Chemical Geology 6, 173.

Schenck, P.A., de Leeuw, J.W., van Grass, G., Haverkamp, J., Bouman, M., 1981. Analysis of recent spores and pollen and of thermally altered sporopollenin by flash pyrolysis-mass spectrometry and flash pyrolysis-gas chromatograpy-mass spectrometry. In: Brooks, J. (Ed.), Organic maturation studies and fossil fuel exploration. Academic Press, London, New York, pp. 225-237.

Servais, T., Wellman, C., 2004. New directions in Palaeozoic palynology. Review of Palaeobotany and Palynology 130, 1-15.

Shaw, G., 1971. The chemistry of sporopollenin. In: Brocks, J., Grant, P., Muir, M.D., Shaw, G., van Gijzel, P. (Eds.), Sporopollenin, Academic Press, London, pp. 305-350.

Stankiewicz, B.A., Briggs, D.E.G., Evershed, R.P., 1997. Chemical composition of Paleozoic and Mesozoic fossil invertebrate cuticles as revealed by pyrolysis-gas chromatography/mass spectrometry. Energy and Fuels 11, 515-521

Stankiewicz, B.A., van Bergen, P.F., Smith, M.B., Carter, J.F., Briggs, D.E.G., Evershed, R.P., 1998. Comparison of the analytical performance of filament and Curie-point pyrolysis devices. Journal of Analytical and Applied Pyrolysis 45, 133-151.

Stankiewicz, B.A., Briggs, D.E.G., Michels, R., Collinson, M.E., Flannery, M.B., Evershed, R. P., 2000. Alternative origin of aliphatic polymer in kerogen. Geology 28, 559-562.

Stout, S.A., 1993. Lasers in organic petrology and organic geochemistry. II. In situ laser micropyrolysis-GCMS of coal macerals. International Journal of Coal Geology 24, 309-331.

Szaniawski, H., 1996. Chapter 12. Scolecodonts; In: Jansonius, J., McGregor, D.C. (Eds.), Palynology: principles and applications; American Association of Stratigraphic Palynologists Foundation, vol. 1, pp. 337-354.

Talyzina, N.M., Moldowan, J.M., Johannisson, A., Fago, F.J., 2000. Affinites of Early Cambrian acritarchs studied by using microscopy, fluorescence flow cytometry and biomarkers. Review of Paleobotany and Palynology 108, 37-53.

Tegelaar, E.W., de Leeuw, J.W., Derenne, S., Largeau, C., 1989. A reappraisal of kerogen formation. Geochimica et Cosmochimica Acta 53, 3103-3106.

Tissot, B.P., Welte, D.H., 1984. Petroleum formation and occurrence. Springer, Berlin, pp. 699.

Tricker, P.M., Marshall, J.E.A., Badman, T.D., 1992. Chitinozoan reflectance: a lower Paleozoic thermal maturity indicator. Marine and Petroleum Geology 9, 302-307.

Tsuge, S., 1995. Analytical pyrolysis-past, present and future. Journal of Analytical and Applied Pyrolysis 32, 1-6.

Versteegh, G.J.M., Blokker, P., 2004. Resistant macromolecules of extant and fossil microalgae. Phycological Research 52, 325-339.

Versteegh, G.J.M., Blokker, P., Wood, G., Collinson, M.E., Sinninghe Damsté, J.S., de Leeuw, J.W., 2004. An example of oxidative polymerization of unsaturated fatty acids as a preservation pathway for dinoflagellate organic matter. Organic Geochemistry 35, 1129-1139.

Wehling, K., Niester, C., Boon, J.J., Willemse, M.T.M., Wiermann, R., 1989. *p*-Coumaric acid – a monomer in the sporopollenin skeleton. Planta 179, 376-380.

# CHAPTER 2

## Molecular Composition of Upper Silurian/Lower Devonian *Tasmanites* and *Leiosphaeridia* (Dadas Formation, SE Turkey)

**Abstract**

**Extraordinarily well-preserved *Tasmanites* and *Leiosphaeridia* prasinophytes from a new Silurian-Devonian sedimentary sequence in South-East Turkey were handpicked from different stratigraphic levels, cleaned and analysed by Curie point pyrolysis-gas chromatography-mass spectrometry. Tricyclic terpenoids in the pyrolysates (e.g., mono and diunsaturated terpenes and monoaromatics) were detected from the genus *Leiosphaeridia,* but not from the genus *Tasmanites.* These results suggest that an inherent source-biomarker relationship between taxa of *Tasmanites* and tricyclic terpenoids may not always exist. Moreover, the detection of tricyclic terpenoid compounds from *Leiosphaeridia* indicates these pyrolysis products are not exclusive to the genus *Tasmanites.***

### 2.1. Introduction

Organic-walled acid-resistant *Tasmanites* microfossils known to occur from the Precambrian throughout the Phanerozoic, have been a long time interest of palynologists. Specimens of *Tasmanites* were first described by Hooker in 1852 as possible lycopod seed cases (see Mendelson, 1993), but in a significant report published in 1875 Newton erected the genus *Tasmanites*, named after the Permian oil shales of Tasmania in which they occurred in high abundance. They were initially thought to be some sort of spore, but Schopf et al. (1944) and Eisenack (1958) later suggested they might be of algal origin. Today, they are generally regarded as phycomata of prasinophyte algae (e.g., Tappan, 1980). Morphological characteristics identified by transmitted light, scanning electron and transmission electron microscope studies, suggest similarities between the *Tasmanites* and the living green alga *Pachysphaera* (Wall, 1962; Tappan, 1980; Guy-Ohlson and Boalch, 1992; Guy-Ohlson, 1996).

Molecular characterisation of Tasmanite oil shales have frequently shown high abundances of tricyclic terpenoids which were soon believed to be biomarkers diagnostic of the *Tasmanites*

phycomata (Philp et al., 1982; Simoneit et al., 1990, 2005; Aquino Neto et al., 1992; Azevedo et al., 1990, 1994, 1995; Revill et al., 1994; Greenwood and George, 1999). Further evidence to support this precursor-biomarker relationship was provided by laser micropyrolysis-gas chromatography/mass spectrometry of isolated *Tasmanites* (Greenwood et al., 2000). Products of this analysis included $C_{19}$-$C_{28}$ tricyclic terpanes, including 13-methyl, 14-alkylpodocarpanes, a $C_{19}$ monoaromatic hydrocarbon and $C_{19}$-$C_{21}$ tricyclic terpenes. The tricyclic terpenoid composition of the kerogen and extractable organic fractions of Tasmanite oil shales typically comprise saturated, unsaturated and aromatic tricyclic hydrocarbons (e.g., Philp et al., 1982; Aquino Neto et al., 1992; Azevedo et al., 1995).

Not all of the analytical data obtained from tricyclic terpenoid products of Tasmanite oil shales has been entirely consistent with their derivation from a *Tasmanites*/algal source. Carbon isotopic values of the extractable tricyclic terpanes from Tasmanite oil shale revealed an isotopic enrichment compared to co-occurring *n*-alkanes (Simoneit et al., 1993; Revill et al., 1994). Simoneit et al. (1993) suggested the divergence of this isotopic data may be due to different sources with the tricyclic compounds deriving from an isoprene pool and the alkanes from the algeanan part of the same organism. In accounting for the isotopic anomaly, Revill et al. (1994) similarly suggested that the *n*-alkanes were derived from thermal cracking of algal aliphatic biopolymer whereas the tricyclic terpenoids were derived from other sources, whilst also emphasizing that tricyclic compounds have been identified in a wide range of sediments and petroleum and not just those associated with high *Tasmanites* content. Furthermore, the *Tasmanites* rich palynomorph fraction obtained from the Lower Cambrian Lükti Formation in Estonia showed few tricyclic terpanes on pyrolysis GC-MS analysis (Talyzina et al., 2000). De Grande et al. (1993) reported prominent tricyclic terpanes in saline lacustrine and marine carbonate environments, indicating that the precursor organisms lived in a moderate salinity conditions, but Peters (2000) suggested caution is needed during these interpretations as tricyclic terpanes are thermally more stable than many other terpanes and these biomarkers are commonly abundant in mature petroleum, regardless of source-rock organic matter origin (see Peters and Moldowan, 1993). Recently, Kranendonck (2004) analysed the saturated fraction extracted from shale horizons of the Fetlika-1 core (including several rich in *Tasmanites*) by GC/MS and found little evidence of $C_{19}$ to $C_{29}$ tricyclic hydrocarbons, but high abundances of hopanes and steranes were observed. Farrimond et al. (1999), similarly pointed out that tricyclic compounds have been detected in an extremely wide range of sediments and oils of different ages, suggesting additional

sources must exist. Data from a larger range of *Tasmanites* related OM reflecting different localities and a range of palaeoenvironments need to be studied.

The present study aims to further investigate the *Tasmanites*-tricyclics (source-product) relationship by assessing the tricyclic terpenoid composition of extremely well preserved *Tasmanites* (Fig. 2.1a, 2.1b) fossils recovered from Silurian/Devonian rocks of the Dadas Formation, SE Turkey. The interpretation of biomarkers detected in soluble organic matter from total rock samples might be ambiguous, with sources from other microfossils, or non-indigenous bitumen by migrated soluble organic matter or with contamination from anthropogenic or other contaminant sources a possibility. To minimise the chance of misinterpretations, the current analyses were performed on handpicked individual microfossils which are taxonomically well assigned. These organic-walled, acid-resistant microfossils have been analysed by Curie point pyrolysis-gas chromatography-mass spectrometry (Cupy-GC-MS). The molecular composition of co-occurring specimens of *Leiosphaeridia* (Fig. 2.1e, 2.1f) has also been investigated. In general, both genera *Leiosphaeridia* and *Tasmanites,* are assigned to prasinophycean algae (Wall, 1962; Tappan, 1980; Guy-Ohlson, 1996), although leiosphaerids are a subject of some considerable taxonomic confusion (see Colbath and Grenfell, 1995).

### 2.2. Samples and preparation

For the present study, specimens of *Tasmanites* and *Leiosphaeridia* were obtained from rocks close to the Silurian/Devonian boundary of the Dadas Formation (a shallow borehole, Hazro area, South-East Turkey). These microfossils and their host sedimentary environment have suffered low thermal conditions (Rock-Eval $T_{max}$ = 430°C; Kranendonck, 2004), similar to the low thermal maturity ($T_{max}$ = 444°C) of Latrobe Tasmanite oil shale in Australia (Revill et al., 1994). Diagnostic morphological features like radial pores or canals, confirms the identity of the genus *Tasmanites*. Their overall morphological appearance (i.e., thick walled phycomata) is in accordance to other geographically unrelated *Tasmanites*. The wall thickness of Turkish *Tasmanites* is comparatively higher than that of Tasmanian *Tasmanites*. Specimens assigned to the genus *Leiosphaeridia* are comparatively thin walled and have no pores or canals. Based on morphological criteria, the genus *Leiosphaeridia* shows similarities with extant prasinophycean alga *Halosphaera* (Wall, 1962; Mendelson, 1993; Strother, 1996).

The present Upper Silurian/Lower Devonian sedimentary sequences characterised by both fine-grained siliciclastic and calcareous sediments were deposited in a marine shoreline

environment that belonged to a pericontinental shelf platform adjacent to the northern margin of Gondwana (Kranendonck, 2004). The sediments of Tasmanian oil shale were deposited in a shallow marine environment associated with cold waters and seasonal sea-ice cover (e.g. Banks and Clarke, 1987; Revill et al., 1994).

Organic residues were isolated from the sedimentary rock matrix by using HF and HCl and water filtration. No oxidising agents were used as they can alter the colour and chemical composition of the organic residues (Saxby, 1970). The organic residue has been separated into two fractions of bigger than 10 μm and bigger than 63 μm. For each analysis, about 300 to 500 individual microfossils were selectively handpicked from the larger fractions, under a stereomicroscope. Altogether 17 samples have been analysed. In order to avoid any misinterpretations due to compositional mixing by signals from other microfossils, we have exclusively used hand picked palynomorphs which have taxonomically been well assigned. Prior to chemical investigations, these palynomorphs were cleaned several times with dichloromethane to remove free hydrocarbons For comparative purposes, Late Carboniferous to Early Permian *Tasmanites* (Fig. 2.1c, 2.1d) isolated from the Latrobe Tasmanite oil shale (Tasmania, Australia; Greenwood et al., 2000) have also been studied using the exact same analytical protocols.

### 2.3. Experimental

Samples were pyrolysed at 650°C for 10 s using a Curie-point pyrolyser (Pyromat) coupled directly to a HP gas chromatography-mass spectrometer (Cupy-GC-MS) system (Model No: HP GC/MS 5973). The GC was operated in the splitless mode and was equipped with a 50 m SGE BPX5 fused silica capillary column with an inner diameter of 220 μm and film thickness of 0.25 μm. An initial oven temperature of 50°C was held for 2 min, and then heated with 10°C $min^{-1}$ to 310°C. The oven was then maintained isothermally for 12 min. Carrier gas was helium. MS parameters included 70 eV EI ionisation, a source temperature of 230ºC and a mass range of 30-550 dalton. Peak assignments were based on GC retention time and mass spectral data including comparison to MS libraries. Full scan analyses were carried out at GSG Mess-und Analysengeräte GmbH, Bruchsal, Germany.

SIM analyses were carried out at Department of Applied Chemistry, Curtin University of Technology, Australia. Both Tasmanite oil shale and *Tasmanites* from SE Turkey were pyrolysed

at 550°C for 10 s. Conditions for the GC system were as follows: splitless injection onto a 50 m DB5 column with an initial oven temperature of 40°C held for 2 min, then heated with 4°C $min^{-1}$

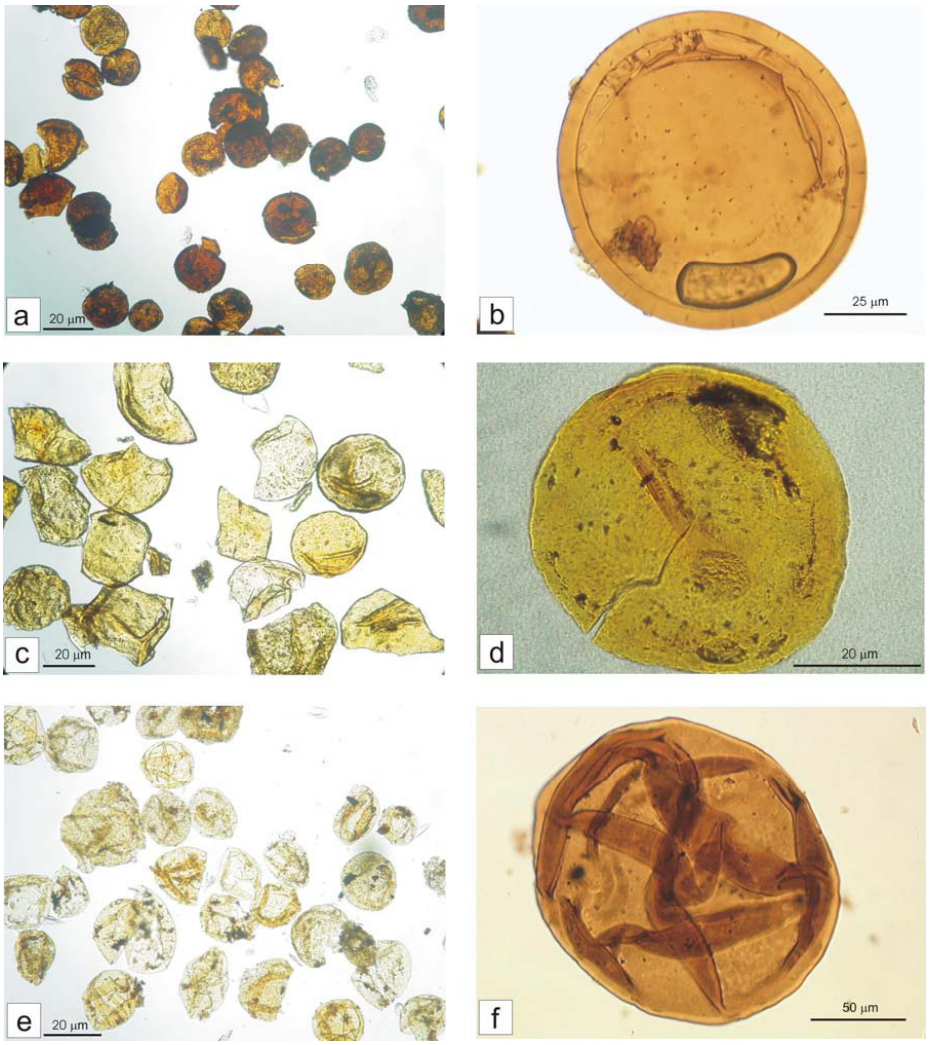


**Figure 2.1.** Photomicrographs of palynomorphs. (a) handpicked *Tasmanites* palynomorphs from the Dadas Formation in lower magnification; (b) Magnified view of single *Tasmanites* from the Dadas Formation; (c) Handpicked *Tasmanites* palynomorphs from Tasmania in lower magnification; (d) Magnified view of single *Tasmanites* from Tasmania; (e) Handpicked *Leiosphaeridia* palynomorphs from the Dadas Formation in lower magnification; (f) Magnified view of single *Leiosphaeridia* from the Dadas Formation.

to 300°C. The oven was then maintained isothermally for 15 min. Inner diameter of the column was 250 μm and film thickness was 0.25 μm. Carrier gas was helium. Mass Spectrometric acquisition was conducted on a 5970 MSD system. Dwell times were 65 μs for cycle time of ~1.4/s.

### 2.4. Results and discussion

#### *2.4.1. Py-GC-MS analysis of Tasmanites*

The total ion chromatogram obtained by Cupy-GC-MS of the *Tasmanites* from Turkey is shown in Figure 2.2. The pyrolysates predominantly consist of *n*-alkane/alkene doublets ranging

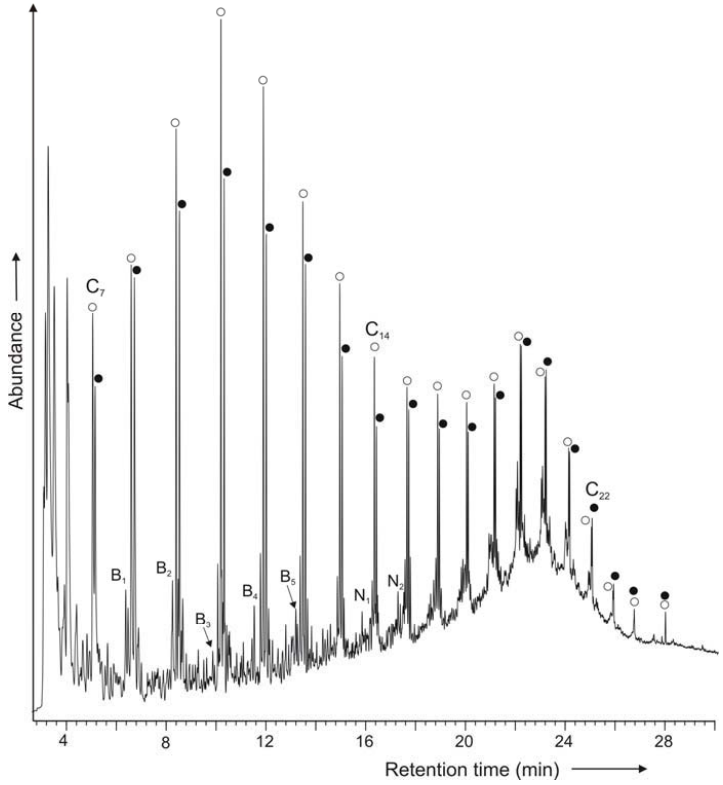


**Figure 2.2.** Total ion chromatogram resulting from Curie point pyrolysis-GC-MS of *Tasmanites* from the Dadas Formation, SE Turkey. Each doublet corresponds to an alkene (○) and an alkane (●); selected C-numbers are indicated. B and N indicate alkylbenzenes and alkylnaphthalenes respectively and their subscripts indicate total number of methyl groups.

from $C_6$ to at least $C_{22}$ in a distribution typical of algaenan, the microbiological resistant algal biopolymer (Hatcher and Clifford, 1997). Lower abundances of aromatic hydrocarbons such as

alkylbenzenes, alkylnaphthalenes and alkylphenanthrenes are also detected. A low relative concentration of these aromatic compounds is also a common feature of algaenan (e.g. Derenne et al., 1992a). The alkylated aromatic products probably derive from biological precursors although pyrolysis-induced aromatisation processes can contribute to the abundance of simple polycyclic hydrocarbons (see Larter and Horsfield, 1993). Significantly, no tricyclic terpenoids were detected in the pyrolysates from the Turkish *Tasmanites*. Similar pyrolysis distributions comprising prominent *n*-alkane/alkene doublets and devoid of tricyclic terpenoids were observed from *Tasmanites* collected from several stratigraphic horizons at either side of the

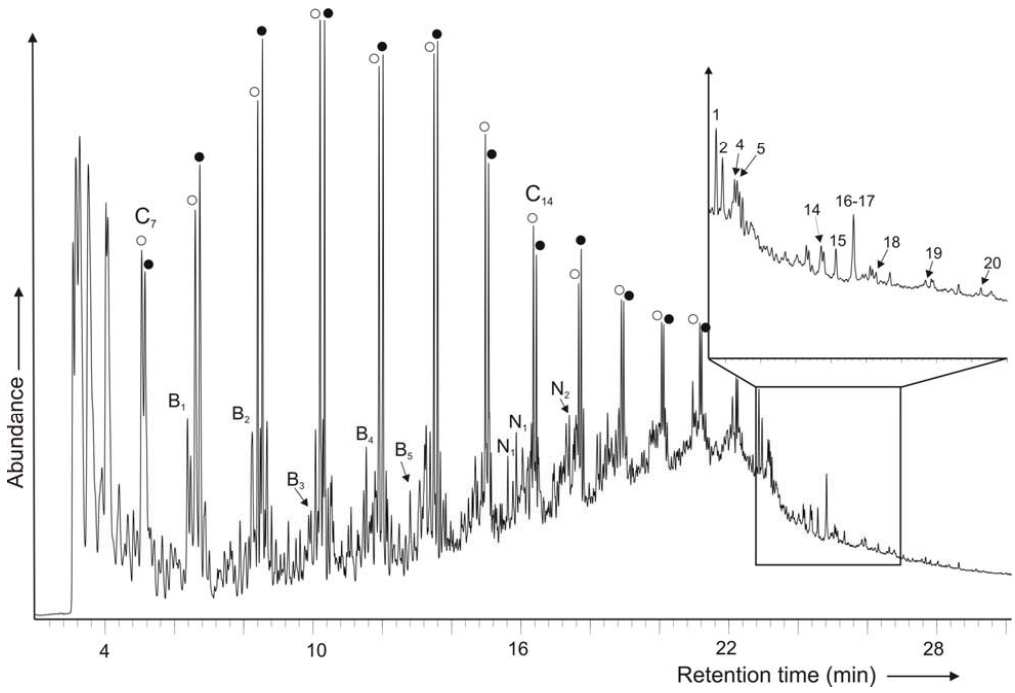


**Figure 2.3.** Total ion chromatogram resulting from Curie point pyrolysis-GC-MS of *Tasmanites* from Tasmania, Australia. Each doublet corresponds to an alkene (○) and an alkane (●); selected C-numbers are indicated. The assigned peaks are listed in Table 2.1. B and N indicate alkylbenzenes and alkylnaphthalenes respectively and their subscripts indicate total number of methyl groups attached.

Silurian/Devonian boundary. The corresponding analysis of Tasmanian *Tasmanites* showed similarly abundant *n*-alkane/alkene profiles from $C_6$ to at least $C_{22}$ (Fig. 2.3) and several tricyclic terpenoidal compounds were observed from this sample and these are listed among other detected

products in Table 2.1. The consistency of this data to previous analyses of these same type of *Tasmanites* (Greenwood et al., 1998, 2000) confirms the integrity of the present analysis. It can therefore be concluded that the Turkish *Tasmanites* contain no tricyclic terpenoidal structures, or are below the detection limits of the Cupy-GC-MS approach.

*2.4.2. Py-GC-MS analysis of Leiosphaeridia*

The total ion chromatogram obtained from the pyrolysis GC-MS of the *Leiosphaeridia* specimens is shown in Figure 2.4. These pyrolysates reflect similar *n*-alkane/alkene doublets ($C_6$ to at least $C_{22}$ with maximum at $C_{10}/C_{11}$) and alkylaromoatic distributions to those observed from

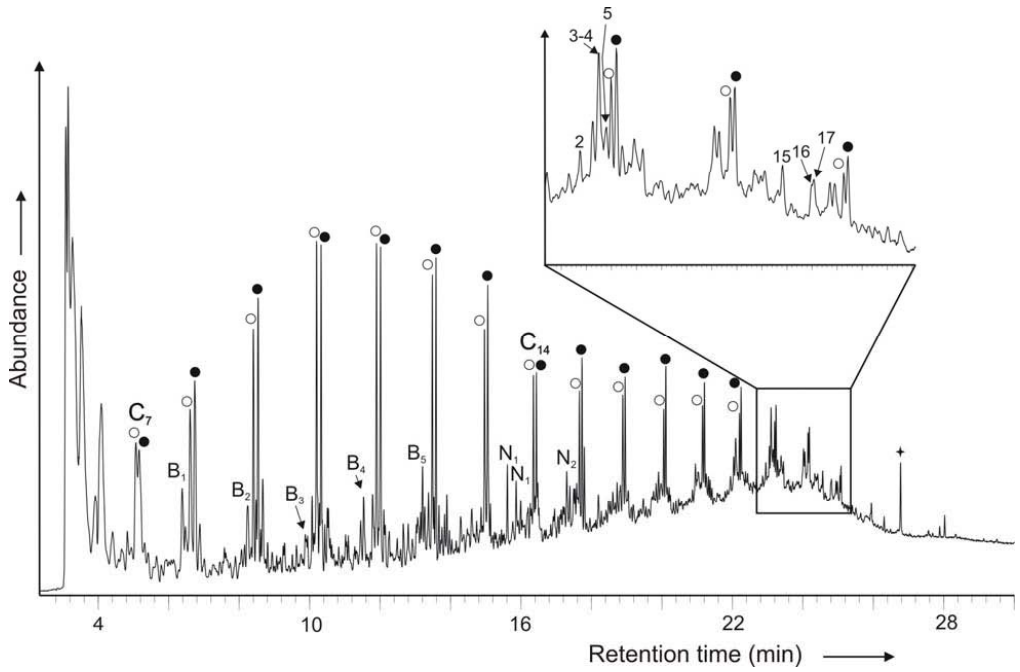


**Figure 2.4.** Total ion chromatogram resulting from Curie point pyrolysis-GC-MS of *Leiosphaeridia* from the Dadas Formation, SE Turkey. Each doublet corresponds to an alkene (○) and an alkane (●); selected C-numbers are indicated. The assigned peaks are listed in Table 2.1. B and N indicate alkylbenzenes and alkylnaphthalenes respectively and their subscripts indicate total number of methyl groups attached. ✦ indicates contaminant.

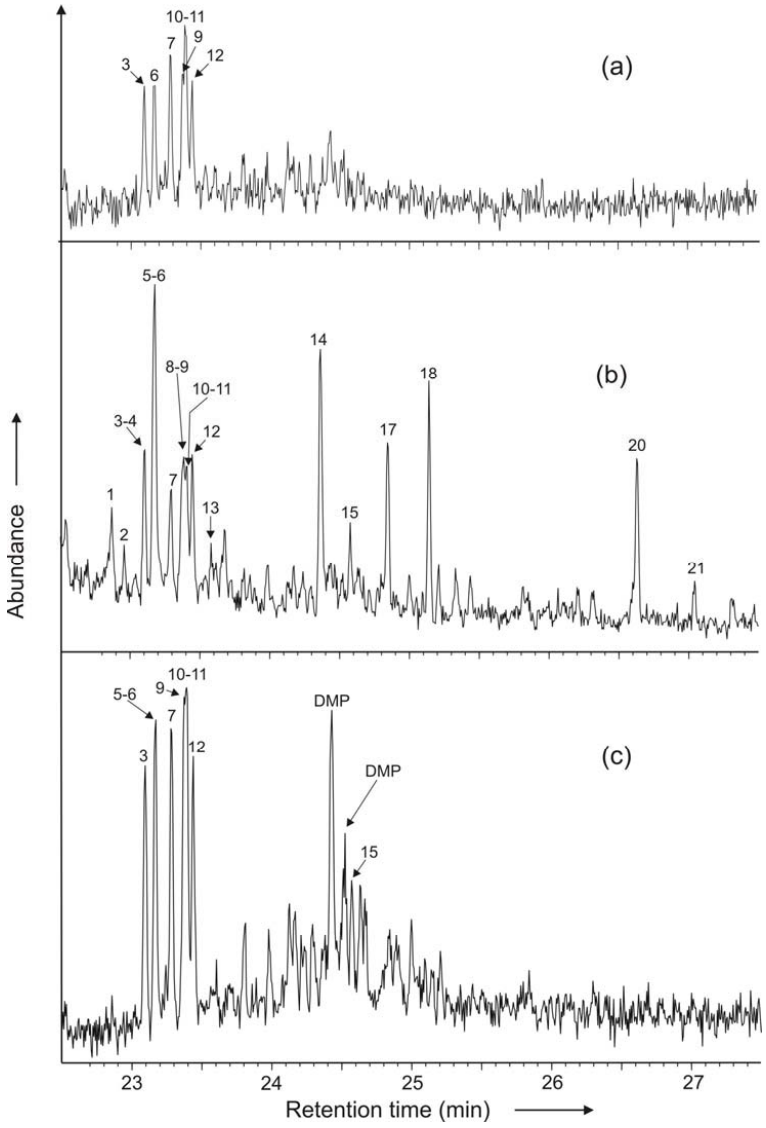


**Figure 2.5.** Partial mass chromatograms at *m/z* 191 from the Curie point pyrolysis-GC-MS analysis of (a) *Tasmanites* from SE Turkey; (b) *Tasmanites* from Tasmania and (c) *Leiosphaeridia* from SE Turkey. The assigned peaks are listed in Table 2.1; DMP indicates $C_2$ phenanthrene.

the *Tasmanites*. However, the products from this palynomorph also include relatively low concentrations of mono- and di-unsaturated tricyclic terpenes and ring-C monoaromatic tricyclic terpanes. No saturated tricyclic terpanes were detected. The mass spectra of tricyclic and other

terpenoids typically show an abundant *m/z* 191 ion which can be used to selectively highlight these products from more complex full scan data. The reconstructed *m/z* 191 chromatogram from full scan analysis of Turkish *Tasmanites*, Tasmanian *Tasmanites* and Turkish *Leiosphaeridia* are shown in Figure 2.5. The Tasmanian *Tasmanites* data comprises the characteristic $C_{19}$-$C_{24}$ tricyclic terpenoid

**Table 2.1.** Tricyclic terpenoids from pyrolysis-GC-MS analyses of *Tasmanites* and *Leiosphaeridia*. Coeluting methylphenanthrenes, methylanthracenes and alkylbenzene are also identified.

| Peak | Product |
|---|---|
| 1 | $C_{19}$ 13ß(H) tricyclic terpane |
| 2 | $C_{19}$ monounsaturated tricyclic terpene |
| 3 | 3-methylphenanthrene |
| 4 | $C_{18}$ monoaromatic tricyclic terpane |
| 5 | $C_{19}$ monounsaturated tricyclic terpene |
| 6 | 2-methylphenanthrene |
| 7 | 2-methylanthracene |
| 8 | $C_{19}$ tricyclic terpane |
| 9 | $C_{13}$ alkylbenzene |
| 10 | 9-methylphenanthrene |
| 11 | 1-methylanthracene |
| 12 | 1-methylphenanthrene |
| 13 | $C_{19}$ tricyclic terpane |
| 14 | $C_{20}$ tricyclic terpane |
| 15 | $C_{20}$ monounsaturated tricyclic terpene |
| 16 | $C_{20}$ diunsaturated tricyclic terpene |
| 17 | $C_{19}$ monoaromatic tricyclic terpane |
| 18 | $C_{21}$ tricyclic terpane |
| 19 | $C_{20}$ monoaromatic tricyclic terpane |
| 20 | $C_{23}$ tricyclic terpane |
| 21 | $C_{24}$ tricyclic terpane |

(Fig. 2.5b; Table 2.1) distribution typical of this sample (Philp et al., 1982; Greenwood et al., 2000). The $C_{22}$ tricyclic terpane is of low relative abundance because of the thermodynamic instability of the C-22 methyl substituent of the isoprenoid side chain (Aquino Neto et al., 1983; Ekweozor and Strausz, 1983). The *m/z* 191 mass chromatogram also shows peaks attributed to methylphenanthrenes, methylanthracenes and $C_{13}$-alkylbenzene. These aromatics were the only

products evident in the *m/z* 191 chromatogram of the Turkish *Tasmanites* (Fig. 2.5a). The Cupy-GC-MS analysis of *Leiosphaeridia*, on the other hand, also showed $C_{19}$ and $C_{20}$ monounsaturated and $C_{20}$ diunsaturated tricyclic terpenes in low abundance (Fig. 2.4; Fig. 2.6(c)-e)). Respective parent ion chromatograms can be used to identify tricyclic products of different carbon number or unsaturation. The *m/z* 260 chromatogram (Fig. 2.6c) shows two unsaturated $C_{19}$ tricyclic isomers in the *Leiosphaeridia* data; and the *m/z* 272 chromatogram a $C_{20}$ diunsaturated tricyclic terpene (Fig. 2.6d). These compounds are also found in Tasmanian *Tasmanites* (Fig. 2.3; Fig. 2.7 (a)-(e)), but they have not been detected for Turkish *Tasmanites* (Fig. 2.8(a)-(e)), They are present in Tasmanite oil shale (Fig. 2.9(a)-(e)).

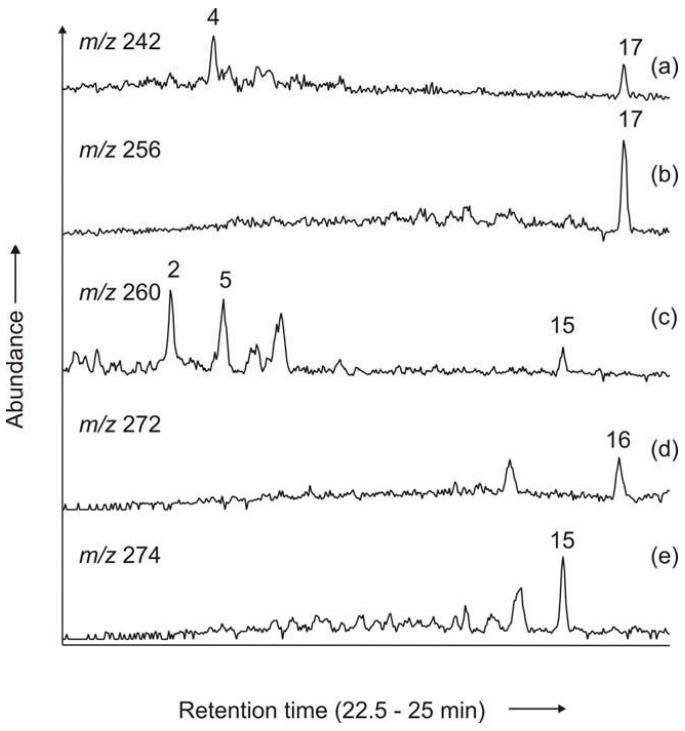


**Figure 2.6.** Partial mass chromatograms from the Curie point pyrolysis-GC-MS analysis of *Leiosphaeridia* from SE Turkey at (a) *m/z* 242; (b) *m/z* 256; (c) *m/z* 260; (d) *m/z* 272; (e) *m/z* 274. The assigned peaks are listed in Table 2.1.

To enhance sensitivity, selective ion acquisition mode of mass spectral detection was carried out, but no aromatic and/or unsaturated tricyclic terpenoids were detected (Fig. 2.10(a)-(c)) from *Tasmanites* of Turkey. Philp et al. (1982) and Greenwood et el. (2000) recognised several

tricyclic terpenes in their pyrolytic studies of Tasmanite oil shale including the same $C_{19}$ and $C_{20}$ monounsaturated and $C_{20}$ diunsaturated tricyclic terpenes detected here in the pyrolysates of *Leiosphaeridia*. These tricyclic terpene pyrolysates can be distinguished on the basis of mass spectra from the tricyclic terp-(9,11)-enes and terp-(13,14)-enes series previously identified (Azevedo et al., 1995) in the extractable fraction of the Tasmanite oil shale. Structural interpretation of mass spectrometric data, including delineation of probable location of unsaturation have already been discussed in detail (Greenwood et al. 2000). $C_{18}$ and $C_{19}$ ring-C monoaromatic tricyclic terpanes are both observed in the pyrolysates of *Leiosphaeridia* (Fig. 2.6(a)-(b)).

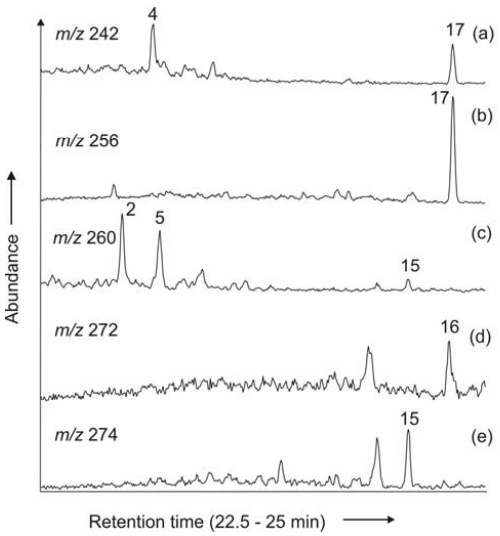


**Figure 2.7.** Partial mass chromatograms from the Curie point pyrolysis-GC-MS analysis of *Tasmanites* from Tasmania at (a) *m/z* 242; (b) *m/z* 256; (c) *m/z* 260; (d) *m/z* 272; (e) *m/z* 274. The assigned peaks are listed in Table 2.1.

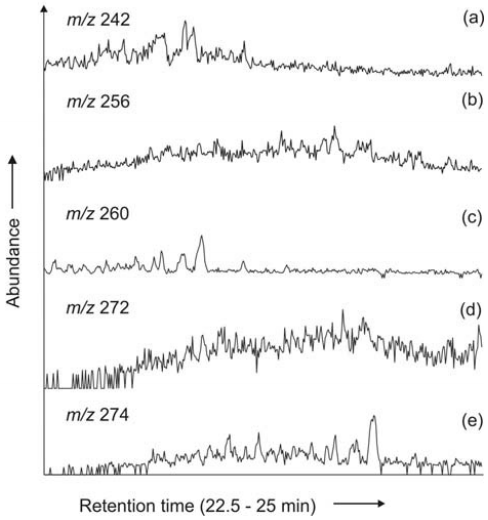


**Figure 2.8.** Partial mass chromatograms from the Curie point pyrolysis-GC-MS analysis of *Tasmanites* from SE Turkey at (a) *m/z* 242; (b) *m/z* 256; (c) *m/z* 260; (d) *m/z* 272; (e) *m/z* 274.

Cupy-GC-MS of the Tasmanian *Tasmanites* both in this study (Fig. 2.3) and previously (e.g., Philp et al., 1982; Greenwood et al., 2000) has similarly shown $C_{18}$-$C_{20}$ ring-C monoaromatic tricyclic terpanes. Monoaromatic tricyclic compounds have also been observed in the extractable fraction of Tasmanite oil shale (Azevedo et al., 1990, 1992; Boreham and Wilkins, 1995). The presence of monoaromatic and unsaturated tricyclic compounds in these immature palynomorphs

suggests the biological precursors of the tricyclic terpenoids may be aromatic in nature. Azevedo et al. (1992) reported the occurrence of aromatic tricyclic terpane series with high concentrations from the immature Tasmanite oil shale suggesting 'early diagenetic or possibly even *in vivo*' generation of these compounds.

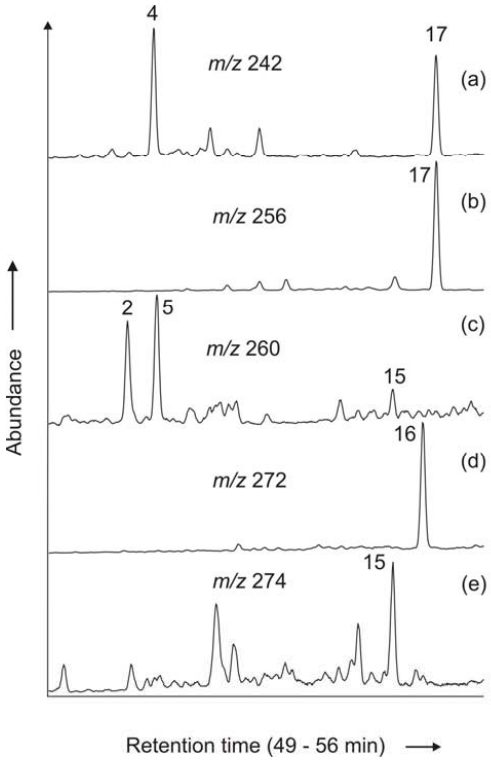


**Figure 2.9.** Partial mass chromatograms (SIM analysis) from the pyroprobe pyrolysis-GC-MS analysis of Tasmanite oil shale at (a) *m/z* 242; (b) *m/z* 256; (c) *m/z* 260; (d) *m/z* 272; (e) *m/z* 274. The assigned peaks are listed in Table 2.1.

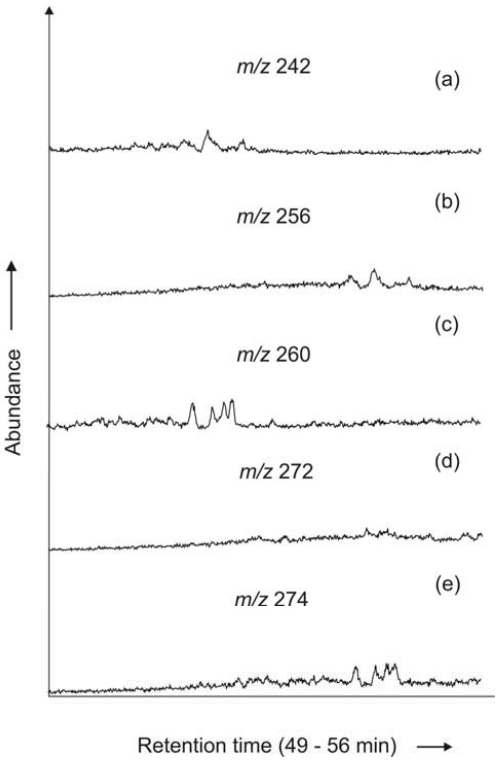


**Figure 2.10.** Partial mass chromatograms (SIM analysis) from the pyroprob pyrolysis-GC-MS analysis of *Tasmanites* from SE Turkey at (a) *m/z* 242; (b) *m/z* 256; (c) *m/z* 260; (d) *m/z* 272; (e) *m/z* 274.

The present pyrolysis study provides little indication of the true precursor of the tricyclic compounds. Aquino Neto et al. (1982) postulated that the regular tricyclic terpane series might have originated from the cyclization of regular hexaprenol which occur in the lipid of archaebacteria. Very recently, Simoneit et al. (2005) carried out Raney nickel

reduction/desulphurization experiments on the polar bitumen fractions from the Latrobe sample (enriched with *Tasmanites*) which shows the dominance of $C_{23}$, $C_{39}$ and $C_{40}$ tricyclic terpenoids and *n*-alkanes ranging from $C_{15}$ to $C_{35}$ and proposed $C_{40}$ head-to-tail acyclic polyprenol (regular octaprenol) is a potential precursor of the tricyclic compounds. Considering the occurrences of these biomarkers in a wide range of sediments and petroleum, it is possible that there are multiple precursors which may yield tricyclic compounds during diagenetic processes.

Talyzina et al. (2000) carried out pyrolysis of the low-fluorescent fraction of palynomorphs enriched in *Leiosphaeridia* (75% of total fraction) and detected $C_{27}$-$C_{29}$ steranes with the $C_{29}$ steranes the most predominant of these. However, no steranes were observed in the present pyrolysis of *Leiosphaeridia.* As stated earlier, leiosphaerids are a subject of considerable taxonomic confusion (Martin, 1993; Colbath and Grenfell, 1995). Leiosphaerids have been compared with prasinophycean green algae (Wall, 1962; Tappan, 1980; Guy-Ohlson, 1996), alete spores (Chaloner and Orbell, 1971) and dinoflagellates (Butterfield and Rainbird, 1998). Strother (1996) proposed that some species of *Leiosphaeridia* may be prasinophytes, but these microfossils may have a wide variety of natural affinities and sources. So, it is possible that all morphotypes of *Leiosphaeridia* will not show similar chemical signatures upon pyrolysis. The predominance of *n*-aliphatic pyrolysates of the presently studied *Leiosphaeridia* is consistent with the highly aliphatic nature and algal affinity.

The apparent absence of any tricyclic terpenoids in the Turkish *Tasmanites* is noteworthy. This result supports Kranendonck's (2004) observations that only very low (sometimes undetectable) concentrations of tricyclic terpanes may be associated with some *Tasmanites*. Furthermore, the closely related palynomorph *Leiosphaeridia* can represent an alternative source of sedimentary tricyclic terpenoids. Talyzina et al. (2000) similarly suggested that trace levels of the compounds might be attributable to amorphous kerogen containing bacterial or algal remains. The detection of tricyclic products from *Leiosphaeridia* support the likelihood of a wide range of sources of tricyclic terpenoids consistent with their detection in a wide range of sediments and oils of different ages (Farrimond et al., 1999).

However, several factors (e.g., thermal maturity, paleo-environment, geological time difference) may affect the chemical composition of the *Tasmanites* microfossils. As mentioned above, the sedimentary environment of the Dadas Formation has suffered low thermal conditions (Rock Eval $T_{max}$ = 430°C; Kranendonck, 2004), similar to the low thermal maturity ($T_{max}$ =

444°C) of Latrobe Tasmanite oil shale (Revill et al., 1994). Moreover, detection of tricyclic biomarkers by analytical pyrolysis of *Leiosphaeridia,* recovered from the same stratigraphic horizon suggests that thermal maturity is not responsible for the absence of these terpenoids compounds in Turkish *Tasmanites*. Although, the geographically unrelated *Tasmanites* were recovered from a shallow marine environment, other localised paleo-environmental factors (e.g., water salinity) may account for their different chemical signatures. Derenne et al. (1992b) observed the growth of extant algae *Botryococcus braunii* in a media of different salinity and noticed the morphology of the alga shifted from "open" to "closed" type with increasing salinity. The chemical composition of the cell walls of the extant algae was also observed to change with salinity. As stated earlier, the wall thickness of Turkish *Tasmanites* is comparatively higher than that of Tasmanian *Tasmanites*. The salinity characteristics of the two geographically unrelated *Tasmanites* are not known but may be a factor in their different wall thickness and tricyclic terpenoid compositions. Tasmanian *Tasmanites* are of Late Carboniferous to Early Permian age, while Turkish *Tasmanites* have been recovered from the Silurian/Devonian boundary. It is also possible that the modest age difference of the palynomorphs leads to chemical changes whilst not significantly altering their morphologies. This issue will be better understood by establishing a database comprising molecular data from *Tasmanites* reflecting a wide range of paleo-environments and- geological times.

### 2.5. Conclusions

1. The highly aliphatic nature (i.e., predominance of *n*-aliphatic pyrolysates) of the *Tasmanites* and *Leiosphaeridia* from Turkey is typical of algal kerogen.
2. An absence of tricyclic terpenoids in pyrolysates from the Turkish *Tasmanites* reflects that an inherent source-biomarker relationship between the *Tasmanites* and tricyclic terpenoids does not always exist.
3. Furthermore, tricyclic terpenoid pyrolysates of the *Leiosphaeridia* confirms that there are more than one biological source(s) of these biomarkers and they are not exclusively from or always diagnostic of *Tasmanites*.

**Acknowledgements**

This research is part of the “Silurian-Devonian Boundary Project” within the DFG Priority Programme SPP 1054 “Evolution of the System Earth During the Late Palaeozoic clues from Sediment Geochemistry”. This project is also related to IGCP Project 499, “Devonian Land-Sea Interactions: Evolution of Ecosystems and Climate (DEVEC)”. We would like to thank Deutsche Forschungsgemeinschaft (DFG), Bonn (grants no. Ma 1861/2 and /4; Br 1943/3-1 and /2) for financial support. S.D. thanks Prof. G. Schleser for continuous interest and support of these studies. For technical assistance, we thank U. Disko, W. Benders, F. Leistner and H. Willsch. O. Kranendonck first recognised the significant occurrences of *Tasmanites* in Fetlika-1 sediments. The authors are grateful to Prof. B. R. T. Simoneit and an anonymous reviewer for their valuable comments on an earlier version of this paper. Support during fieldwork by TPAO (Türkiye Petrolleri Anonim Ortakliği), Ankara, is gratefully acknowledged.

## 2.6. References


Aquino Neto, F.R., Restle, A., Connan, J., Albrecht, P., Ourisson, G., 1982. Novel tricyclic terpanes ($C_{19}$, $C_{20}$) in sediments and petroleums. Tetrahedron Letters 23, 2027-2030.

Aquino Neto, F.R., Trendel, J.M., Restle, A., Connan, J., Albrecht, P.A., 1983. Occurrence and formation of tricyclic and tetracyclic terpanes in sediments and petroleums. In: Bjorøy, M. et al. (Eds.), Advances in Organic Geochemistry 1981. Wiley, Chichester, pp. 659-667.

Aquino Neto, F.R., Trigüis, J., Azevedo, D.A., Rodrigues, R., Simoneit, B.R.T., 1992. Organic geochemistry of geographically unrelated tasmanites. Organic Geochemistry 18, 791-803.

Azevedo, D.A., Aquino Neto, F.R., Simoneit, B.R.T., 1990. Mass spectrometric characteristics of a novel series of ring-C monoaromatic tricyclic terpanes found in Tasmanian tasmanite. Organic Mass Spectrometry 25, 475-480.

Azevedo, D.A., Aquino Neto, F.R., Simoneit, B.R.T., Pinto, A.C., 1992. Novel series of tricyclic aromatic terpanes characterized in Tasmanian tasmanite. Organic Geochemistry 18, 9-16.

Azevedo, D.A., Aquino Neto, F.R., Simoneit, B.R.T., 1994. Extended saturated and monoaromatic tricyclic terpenoid carboxylic acids found in Tasmanian tasmanite. Organic Geochemistry 22, 991-1004.

Azevedo, D.A., Aquino Neto, F.R., Simoneit, B.R.T., 1995. Mass spectrometric characteristics of two novel series of ring- C monounsaturated tricyclic terpenes found in Tasmanian tasmanite. Journal of Mass Spectrometry 30, 247-256.

Banks, M.R., Clarke, M.J., 1987. Changes in the geography of the Tasmania Basin in the late Paleozoic. In: McKenzie, G.D. (Ed.) Gondwana Six: Stratigraphy, Sedimentology and Paleontology, 41. American Geophysical Union, Geophysics Monograph, pp. 1-14.

Boreham, C.J., Wilkins, A.L., 1995. Structure and origin of the two major monoaromatic hydrocarbons in Tasmanite oil shale from Tasmania, Australia. Organic Geochemistry 23, 461-466.

Butterfield, N.J., Rainbird, R.H., 1998. Diverse organic-walled fossils, including 'possible dinoflagellates', from the early Neoproterozoic of arctic Canada. Geology 26, 963-966.

Chaloner, W.G., Orbell, G., 1971. A palaeobiological definition of sporopollenin. In: Brooks, J. et al. (Eds.), Sporopollenin. Academic Press, London. pp. 273-294.

Colbath, G.K., Grenfell, H.R., 1995. Review of biological affinities of Paleozoic acid-resistant, organic walled eukaryotic algal microfossils (including "acritarchs"). Review of Paleobotany and Palynology 86, 287-314.

De Grande, S.M.B., Aquino Neto, F.R., Mello, M.R., 1993. Extended tricyclic terpanes in sediments and petroleum. Organic Geochemistry 20, 1039-1047.

Derenne, S., Largeau, C., Berkaloff, C., Rousseau, B., Wilheim, C., Hatcher, P., 1992a. Non-hydrolysable macro-molecular constituents from outer walls of *Chlorella fusca* and *Nanochlorum eucaryotum*. Phytochemistry 31, 1923-1929.

Derenne, S., Metzger, P., Largeau, C., Bergen, P.F.V., Gatellier, J.P., Sinninghe Damsté, J.S., de Leeuw, J.W., Berkaloff, C., 1992b. Similar morphological and chemical variations of *Gloeocapsomorpha prisca* in Ordovician sediments and cultured *Botryococcus braunii* as a response to changes in salinity. Organic Geochemistry 19, 299-313.

Eisenack, A., 1958. *Tasmanites* Newton 1875 und *Leiosphaeridia* n.g. als Gattungen den Hystrichosphaeridia. Palaeontographica, Abteilung A. Paläozoologie 110, 1-19.

Ekweozor, C.M., Strausz, O.P., 1983. Tricyclic terpanes in the Athabasca Oil Sands: Their geochemistry. In: Bjorøy, M. et al. (Eds.), Advances in Organic Geochemistry 1981. Wiley, Chichester, pp. 746-766.

Farrimond, P., Bevan, J.C., Bishop, A.N., 1999. Tricyclic terpane maturity parameters: response to heating by an igneous intrusion. Organic Geochemistry 30, 1011-1019.

Greenwood, P.F., George, S.C., 1999. Mass spectral characteristics of $C_{19}$ and $C_{20}$ tricyclic terpanes detected in Latrobe Tasmanite oil shale. European Journal of Mass Spectrometry 5, 221-230.

Greenwood, P.F., George, S.C., Hall, K., 1998. Applications of laser micropyrolysis-gas chromatography-mass spectrometry. Organic Geochemistry 29, 1075-1089.

Greenwood, P.F., Arouri, K.R., George, S.C., 2000. Tricyclic terpenoid composition of *Tasmanites* kerogen as determined by pyrolysis GC-MS. Geochimica et Cosmochimica Acta 64, 1249-1263.

Guy-Ohlson, D., 1996. Prasinophycean algae. In: Jansonius, J., McGregor, D.C. (Eds.), Palynology: Principles and Applications. American Association of Stratigraphic Palynologist Foundation-1. pp. 181-189.

Guy-Ohlson, D., Boalch, G.T., 1992. Comparative morphology of the genus *Tasmanites* (Pterospermales, Chlorophyta). Phycologia 31, 523-528.

Hatcher, P.G. and Clifford, D.J., 1997. The organic geochemistry of coal: from plant materials to coal. Organic Geochemistry 27, 251-274.

Kranendonck, O., 2004. Geo- and biodynamic evolution during Late Silurian to Early Devonian time (Hazro Area, SE Turkey). Schriften des Forschungszentrum Jülich, Reihe Umwelt/Environment 49, pp. 268.

Larter, S.R., Horsfield, B., 1993. Determination of structural components of kerogens by the use of analytical pyrolysis methods. In: Engel, M.H, Macko, S.A. (Eds.), Organic Geochemistry. Plenum Press, pp. 271-288.

Martin, F., 1993. Acritarchs Review: a review. Biological Reviews. Cambridge, Philosophical Society 68, 475-538.

Mendelson, C.V., 1993. Acritarchs and prasinophytes. In: Lipps, J.H. (Ed.), Fossil Prokaryotes and Protist. Blackwell, Boston, pp. 77-104.

Newton, E.T., 1875. On 'Tasmanite' and Australian 'White coal' Geological Magazine 12, 337-342.

Peters, K.E., 2000. Petroleum tricyclic terpanes: predicted physicochemical behaviour from molecular mechanics calculations. Organic Geochemistry 31, 497-507.

Peters, K.E., Moldowan, J.M., 1993. The Biomarker Guide: Interpreting Molecular Fossils in Petroleum and Ancient Sediments. Prentice-Hall, Englewood Cliffs, New Jersey, p. 363.

Philp, R.P., Gilbert, T.D., Russell, N.J., 1982. Characterisation by pyrolysis-gas chromatography- mass spectrometry of the insoluble organic residues derived from the hydrogenation of *Tasmanites* sp. oil shale. Fuel 61, 221-226.

Revill, A.T., Volkman, J.K., O'Leary, T., Summons, R.E., Boreham, C.J., Banks, M.R., Denwar, K., 1994. Hydrocarbon biomarkers, thermal maturity and depositional setting of tasmanite oil shales from Tasmania, Australia. Geochimica et Cosmochimica Acta 58, 3803-3822.

Saxby, J.D., 1970. Isolation of kerogen in sediments by chemical methods. Chemical Geology 6, 173.

Schopf, J.M., Wilson, L.R., Bentall, R., 1944. An annotated synopsis of Paleozoic fossil spores and the definition of generic groups. Illinois State Geological Survey Report of Investigations 91, 1-72.

Simoneit, B.R.T., Leif, R.N., Aquino Neto, F.R., Azevedo, D.A., Pinto, A.C., Albrecht, P., 1990. On the presence of tricyclic terpane hydrocarbons in Permian tasmanite algae. Naturwissenschaften 77, 380-383.

Simoneit, B.R.T., Schoell, M., Dias, R.F., Aquino Neto, F.R., 1993. Unusual carbon isotope compositions of biomarker hydrocarbons in a Permian tasmanite. Geochimica et Cosmochimica Acta 57, 4205-4211.

Simoneit, B.R.T., McCaffrey, M.A., Schoell, M., 2005. Tasmanian tasmanite: II – compound specific isotope analyses of kerogen oxidation and Raney Ni reduction products. Organic Geochemistry 36, 399-404.

Strother, P.K., 1996. Acritarchs. In: Jansonius, J., McGregor, D.C. (Eds.), Palynology: Principles and Applications. American Association of Stratigraphic Palynologist Foundation-1, pp. 81-106.

Talyzina, N.M., Moldowan, J.M., Johannisson, A., Fago, F.J., 2000. Affinities of Early Cambrian acritarchs studied by using microscopy, fluorescence flow cytometry and biomarkers. Review of Paleobotany and Palynology 108, 37-53.

Tappan, H., 1980. The Paleobiology of Plant Protists. Freeman, San Francisco, CA.

Wall, D., 1962. Evidence from recent plankton regarding the biological affinities of *Tasmanites* Newton 1875 and *Leiosphaeridia* Eisenack 1958. Geological Magazine 99, 353-362.

# CHAPTER 3

## Molecular composition of Upper Silurian Chitinozoa from the Dadas Formation, SE Turkey as revealed by spectroscopic and pyrolytic investigations

**Abstract**

**Extraordinarily well-preserved chitinozoans from an Upper Silurian sedimentary sequence in South-East Turkey were recovered from different depth levels, handpicked from the palynological residues, cleaned and analysed by micro-FTIR and Curie point pyrolysis-gas chromatography-mass spectrometry. Handpicked chitinozoans were predominantly represented by the genera *Bursachitina, Cingulochitina, Ancyrochitina* and *Pterochitina*. Both spectroscopic and pyrolytic investigations suggest that biomacromolecules of these Chitinozoa consist of both aliphatic and aromatic moieties. The micro-FTIR spectra of Chitinozoa are characterised by aliphatic $CH_x$ (3000-2800 and 1460-1450 $cm^{-1}$) and $CH_3$ (1375 $cm^{-1}$) absorptions and aromatic C=C (1560-1610 $cm^{-1}$) and CH (3050 $cm^{-1}$ and 700-900 $cm^{-1}$) absorptions. Major pyrolysis products from the Chitinozoa include both aromatic compounds such as akylbenzenes, alkylnaphthalenes, alkylphenols and alkylphenanthrenes and aliphatic hydrocarbons including a homologous series of *n*-alkene/*n*-alkane doublets. Aromatic compounds predominate over aliphatic compounds. 1,2,3,4-Tetramethylbenzene is the most abundant pyrolysis product of the studied Chitinozoa. No pyrolysis products diagnostic of chitin were detected in the present study and it is concluded that the original biomacromolecules of Chitinozoa before fossilization were not made up of chitin.**

### 3.1. Introduction

Chitinozoans represent a group of organic walled microfossils (OWM), which lived in the marine realm from the Early Ordovician to at least the Late Devonian (Paris et al., 1999). They reached their greatest diversity during the Silurian (Paris and Nõlvak, 1999). Chitinozoans are extensively used as biostratigraphic and palaeobiogeographical index fossils of Lower and Middle Paleozoic sequences. Chitinozoans also offer promising applications in the field of organic-petrography, for instance by measuring the reflectance of their vesicle wall so that the thermal maturity of the host rock can be assessed. This is especially important

for pre-Devonian sediments where the organic remains from higher plants are absent or very rare (see Obermajer et al., 1996 and references therein). Chitinozoans appear exclusively in marine sediments and have been assigned to Protozoa (e.g., foraminifers, ciliates), various Metazoa (e.g., eggs of annelids, graptolites), algae or even fungi (see references in Miller, 1996). More recently, chitinozoans are assigned to ontogenetic vesicles ("eggs") of unknown soft-bodied organisms (Paris and Nõlvak, 1999). Eisenack (1931) established this group of palynomorphs for the first time and classified them by morphological criteria. He believed that they were chitinous remains of animals and therefore created the name by linking the terms "chitin" and "zoa". Chitin was not identified from the Ordovician Chitinozoa *Cyathochitina campanulaeformis* (Voss-Foucart and Jeuniaux, 1972) by using an enzymatic method. Later, Bailey (1981), using pyrolysis-gas chromatography, concluded that Chitinozoa chemistry is similar to that of wood and gas-prone biogeomacromolecules. However, the chemical nature of the vesicle wall of these extinct organisms has never been elucidated in detail. It was speculated that the vesicle wall of these microfossils consists of scleroprotein (Lacquin, 1981) or polysaccharide-protein (Mierzejewski, 1981). Thus, this study presents for the first time a detailed report on molecular composition of these cryptic fossils using micro-FTIR and pyrolysis-gas chromatography-mass spectrometry.

### 3.2. Geological setting

For the present study, specimens of Chitinozoa were obtained from rocks of three depth levels of the Upper Silurian part the Dadas Formation (Fetlika-1 borehole, Hazro area, South-East Turkey). The generalised stratigraphy and lithological settings of the investigated sequences are shown in Figure 3.1. Sedimentation took place in the outer shelf environment under low energy conditions which led to the accumulation of very fine silt-sized mud settling out of a uniform suspension (Kranendonck, 2004). Occasionally, the sea floor was affected by storm driven currents, transporting coarse silts and brachiopod shells from the shallower environment into the offshore zone.

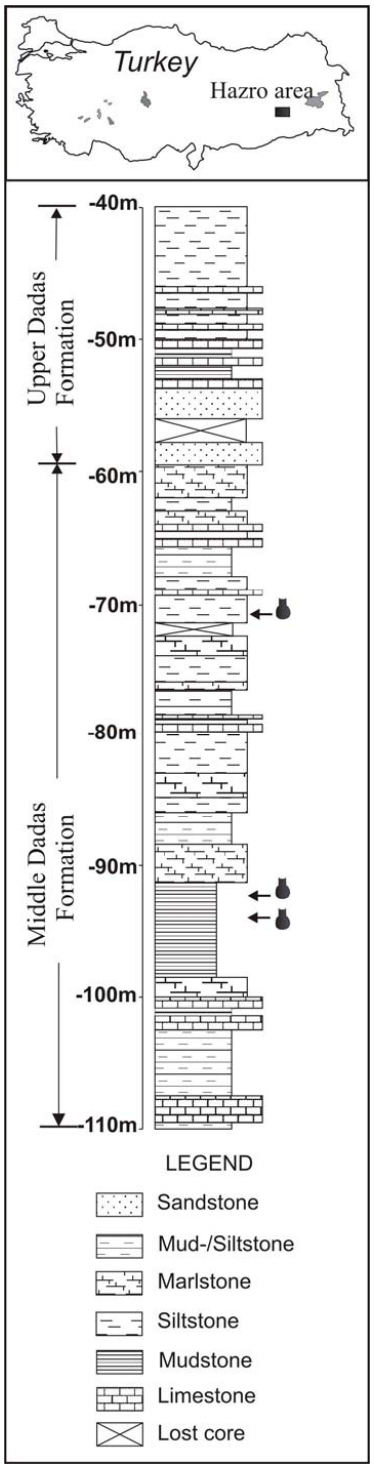


**Figure 3.1.** Stratigraphic column of the Fetlika-1 core between –110 m and –40 m (Dadas Formation) around Hazro area, SE Turkey. Sample positions in the core are indicated by arrows.

### 3.3. Experimental

*3.3.1. Samples and preparation*

Organic remains, including the organic walled microfossils and their host sedimentary environment have suffered low thermal alteration (Rock-Eval $T_{max} \approx 430°C$; Table 3.1). Due to low thermal maturity and the propitious depositional conditions, palynomorphs are extraordinarily well preserved, and hence suitable for combined palynological and organic geochemical studies. For the present paper the three core samples CFE-18, Fe1 PP-99 and Fe1 PP-101 from the Fetlika 1 borehole have been selected because of their primary comparatively high abundance of chitinozoan taxa. In general, analysed palynological assemblages from this borehole consist of different groups of marine OWM like acritarchs, prasinophytes, chitinozoans, scolecodonts and fragments of zooclasts (e.g., arthropods). The terrestrial derived OWM is very sparse in these assemblages and represented by very few spores, and occasionally by cuticles and tissues of land plants. Above all, comparatively thin-walled acritarchs and prasinophytes are prevailing. Chitinozoans occur in various frequency and diversity throughout the successions. They are thicker walled and thus when using the light microscope usually brownish to black or even opaque. Black colour and opaque specimens often results from pyrite inside the vesicles. Diagnostic internal structures, morphology and pyrite can be visualized only when applying inrafred (IR) video technique (Brocke & Wilde, 2001; Plate 3.1 this chapter). Figured chitinozan specimens of the genera *Bursachitina* Taugourdeau, 1966, *Calpichitina* Wilson and Hedlund, 1964, *Cingulochitina* Paris, 1981, *Pterochitina* Eisenack, 1955, *Ancyrochitina* Eisenack, 1955, and *Angochitina* Eisenack, 1931 (Plate 3.1) represents the most characteristic taxa from the three analysed samples. In addition, specimens of the genera *Urnochitina* Paris, 1981, cf. *Conochitina* Eisenack, 1931 emend. Paris, Grahn, Nestor, and Lakova, 1999, and cf. *Eisenackitina* Jansonius, 1964 occur in various frequencies.

Organic residues were isolated from the sedimentary rock matrix by using HF and HCl and water filtration. No oxidising agents were used as they do alter the colour and chemical composition of the organic residues (Saxby, 1970). The organic residue has been separated into two fractions (10-63 μm and >63 μm). For each analysis, about 300 to 500 individual chitinozoans were selectively handpicked from the larger fractions, under a stereomicroscope. In order to avoid any misinterpretations due to compositional mixing by signals from other microfossils (e.g., *Tasmanites*, *Leiosphaeridia,* see Dutta et al., 2006), we have exclusively used hand picked chitinozoans which have taxonomically been well assigned.

**Table 3.1.** Total organic carbon and Rock Eval data of Chitinozoa bearing sediments from the Dadas Formation, SE Turkey.

| Sample No. | Depth (m) | TOC | $S_1$ | $S_2$ | HI | $T_{max}$ (°C) |
|---|---|---|---|---|---|---|
| C Fe-18* | -72.70 | 0.81 | 0.22 | 1.75 | 215 | 429 |
| Fe1 PP-101 | -92.30 | 1.06 | 0.09 | 1.02 | 96 | 432 |
| Fe1 PP-99 | -94.00 | 1.07 | 0.11 | 1.42 | 133 | 433 |

*Data based on Kranendonck, 2004

Prior to chemical investigations, these palynomorphs were cleaned several times with dichloromethane to remove soluble organic compounds.

---

**Plate 3.1.** Photomicrographs of chitinozoans from the Dadas Formation (Fetlika 1 borehole, Dadas Formation, SE Turkey, Upper Silurian). Location by sample, slide number and England finder coordinates (E.F.) are indicated. Scales equal 20 µm. Pictured chitinozoan specimens by both, transmitted light microscopy (a) and using infrared (IR) video technique (b). SMB: slides stored in the collections of the Forschungsinstitut Senckenberg, Frankfurt am Main, Germany.
1a. *Cingulochitina* Paris, 1981; Fe1 PP-99; SMB 20865; E.F. O35-4.
1b. Same specimen in IR mode, showing operculum in situ, and carina at the margin of the chamber near at its base.
2a. *Pterochitina* Eisenack, 1955, Fe1 PP-99; SMB 20865; E.F. C 30-2. Spherical chamber remains opaque under transmitted light, thus internal structures and details are not visible. Membranous carina is incomplete (parts lost during the preparation).
2b. Same specimen in IR mode, showing operculum in situ and the membranous carina which is covering the chamber.
3a. *Ancyrochitina* Eisenack, 1955; Fe1 PP-99; SMB 20865; E.F. N52-3.
3b. Same specimen in IR mode, showing the internal plug (prosome) at the base of the neck. The chamber bears hollow and branched processes (incomplete) near at its base, and numerous more or less simple hairs and spines around the neck.
4a. *Bursachitina* Taugourdeau, 1966; Fe1 PP-99; SMB 20865; E.F. Q40-2. Specimen is comparatively thick-walled and thus opaque when using transmitted light microscope.
4b. Same specimen in IR mode, showing operculum at the base of the neck, and chamber with smooth to finely granulate ornamentation. Ruptures on the chamber are frequently observed in those specimens and are mainly caused by the preparation, indicating a generally rigid wall of this taxa.
5a. *Bursachitina* Taugourdeau, 1966; Fe1 PP-101; SMB 20866; E.F. Z30-4. Thick-walled specimen with discrete rim (mucron) at the apex.
5b. Same specimen in IR mode, showing operculum situated at the base of the neck, and chamber with a granulate ornamentation.
6a. *Angochitina* Eisenack, 1931; CFE-18; SMB 20867; E.F. U33. Specimen of this genus with numerous, evenly distributed spiny ornamentation.
6b. Same specimen in IR mode, showing prosome with several horizontal septa situated at the base of the neck.
7a. *Calpichitina* Wilson and Hedlund, 1964; CFE-18; SMB 20867; E.F. X38-2. Specimen of this genus with a smooth to finely granulate ornamentation of the outer layer of the chamber.
7b. Same specimen in IR mode, showing a discrete rim around aperture.
8a. *Cingulochitina* Paris, 1981; Fe1 PP-101; SMB 20866; E.F. W54-3. Chain of four individuals of this genus.
8b. Details of two individuals of this chain showing disk-like operculum and membranous extension (copula) at the apex when applying IR video microscopy.

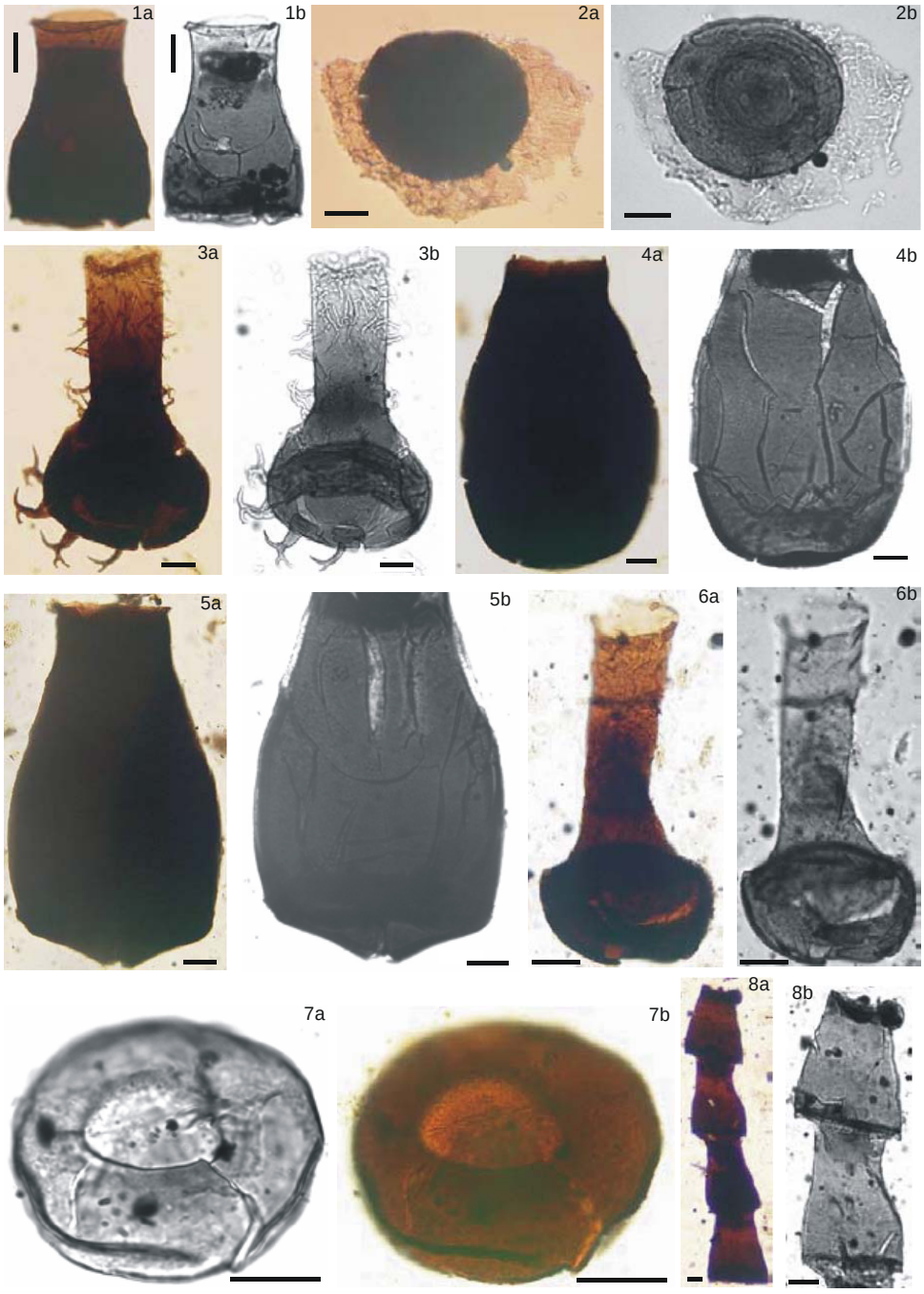


**Plate 3.1**

*3.3.2. Micro-FTIR spectroscopy*

Micro-FTIR spectroscopic analyses were performed in transmission mode using a Nic-Plan microscope and a Protégé 460 FT-IR optical bench operated by the OMNIC® software. The microscope is equipped with an objective 15x/N.A. 0.58 with reflecting lenses of a Cassegrainian design and a Cassegrainian condenser. Two adjustable rectangular apertures allow to precisely define the size and shape of the measured area. The optical bench includes an Ever-Glo source, a KBr beamsplitter, and MCT-A detector which requires liquid-nitrogen cooling during data collection. Spectra were obtained of a defined area by co-adding up to 1024 scans with a spectral resolution of 4 $cm^{-1}$. The standard setting was 1024 scans/4 $cm^{-1}$ or 512 scans/4 $cm^{-1}$. The recorded spectral range was within 4000-650 $cm^{-1}$. Back ground spectra were collected after every sample. As the air in the system was not purged the spectra show the $CO_2$ band at 2360 $cm^{-1}$. All specimens were placed on a NaCl sample support (size 13 x 2 mm). This analysis was carried out at the school of Ocean and Earth Science, Southampton Oceanography Centre, University of Southampton, UK.

*3.3.3. Curie point pyrolysis-gas chromatograph-mass spectrometry (Cupy-GC-MS)*

Samples were pyrolysed at 650°C for 10 s using a Curie-point pyrolyser (Pyromat) coupled directly to a HP gas chromatograph-mass spectrometer (Cupy-GC-MS, Model No: HP GC-MS 5973). The GC was operated in the splitless mode and was equipped with a 50 m SGE BPX5 fused silica capillary column with an inner diameter of 220 μm and film thickness of 0.25 μm. An initial oven temperature of 50°C was held for 2 min, and then heated with 10°C $min^{-1}$ to 310°C. The oven was then maintained isothermally for 12 min. Carrier gas was helium. MS parameters included 70 eV EI ionisation, a source temperature of 230ºC and a mass range of 30-550 dalton. Peak assignments were based on mass spectra, GC retention time and literature data (e.g. Hartgers et al., 1992; Mastalerz et al., 1998; Armstroff et al., in press). This analysis was carried out at GSG Mess- und Analysengeräte GmbH, Bruchsal, Germany.

For a comparison with chitin derived compounds, we have analysed a chitin standard from crab (*Cancer magister,* purchased from Sigma-Aldrich) shells (Fig. 3.2; see Stankiewicz et al., 1996) using identical analytical protocols to confirm the integrity of the present investigations.

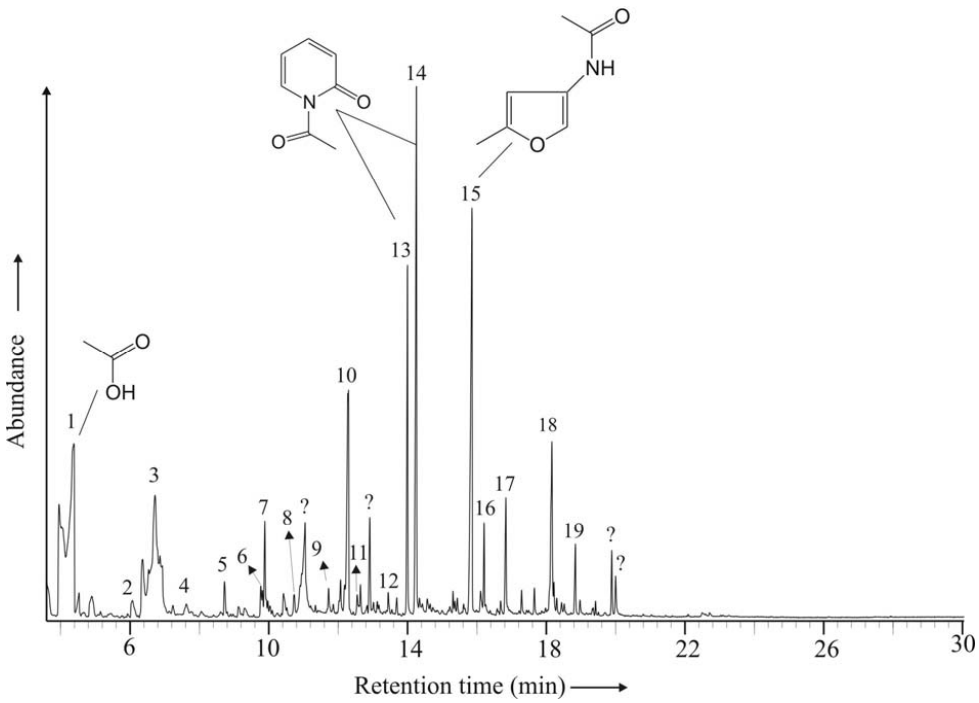


**Figure 3.2.** Total ion chromatogram resulting from Curie point pyrolysis-GC-MS (pyrolysis at 610ºC for 10 s) of chitin standard from crab (*Cancer magister*) shells. The numbers indicate major pyrolysis products derived from chitin: 1, acetic acid; 2, pyridine; 3, acetamide; 4, $C_1$-pyridone; 5, 3-hydroxy-2-pyridone; 6, 2-pyridinecarboxaldehyde; 7, acetylpyrroline; 8, levoglucocenone; 9, acetylpyrrolidone; 10, acetylpyrrolidone; 11, acetoxypyridine; 12, acetyldihydropyridine; 13, acetylpyridone; 14, acetylpyridone; 15, 3-acetamido-5-methylfuran; 16, 3-acetamido-4-pyrone; 17, N-hydroxyphenylacetamide; 18 and 19, oxazoline derivatives.

### *3.3.4. GC-MS of rock extract*

Soluble organic matter was extracted from rock samples from the core, using dichloromethane and methanol (99:1, v/v) following the modified flow-blending method after Radke *et al*. (1978). Separation of the soluble organic matter into $C_{15+}$ saturated hydrocarbons (SAT), $C_{11+}$ aromatic hydrocarbons (ARO) and nitrogen, sulphur and oxygen (NSO) compound fractions was performed by medium pressure liquid chromatography (MPLC) after Radke *et al*. (1980). The aromatic hydrocarbon fraction of host sediment extract was analysed by gas chromatography-mass spectrometry (GC-MS). Gas chromatography-mass spectrometry was accomplished using a gas chromatograph (HP 5890 Series II GC) coupled with a Finnigan MAT 95SQ mass spectrometer. The gas chromatograph was equipped with a temperature-programmable injection system (Gerstel KAS) and a SGE BPX5 fused silica capillary column (50 m length, 0.22 mm inner diameter, 0.25 μm film thickness). Helium was used as carrier gas at a flow rate of 1 ml/min. The oven temperature was programmed from 120 to 320°C

(initial hold time 2 min and final hold time 21 min) for the ARO fractions, at a rate of 3°C/min. The MS was operated in electron impact ionization mode at ionization energy of 70 eV and a source temperature of 260°C. Full scan mass spectra were recorded over a mass range of 50 to 1050 Da at a total scan time of 1.0 s.

### 3.4. Results and discussion

*3.4.1. Micro-FTIR spectroscopy*

A micro-FTIR spectrum from Chitinozoa is shown in Figure 3.3. Spectral bands were assigned with reference to the literature (for example, Arouri et al., 1999; Yule et al., 2000; Marshall et al., 2005). The micro-FTIR signals from Chitinozoa include both aliphatic and aromatic components (Fig. 3.3).

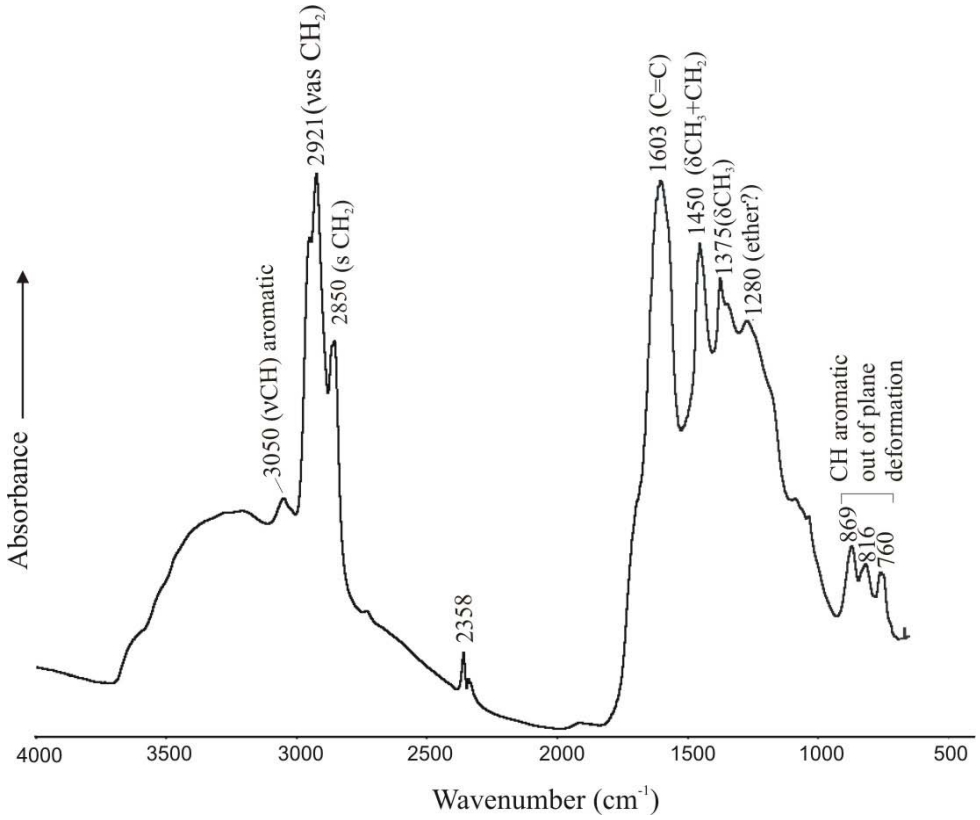


**Figure 3.3.** A micro-FTIR spectrum of Chitinozoa. Assignments of absorption bands and vibration modes (δ=deformation; ν=stretching; s=symmetric; as=asymmetric) are indicated in parentheses.

The aliphaticity is indicated by prominent alkyl group bands between 2800-3000 and 1300-1500 $cm^{-1}$. The strong narrow absorption at 2921 $cm^{-1}$ is due to asymmetric stretching vibration of $CH_2$. The peak at 2850 $cm^{-1}$ represents symmetric stretching vibration of $CH_2$. The absorptions of deformational asymmetric bending of $CH_2$ and $CH_3$ centered at 1450 $cm^{-1}$. The absorption at 1375 $cm^{-1}$ is assigned to deformational vibration of $CH_3$ with possible contribution from $[CH]_n$ bending (Arouri et al., 1999). A strong absorption signal attributed to aromatic C=C stretching vibration (1560-1610 $cm^{-1}$) is peaking at 1603 $cm^{-1}$. The prominent absorption signals at 700-900 $cm^{-1}$ (peaking at 869 $cm^{-1}$, 816 $cm^{-1}$ and 760 $cm^{-1}$) are due to aromatic CH out of plane deformation. A moderate absorption at 3050 $cm^{-1}$ is assigned to aromatic CH stretching vibration. FTIR spectroscopy clearly indicates that the biomacromolecules of these fossils consist of aliphatic and aromatic moieties.

*3.4.2. Curie point pyrolysis-gas chromatography-mass spectrometry*

A total ion chromatogram (TIC) representing the GC amenable pyrolysis products of Chitinozoa is shown in Figure 3.4a. The pyrolysate consists of both aliphatic and aromatic compounds. Aliphatic compounds are dominated by a series of *n*-alkenes and *n*-alkanes ranging from $C_6$ to at least $C_{22}$. The major aromatic compounds are alkylbenzenes, alkylnaphthalenes, alkylphenanthrenes and alkylphenols. No chitin derived pyrolysis products have been detected from the Chitinozoa. The corresponding analysis of total kerogen fraction (size> 63 μm) shows a series of *n*-alkenes and *n*-alkanes, ranging from $C_6$ to $C_{28}$ with a significantly lower amount of aromatic compounds (Fig. 3.4b). The macromolecular matter of chitinozoans has a much more aromatic character (Figs. 3.5 a, b, c) than that of the entire kerogen (Fig. 3.5d). All three pure chitinozoan concentrates show very similar pattern of pyrolysis products. The relative abundances of the individual compound classes (e.g., alkylbenzenes and alkylnaphthalenes) are different in the three samples; this could be due to the variation in abundance of different Chitinozoa genera. A detailed discussion of the distribution pattern of the various major compound classes is given below.

*3.4.2.1. n-Alkenes/n-alkanes*

The *m/z* 57 mass chromatogram (Fig. 3.6a) derived from the pyrolysates of Chitinozoa, shows a homologous series of *n*-alkanes ranging from $C_6$ to $C_{22}$ with a maximum at $C_{11}/C_{12}$. The abundance of *n*-$C_{17}$ alkane is somewhat high compared to the overall *n*-alkane envelope. *n*-Alkanes predominate over *n*-alkenes (Fig. 3.5a-c). The corresponding *m/z* 57 data (Fig. 3.6b) derived from the pyrolysates of total organic residues (size>63 μm), shows a homologous

series of *n*-alkanes ranging from $C_6$ to $C_{28}$ with maxima at $C_{11}$. High abundance of *n*-alkene/*n*-alkane pyrolysates of highly aliphatic resistant biopolymers are present in fossil remains such as algal walls (algaenan; see Hatcher and Clifford, 1997), higher plant cuticles (cutan; see Mösle et al., 1998), and periderm tissues (suberans; see Collinson et al., 1994). As mentioned earlier, total organic residues of the sedimentary sequence studied are dominated by acritarchs and prasinophycean algae e.g., *Tasmanites* and *Leiosphaeridia* (see Dutta et al., 2006). Therefore, the abundant *n*-alkenes/*n*-alkanes (up to $C_{28}$, Fig. 3.6b) in the pyrolysates of the total organic residues are probably indicative of algaenan. It is uncertain whether the vesicle of Chitinozoa is the source of these aliphatic products. Mobilisation and migration during diagenesis of aliphatic moieties from aliphatic-rich substance (liptinites) to nonaliphatic ones (vitrinite) has been used to explain chemical alteration of coal macerals derived from aliphatic-poor macromolecules such as lignin (Zhang et al., 1993). However, recently, Stankiewicz et al. (2000) carried out thermal maturation studies on modern arthropods cuticles which consist of a chitin-protein complex (with major chitin and protein derived biomarkers in the pyrolysates). They found that thermal maturation at 350°C resulted in extensive alteration of the macromolecular composition, the *n*-alkenes/*n*-alkanes doublets being the dominant pyrolysis products. Hence, aliphatic compounds must be present in the arthropod cuticles. Similarly, we also believe that the abundant *n*-alkenes/*n*-alkanes in the pyrolysates of Chitinozoa should be a product of aliphatic macromolecules of the vesicle of these micro-fossils.

*3.4.2.2. Aromatic compounds*

Alkylbenzenes represent a relatively important contribution to the TIC traces of the chitinozoan pyrolysates (Fig. 3.4a). Alkylbenzenes ($C_1$-$C_4$) were identified by selective ion detection at *m/z* 91+105+106+119+120+134 (Fig. 3.7; Table 3.2). These alkylbenzenes (i.e. $C_1$-$C_4$) were not found in the host rock extract. *n*-Alkylbenzenes with a $C_5$-$C_{16}$ chain could be secondary pyrolysis products produced by cyclisation/aromatisation processes (Hartgers et al., 1994a). However, *n*-alkylbenzenes with a low alkyl carbon number (i.e. in the $C_1$-$C_4$ range) might also be pyrolysis products formed by β-cleavage of the substituted aromatic rings linked to the macromolecular structure via an alkyl chain (Hartgers et al., 1994b). Benzene and its alkylated homologs are found in the pyrolysates of various types of geochemical samples and therefore have little potential as biomarkers, nevertheless 1,2,3,4-tetramethylbenzene (TMB, Peak 15, Fig. 3.7) is the most abundant pyrolysis product of Chitinozoa. The presence of 1,2,3,4-TMB in the pyrolysates of various kerogens was ascribed

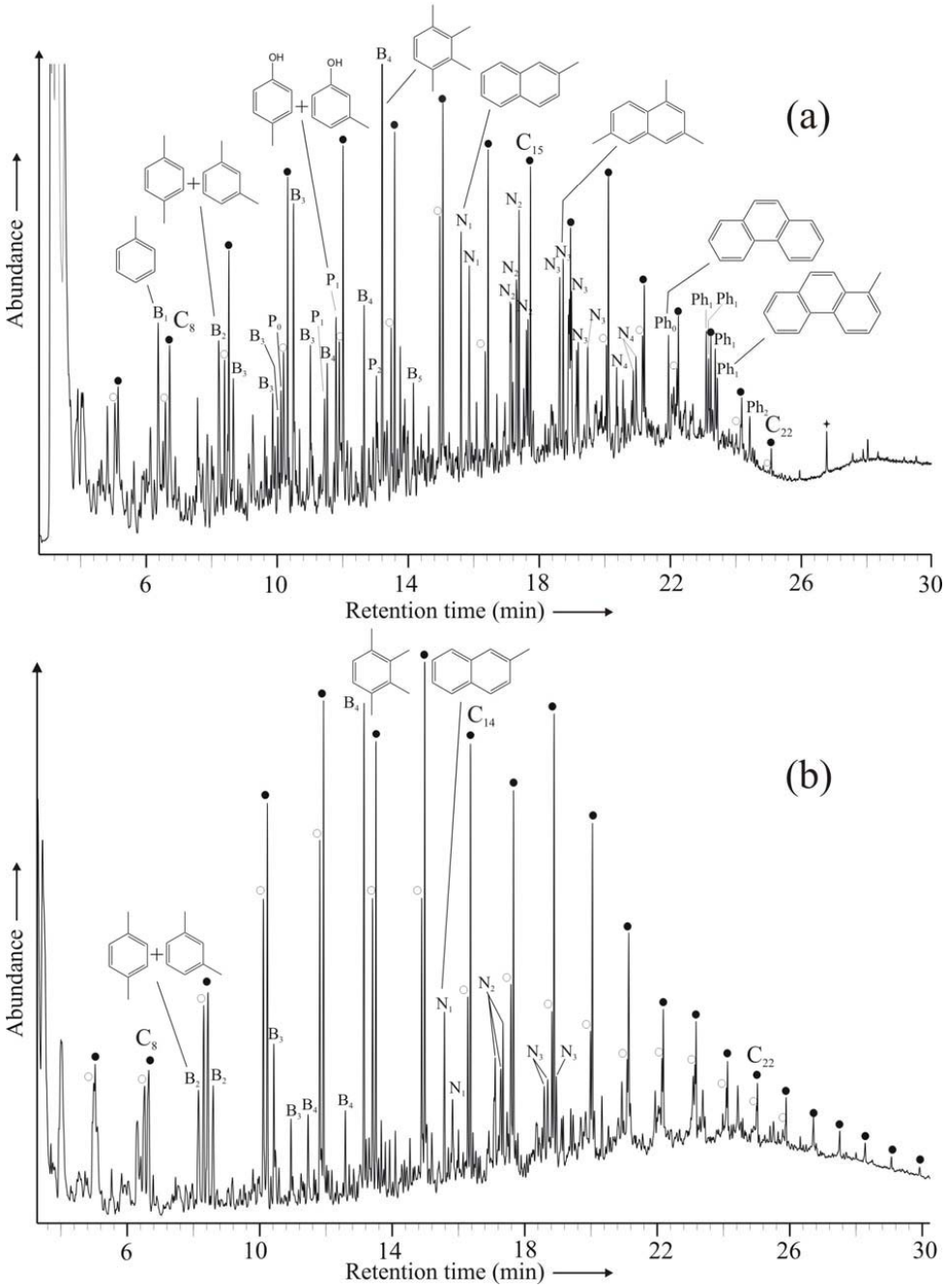


**Figure 3.4.** Total ion chromatogram resulting from Curie point pyrolysis-GC-MS (pyrolysis at 610ºC for 10s) of (a) handpicked Chitinozoa from the Dadas Formation, SE Turkey (Fe1 PP-101); (b) total organic residues (Fe1 PP-101, size> 63 µm). Each doublet corresponds to an alkene (○) and an alkane (●); selected C-numbers are indicated, $B_n$ = (alkyl)benzene, $P_n$ = (alkyl)phenol, $N_n$ = (alkyl)naphthalene, $Ph_n$ = (alkyl)phenanthrene, (where n = 1 is methyl, n = 2 is dimethyl or ethyl etc.).

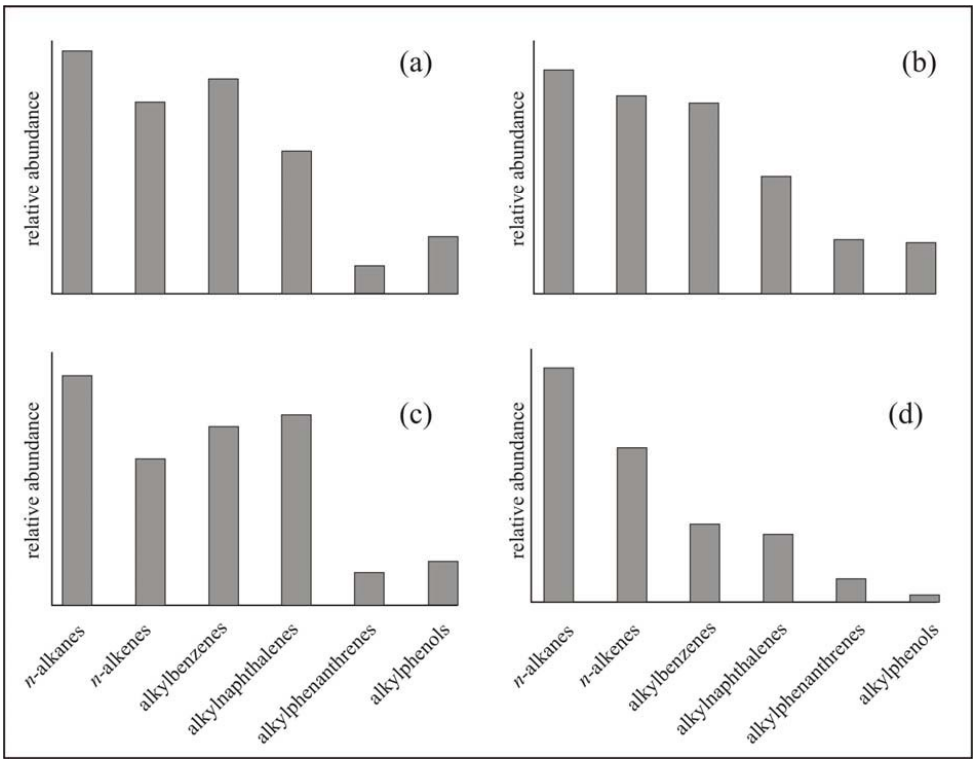


**Figure 3.5.** Histograms showing relative abundance of various compound classes in the pyrolysates of handpicked chitinozoans from the Dadas Formation, SE Turkey at depth (a) -72.70 m (C Fe 18); (b) -94.00 m (Fe1 PP-99); (c) -92.30 m (Fe1 PP-101); (d) histogram showing relative abundance of various compound classes in the pyrolysate of the total organic residues at depth -92.30 m (Fe1 PP-101, size> 63 μm).

to macromolecularly bound diaromatic carotenoids derived from *Chlorobiaceae* (Hartgers et al., 1994a, b; Clegg et al., 1997). *Chlorobiaceae* are anaerobic, photosynthetic, green sulphur bacteria. Since green sulphur bacteria require light and hydrogen sulphide, their presence is an indicator of anoxia in the photic zone. It is believed that diaromatic carotenoids are incorporated within the kerogen during diagenesis, although the method of incorporation is not known (Clegg et al., 1997). However, Hoefs et al. (1995) proposed that 1,2,3,4-TMB could be derived from marine algae and suggested that the assessment of photic zone anoxia on the basis of abundant presence of 1,2,3,4-TMB in the pyrolysate is not possible without determination of its stable carbon isotope composition and comparison with those of algal lipids. The molecular characterisation of organic matter of carbonate facies from Keg River Formation, western Canada revealed that 1,2,3,4-TMB was a major peak in most samples (Clegg et al., 1997) and also showed that 1,2,3,5-tetramethylbenzene, 1-ethyl-3,4,5-

trimethylbenzene and 1-ethyl-2,3,6-trimethylbenzene occurred in significant amount. These compounds could be derived from γ-cleavage of macromolecularly bound diaromatic carotenoids (e.g., isorenieratene). 1,2,3,5-Tetramethylbenzene (Peak 14, Fig. 3.7) is also abundant in the pyrolysates of chitinozoans. We also analysed aromatic fractions of host sediment extract of the core where we found $C_{13}$-$C_{26}$ aryl isoprenoids (Fig. 3.8) which are believed to be derived from isorenieratene from *Chlorobiaceae* as well (Summons and Powell, 1987).

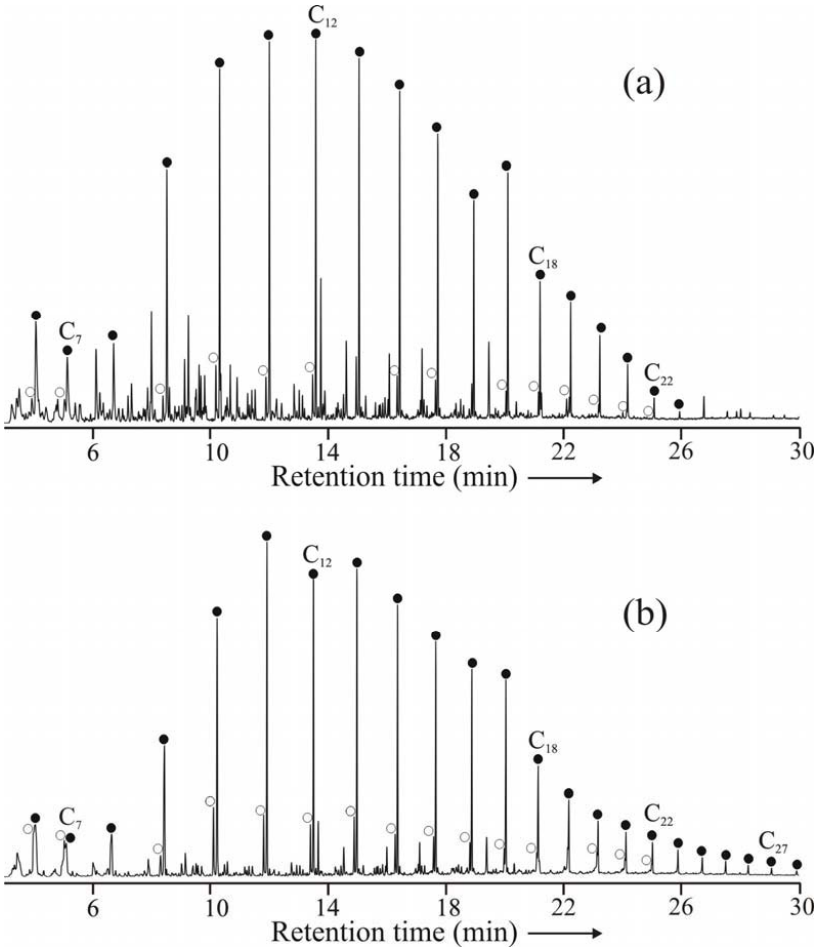


**Figure 3.6.** Mass chromatogram (*m/z* 57) of the 610°C Curie-point pyrolysates of (a) handpicked Chitinozoa (Fe1 PP-101); (b) total organic residues (Fe1 PP-101, size> 63 µm) showing the homologous series of *n*-alkenes (○) and *n*-alkanes (●). Numbers on top of the chromatogram indicate the number of carbon atoms in the respective alkene/alkane pair.

Considering the chemical structure, it appears that both 1,2,3,4-TMB and aryl isoprenoids have been derived from the same diaromatic precursor compound. It is difficult to infer

whether the precursor compound of TMB was either a constituent of the original macromolecular structure of Chitinozoa or whether it was incorporated into macromolecules of Chitinozoa during diagenesis. If the latter is true, then all chemical compounds which are produced upon pyrolysis of pure chitinozoan concentrate may not necessarily derive from the original macromolecules of Chitinozoa. If we assume, TMB has been derived from the original macromolecules of Chitinozoa then this would be an example of another source of TMB which so far has been typically attributed to green sulphur bacteria or marine algae. We also analysed pure handpicked *Tasmanites* and *Leiosphaeridia* (see Dutta et al., 2006) from several depth levels of Fetlika-1 core where TMB is absent in the pyrolyastes of those prasinophytes. Therefore, it is likely that TMB has been derived from the original macromolecules of Chitinozoa.

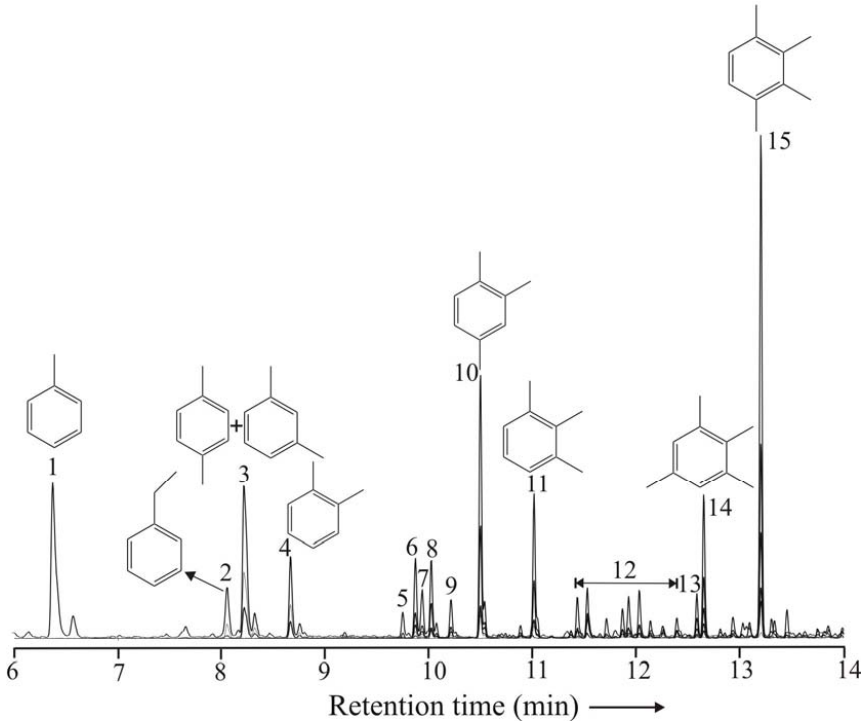


**Figure 3.7.** Mass chromatogram (*m/z* 91+105+106+119+120+134) of the 610°C Curie-point pyrolysates of handpicked Chitinozoa (Fe1 PP-101) showing the distribution of alkylbenzenes. The identification of the numbered peaks is listed in Table 3.2.

Alkylnaphthalenes are also abundant in the pyrolysates of Chitinozoa. Naphthalene and its alkylated homologs were identified by selective ion detection of *m/z* 128, 142, 156 and 170 (Fig. 3.9; Table 3.3). Alkylnaphthalenes are not very source specific compounds. They have

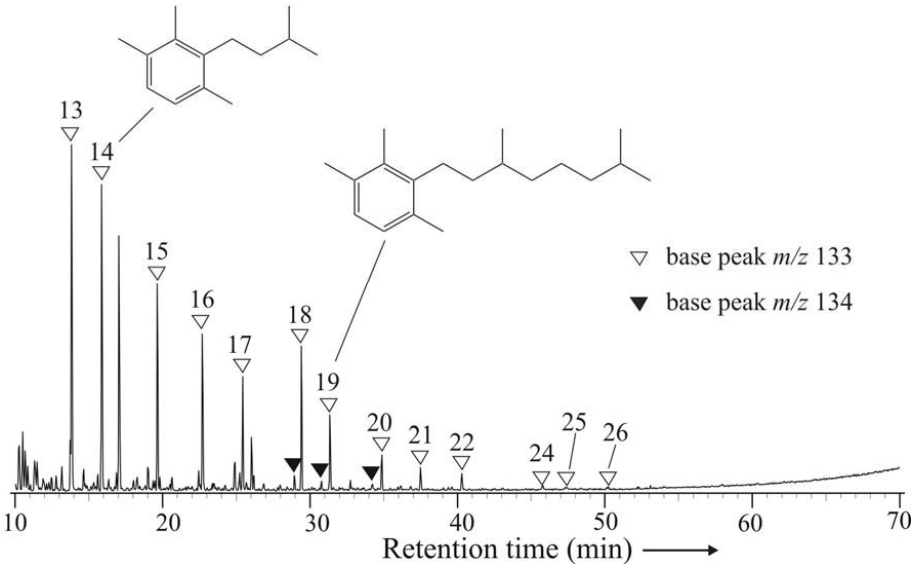


**Figure 3.8.** Mass chromatogram (*m/z* 133+134) of aromatic hydrocarbon fraction from sediment extract at depth –92.30 m (Fe1 PP-101, Fetlika 1 borehole, Dadas Formation, SE Turkey) revealing typical distributions of aryl isoprenoids. C-numbers are indicated.

been detected upon the pyrolysis of different kinds of fossil remains and and extant plant material. They have been detected in the pyrolysates of *Protosalvinia* (Mastalerz et al., 1998) which is a Paleozoic index fossil of problematic botanical origin. Abundant $C_0$-$C_4$ naphthalenes have been detected in the pyrolysates of resinite and vitrinite macerals of coal from China (Greenwood et al., 2001). Radke et al. (1994) suggested that alkylnaphthalenes are mainly derived from terrestrial sources. During the last few years, the occurrence of alkylnaphthalenes in the bitumens of various sediments has attracted some interest (Armstroff et al., in press and references therein). Strachan et al. (1988) suggested that 1,2,5- and 1,2,7-trimethylnaphthalene (Peak 20 and 16, Fig. 9) are the degradation products of an oleanane type pentacyclic triterpenoid. Alexander et al. (1992) suggested microbially produced 1,2,2,5-tetramethyltetralin and 1,2,2,5,6-pentamethyltetralin may be precursors of 1,2,6-trimethylnaphthalene (Peak 18, Fig. 3.9). Chitinozoans appear exclusively in marine sediments and their morphology is not typical of higher plant or microbial origin. It is evident that naphthalene and its alkylated homologs which are found in the pyrolysates of chitinozoans are also present with similar distribution pattern in the host sediment extract (Fig. 3.9b). Therefore, we believe that chitinozoans are the biological precursor of Naphthalenes.

**Table 3.2**. Major alkylbenzenes (Fig. 3.7) identified in the pyrolysates of the handpicked Chitinozoa.

| Peaks | Compounds |
|---|---|
| 1 | Toluene |
| 2 | Ethylbenzene |
| 3 | 1,3- and 1,4-Dimethylbenzene |
| 4 | 1,2-Dimethylbenzene |
| 5 | *n*-Propylbenzene |
| 6 | 1-Methyl-3-ethylbenzene |
| 7 | 1,3,5-Trimethylbenzene |
| 8 | 1-Methyl-4-ethylbenzene |
| 9 | 1-Methyl-2-ethylbenzene |
| 10 | 1,2,4-Trimethylbenzene |
| 11 | 1,2,3-Trimethylbenzene |
| 12 | Dimethylethylbenzenes |
| 13 | 1,2,4,5-Tetramethylbenzene |
| 14 | 1,2,3,5-Tetramethylbenzene |
| 15 | 1,2,3,4-Tetramethylbenzene |

**Table 3.3.** Major alkylnaphthalenes (Fig. 3.9) identified in the pyrolysates of the handpicked Chitinozoa and in the host rock extract.

| Peaks | Compounds |
|---|---|
| 1 | Naphthalene |
| 2 | 2-Methylnaphthalene |
| 3 | 1-Methylnaphthalene |
| 4 | 2-Ethylnaphthalene |
| 5 | 2,6-Dimethylnaphthalene |
| 6 | 2,7-Dimethylnaphthalene |
| 7 | 1,3- and 1,7-Dimethylnaphthalene |
| 8 | 1,6-Dimethylnaphthalene |
| 9 | 1,4- and 2,3-Dimethylnaphthalene |
| 10 | 1,5-Dimethylnaphthalene |
| 11 | 1,2-Dimethylnaphthalene |
| 12 | 1,3,7-Trimethylnaphthalene |
| 13 | 1,3,6-Trimethylnaphthalene |
| 14 | 1,3,5 and 1,4,6-Trimethylnaphthalene |
| 15 | 2,3,6-Trimethylnaphthalene |
| 16 | 1,2,7-Trimethylnaphthalene |
| 17 | 1,6,7-Trimethylnaphthalene |
| 18 | 1,2,6-Trimethylnaphthalene |
| 19 | 1,2,4-Trimethylnaphthalene |
| 20 | 1,2,5-Trimethylnaphthalene |
| 21 | 1,3,6,7-Tetramethylnaphthalene |

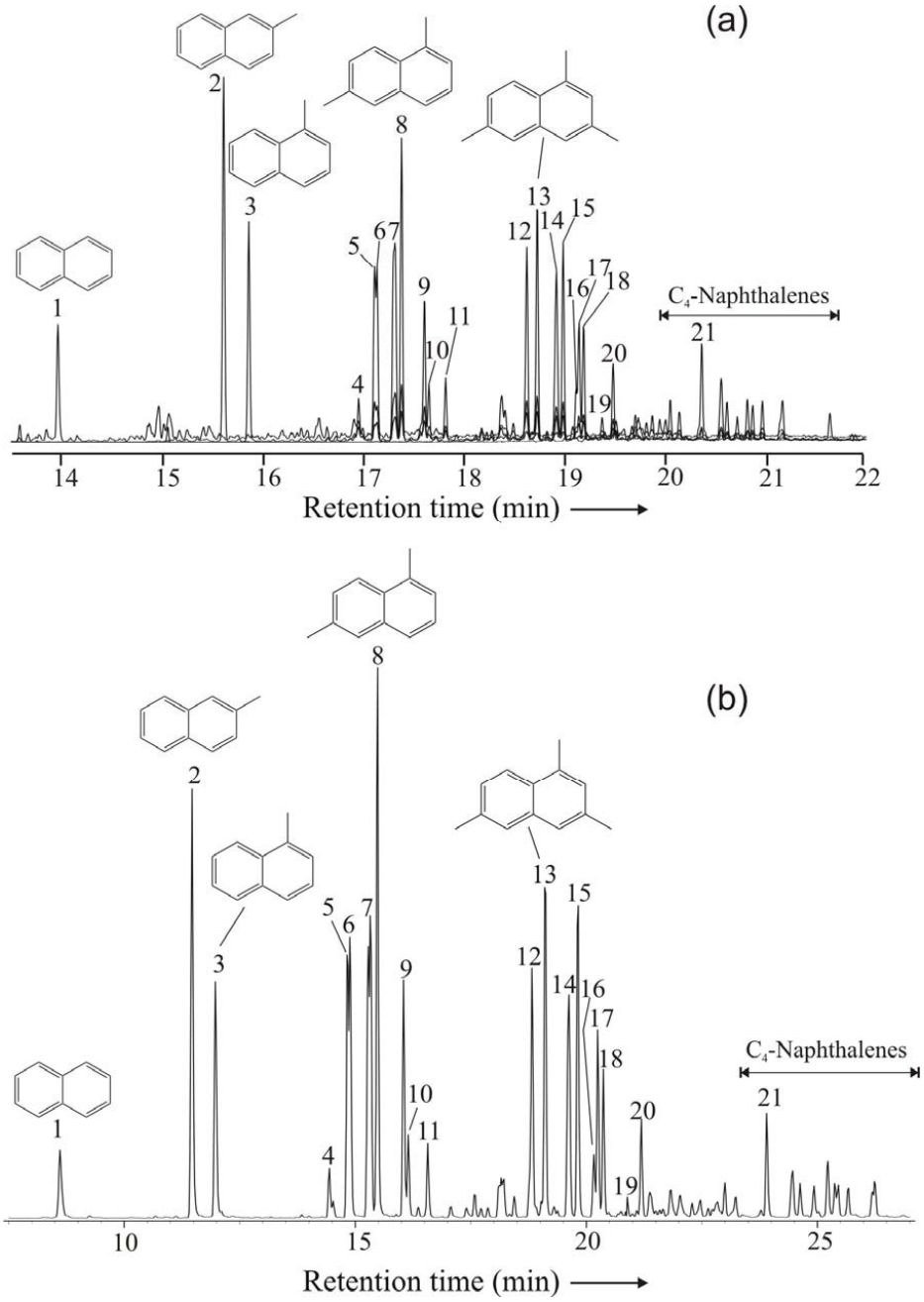


**Figure 3.9.** Mass chromatogram (*m/z* 128+142+156+170+184) of (a) the 610°C Curie-point pyrolysates of handpicked Chitinozoa (Fe1 PP-101) and (b) the aromatic hydrocarbon fraction from sediments at depth -92.30 m (Fe1 PP-101, Fetlika 1 borehole, Dadas Formation, SE Turkey) revealing the distribution of alkylnaphthalenes. The identification of the numbered peaks is listed in Table 3.3.

alkylnaphthalenes and these compounds are not always diagnostic of higher plants.

Phenanthrene and its alkylated homologs which have been found in the pyrolysates of Chitinozoa are not very source specific compounds. They have been found in the pyrolysates of different coal macerals (see Nip et al., 1992; Greenwood et al., 2001) and as well in extant marine algae (Derenne et al., 1996).

Phenols are found in all pyrolysates of all three samples. Selective ion detection at *m/z* 94+107+108+121+122 (Fig. 3.10) is used to highlight phenol and its alkylated homologs from the full scan data. Phenolic moieties are found as part of lignin (see Hatcher and Clifford, 1997), seed coats of higher plants (van Bergen et al., 1994), plant cuticles (Mösle et al., 1998) and as spore coverings of sporopollenin (van Bergen et al., 1993). Phenolic compounds played a very significant role in the evolution of the first photosynthetic plants on land during the Silurian-Devonian time (see Cooper-Driver, 2001). The significance of phenolic compounds in the macromolecular structure of extinct marine organism like Chtinozoa is not yet clear.

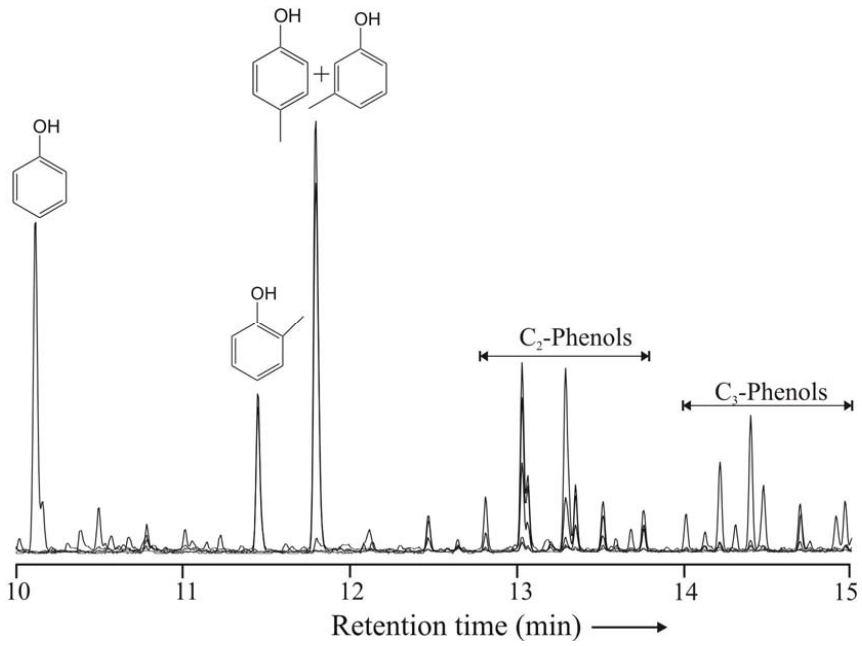


**Figure 3.10.** Mass chromatogram (*m/z* 94+107+108+121+122) of the 610°C Curie-point pyrolysates of handpicked Chitinozoa (Fe1 PP-101) showing the distribution of alkylphenols.

Phenol and its alkylated homologs, found in the present study, might have derived from protein/amino acid (e.g., tyrosine) related precursor compounds (Tsuge and Matsubara, 1985).

It was speculated that the vesicle wall of these microfossils consisted of scleroprotein (Locquin, 1981) or polysaccharide-protein (Mierzejewski, 1981). However, protein/amino acids derived biomarkers have not been detected in the present study. Hence, it appears that chitinozoan derived macromolecules have certain structural features in common with lignin or tannins, i.e., biomacromolecules known to contain significant proportions of phenolic moieties.

*3.4.2.*3. *Chitin derived compounds*

We have analysed a chitin standard obtained from crab (*Cancer magister*) shells (Fig. 3.2) where chitin derived biomarkers (see Stankiewicz et al., 1996; 1997a; 1997b) e.g. acetamide, acetic acid, acetylpyridone, 3-methyl-5-acetamidofuran have been detected. It is very clear that some specific compounds, which are abundant in the pyrolysate of chitin standard, are absent in the pyrolysates of Chitinozoa. Chitin biomarkers were also absent from the Ordovician Chitinozoa *Cyathochitina campanulaeformis* (Voss-Foucart and Jeuniaux, 1972) upon characterisation by an enzymatic method. The chemical composition of cuticles from modern invertebrates consists of chitin derived compounds (Stankiewicz et al. 1996) but the cuticles of fossil invertebrates collected from Silurian to Cretaceous sediments do not yield chitin derived compounds upon pyrolysis (Stankiewicz et al. 1997b). The fossil cuticles fall into two, chemically distinct groups: aliphatic, yielding *n*-alkene/*n*-alkane doublets upon pyrolysis and aromatic, producing pyrolysates dominated by alkylbenzenes and alkylindenes. The compounds and their distribution pattern, which are found in the pyrolysates of Chitinozoa are not comparable to the compounds that are produced upon the pyrolysis of fossil cuticles consisting of degraded chitin biomacromolecules. Therefore, it is evident that original macromolecules of Chitinozoa before fossilization were not made of chitin related compounds and hence, the incorporation of the word “chitin” into the name of these extinct organisms was not appropriate.

Bailey (1981) analysed algal-chitinozoan assemblages in which the chitinozoans are equally or more abundant than algal material based on pyrolysis-gas chromatography data. It was suggested that the pyrolysis products from Chitinozoa may resemble those obtained from wood. It is obvious that pyrolysates of Chitinozoa, investigated in the present study are dominated by many aromatic compounds including phenols which are also commonly found in the pyrolysates of type-III kerogen originating from terrestrial higher plants. As mentioned earlier, chitinozoans appear exclusively in marine sediments. Generally, organic remains of marine origin do not show aromatic macromolecular character. However, pyrolysates of

modern microalgae *Chorella marina* yield predominantly aromatic components compared to *n*-alkene/*n*-alkane doublets (Derenne et al., 1996). Kokinos et al. (1998) documented the molecular composition of an extant marine dinoflagellate (*Lingulodinium polyedrum*) and suggested that the biomacromolecules of these marine organisms predominantly consist of aromatic compounds. From a morphological point of view, there is no similarity between chitinozoans and algae or dinoflagellates. Moreover, *Protosalvinia* being a problematic marine fossil from the Devonian yields both aliphatic and aromatic pyrolysates and it was concluded that *Protosalvinia* belongs to rare marine organisms that yield aromatic pyrolysates (Mastalerz et al., 1998). Similarly, we also believe that chitinozoans belong to another group of rare marine fossils that have substantial amount of 'lignin-like' macromolecular matter.

### 3.5. Conclusions

For the first time, the present investigation provides a detailed insight into the molecular composition of Chitinozoa. Biomacromolecules of this extinct microfossil group consist of both aliphatic and aromatic moieties. A series of *n*-alkene/*n*-alkane doublets represents the aliphatic moiety. Alkylbenzenes, alkylnaphthalenes, alkylphenols and alkylphenanthrenes are the major aromatic compounds found in the pyrolysates of Chitinozoa. Aromatic compounds predominate over aliphatic compounds. 1,2,3,4-Tetramethylbenzene is the most abundant pyrolysis product of Chitinozoa analysed in this study. Aryl isoprenoids are also present in the host sediment extract. Both, 1,2,3,4-tetramethylbenzene in the pyrolysates of chitinozoans and aryl isoprenoids in the host sediment extract have been derived from same precursor diaromatic compound, but the biological precursor of those compounds is yet not clear. The presence of abundant alkylnaphthalenes in the pyrolysates of Chitinozoa and the host sediment extract suggests that chitinozoans are the biological precursor of alkylnaphthalenes and these compounds are not always diagnostic of higher plants. Micro-FTIR data are consistent with the pyrolytic studies emphasizing that biomacromolecules of the Chitinozoa investigated in the present study consist of both aliphatic and aromatic components. No pyrolysis products diagnostic of chitin have been detected in the present study and it is also concluded that original biomacromolecules of Chitinozoa before fossilization were not made of chitin. Chitinozoans belong to rare marine fossils that contained substantial amount of 'lignin-like' macromolecular matter. No specific biomarker(s) has been recognised in the pyrolysates of Chitinozoa providing information about the biological affinity of this enigmatic, marine, fossil group.

**Acknowledgements**

This research is part of the “Silurian-Devonian Boundary Project”. We would like to thank Deutsche Forschungsgemeinschaft, Bonn (grants no. Ma 1861/2 and /4; Br 1943/3-1 and /2) and Forschungszentrum Jülich for financial support. The authors are grateful to P. F. Greenwood (University of Western Australia) for his contributions to improve the manuscript and useful discussions. S. Roberts (University of Southampton) is acknowledged for supporting with Micro-FTIR investigations. We are thankful to R. Woisch (GSG Mess-und Analysengeräte GmbH, Bruchsal) for supporting with some of the Py-GC-MS analyses. For technical assistance, we would like to thank U. Disko, F. Leistner and H. Willsch. Support during fieldwork by TPAO (Türkiye Petrolleri Anonim Ortakliği), Ankara, is gratefully acknowledged. This project is also related to IGCP Project 499, “Devonian Land-Sea Interactions: Evolution of Ecosystems and Climate (DEVEC)”.

### 3.6. References


Alexander, R., Bastow, T.P., Kagi, R.I., Singh, R.K., 1992. Identification of 1,2,2,5-tetramethyltetralin and 1,2,2,3,4-pentamethyltetralin as racemates in petroleum. Journal of the Chemical Society, Chemical Communications 1906, 1712-1714.

Armstroff, A., Wilkes, H., Schwarzbauer, J., Littke, R., Horsfield, B., Aromatic hydrocarbon biomarkers in terrestrial organic matter of Devonian to Permian age. Palaeogeography, Palaeoclimatology, Palaeoecology (in press).

Arouri, K., Greenwood, P.F., Walter, M.R., 1999. A possible chlorophycean affinity of some Neoproterozoic acritarchs. Organic Geochemistry 30, 1323-1337.

Bailey, N.J.L., 1981. Hydrocarbon potential of organic matter. In: Brooks, J. (Ed.), Organic maturation studies and fossil fuel exploration, pp. 283-302.

van Bergen, P.F., Collinson, M.E., de Leeuw, J.W., 1993. Chemical composition and ultrastructure of fossil and extant salvinialean microspore massulae and megaspores. Grana Suppl. 1, 18-30.

van Bergen, P.F., Goñi, M., Collinson, M.E., Barrie, P.J., Sinninghe Damsté, J.S., de Leeuw, J.W., 1994. Chemical and microscopic characterization of outer seed coats of fossils and extant water plants. Geochimica et Cosmochima Acta 58, 3823-3844.

Brocke, R., Wilde, V., 2001. Infrared video microscopy – an efficient method for the routine investigation of opaque organic-walled microfossils. Facies 45, 157-164.

Clegg, H., Horsfield, B., Stasiuk, L., Fowler, M.G., Vliex, M., 1997. Geochemical characterisation of organic matter in Keg River Formation (Elk point group, Middle Devonian), La Crete Basin, western Canada. Organic Geochemistry 26, 627-643.

Collinson, M.E., van Bergen, P.F., Scott, A.C., de Leeuw, J.W., 1994. The oil-generating potential of plants from coal and coal-bearing strata through time: a review with new evidence from Carboniferous plants. In: Scott, A.C., Fleet, A.J. (Eds.), Coal and coal-bearing strata as oil prone source rocks? Geological Society Special Publication 77, pp. 31-70.

Cooper-Driver, G.A., 2001. Biological roles for phenolic compounds in the evolution of early land plants. In: Gensel, P.G., Edwards, D. (Eds.), Plants Invade the Land. Evolutionary and Environmental Perspectives. New York: Columbia University Press, pp.159-172.

Derenne, S., Largeau, C., Berkaloff, C., 1996. First example of an algaenan yielding an aromatic rich pyrolysates, possible geochemical implications on marine kerogen formation. Organic Geochemistry 24, 617-627.

Dutta, S., Greenwood, P.F., Brocke, R., Schaefer, R.G., Mann, U., 2006. New insights into the relationship between *Tasmanites* and tricyclic terpenoids. Organic Geochemistry 37, 117-127.

Eisenack, A., 1931. Neue Mikrofossilien des baltischen Silurs I, Palaeontologische Zeitschrift 13, 74-118.

Greenwood, P.F., George, S.C., Pickel, W., Zhu, Y., Zhong, N., 2001. In situ analytical pyrolysis of coal macerals and solid bitumens by laser micropyrolysis GC-MS. Journal of Analytical and Applied Pyrolysis 58-59, 237-253.

Hartgers, W.A., Sinninghe Damsté J.S., de Leeuw, J.W., 1992. Identification of $C_2$-$C_4$ alkylated benzenes in flash pyrolysates of kerogens, coals and asphaltenes. Journal of Chromatography 606, 211-220.

Hartgers, W.A., Sinninghe Damsté J.S., de Leeuw, J.W., 1994a. Geochemical significance of alkylbenzene distributions in flash pyrolysates of kerogens, coals, and asphaltenes. Geochimica et Cosmochima Acta 58, 1759-1775.

Hartgers, W.A., Sinninghe Damsté, J.S., Requejo, A.G., Allan, J., Hayes, J.M., Ling, Y., Xie, T-M., Primack, J., de Leeuw, J.W., 1994b. A molecular and carbon isotopic study towards the origin and diagenetic fate of diaromatic carotenoids. In: Øygard, K., et al. (Eds.), Advances in Organic Geochemistry 1993, 22, 703-725.

Hatcher, P.G., Clifford, D.J., 1997. The organic geochemistry of coal: from plant materials to coal. Organic Geochemistry 27, 251-274.

Hoefs, M.J.L., van Heemst, J.D.H., Gelin, F., Koopmans, M.P., van Kaam-Peters, H.M.E., Schouten, S., de Leeuw, J.W., Sinninghe Damsté, J.S., 1995. Alternative biological sources for 1,2,3,4-tetramethylbenzene in flash pyrolysates of kerogen. Organic Geochemistry 23, 975-979.

Kokinos, J.P., Eglinton, T.I., Goni, M.A., Boon, J.J., Martoglio, P.A., Anderson, D.M., 1998. Characterization of a highly resistant biomacromolecular material in the cell wall of a marine dinoflagellate resting cyst. Organic Geochemistry 28, 265-288.

Kranendonck, O., 2004. Geo- and biodynamic evolution during Late Silurian to Early Devonian time (Hazro Area, SE Turkey). Schriften des Forschungszentrum Jülich, Reihe Umwelt/Environment 49, pp. 268.

Locquin, M.V., 1981. Technique de regonflement des micro-organismes fossiles contenant des scleroproteines. Cahiers de Micropaleontologie 1, 57-58.

Marshall, C.P., Javaux, E.J., Knoll, A.H., Walter, M.R., 2005. Combined micro-Fourier transform infrared (FTIR) spectroscopy and micro-Raman spectroscopy of Proterozoic acritarchs: A new approach to Paleobiology. Precambrian Research 138, 208-224.

Mastalerz, M., Hower, J.C., Carmo, A., 1998. In situ FTIR and flash pyrolysis/GC-MS characterization of *Protosalvinia* (Upper Devonian, Kentucky, USA): implications for maceral classification. Organic Geochemistry 28, 57-66.

Mierzejewski, P., 1981. TEM study on ultrastructure of chitinozoan vesicle wall. Cahiers de Micropaleontologie 1, 59-70.

Miller, M.A., 1996. Chitinozoa, In: Jansonius, J., McGregor, D.C., (Eds.) Palynology: principles and applications; American Association of Stratigraphic Palynologist Foundation. Vol. 1, pp. 307-336.

Mösle, B., Collinson, M., Finch, P., Stankiewicz, B.A., Scott, A.C., Wilson, R., 1998. Factors influencing the preservation of plant cuticles: a comparison of morphology and chemical composition of modern and fossil examples. Organic Geochemistry 29, 1369-1380.

Nip, M., de Leeuw, J.W., Creeling, J.C., 1992. Chemical structure of bituminous coal and its constituting macerals fractions as revealed by Flash pyrolysis. Energy and Fuels 6, 125-136.

Obermajer, M., Fowler, M.G., Goodarzi, F., Snowdon, L.R., 1996. Assessing thermal maturity of Paleozoic rocks from reflectance of chitinozoa as constrained by geochemical indicators: an example from southern Ontario, Canada. Marine and Petroleum Geology 13, 907-919.

Paris, F., Grahn, Y., Nestor, V., Lakova, I., 1999. A revised chitinozoan classification. Journal of Paleontology 73, 549-570.

Paris, F., Nõlvak, J., 1999. Biological interpretation and palaeodiversity of a cryptic fossil group: the “chitinozoan animal”. Geobios 32, 315-324.

Radke, M., Sittardt, H.G., Welte, D.H. 1978. Removal of soluble organic matter from rock samples with a flow-through extraction cell. Analytical Chemistry 50, 663-665.

Radke, M., Willsch, H., Welte, D.H., 1980. Preparative hydrocarbon group type determination by automated medium pressure liquid chromatography. Analytical Chemistry 52, 406-411.

Radke, M., Rullkötter, J., Vriend, S.P., 1994. Distribution of naphthalenes in crude oils from the Java Sea: Source and maturation effects. Geochimica et Cosmochimica Acta 58, 3675-3689.

Saxby, J.D., 1970. Isolation of kerogen in sediments by chemical methods. Chemical Geology 6, 173.

Stankiewicz, B.A., van Bergen, P.F., Duncan, I.J., Carter, J.F., Briggs, D.E.G., Evershed, R. P., 1996. Recognition of chitin and proteins in invertebrate cuticles using analytical pyrolysis/gas chromatography and pyrolysis/gas chromatography/mass spectrometry. Rapid Communications in Mass spectrometry 10, 1747-1757.

Stankiewicz, B.A., Briggs, D.E.G., Evershed, R.P., Flannery, M.B., Wuttke, M., 1997a. Preservation of chitin in 25-million-year-old fossils. Science 276, 1541-1543.

Stankiewicz, B.A., Briggs, D.E.G., Evershed, R.P., 1997b. Chemical composition of Paleozoic and Mesozoic fossil invertebrate cuticles as revealed by pyrolysis-gas chromatography/mass spectrometry. Energy and Fuels 11, 515-521.

Stankiewicz, B.A., Briggs, D.E.G., Michels, R., Collinson, M.E., Flannery, M.B., Evershed, R. P., 2000. Alternative origin of aliphatic polymer in kerogen. Geology 28, 559-562.

Strachan, M.G., Alexander, R., Kagi, R.I., 1988. Trimethylnaphthalenes in crude oils and sediments: effects of source and maturity. Geochimica et Cosmochimica Acta 52, 1255-1264.

Summons, R.E., Powell, P.G., 1987. Identified of aryl isoprenoids in source rocks and crude oils: biological markers for the green sulphur bacteria. Geochimica et Cosmochimica Acta 51, 557-566.

Tsuge, S., Matsubara, H., 1985. High-resolution pyrolysis-gas chromatography of proteins and related materials. Journal of Analytical and Applied Pyrolysis 8, 49-64.

Voss-Foucart, M.F., Jeuniaux, C., 1972. Lack of chitin in a sample of Ordovician Chitinozoa. Journal of Paleontology 46, 769-770.

Yule, B.L., Roberts, S., Marshall, J.E.A., 2000. The thermal evolution of sporopollenin. Organic Geochemistry 31, 859-870.

Zhang, E., Hatcher, P.G., Davis, A., 1993. Chemical composition of pseudo-phlobaphinite precursors: implications for the presence of aliphatic biopolymers in vitrinite from coal. Organic Geochemistry 20, 721-734.

# CHAPTER 4

## The molecular composition of sporopollenin from fossil megaspores as revealed by micro-FTIR and pyrolysis-GC-MS

**Abstract**

**In order to investigate the chemical composition of fossil sporopollenin, three megaspore samples of Pennsylvanian age and three megaspore samples of Cretaceous age were analysed using micro-FTIR and Curie-point pyrolysis-gas chromatography-mass spectrometry. Both spectroscopic and pyrolytic investigations demonstrate that the sporopollenin of the fossil megaspores consists of both aliphatic and aromatic moieties. The micro-FTIR spectra of the spore wall of all megaspores are characterised by aliphatic $CH_x$ (3000-2800 and 1460-1450 $cm^{-1}$) and $CH_3$ (1375 $cm^{-1}$) absorptions, aromatic C=C (1560-1610 $cm^{-1}$) and CH (700-900 $cm^{-1}$) absorptions and various acid C=O group absorptions at 1740-1700 $cm^{-1}$. In the pyrolysates, alkylbenzenes and alkylphenols are the major aromatic compounds. A homologous series of *n*-alkenes/*n*-alkanes is also present in the pyrolysates of all fossil sporopollenin. Acetophenone has been found in the pyrolysates of all three megaspores of Cretaceous age, but is absent in the megaspores of Pennsylvanian age. The relative abundance of phenols compared to other compounds is higher in samples from the Cretaceous than those from the Pennsylvanian. It is suggested that oxygenated aromatic compounds were selectively degraded during burial and diagenesis with increasing thermal maturation and time. On the other hand, the relative abundance of aliphatic moieties selectively increased during burial and diagenesis with increasing thermal maturation and time. Aromatic compounds like cadalene, retene, dehydroabietane, simonellite and ferruginol are generally believed to represent the biomarkers of coniferous resins. However, these compounds were also detected in the pyrolysates of the megaspore *Paxillitriletes midas*. More investigations are needed to reveal the relationship between these biomarkers and sporopollenin.**

### 4.1. Introduction

Sporopollenins are the naturally occurring macromolecules that constitute the chemically resistant component of the outer wall (exine) of spores and pollens. Fossil sporopollenin is of

particular interest as it makes up the maceral sporinite which is an important component of some coals. Previously, it was believed that sporopollenin was chemically similar to carotenoids (Brocks and Shaw, 1968; Shaw, 1971). However, later investigations suggested that carotenoids do not contribute to sporopollenins (Herminghaus et al., 1988; Wehling et al., 1989) and that their identification could be due to incomplete purification of sporopollenin isolates (see de Leeuw and Largeau, 1993). More recent studies suggest that sporopollenins may have two different types of chemical structures. In one type the main building blocks are oxygenated aromatic compounds (e.g. Schenck et al., 1981; Schulze Osthoff and Wiermann 1987; Herminghaus et al., 1988; Wehling et al., 1989), while in the other, the main building blocks are aliphatic compounds (Guilford et al., 1988; Hayatsu et al., 1988; Stout 1993; Hemesly et al. 1992, 1996). van Bergen et al. (1993) showed that sporopollenin is composed of aliphatic compounds yielding *n*-alkane/*n*-alkene doublets on py-GC-MS, but also a series of oxygenated aromatic compounds which appeared to diminish in relative abundance with increasing maturation. Kawase and Takahashi (1995) carried out several spectroscopic analyses on sporopollenin from extant pollen and concluded that the main structure of sporopollenin is a simple aliphatic polymer containing aromatic or conjugated side chains. With respect to fossil material, very few papers have been published on well characterized spore material (see van Bergen et al., 2004 and references therein) and the definite chemical structure of this resistant macromolecule remains unclear. The present study aims to provide further insights into the chemical composition of the sporopollenin of handpicked fossil megaspores which have been isolated from sediments of low thermal maturity and which are taxonomically well assigned.

## 4.2. Experimental

### *4.2.1. Samples*

Six samples have been investigated from Pennsylvanian and Cretaceous sediments of Germany (Fig. 4.1). Three samples have been collected from Pennsylvanian sediments. Trilete megaspores (sample E51993) of black colour were isolated from a dark grey mudstone intercalated in seam V1/2 (Upper Horst Formation, upper Duckmantian, Pennsylvanian) encountered in borehole PH175/04 north of Bottrop, western Germany (Fig. 4.1). The borehole is located in the Ruhr Basin, western Germany. In this basin sediments of Duckmantian age have been deposited in a paralic environment. Organic carbon rich mudstones overlying coal seams are especially rich in a diverse, hygro- and hydrophilous plant association. A detailed account on the litho- and biostratigraphy of the Pennsylvanian of

the Ruhr Basin has recently been published by Wrede (2005) and on the coal evolution by Littke (1987) and Littke and ten Haven (1989). All selected megaspores are large (up to 2500 µm in diameter), laevigate, and the contact faces are indistinct (Plate 4.1, Figs. 1-2). Hence, all specimens have been assigned to the genus *Laevigatisporites* Ibrahim 1933 and most, if not all, belong to the species *Laevigatisporites reinschii* Ibrahim 1933. This megaspore genus was produced by Sigillariaceans (*Mazocarpon* and *Sigillariostrobus*; e.g. *Laevigatisporites reinschii* was isolated from the cone *Mazocarpon bensonii*) (Balme, 1995).

The organic rich mudstone from the Saarland (sample E51956) yielded small megaspores. The sample comes from a museum collection. The material was collected from an old slagheap near Weilerbach (Saarland, southwestern Germany) originating from a coal mine. Presumably, the coal produced is of Bolsovian or Asturian age (late Pennsylvanian). Detailed accounts on the geology, litho- and chronostratigraphy and thermal history of the Pennsylvanian in the Saar-Basin have recently been given by Hertle and Littke (2000) and Schäfer (2005). The megaspores are trilete, heavily folded, and laevigate (Plate 4.1, Figs. 3-4) which is diagnostic for the genus *Calamospora*. More than 100 species of this genus have been erected which makes it difficult to assign them undoubtedly to a taxon. However, most of the species are less than 200 µm and hence are miospores (for definition see Guennel, 1952). Contrary, the specimens from the Saarland sample are above 200 µm (around 300 µm) and therefore classified as megaspores. Lachkar (1975) described two *Calamospora* megaspore species from the Pennsylvanian of the Saar-Basin of which *Calamospora laevigata* (Ibrahim 1933) Schopf, Wilson & Bentall, 1944 fits well into the size range of the analysed specimens. During the Pennsylvanian most of *Calamospora* species have been produced by Equisetopsida and Noeggerathiales (Balme, 1995).

A third sample (E51996) was recovered from sediments of Asturian (Pennsylvanian) age cropping out at the banks of the river Mulde in the Zwickau Basin, eastern Germany. The sample was collected from the Zwickau Formation, about 3 m above the Cainsdorf volcanite near the equivalents of the Amandus-Seam. Documentation of the coal production in the Zwickau Basin goes back to the famous Agricola in the 15$^{th}$ century and because of the low thermal maturity samples of Pennsylvanian age from this basin were used for one of the very first publications on palynology (Reinsch, 1884). A detailed description of the Mulde section was published by Schneider et al. (2005). Despite the mudstones being unconsolidated due to weathering and frequent flooding by the Mulde River, the sediments in this section are rich in macrofloras and miospores (Herrmann, 2006). The sample processed for megaspores yielded a mono-generic assemblage of *Tuberculatisporites* sp., a genus which is characterised by

large ornaments along the equatorial outline and the distal face and by small cones on the contact areas (Plate 4.1, Figs. 5-6). *Tuberculatisporites* has been found *in situ* in cones of Sigillariaceae (*Mazocarpon*, *Sigillariostrobus*) (Balme, 1995).

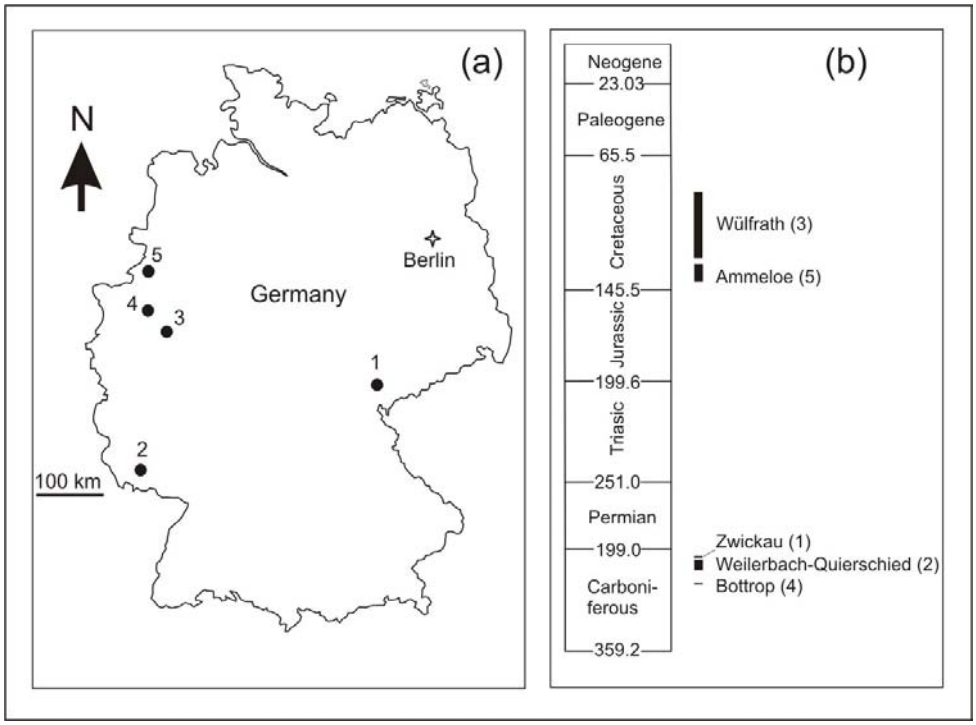


**Figure 4.1.** (a) Map of Germany showing megaspore sample localities; 1-Zwickau (E51996); 2-Weilerbach-Quierschied (E51956); 3- Wülfrath (E51997 & E51998); 4-Bottrop (E51993); 5-Ammeloe (Alstätte Embayment) (E51994); (b) Stratigraphic position of the megaspore samples. The age of the Carboniferous samples is well known while biostratigraphic control of the Cretaceous material is still poor. Absolute ages of the period boundaries are taken from Gradstein et al. (2004).

Cretaceous megaspores have been studied from two localities in western Germany. Sample E51994 comes from the borehole Ammeloe 36 located in the Alstätte Embayment close to the German-Dutch border. In this borehole a sequence of sands and grey clay-silt which is part of the Kuhfeld-Formation has been encountered. Samples were collected between 66.0-67.5 m. The Kuhfeld-Formation was deposited in a limnic-terrestrial and marine environment. The age of the base is Ryazanian-Valanginian and higher parts of the formation are of early to late Hauterivian age (Herngreen et al., 1994). These megaspores are assigned to the species

**Table 4.1.** Sample descriptions, bulk chemical and Rock-Eval data of the megaspore bearing host rock.

| Sample No. | Investigated Spore | Locality (within Germany) | Age | TOC (%) | $S_1$ | $S_2$ | HI | $T_{max}$ [°C] |
|---|---|---|---|---|---|---|---|---|
| E 51956 | *Calamospora laevigata* | Saarland | Pennsylvanian | 44.90 | 3.55 | 177.89 | 396 | 432 |
| E 51993 | *Laevigatisporites reinschii* | Ruhr Basin | Pennsylvanian | 5.47 | 0.09 | 12.32 | 225 | 437 |
| E 51996 | *Tuberculatisporites* sp. | Zwickau | Pennsylvanian | 2.17 | 0.02 | 1.49 | 36 | 429 |
| E 51994 | *Paxillitriletes midas* | Alstätte Embayment | Early Cretaceous | 4.79 | 0.15 | 5.92 | 124 | 419 |
| E 51997 | Megaspores | near Wülfrath | late Early to early Late Cretaceous | 2.62 | 0.05 | 0.94 | 36 | 422 |
| E 51998 | *Dijkstraisporites helios* | near Wülfrath | late Early to early Late Cretaceous | 6.74 | 0.11 | 2.05 | 30 | 418 |

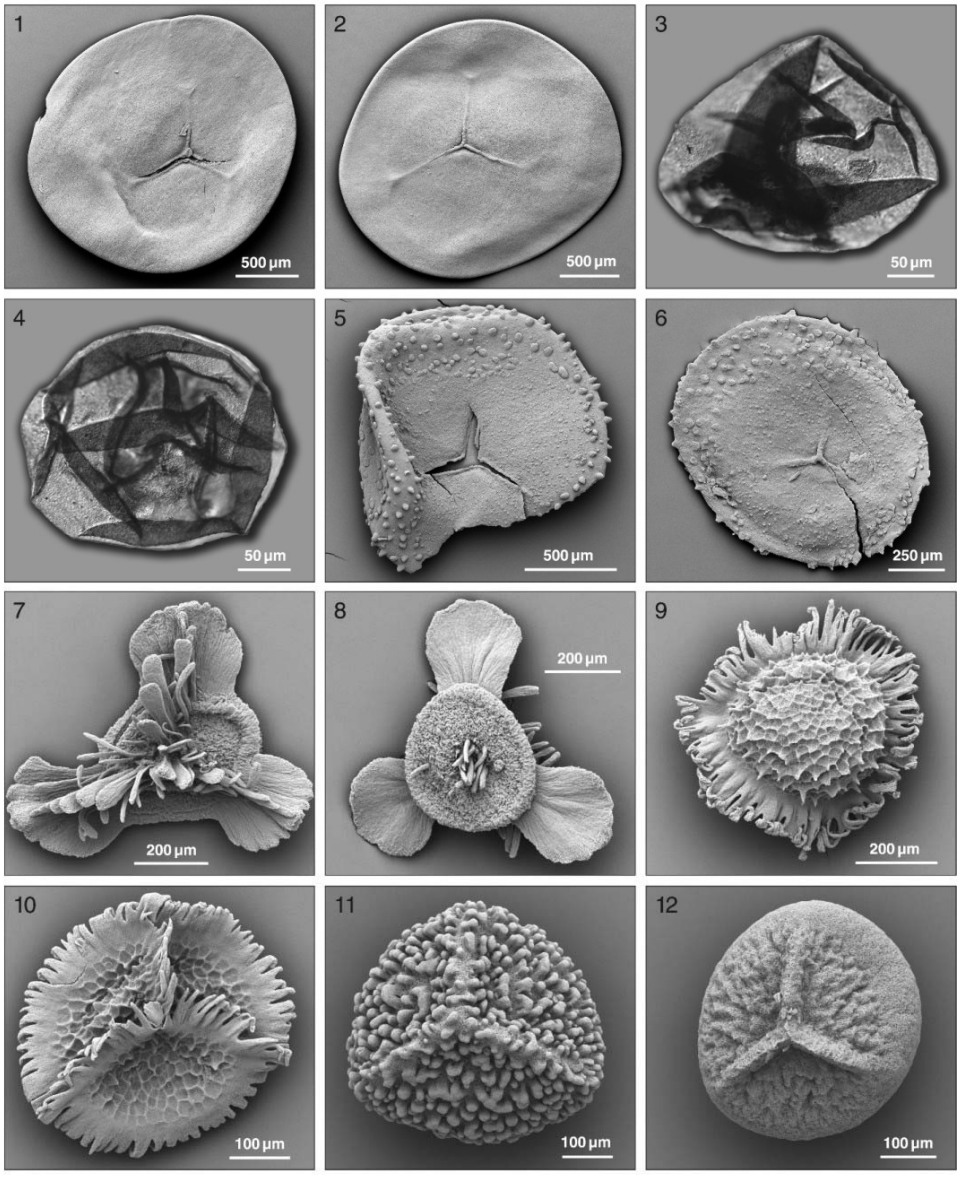
1
500 µm
2
500 µm
3
50 µm
4
50 µm
5
500 µm
6
250 µm
7
200 µm
8
200 µm
9
200 µm
10
100 µm
11
100 µm
12
100 µm

Plate 4.1

**Plate 4.1**

Scanning electron micrographs (except Figs. 3-4) of megaspores. All S.E.M. stubs and slides are housed in the Geological Survey of North Rhine-Westphalia.
**Figs. 1-2.** *Laevigatisporites reinschii* Ibrahim, 1933, Ruhr Basin, sample E51993.
**Figs. 3-4.** *Calamospora laevigata* (Ibrahim 1933) Schopf, Wilson & Bentall 1944, Saar Basin, sample E51956, transmitted light illumination, Nomarski differential interference contrast.
**Figs. 5-6.** *Tuberculatisporites* sp. Zwickau Basin, sample E51996.
**Figs. 7-8.** *Paxillitriletes midas* (Dijkstra 1951) Hall & Nicolson 1973, Alstätte Embayment, sample E51994. Fig. 7 proximal face, Fig. 8 distal face.
**Figs. 9-10.** *Dijkstraisporites helios* (Dijkstra) Potonié 1956, Cretaceous karst infills near Wülfrath, sample E51998. Fig. 9 distal face, Fig. 10 proximal face.
**Figs. 11-12.** unidentified megaspores, Cretaceous karst infills near Wülfrath, sample E51997.

---

*Paxillitriletes midas* (Dijkstra 1951) Hall & Nicolson 1973 (Plate 4.1, Figs. 7-8). Based on the wall ultrastructure, *Paxillitriletes midas* is thought to have isoetalean origin (Batten & Koppelhus, 1993). Two samples (E51997, E51998) have been collected from Cretaceous karst infills near Wülfrath, Bergisches Land, western Germany. Sediments of these karst deposits have never experienced overburden as they are preserved in Devonian limestones up to 200 m below the present surface (Drozdzewski et al., 1998). The sediment is rich in well preserved plant remains including angiosperm flowers. Most of the plant remains are charred by wildfires. Age assignment is still difficult but palynological data indicate a late Early to early Late Cretaceous age. Sample E51998 exclusively consists of a reticulate megaspore with an encircling equatorial zona, and raised fimbriate laesural lips (Plate 4.1, Figs. 9-10). These megaspores have been assigned to *Dijkstraisporites helios* (Dijkstra) Potonié 1956. For this species an isoetalean affinity has been suggested by Wilde and Hemsley (2000). Sample E51997 comprises megaspores of different genera and hence no biological affinity can be deduced. Two specimens demonstrating the wide range of morphological features of these megaspores are shown on Plate 4.1, Figs. 11-12.

### *4.2.2. Palynological preparation*

Megaspores from indurated sediments of Pennsylvanian age have been isolated using standard palynological techniques, i.e. HF and HCl acid maceration. The resultant residue was further concentrated by sieving with a 200 μm polyester fabric to recover the megaspores and rinsed in bi-distilled water. The megaspores were first air-dried before selecting specimens with no adhering sediment particles using a dissecting binocular microscope. No oxidants were applied and samples were not heated during processing.

Sediments from the Cretaceous were not consolidated and could be disaggregated using warm tap water (< 38 °C), only. After breakdown of the matrix the slurry was washed through a sieve with mesh openings of 200 µm. The residue usually consisting of a large amount of sand grains and organic matter was subjected to the swirling technique to get off the siliciclastic fraction. The resultant organic matter was washed with bi-distilled water and air-dried. From the rich and diverse megaspore assemblage usually the most abundant genus/species was selected using a dissecting binocular microscope. Hence, most samples analysed consist of a pure concentrate of a single megaspore genus or species. As to most specimens some sediment was still adhering they were all submitted to HF treatment following frequent rinsing in bi-distilled water and then air-dried.

Some well-preserved specimens were thoroughly cleaned with hydrofluoric acid, rinsed in bi-distilled water, air-dried, and mounted with adhesive tabs on stubs. These were then gold coated and examined using a CamScan MV 2300 at the University of Bonn, Palaeontological Institute. Permanent mounts for transmitted light microscopy were produced with PVA as the mounting medium and Elvacite 2044$^{TM}$ epoxy resin as the embedding medium.

*4.2.3. Micro-FTIR Spectroscopy*

Micro-FTIR spectroscopic analyses were performed in transmission mode using a Nic-Plan microscope and a Protégé 460 FT-IR optical bench operated by the OMNIC® software. The microscope is equipped with an objective 15x/N.A. 0.58 with reflecting lenses of a Cassegrainian design and a Cassegrainian condenser. Two adjustable rectangular apertures allow to precisely define the size and shape of the measured area. The optical bench includes an Ever-Glo source, a KBr beamsplitter, and MCT-A detector which requires liquid-nitrogen cooling during data collection. Spectra were obtained of a defined area by co-adding up to 1024 scans with a spectral resolution of 4 $cm^{-1}$. The standard setting was 1024 scans/4 $cm^{-1}$ or 512 scans/4 $cm^{-1}$. The recorded spectral range was within 4000-650 $cm^{-1}$. Background spectra were collected after every sample. As the air in the system was not purged the spectra show the $CO_2$ band at 2360. All specimens were placed on a NaCl sample support (size 13 x 2 mm). This analysis was carried out at the school of Ocean and Earth Science, Southampton Oceanography Centre, University of Southampton, UK.

*4.2.3. Curie point pyrolysis-gas chromatography-mass spectrometry*

Samples were pyrolysed at 650°C for 10 s using a Curie-point pyrolyser (Pyromat) coupled directly to a HP gas chromatography-mass spectrometer (Cupy-GC-MS) system (Model No:

HP GC-MS 5973). The GC was operated in the splitless mode and was equipped with a 50 m SGE BPX5 fused silica capillary column with an inner diameter of 220 μm and film thickness of 0.25 μm. An initial oven temperature of 50°C was held for 2 min and then heated with 4°C $min^{-1}$ to 310°C. The oven was then maintained isothermally for 12 min. Carrier gas was helium. MS parameters included 70 eV EI ionisation, a source temperature of 230ºC and a mass range of 30-550 dalton. Peak assignments were based on GC retention time and mass spectral data including comparison to MS libraries. This analysis was carried out at GSG Mess-und Analysengeräte GmbH, Bruchsal, Germany.

### 4.3. Results and discussion

*4.3.1. FTIR spectral characteristics of fossil sporopollenin*

Sporopollenin of all the megaspore samples from the Pennsylvanian and Cretaceous shows similar functional groups distribution (Figs. 4.2a-c; 4.3a-c). Spectral bands were assigned with reference to the literature (for example, Guo and Bustin, 1998; Arouri et al., 1999; Yule et al., 2000). These fossil megaspores contain abundant aliphatic structures as indicated by the very strong aliphatic $CH_x$ band in the region 2930-2850. Strong narrow absorptions centered in the range from 2920 $cm^{-1}$ to 2930 $cm^{-1}$ and from 2852 $cm^{-1}$ to 2856 $cm^{-1}$ are due to asymmetric stretching vibration from $CH_2$ methylene and symmetric stretching vibrations from $CH_2$ methylene groups, respectively. The peak at 1700-1710 $cm^{-1}$ is assigned to aromatic carbonyl/carboxyl C=O groups which is more intense in the megaspore samples from the Cretaceous (Figs. 4.3a-c) than that of megaspores from the Pennsylvanian (Figs. 4.2a-c). The aromatic carbonyl/carboxyl C=O group in the IR spectra of megaspores from the Pennsylvanian occur as a slight shoulder (Figs. 4.2a-c). The increase in the absorbance of the 1700 $cm^{-1}$ carbonyl/carboxyl C=O group band may be related to oxidation affecting megaspores from the Cretaceous. Guo and Bustin (1998) reported IR spectra of sporinite where the intensity of C=O groups is very low. They suggested that the strong C=O group absorption may be due to oxidation effects of sporopollenin during diagenesis or sample preparation. It is worthwhile to mention that no oxidants were applied during sample preparation. The peak due to aromatic C=C ring stretching has moderate intensity and occurs at about 1610 $cm^{-1}$. The peak at 1450 $cm^{-1}$ to 1460 $cm^{-1}$ is assigned to $CH_2$ and $CH_3$ deformation. The peak at 1450-1460 $cm^{-1}$ is made up of the $CH_2$ deformation at 1465 $cm^{-1}$ and $CH_3$ deformation at 1450 $cm^{-1}$ and peak shift from 1450 to 1460 $cm^{-1}$ may represent an increase in the $CH_2$ component in the structure (Guo and Bustin, 1998). A low

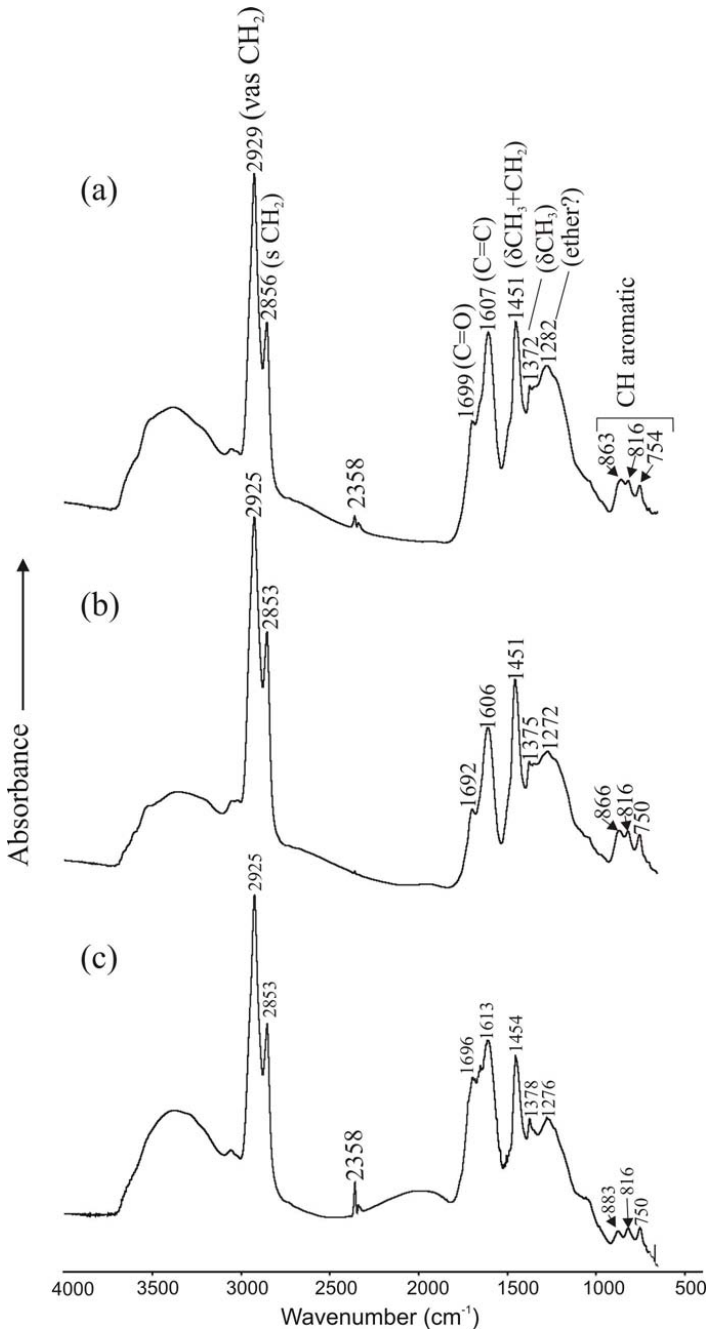


**Figure 4.2.** Micro-FTIR spectra of megaspores from the Pennsylvanian. (a) *Tuberculatisporites* sp.; (b) *Laevigatisporites reinschii*; (c) *Calamospora laevigata*. Assignments of absorption bands and vibration modes (δ=deformation; ν=stretching; s=symmetric; as=asymmetric) are indicated in parentheses.

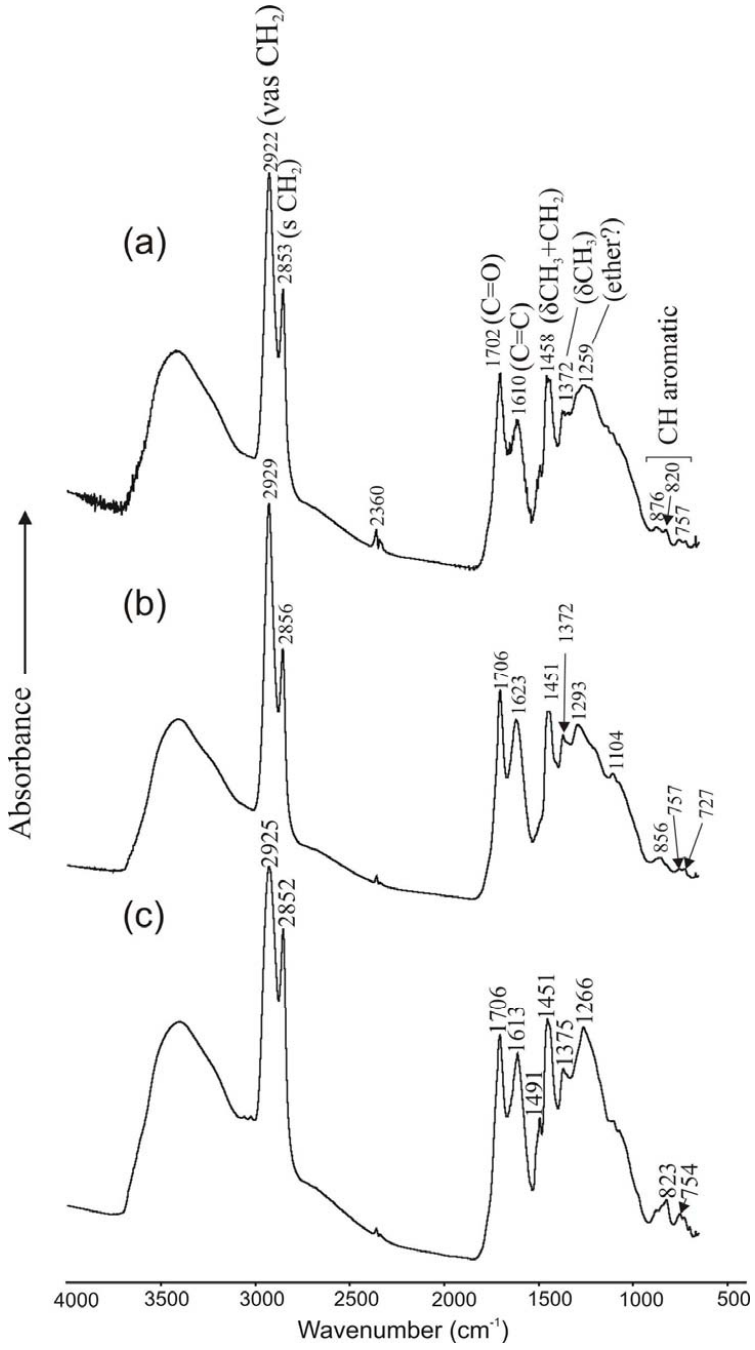


**Figure 4.3.** Micro-FTIR spectra of megaspores of Cretaceous age. (a) *Dijkstraisporites helios*; (b) Megaspore E51997 (not identified); (c) *Paxillitriletes midas*. Assignments of absorption bands and vibration modes (δ=deformation; ν=stretching; s=symmetric; as=asymmetric) are indicated in parentheses.

absorption for aliphatic bending occurs at 1375 $cm^{-1}$ in all spores. The C-O wide band centered at about 1260 $cm^{-1}$, mainly reveals ether functions (see Pradier et al., 1992). This wide peak is found in IR spectra of all megaspore specimens. All megaspores show a similar pattern of absorption due to aromatic CH out of plane deformation at 700-900 $cm^{-1}$. The CH out of plane region is much more prominent in the megaspores from the Pennsylvanian compared to Cretaceous megaspores. A moderate broad absorption occurs at about 3400 $cm^{-1}$ which could be due to phenolic OH, and/or carboxylic OH. It is also possible that atmospheric moisture became absorbed onto the spore surface during sample preparation.

*4.3.2. Curie point pyrolysis-gas chromatography-mass spectrometry*

The reconstructed total ion chromatograms of pyrolysates from different megaspores are shown in Figures 4.4, 4.5 and 4.6. The pyrolysates of megaspores (Figs. 4.4a-c) from the Pennsylvanian predominantly consist of *n*-alkenes and *n*-alkanes, ranging from $C_6$ to at least $C_{24}$. The major aromatic compounds (Table 4.2) are alkylbenzenes, alkylphenols and methylnaphthalenes. The predominant pyrolysates of all megaspores, i.e alkylbenzenes, alkylphenols, and methylnaphthalenes indicate an aromatic macromolecular moiety, whereas the homologous series of *n*-alkenes and *n*-alkanes indicate an aliphatic macromolecular moiety.

The pyrolysates of *Dijkstraisporites helios* and another megaspore concentrate (E51997) from the Cretaceous consist of both aliphatic and aromatic compounds (Fig. 4.5). Aliphatic compounds consist of a series of *n*-alkenes and *n*-alkanes, ranging from $C_6$ to at least $C_{18}$. The major aromatic compounds are alkylbenzenes and alkylylphenols (Table 4.2). Other aromatic compounds like acetophenone occur in subordinate amount in the pyrolysates of all fossil spores of Cretaceous age.

The pyrolysis products of the megaspore *Paxillitriletes midas* (Fig. 4.6) of Cretaceous age are dominated by aromatic compounds. Oxygenated aromatic compounds like alkylphenols and acetophenone have been detected in the pyrolysates. A series of alkylbenzenes and alkenylbenzenes (up to $C_{12}$) are present in the pyrolysates. *n*-Alkenes and *n*-alkanes, ranging from $C_7$ to at least $C_{18}$ are also present. Aromatic compounds like cadalene, retene, dehydroabietane, simonellite and ferruginol (Fig. 4.7) are found in the pyrolysates of *Paxillitriletes midas*.

Both spectroscopic and pyrolytic investigations of the present study as well as previous investigations clearly demonstrate that aliphatic moieties are significant constituents of fossil

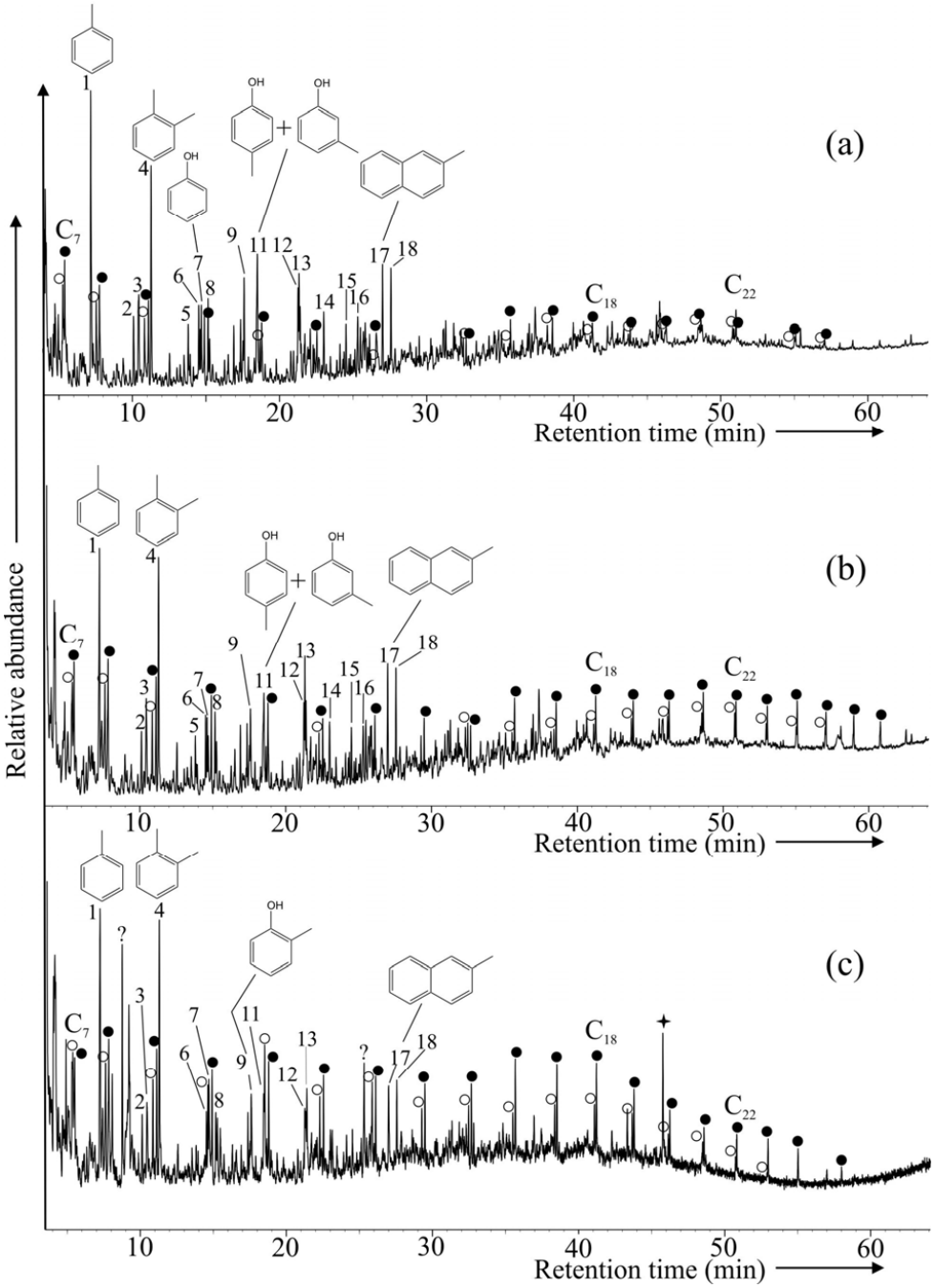


**Figure 4.4.** Total ion chromatograms resulting from the Curie point pyrolysis-GC-MS (pyrolysis at 610ºC for 10 s) of megaspores from the Pennsylvanian. (a) *Tuberculatisporites* sp.; (b) *Laevigatisporites reinschii***;** (c) *Calamospora laevigata*. The identification of the numbered peaks is listed in Table 4.2. Each doublet corresponds to an alkene (○) and an alkane (●); selected C- numbers are indicated. ✦ indicates contaminant.

sporopollenin. van Bergen et al. (1993) reported that the pyrolysis products of fossil megaspores of *Parazolla* include both oxygenated aromatics and a homologous series of *n*-alkenes and *n*-alkanes. Similarly, pyrolysis products of the Carboniferous megaspore (*Tuberculatisporites*) consist of several aromatic compounds and a series of *n*-alkenes and *n*-alkanes (Collinson et al., 1994). Hayatsu et al. (1988) suggested that sporopollenin was composed of oxygenated aromatic and aliphatic moieties which were linked together through ether/ester linkages. van Bergen et al. (1993) alternatively evoked that both moieties, aromatic and aliphatic, may represent macromolecules which are present in different layers of both, the resistant tissues outside the exine as well as within the exine. Kawase and Takahashi (1995) carried out several spectroscopic investigations of sporopollenin and suggested that the main structure of sporopollenin is a simple aliphatic polymer containing aromatic or conjugated side chains. On the contrary, the pyrolysates of the extant spore walls consist almost exclusively of aromatic compounds and very low amounts of aliphatic constituents represented by $C_{16}$ and $C_{18}$ fatty acids (see van Bergen et al., 1993; 2004; de Leeuw et al., 2006). It is worthwhile to mention that the migration of aliphatic moieties from sediment matrix to fossil remains is a topic of considerable debate in the field of organic geochemistry (see Zhang et al., 1993; Stankiewicz et al., 2000; Versteegh et al., 2004; de Leeuw et al., 2006). Mobilisation and migration of aliphatic moieties from aliphatic-rich components (liptinites) to nonaliphatic ones (vitrinite) with increasing diagenesis has been used to explain chemical alterations in composition of coal macerals derived from aliphatic-poor macromolecules such as lignin (Zhang et al., 1993). Very recently, de Leeuw et al. (in press) suggested that aliphatic compounds represent an aliphatic geopolymer produced during burial and diagenesis from low such-molecular-weight lipids such as plant waxes consisting of saturated and unsaturated hydrocarbons, alcohols, fatty acids or, even, from unsaturated lipids present in the original spores or pollen that may get attached to the spore wall serving as a matrix through oxidative cross linking (see also Versteegh et al., 2004). However, Stankiewicz et al. (2000) carried out thermal maturation studies on modern arthropod cuticles which consist of chitin-protein complex (with major chitin and protein derived biomarkers in the pyrolysates). They found that thermal maturation at 350°C results in extensive alteration of the macromolecular composition without change in morphology. *n*-Alkene/*n*-alkane doublets are the dominant pyrolysis products of cuticles. They concluded that aliphatic hydrocarbons must be present in the arthropod cuticles. We also believe that *n*-alkene/*n*-alkane doublets should be a product of aliphatic macromolecules of the fossil spore wall. The relative abundance of *n*-alkenes/*n*-alkanes in pyrolysates of megaspores from Pennsylvanian

sediments is higher than in those from the Cretaceous. As the megaspores from the Pennsylvanian are older as well as thermally more mature than those from the Cretaceous

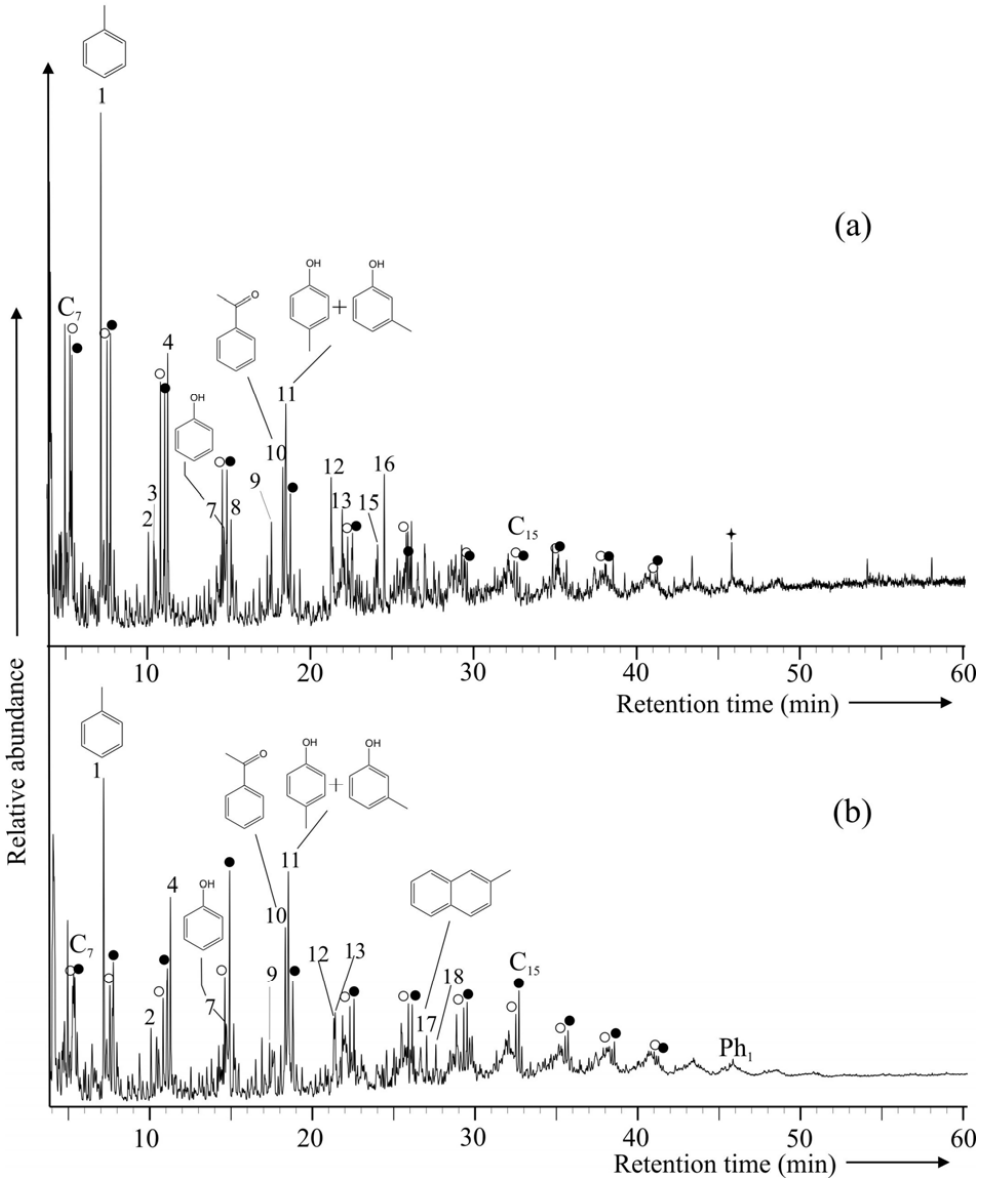


**Figure 4.5.** Total ion chromatogram resulting from the Curie point pyrolysis-GC-MS (pyrolysis at 610ºC for 10 s) of Cretaceous megaspores. (a) *Dijkstraisporites helios*; (b) Megaspore concentrate E51997 (not identified). The identification of the numbered peaks is listed in Table 4.2. Each doublet corresponds to an alkene (○) and an alkane (●); selected C- numbers are indicated.

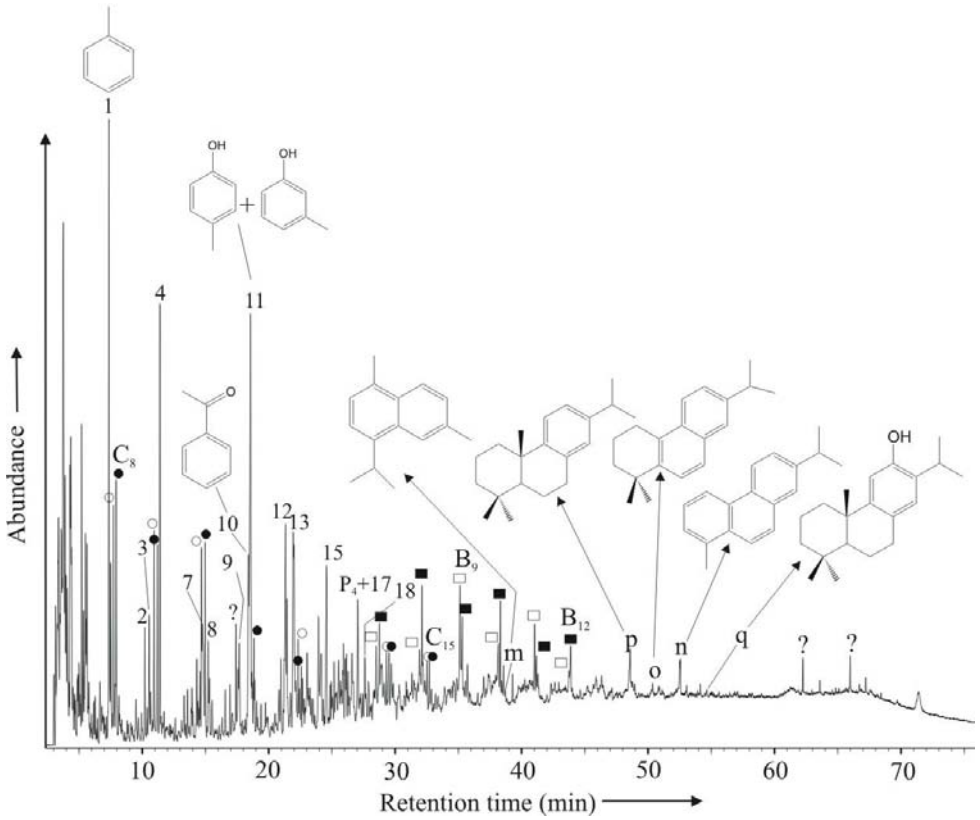


**Figure 4.6.** Total ion chromatogram resulting from the Curie point pyrolysis-GC-MS (pyrolysis at 610ºC for 10 s) of *Paxillitriletes midas* of Cretaceous age. The identification of the numbered peaks is listed in Table 4.2. Each doublet corresponds to an alkene (○) and an alkane (●); selected C- numbers are indicated. $P_4$ indicates $C_4$ phenol.

(see Table 4.1), it is apparent that the aliphatic building blocks were selectively preserved during burial and diagenesis with increasing thermal maturity and time.

Among the oxygenated aromatic compounds phenols are quite dominant and appear to be characteristic for sporopollenin. The phenols are not only present in the biomacromolecule of sporopollenin but also present in other parts of higher plants. They are also found as part of lignin (see Hatcher and Clifford, 1997), seed coats of higher plants (van Bergen et al., 1994) and plant cuticles (Mösle et al., 1998). The phenolic compounds played a central role in the evolution of land plants; because the ability for early land plants in colonizing the lands required evolutionary innovations which were not only anatomical or morphological but also

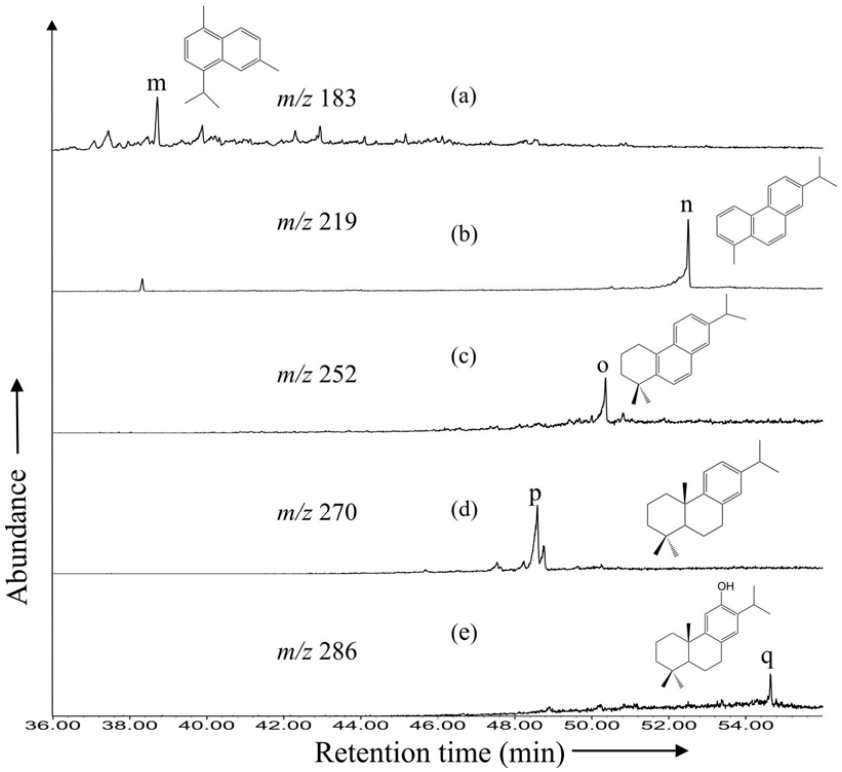


**Figure 4.7.** Partial mass chromatograms resulting from Curie point pyrolysis-GC-MS (pyrolysis at 610ºC for 10s) of the megaspore *Paxillitriletes midas* of Cretaceous age at (a) *m/z* 183; (b) *m/z* 219; (c) *m/z* 252; (d) *m/z* 270; (e) *m/z* 286. The identification of the peaks is listed in Table 4.2.

biochemical (see Cooper Driver, 2001 for review). Pyrolysates of sporopollenin from miospore massulae of the modern *Azolla* and the megaspore *Salvinia* showed the presence of *p*-vinylphenol which is the pyrolysis product of *p*-coumaric acid, and also 4-vinyl-2-methoxyphenol (found in pyrolysates of the megaspore *Salvinia*) which is the pyrolysis product derived from ferulic acid (van Bergen et al., 1993). It has been suggested that both *p*-coumaric acid and ferulic acid protect the spore from UV radiation and the relative proportion of these acids can be used for the reconstruction of historic variation in solar UV-B levels (Rozema et al., 2001, 2002). However, pyrolysates of megaspores of the present study do contain phenol and its alkylated homologs which do not have direct structural link with cinnamic acids. The pyrolysates of sporinite rich maceral concentrates did not show any cinnamic acid derived pyrolysis products (Nip et al., 1988). Collinson et al. (1994) also reported several simple aromatics and phenols in the pyrolysates of Carboniferous miospores and megaspores, but no cinnamic acid derived compounds have been reported.

**Table 4.2.** Aromatic products detected from Curie point pyrolysis of different megaspores of Pennsylvanian and Cretaceous age.

| Peak | Product |
|---|---|
| 1 | Toluene |
| 2 | Ethylbenzene |
| 3 | 1,3- and 1,4-Dimethylbenzene |
| 4 | 1,2-Dimethylbenzene |
| 5 | 1-Methyl-3-ethylbenzene |
| 6 | 1-Methyl-2-ethylbenzene |
| 7 | Phenol |
| 8 | 1,2,4-Trimethylbenzene |
| 9 | 2-Methylphenol |
| 10 | Acetophenone |
| 11 | 3-and 4-Methylphenol |
| 12 | $C_2$-Phenol |
| 13 | $C_2$-Phenol |
| 14 | Naphthalene |
| 15 | $C_3$-Phenol |
| 16 | $C_3$-Phenol |
| 17 | 2-Methylnaphthalene |
| 18 | 1-Methylnaphthalene |
| m | Cadalene |
| n | Retene |
| o | Simonellite |
| p | Dehydroabietane |
| q | Ferruginol |

Acetophenone is another oxygenated aromatic compound which is present in subordinate amount in the pyrolysates of Cretaceous megaspores. However, alkylated homologs of acetophenone have not been detected. High abundance of acetophenone and its alkylated homologs have been reported from rock extract of the Posidonia Shale by Wilkes et al. (1998). Acetophenone has been detected in high abundance in the pyrolysates of extant spores (see van Bergen et al., 1993; 2004), but is absent in the pyrolysates of the Pennsylvanian megaspores of the present investigation. It is also noteworthy to mention that relative abundance of phenols compared to other compounds is higher in the Cretaceous megaspores than in the Pennsylvanian megaspores (Fig. 4.8). As the spores from the Pennsylvanian are older as well as thermally more mature than those from the Cretaceous (see Table 4.1), it is possible that the oxygenated aromatic compounds were selectively degraded during burial and diagenesis with increasing thermal maturation and time.

The pyrolysis products of the megaspore *Paxillitriletes midas* (Fig. 4.6) of Cretaceous age are different compared to other spores of the present investigation. A homologous series of *n*-alkylbenzenes and *n*-alkenylbenzenes ranging up to $nC_{12}$ is revealed by the *m/z* 91 and *m/z*

104 mass chromatograms, respectively (data not shown). A similar distribution of *n*-alkylbenzenes (up to $C_{10}$) was reported from the pyrolysates of megasporinite (Stout, 1993).

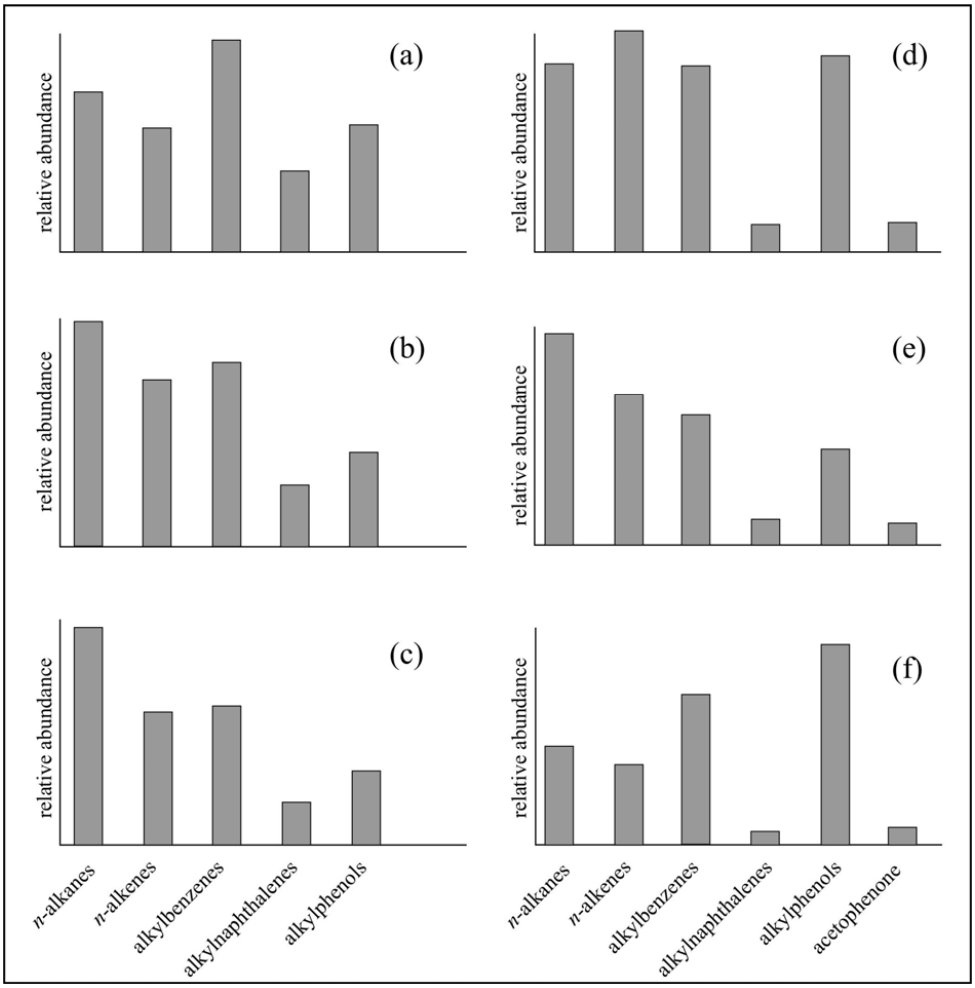


**Figure 4.8.** Histograms showing relative abundance of various compound classes in the pyrolysates of megaspores (a) *Tuberculatisporites* sp.; (b) *Laevigatisporites reinschii*; (c) *Calamospora laevigata*; (d) *Dijkstraisporites helios*; (e) Megaspore concentrate E51997 (not identified); (f) *Paxillitriletes midas*.

As mentioned earlier, compounds like cadalene, retene, dehydroabietane, simonellite and ferruginol (Fig. 4.7a-e) are found in the pyrolysates of *Paxillitriletes midas*. These compounds are believed to be derived from conifer resins (Simoneit, 1977, Ellis et al., 1996; Haberer et al., 2006). However, retene and dehydroabietane have also been identified in pyrolysates of algal and bacterial organic matter (Zhou et al., 2000). Cadalene is believed to be derived from cadinenes and cadinols in plants, bryophytes, fungi (Bordoloi et al., 1989) and plant resins

(van Aarssen et al., 1990). To our best knowledge, these biomarkers are being reported for the first time from the pyrolysates of a fossil spore. It is noteworthy to remind that handpicked spore samples were extracted several times with dichloromethane to remove soluble organic matter. The extract has been analysed, but these biomarkers have not been detected. Therefore, it is evident that these aromatic compounds are derived from the macromolecule of the spore wall. More investigations are inevitable to reveal the relationship between these biomarkers and sporopollenin.

van Bergen et al. (2004) provided a tentative structure of sporopollenin in which long chain aliphatic units form the backbone of the structure and the cinnamic acids are the cross-linking units. They speculated that the hydrophobic long-chain aliphatic backbone could provide water repellent properties, and cinnamic acid units could provide UV protection. As the macromolecular structure of fossil sporopollenin is still not well understood, it is very difficult to propose any physiological properties of those compounds which might be significant building units of sporopollenin of some selected spores.

### 4.4. Conclusions

The present spectroscopic and pyrolytic investigations demonstrate that the sporopollenin from fossil megaspores of Pennsylvanian and Cretaceous age consists of both aromatic and aliphatic components. The micro-FTIR spectra of the spore walls are characterised by aliphatic $CH_x$ absorptions at 3000-2800 and 1460-1450 $cm^{-1}$, aromatic C=C ring stretching vibration and aromatic CH out of plane deformation at 1610-1560 and 900-700 $cm^{-1}$, respectively, and various acidic C=O group absorptions at 1740-1700 $cm^{-1}$.

Alkylated benzenes and alkylphenols are the major aromatic compounds present in the pyrolysates of all investigated megapores. Aliphatic compounds consist of a series of *n*-alkenes/*n*-alkanes. Acetophenone which has been found in the pyrolysates of extant spores, is also present in the pyrolysates of all three Cretaceous megaspores, but is absent in the pyrolysates of the Pennsylvanian megaspores. Moreover, the relative abundance of phenols compared to other compounds is higher in the Cretaceous megaspores than in those of the Pennsylvanian age. It is suggested that oxygenated aromatic compounds were selectively degraded during burial and diagenesis in older samples. The chemical composition of the megaspore *Paxillitriletes midas* differs from that of other megaspores which could be due to its taxonomic affiliation. Aromatic biomolecules like cadalene, retene, dehydroabietin, simonellite and ferruginol which are generally believed to be the biomarkers of coniferous

resins have been detected in the pyrolysates of *Paxillitriletes midas*. More investigations are needed to reveal the relationship between these biomarkers and sporopollenin.

The pyrolytic data reveal that the relative abundance of *n*-alkenes/*n*-alkanes in pyrolysates of megaspores from Pennsylvanian sediments is higher than in those from Cretaceous sediments. As the megaspores from the Pennsylvanian are older as well as thermally more mature than those of Cretaceous age, it is apparent that abundance of aliphatic moieties selectively increased during burial and diagenesis with increasing thermal maturation and time.

**Acknowledgements**

We would like to thank Deutsche Forschungsgemeinschaft (DFG), Bonn (grants no. Ma 1861/2 and /4) and Forschungszentrum Jülich for financial support. S. Roberts (University of Southampton) is thanked for supporting with Micro-FTIR investigations. For technical assistance, we thank U. Disko, F. Leistner and H. Willsch (all Forschungszentrum Jülich). We thank K. Jasper (University of Aachen) for providing us with the sample from the Ruhr Basin and H. Kerp (University of Münster) who placed the sample from the Saarland at our disposal. We are grateful to J. Galus (Geological Survey NRW) for support with kerogen separation.

**4.5. References**

van Aarssen, B.G.K., Cox, H.C., Hoogendoorn, P., de Leeuw, J.W., 1990. A cadinene biopolymer present in fossil and extant dammar resins as a source of cadinanes and bicadinanes in crude oils from South East Asia. Geochimica et Cosmochimica Acta 54, 3021-3031.

Arouri, K., Greenwood, P.F., Walter, M.R., 1999. A possible chlorophycean affinity of some Neoproterozoic acritarchs. Organic Geochemistry 30, 1323-1337.

Balme, B.E., 1995. Fossil in situ spores and pollen grains: an annotated catalogue. Review of Palaeobotany and Palynology 87, 81-323.

Batten, D.J., Koppelhus, E.B., 1993. Morphological reassessment of some zonate and coronate megaspore genera of mainly post-Palaeozoic age. Review of Palaeobotany and Palynology 78, 19-40.

van Bergen, P.F., Collinson, M.E., de Leeuw, J.W., 1993. Chemical composition and ultrastructure of fossil and extant salvinialean microspore massulae and megaspores. Grana Suppl. 1, 18-30.

van Bergen, P.F., Goñi, M., Collinson, M.E., Barrie, P.J., Sinninghe Damsté, J.S., de Leeuw, J.W., 1994. Chemical and microscopic characterization of outer seed coats of fossil and extant water plants. Geochimica et Cosmochima Acta 58, 3823-3844.

van Bergen, P.F., Blokker, P., Collinson, M.E., Sinninghe Damsté, J. P., de Leeuw, J.W., 2004. Structural biomacromolecules in plants: what can be learnt from the fossil records? In: Hemesly, A.R., Poole, I. (Eds.), Evolution of Plant Physiology, Elsevier, Amsterdam, pp. 133-154.

Bordoloi, M., Shukla, V.S., Nath, S.C., Sharma, R.P., 1989. Naturally occurring cadinenes. Photochemistry 28, 2007-2037.

Brocks, J., Shaw, G., 1968. Chemical structure of the exine of pollen walls and a new function for cartenoids in nature. Nature 219, 532-533.

Collinson, M.E., van Bergen, P.F., Scott, A.C., de Leeuw, J.W. 1994. The oil-generating potential of plants from coal and coal-bearing strata through time. In: Scott, A.C., Fleet A.J., (Eds.), Coal and Coal bearing Strata as Oil-prone Source Rocks? Geological Society Special Publication 77, 31-70.

Cooper-Driver, G.A., 2001. Biological roles for phenolic compounds in the evolution of early land plants. In: Gensel P.G., Edwards, D. (Eds.), Plants Invade the Land. Evolutionary and Environmental Perspectives. New York: Columbia University Press, pp. 159-172.

de Leeuw, J.W., Largeau, C., 1993. A review of macromolecular organic compounds that comprise living organism and their role in kerogen, coal and petroleum formation. In: Engel, M.H., Macko, S.A. (Eds.), Organic Geochemistry. Plenum Publishing Corp., New York, pp. 23-72.

de Leeuw, J.W., Versteegh, G.J.M., van Bergen, P.F., 2006. Biomacromolecules of algae and plants and their fossil analogues. Plant Ecology 182, 209-233.

Drozdzewski, G., Hartkopf-Fröder, C., Lange, F.G., Oesterreich, -B., Ribbert, K.-H., Voigt, S., Wrede, V., 1998. Vorläufige Mitteilung über unterkretazischen Tiefenkarst im Wülfrather Massenkalk (Rheinisches Schiefergebirge). Mitteilungen des Verbandes der deutschen Höhlen- und Karstforscher 44**,** 54-64.

Ellis, L., Singh, R.K., Alexander, R., Kagi, R.I., 1996. Formation of isohexyl alkylaromatic hydrocarbons from dramatization-rearrangement of terpenoids in the sedimentary environment: A new class of biomarker. Geochimica et Cosmochimica Acta 60, 4747-4763.

Gradstein, F.M., Ogg, J.G., Smith, A.G. (Eds.), 2004. A geologic time scale 2004. XX + 589 pp. Cambridge: Cambridge University Press.

Guennel, G.K., 1952. Fossil spores of the Alleghenian coals in Indiana. Indiana geological Survey Report of Progress 4, 1–40.

Guilford, W.J., Schneider, D.M., Labovitz, J., Opella, S. J., 1988. High resolution solid state $^{13}C$ NMR spectroscopy of sporopollenins from different plant taxa. Plant physiology 86, 134-136.

Guo, Y., Bustin, R.M., 1998. Micro-FTIR spectroscopy of liptinite macerals in coal. International Journal of Coal Geology 36, 259-275.

Haberer, R., Mangelsdorf, K., Wilkes, H., Horsfield, B., 2006. Occurrence and palaeoenvironmental significance of aromatic hydrocarbon biomarkers in Oligocene sediments from the Mallik 5L-38 Gas Hydrate Production Research Well (Canada). Organic Geochemistry 37, 519-538.

Hatcher, P.G., Clifford, D.J., 1997. The organic geochemistry of coal: from plant materials to coal. Organic Geochemistry 27, 251-274.

Hayatsu, R., Botto, R.E., McBeth, R.L., Scott, R.G., Winans, R.E., 1988. Chemical alteration of a biological polymer “sporopollenin” during coalification: Origin, formation, and transformation of the coal maceral sporinite. Energy & Fuels 2, 843-847.

Hemesly, A.R., Scott, A.C., Barrie, P.J., Chaloner, W.G., 1996. Studies of fossil and modern spore wall biomacromolecules using $^{13}C$ solid-state NMR. Annals of Botany 78, 83-94.

Herminghaus, S., Gubatz, S., Arendt, S., Wiermann, R. 1988. The occurrence of phenols as degradation products of natural sporopollenin – a comparison with 'synthetic sporopollenin'. Zeitschrift Naturforschung 43c, 491-500.

Herngreen, G.F.W., Hartkopf-Fröder, C., Ruegg, G.H.J., 1994. Age and depositional environment of the Kuhfeld Beds (Lower Cretaceous) in the Alstätte Embayment (W Germany, E Netherlands). Geologie en Mijnbouw 72, 375-391.

Herrmann, S., 2006. Palynologie, Palökologie und Biostratigraphie des Oberkarbon und Perm im Erzgebirge Becken.- unpubl. Diplomarbeit (Master thesis) Univ. Freiberg, 1-118.

Hertle, M., Littke, R., 2000. Coalification pattern and thermal modelling of the Permo-Carboniferous Saar Basin (SW-Germany). International Journal of Coal Geology 42, 273-296.

Kawase, M., Takahashi, M., 1995. Chemical composition of sporopollenin in *Magnolia grandiflora* (Magnoliaceae) and *Hibiscus syriacus* (Malvaceae). Grana 34, 242-245.

Lachkar, G., 1975. Les mégaspores du bassin houiller sarro-lorrain. Palaeontographica B150, 1-123.

Landais, P., Rochdi, A., Largeau, C., Derenne, S., 1993. Chemical characterization of torbanites by transmission micro-FTIR spectroscopy: Origin and extent of compositional heterogeneities. Geochimica et Cosmochimica Acta 57, 2529-2539.

Littke, R., 1987. Petrology and genesis of Upper Carboniferous seams from Ruhr region, Western Germany. International Journal of Coal Geology 7, 147-184.

Littke, R., ten Haven, H.L., 1989. Palaeoecologic trends and petroleum potential of Upper Carboniferous coal seams of Western Germany as revealed by their petrographic and organic geochemical characteristics. In: Lyons, P.C., Alpern, B. (Eds.), Peat and Coal 1, Origin, Facies and Depositional Models, International Journal of Coal Geology 13, 529-574.

Mösle, B., Collinson, M., Finch, P., Stankiewicz, B.A., Scott, A.C., Wilson, R., 1998. Factors influencing the preservation of plant cuticles: a comparison of morphology and chemical composition of modern and fossil examples. Organic Geochemistry 29, 1369-1380.

Nip, M., de Leeuw, J.W., Schenck, P.A., 1988. The characterization of eight maceral concentrates by means of Curie point pyrolysis-gas chromatography and Curie point pyrolysis-gas chromatography –mass spectrometry. Geochimica et Cosmochimica Acta 52, 637-648.

Pradier, B., Landais, P., Rochdi, A., Davis, A., 1992. Chemical basis of fluorescence alteration of crude oils and kerogens-II. Fluorescence and infrared micro-spectrometric analysis of vitrinite and liptinite. Organic Geochemistry 18, 241-248.

Reinsch, P.F., 1984. Micro-PalaeoPhytologia Formationis Carboniferae. Vol. 1, p. i-viii, 1-80, Vol. 2. p. i-iv, 1-55, Erlangae (Krische), Londinii (Quaritch).

Rozema, J., Broekman, R.A., Blokker, P., Meijkamp, B.B., de Bakker, N., van de Staaij, J., van Beem, A., Ariese, F., Kars, S.M., 2001. UV-B absorbance and UV-B absorbing compounds (*para*-cumaric acid) in pollen and sporopollenin: the perspective to track historic UV-B levels. Journal of Photochemistry Photobiology B: Biology 62, 108-117.

Rozema, J., van Geel, B., Björn, L.O., Lean, J., Madronich, S., 2002. Towards solving the UV puzzle. Science 296, 1621-1622.

Schäfer, A., 2005. Sedimentologisch-numerisch begründeter Stratigraphischer Standard für das Permo-Karbon des Saar-Nahe-Beckens. Courier Forschungsinstitut Senckenberg 254, 369-394.

Schenck, P.A., de Leeuw, J.W., van Grass, G., Haverkamp, J., Bouman, M., 1981. Analysis of recent spores and pollen and of thermally altered sporopollenin by flash pyrolysis-mass spectrometry and flash pyrolysis-gas chromatograpy-mass spectrometry. In: Brooks, J. (Ed.), Organic maturation studies and fossil fuel exploration. Academic Press, London, New York. pp. 225-237.

Schneider, J.W., Hoth, K., Gaitzsch, B.G., Berger, H.J., Steinborn, H., Walter, H., Zeidler, M. K., 2005. Carboniferous stratigraphy and development of the Erzgebirge Basin, East Germany.- Zeitschrift der deutschen Gesellschaft für Geowissenschaften 156, 431-466.

Schulze Osthoff, K., Wiermann, R., 1987. Phenols as integrated compounds of sporopollenin from *pinus* pollen. Journal of Plant Physiology 131, 5-15.

Simoneit, B.R.T., 1977. Diterpenoid compounds and other lipids in deep-sea sediments and their geochemical significance. Geochimica et Cosmochimica Acta 41, 463-476.

Shaw, G., 1971. The chemistry of sporopollenin. In: Brocks, J., Grant, P., Muir, M.D., Shaw, G., van Gijzel, P. (Eds.), Sporopollenin, Academic Press, London, pp. 305-350.

Stankiewicz, B.A., Briggs, D.E.G., Michels, R., Collinson, M.E., Flannery, M.B., Evershed, R.P., 2000. Alternative origin of aliphatic polymer in kerogen. Geology 28, 559-562.

Stout, S.A., 1993. Lasers in organic petrology and organic geochemistry. II. In situ laser micropyrolysis-GCMS of coal macerals. International Journal of Coal Geology 24, 309-331.

Versteegh, G.J.M., Blokker, P., Wood, G., Collinson, M.E., Sinninghe Damsté, J.S., de Leeuw, J.W., 2004. An example of oxidative polymerization of unsaturated fatty acids as a preservation pathway for dinoflagellate organic matter. Organic Geochemistry 35, 1129-1139.

Wehling, K., Niester, Ch., Boon, J.J., Willemse, M.T.M., Wiermann, R., 1989. *p*-Coumaric acid – a monomer in the sporopollenin skeleton. Planta 179, 376-380.

Wilde, V., Hemsley, A.R., 2000. Morphology, ultrastructure and affinity of Barremian (Lower Cretaceous) megaspores *Dijkstraisporites* and *Paxillitriletes* from Brilon-Nehden, Germany. Palynology 24, 217-230.

Wilkes, H., Disko, U., Horsfield, B., 1998. Aromatic aldehydes and ketones in the Posidonia Shale, Hill Syncline, Germany. Organic Geochemistry 29, 107-117.

Wrede, V., 2005. Das Oberkarbon (Silesium) am Nordrand des rechtsrheinischen Schiefergebirges (Ruhrkarbon). Courier Forschungsinstitut Senckenberg 254, 225-254.

Yule, B.L., Robers, S., Marshall, J.E.A., 2000. The thermal evolution of sporopollenin. Organic Geochemistry 31, 859-870.

Zhang, E., Hatcher, P.G., Davis, A., 1993. Chemical composition of pseudo-phlobaphinite precursors: implications for the presence of aliphatic biopolymers in vitrinite from coal. Organic Geochemistry 20, 721-734.

Zhou, W., Wang, R., Radke, M., Wu, Q., Sheng, G., Liu, Z., 2000. Retene in pyrolysates of algal and bacterial organic matter. Organic Geochemistry 31, 757-762.

# CHAPTER 5

## Molecular composition of Silurian scolecodonts (Gotland, Sweden) as revealed by pyrolysis-GC-MS

**Abstract**

**Sedimentary rock samples from the Silurian Högklint Formation of Gotland, Sweden, contain well-preserved scolecodonts. After kerogen separation scolecodonts were handpicked, cleaned and analysed by Curie point pyrolysis-gas chromatography-mass spectrometry to investigate their chemical composition. The major pyrolysis products from the scolecodonts are aromatic compounds such as alkylbenzenes, alkylnaphthalenes and alkylphenols. Aliphatic hydrocarbons are represented by homologous series of *n*-alkenes and *n*-alkanes. The presence of predominantly aromatic products in scolecodont pyrolysates suggests that kerogen consisting of marine zooclasts can yield a similar pattern of aromatic pyrolysis products as terrestrial higher plants. Except for phenols, no compounds diagnostic of amino acids have been recognised. Thus, it is concluded that amino acid related compounds which are commonly found in the extant polychaete jaws were degraded during diagenesis.**

### 5.1. Introduction

Scolecodonts are fossilized jaws of polychaete annelids of the order Eunicida. The oldest scolecodonts have been found in Lower Ordovician rocks, but they are most diverse and numerous in the Upper Ordovician, Silurian and Devonian (see Szaniawski, 1996). They occur in many types of marine sediments, but are most abundant in shallow water limestones and shales.

Despite their currently limited use as biostratigraphic indicators, scolecodonts are useful as indicators for thermal maturity of host rocks (see Goodarzi and Higgins, 1987; Bertrand, 1990). This is especially true for pre-Devonian sediments where the organic remains from higher plants are absent or very rare. Mineralogical/elemental composition of both extant and fossil polychaete jaws has recently been reported (Colbath, 1986; Eriksson and Elfman, 2000). Colbath (1986) suggested that jaw mineralization within the families of eunicean polychaetes is correlated with other features of jaw morphology and masculature and jaw

mineralogical composition may be a useful taxonomic character at the family level. The biogeochemical composition of scolecodonts is poorly known. It was speculated that the fossil jaws from the Paleozoic were made up of chitin (Hinde, 1879; cited in Colbath, 1986). Voss-Foucart et al. (1973) investigated the chemical composition of extant polychaete jaws and concluded that the extant jaws contain amino acids but no chitin. Nature and amount of protein derived compounds differ between taxa. With respect to fossil material, the definite chemical structure of the resistant macromolecules remains unclear. To our best knowledge, the biogeochemical composition of fossil polychaete jaws has never been elucidated. For the first time, the present study reports the biogeochemical composition of scolecodonts by using pyrolysis-gas chromatography-mass spectrometry.

### 5.2. Geological background

The Silurian, latest Llandovery to late Ludlow, of Gotland is known for well preserved scolecodonts. The map of Gotland showing different stratigraphical units and the sample location of the present investigation is given in Figure 5.1. An overview of the geology is presented by Hede (1960). The slight dip of the tectonically undisturbed layers exposes a stratigraphical sequence of about 500 m thickness. The strata are composed of various types of carbonate-rich sediments including biohermal limestone, stratified limestone, oolite, marlstone and siltstone (Bergman, 1989; Munnecke, 1997). Scolecodonts of the present investigation were collected from the Högklint Formation which is characterised by bioherms and argillaceous limestones intercalated with marlstone.

**Table 5.1.** Total organic carbon and Rock Eval data of scolecodont bearing sediments from the Högklint Formation.

| Sample No. | TOC (%) | $S_1$ (mg/g sample) | $S_2$ (mg/g sample) | HI (mg/g TOC) | $T_{max}$ (°C) |
|---|---|---|---|---|---|
| E51960 | 0.25 | 0.01 | 0.14 | 56 | 428 |
| E51961 | 0.18 | 0.01 | 0.09 | 50 | 421 |

The $T_{max}$ values (421°C and 428°C; Table 5.1) of sediments indicate a coalification stage corresponding to a vitrinite reflectance of approximately 0.50% $R_c$ (Espitalié et al., 1985), and thus the investigated samples are considered as immature.

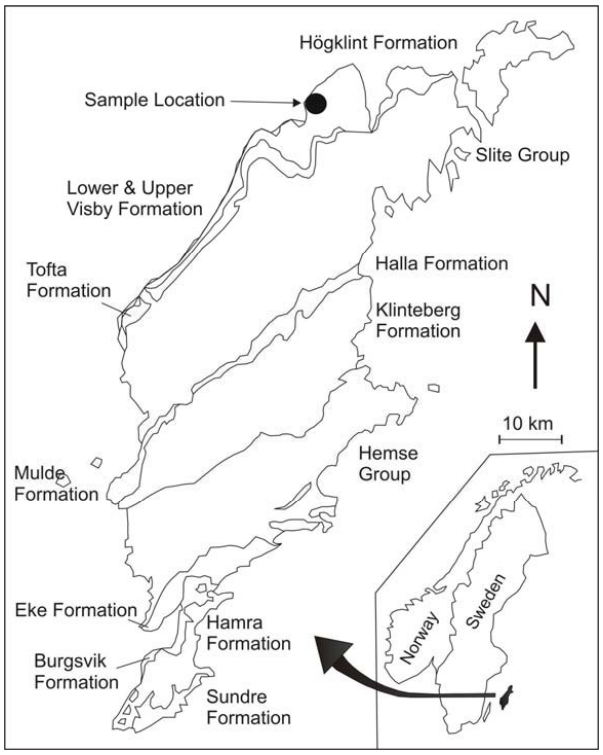


**Figure 5.1.** Map of Gotland showing different stratigraphical units and sample location (based on Hede, 1960).

## 5.3. Experimental

*5.3.1. Sample preparation*

Several samples were processed using standard palynological methods, i.e. HF, HCl and sieving with 20 µm polyester fabric. Two samples (E51960 and E51961) were selected because of high abundance of scolecodonts in the organic residues. By handpicking, a sample consisting of pure scolecodont concentrate was prepared from two kerogen fractions and was cleaned by dichloromethane to remove free hydrocarbons. Finally, about 300 µg (about 300-400 individuals) were analysed by Curie point pyrolysis-gas chromatography-mass spectrometry.

A specimen (Fig. 5.2) was mounted with adhesive tabs on stubs and then gold coated and examined using CamScan 44 scanning electron microscope at the University of Cologne, Geological and Mineralogical Institute.

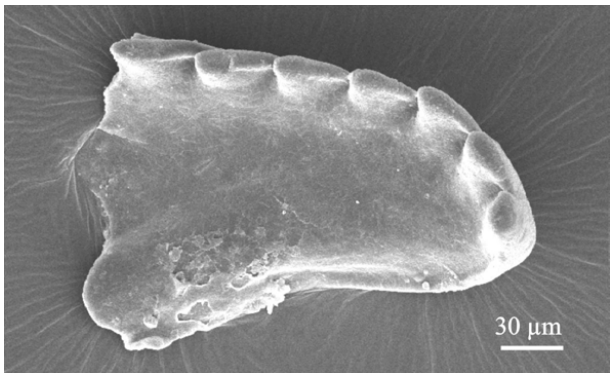


**Figure 5.2.** Scanning electron micrograph of a scolecodont from the Högklint Formation, Gotland, Sweden (micrograph courtesy of C. Hartkopf-Fröder).

*5.3.2. Curie point pyrolysis-gas chromatography-mass spectrometry*

Samples were pyrolysed at 650°C for 10 s using a Curie-point pyrolyser (Pyromat) coupled directly to a HP gas chromatography-mass spectrometer (Cupy-GC-MS) system (Model No: HP GC-MS 5973). The GC was operated in the splitless mode and was equipped with a 50 m SGE BPX5 non-polar column with an initial oven temperature of 50°C held for 2 min, then heated with 4°C $min^{-1}$ to 310°C. The oven was then maintained isothermally for 12 min. Inner diameter of the column was 220 μm and film thickness was 0.25 μm. Carrier gas was helium. MS parameters included 70 eV EI ionisation, a source temperature of 230ºC and a mass range of 30-550 dalton. Peak assignments were based on GC retention time and mass spectral data including comparison to MS libraries.

## 5.4. Results and discussion

The total ion chromatograms (TICs) from Curie point pyrolysis-gas chromatography-mass spectrometry of scolecodonts and the total kerogen fraction (size >20 μm) are shown in Figures 5.3(a) and 5.3(b), respectively. The major pyrolysis products from the scolecodonts include aromatic hydrocarbons such as alkylbenzenes, alkylnaphthalenes and alkylphenols. Aliphatic hydrocarbons are represented by a homologous series of *n*-alkenes and *n*-alkanes. The identification of the aromatic compounds from the pyrolysates is given in Table 5.2. The corresponding analysis of the total kerogen fraction (size > 20 μm) shows a series of *n*-alkenes and *n*-alkanes, ranging from $C_6$ to $C_{19}$ (Fig. 5.3b). The aromatic compounds are represented by alkylbenzenes, alkylnaphthalenes and alkylphenols. The overall chemical composition of the handpicked scolecodont concentrate and total organic residues does not show significant differences (Fig. 5.4).

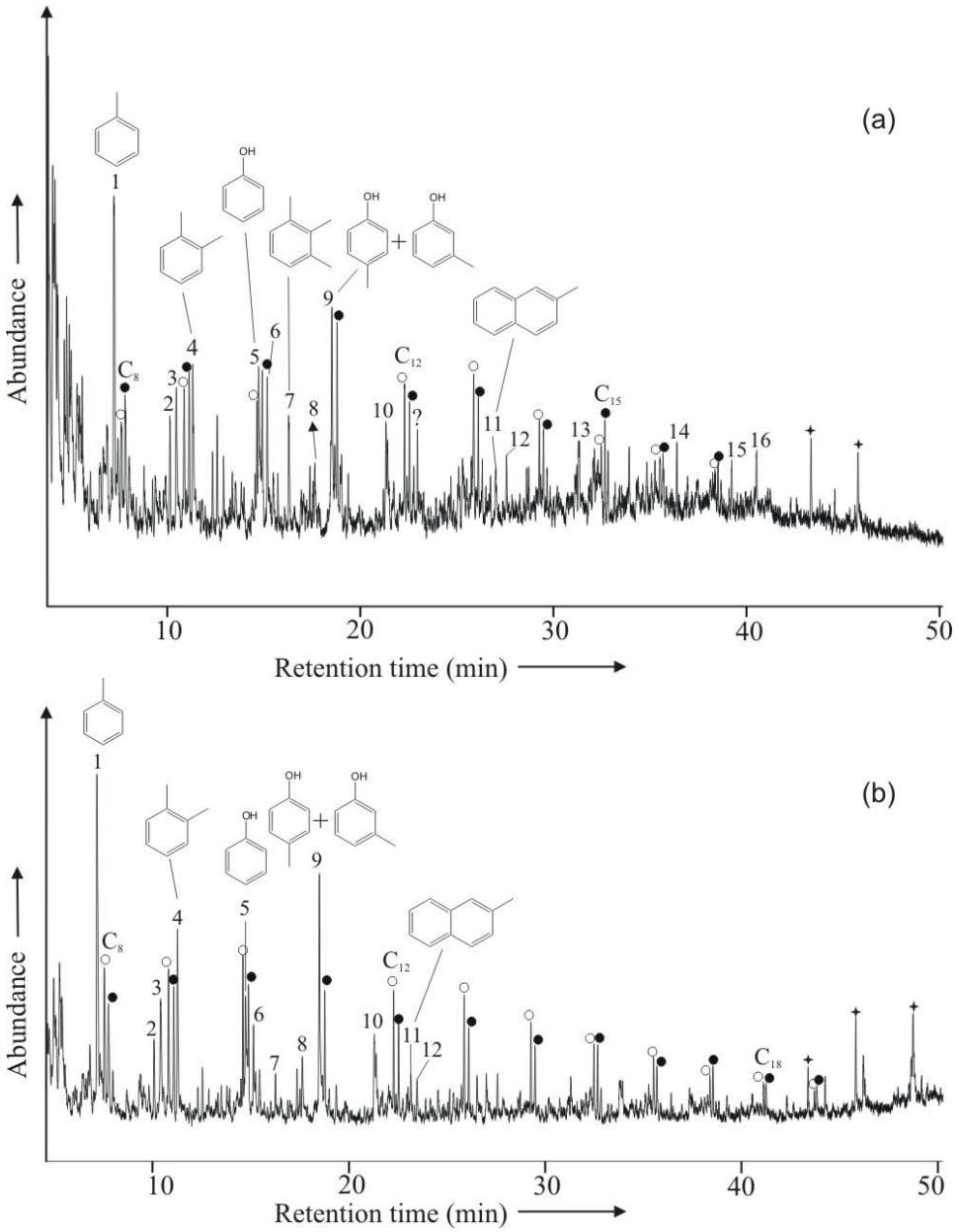


**Figure 5.3.** Reconstructed total ion chromatogram resulting from Curie point pyrolysis-GC-MS (pyrolysis at 610ºC for 10s) of (a) handpicked scolecodonts (E 51960 & E 51961) and (b) total kerogen (E 51960; size>20 μm) from the Högklint Formation, Gotland, Sweden. Each doublet corresponds to an alkene (○) and an alkane (●); selected C-numbers are indicated. ✦ indicates contaminant. Numbers indicating major aromatic compounds in the pyrolysates are listed in Table 5.2.

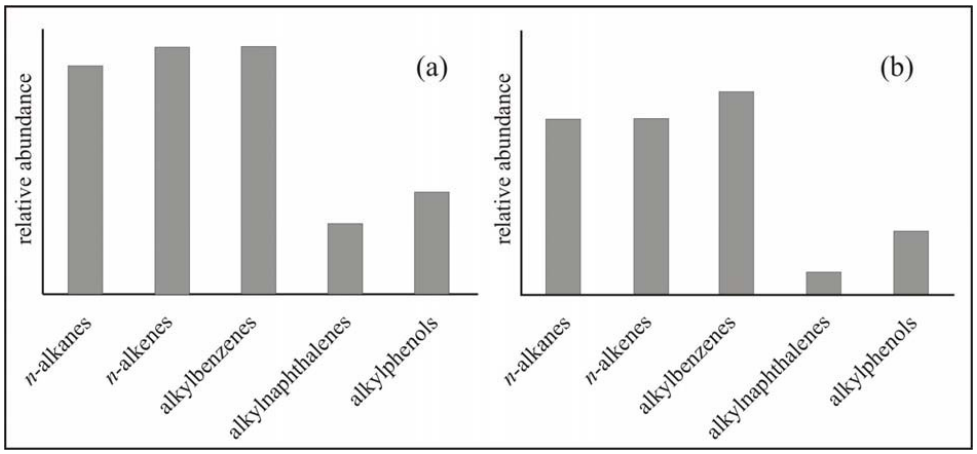


**Figure 5.4.** Histograms showing relative abundance of various compound classes in the pyrolysates of (a) handpicked scolecodonts; (b) total kerogen from the Högklint Formation, Gotland, Sweden.

Aliphatic compounds are characterised by a series of *n*-alkenes and *n*-alkanes ranging from $C_6$ to at least $C_{17}$. *n*-Alkene/*n*-alkane doublets are highly abundant in the pyrolysates of the highly aliphatic, resistant, biopolymere (see chapter 3 and references therein). However, *n*-alkene/*n*-alkane doublets are also found in the pyrolysates of various kerogen (see chapter 4 for discussion).

Alkylbenzenes (Figs. 5.3, 5.5) represent a relatively important contribution to the TIC traces of the scolecodont pyrolysates. *n*-Alkylbenzenes with a $C_5$-$C_{16}$ chain could be derived during pyrolysis by secondary reaction via cyclisation/aromatisation processes (Hartgers et al., 1994a). However, some *n*-alkylbenzenes with a low alkyl carbon number (i.e. in the $C_1$-$C_4$ range) might be pyrolysis products formed by β-cleavage of the substituted aromatic rings linked to the macromolecular structure via an alkyl chain (Hartgers et al., 1994b). Toluene and $C_2$-alkylbenzenes may be produced upon pyrolysis of protein derivatives (Tsuge and Matsubara, 1985).

Naphthalene and its alkylated homologs (Fig. 5.6) occur in the pyrolysates of chitinozoans and other different kinds of fossil remains (see chapter 3 and references therein). Radke et al. (1994) suggested that alkylnaphthalenes are mainly derived from terrestrial sources. We believe that alkylnaphthalenes are not always diagnostic of higher plants (see chapter 3 for detailed discussion) .

**Table. 5.2.** Aromatic compounds found in the pyrolysates from scolecodonts and total kerogen.

| Peak | Compounds |
|---|---|
| 1 | Toluene |
| 2 | Ethylbenzene |
| 3 | 1,3-1,4-Dimethylbenzene |
| 4 | 1,2-Dimethylbenzene |
| 5 | Phenol |
| 6 | 1,2,4-Trimethylbenzene |
| 7 | 1,2,3-Trimethylbenzene |
| 8 | 2-Methylphenol |
| 9 | 4 and 3-Methylphenol |
| 10 | $C_2$-Phenol |
| 11 | 2-Methylnaphthalene |
| 12 | 1-Methylnaphthalene |
| 13 | $C_2$-Naphthalene |
| 14 | $C_3$-Naphthalene |
| 15 | $C_4$-Naphthalene |
| 16 | $C_4$-Naphthalene |

$C_0$-$C_2$ Phenols (Fig. 5.7) which occur in the pyrolysates of scolecodonts are very characteristic compounds. Phenol and its alkylated homologs might have derived from amino acid (e.g., tyrosine) related precursor compounds. Phenols were also found as part of lignin (Collinson et al., 1994), seed coats of higher plants (van Bergen et al., 1994), plant cuticles (Mösle et al., 1998) and spore walls (see chapter 4). As the extant polychaete jaws contain amino acids, we believe that phenols are derived from the amino acid derived precursor compounds. Phenols are very stable compounds; they might have survived during diagenesis. It is now apparent that phenols are not always associated with lignin. Therefore, zooclasts like scolecodonts could be the source of phenols in the Lower Paleozoic sediments where kerogen originating from higher plants is absent.

The overall chemical composition of the handpicked scolecodont concentrate and of total organic residues does not show a significant difference (Fig. 5.4). This is due to the fact that total organic residues (size >20 μm) are highly enriched with scolecodonts. Beside scolecodonts, chitinozoans and cuticles from arthropod and prasniophytes (minor amount) are also present in the kerogen fraction. Chitinozoans and cuticles from arthropods could also yield aromatic compounds including phenols upon pyrolysis (see chapter 3 and references therein). Therefore, the relative intensity of each compound class varies between handpicked scolecodonts and total kerogen but the basic constituents remain the same.

Voss-Foucart et al. (1973) analysed jaws of modern polychaetes and found different types of amino acids. Except phenols, no compounds diagnostic of amino acids have been

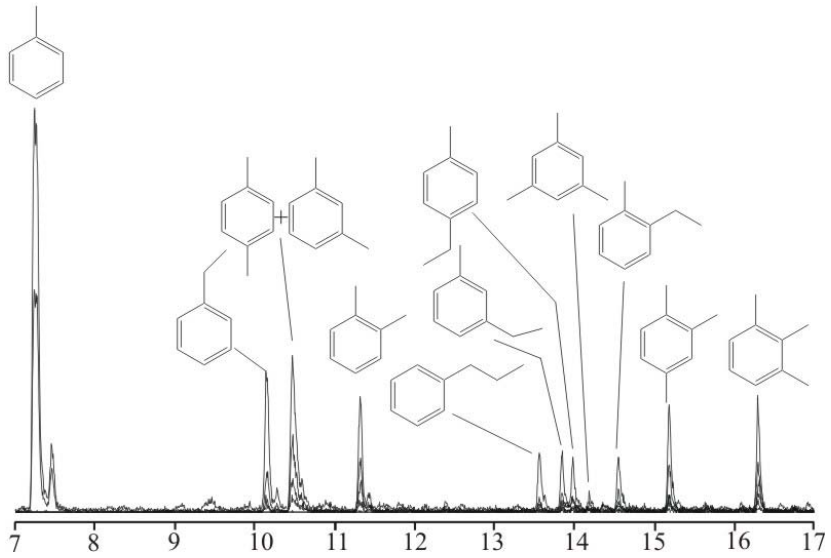


**Figure 5.5.** Mass chromatogram (*m/z* 91+92+105+106+119+120) of the 610°C Curie-point pyrolysates of handpicked scolecodonts showing the distribution of alkylbenzenes.

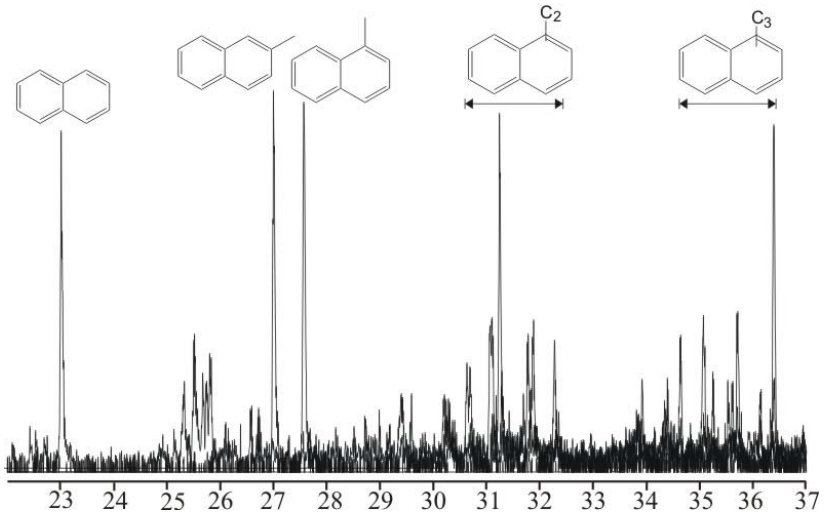


**Figure 5.6.** Mass chromatogram (*m/z* 128+142+156+170) of the 610°C Curie-point pyrolysates of handpicked scolecodonts showing the distribution of alkylnaphthalenes.

recognised in the pyrolysates of fossil polychaete jaws. Briggs et al. (1995) carried out pyrolytic studies of the periderm of the extant hemichordate *Rhabdopleura* which has a close relation with the Paleozoic graptolite. Their pyrolytic study shows the presence of many

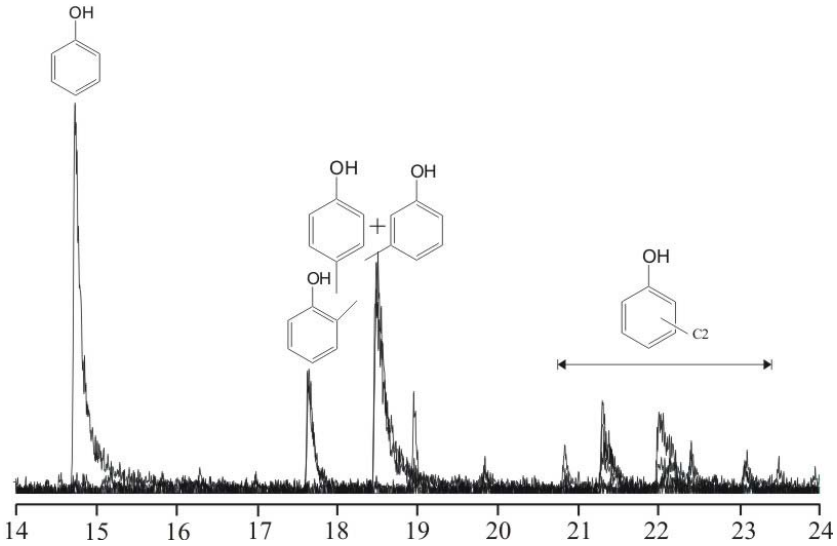


**Figure 5.7.** Mass chromatogram (*m/z* 94+107+108+121+122) of the 610°C Curie-point pyrolysates of handpicked scolecodonts showing the distribution of alkylphenols.

nitrogen bearing compounds (e.g., pyrrole, indole, ethylbenzenecyanide etc.) confirming the proteinaceous organic matter is a major constituent of the periderm of this living form. However, pyrolysis-GC-MS analysis of the periderm of the Ordovician graptolite *Amphigraptus* sp. from the Viola Limestone Formation of Oklahoma shows a homologous series of *n*-alkene/*n*-alkane doublets but no protein derived compounds have been detected (see Briggs et al., 1995). Similarly, it is possible that protein related compounds of scolecodonts might have degraded during diagenesis. It is apparent from the present study the pyrolysates of fossil jaws are enriched with aromatic compounds which are commonly found in the pyrolysates of type-III kerogen originated from terrestrial higher plant remains. However, scolecodonts occur in marine sediments and they are taxonomically related to the animal kingdom. Mastalerz et al. (1998) analysed *Protosalvinia* which is a problematic marine fossil from the Devonian which yields both aliphatic and aromatic pyrolysates. They concluded that *Protosalvinia* belong to rare marine organisms that yield aromatic pyrolysates. Moreover, pyrolysis of algaenan isolated from extant marine green microalgae *Chlorella marina* yields predominantly aromatic compounds compared to *n*-alkane/*n*-alkene doublets (Derenne et al., 1996). Chitinozoans (see chapter 3 for discussion) are exclusively marine micro-fossils which yield substantial amounts of aromatic compounds including phenols upon

pyrolysis. Therefore, kerogen of marine origin can also yield aromatic compounds including phenols upon pyrolysis. Inversely, aromatic compounds generated upon pyrolysis of kerogen may not always be attributed to kerogen derived from terrestrial higher plants.

### 5.5. Conclusions

Biomacromolecules of scolecodonts investigated in the present study consist of both aromatic and aliphatic moieties. The major aromatic pyrolysis products from scolecodonts include alkylbenzenes, alkylnaphthalenes and alkylphenols. The aliphatic compounds are represented by a homologous series of *n*-alkenes and *n*-alkanes. Presence of predominant aromatic pyrolysates in scolecodonts may suggest that kerogen consisting of zooclasts of marine origin can also yield aromatic pyrolysates which are typically attributed to type-III kerogen originating from higher plants. Except phenols, no compounds diagnostic of amino acids have been recognised, and it is concluded that amino acids which are commonly found in the extant polychaete jaws were degraded during diagenesis.

### Acknowledgements

We would like to thank Deutsche Forschungsgemeinschaft, Bonn (grants no. Ma 1861/2 and /4) and Forschungszentrum Jülich for financial support. We are grateful to Dr. A. Munnecke (Erlangen Institute of Palaeontolgy) for providing the sediment samples from Gotland. For technical assistance, we thank U. Disko, F. Leistner and H. Willsch. We are grateful to J. Galus for support with kerogen separation. This research is part of the "Silurian-Devonian Boundary Project" within the Priority Programme SPP 1054 "Evolution of the System Earth during the Late Palaeozoic clues from Sediment Geochemistry". This project is also related to IGCP Project 499, "Devonian Land-Sea Interactions: Evolution of Ecosystems and Climate (DEVEC)".

**5.6. References**

van Bergen, P.F., Goñi, M., Collinson, M.E., Barrie, P.J., Sinninghe Damsté, J.S., de Leeuw, J.W., 1994. Chemical and microscopic characterization of outer seed coats of fossils and extant water plants. Geochimica et Cosmochima Acta 58, 3823-3844.

Bergman, C.F., 1989. Silurian paulinitid polychaetes from Gotland. Fossil and strata 25, 1-128.

Bertrand, R., 1990. Correlations among the reflectances of vitrinite, chitinozoans, graptolites and scolecodonts. Organic Geochemistry 15, 565-574.

Briggs, D.E.G., Kear, A.J., Baas, M., De Leeuw, J.W., Rigby, S., 1995. Decay and composition of hemichordate *Rhabdopleura*: implications for the taphonomy of graptolites. Lethaia 28, 15-23.

Colbath, G.K., 1986. Jaw mineralogy in eunicean polychaetes. Micropaleontology 32, 186-189.

Collinson, M.E., van Bergen, P.F., Scott, A.C., de Leeuw, J.W., 1994. The oil-generating potential of plants from coal and coal-bearing strata through time: a review with new evidence from Carboniferous plants. In: Scott, A.C., Fleet, A.J. (Eds.), Coal and coal-bearing strata as oil prone source rocks? Geological Society Special Publication 77, pp. 31-70.

Derenne, S., Largeau, C., Berkaloff, C., 1996. First example of an algaenan yielding an aromatic rich pyrolysates, possible geochemical implications on marine kerogen formation. Organic Geochemistry 24, 617-627.

Erikkson, M., Elfman M., 2000. Enrichment of metals in the jaws of fossil and extant polychaetes – distribution and function. Lethaia 33, 75-81.

Espitalié, J., Deroo, G., Marquis, F., 1985. La Pyrolyse rock eval et ses applications. Deuxieme partie. Revue de L´Insitut Francais du Pétrole 40,755-784.

Goodarzi, F., Higginst, A.C., 1987. Optical properties of scolecodonts and their use as indicators of thermal maturity. Marine and Petroleum Geology 4, 353-359.

Hartgers, W.A., Sinninghe Damsté J.S., de Leeuw J.W., 1994a. Geochemical significance of alkylbenzene distributions in the flash pyrolysates of kerogens, coals, and asphaltenes. Geochimica et Cosmochima Acta 58, 1759-1775.

Hartgers, W.A., Sinninghe Damsté, J.S., Requejo, A.G., Allan, J., Hayes, J.M., Ling, Y., Xie, T-M., Primack, J., de Leeuw, J.W., 1994b. A molecular and carbon isotopic study towards the origin and diagenetic fate of diaromatic carotenoids. In Advances in Organic Geochemistry 1993 (Eds. K. Øygard et al.). 22, 703-725.

Hede, J.E., 1960. The Silurian of Gotland. In: Regnéll, G., Hede, J.E., (Eds.) The Lower Palaeozoic of Scania. The Silurian Gotland. International Geological Congress, XXI Session, Norden, Guide book, Sweden, 44-89.

Hinde, G.J., 1879. On annelid jaws from the Cambro-Silurian, Ailurian and Devonian formations in Canada and from the Lower Carboniferous in scotland. Quarterly Journal of the Geological Society of London 35, 370-389.

Mastalerz, M., Hower, J.C., Carmo, A., 1998. In situ FTIR and flash pyrolysis/GC-MS characterization of Protosalvinia (Upper Devonian, Kentucky, USA): implications for maceral classification. Organic Geochemistry 28, 57-66.

Mösle, B., Collinson, M., Finch, P., Stankiewicz, B.A., Scott, A.C., Wilson, R., 1998. Factors influencing the preservation of plant cuticles: a comparison of morphology and chemical composition of modern and fossil examples. Organic Geochemistry 29, 1369-1380.

Munnecke, A., 1997. Bildung mikritischer Kalke im Silur auf Gotland. Cour. Forsch. Inst. Senckenberg 198, 1-131.

Radke, M., Rullkötter, J., Vriend, S.P., 1994. Distribution of naphthalenes in crude oils from the Java Sea: source and maturation effects. Geochimica et Cosmochimica Acta 58, 3675-3689.

Szaniawski, H., 1996. Scolecodonts, In: Jansonius, J., McGregor, D.C. (Eds.), Palynology: principles and applications; American Association of Stratigraphic Palynologist Foundation. Vol. 1, p. 337-354.

Tsuge, S., Matsubara, H., 1985. High-resolution pyrolysis-gas chromatography of proteins and related materials. Journal of Analytical and Applied Pyrolysis 8, 49-64.

Voss-Foucart, M.F., Fonze-Vignaux M.T., Jeuniaux, C., 1973. Sytematic characters of some Polychaetes (Annelida) at the level of the chemical composition of the Jaws. Biochemical Sytematics 1, 119-122

# CHAPTER 6

## *Chuaria circularis* from the Early Mesoproterozoic Suket Shale, Vindhyan Supergroup, India: Insights from Microscopy, Spectroscopy and Pyrolysis-Gas Chromatography

**Abstract**

***Chuaria circularis* Walcott (1899) from the Suket Shale of the Vindhyan Supergroup (Central India) has been reinvestigated for its morphology and chemical composition using biostatistics, electron microscopy and pyrolysis-gas chromatography. Morphology and microscopic investigations provide little clues on the specific biological affinity of *Chuaria* as numerous preservational artifacts seem to be incorporated. On the contrary, the predominance of *n*-aliphatic pyrolysates of presently studied *Chuaria* from India rather supports an algal affinity. Micro-FTIR data are consistent with the pyrolytic studies emphasizing that biomacromolecules of the *C. circularis* investigated in the present study consist of aliphatic moiety and supports its algal affinity. Moreover, the reflectance of *C. circularis* can be used to obtain a comparative maturity parameter of the Precambrian sediments. The review of the age and geographical distribution of *C. circularis* constrains that this species cannot be considered as an index fossil for the Proterozoic time.**

### 6.1. Introduction

The origin and nature of *Chuaria circularis* has long been a topic of debate in Precambrian paleobiology since its first recognition by Walcott (1899). *Chuaria* had been related to hyolithids, gastropods, brachiopod, chitinous foraminifera, medusoids, trilobite eggs or even was regarded as inorganic remains in various studies (see Hofmann, 1992). Ford and Breed (1973) concluded that *Chuaria* was a plant, most probably being a large leiospherid acritarch. White (1928) first concluded that *C. circularis* might represent an alga. Later, this view was supported by many authors, e.g. Vidal (1974, 1976), Hofmann (1971, 1977), and Jux (1977). Due to its large size, *C. circularis* was placed into the Megasphaeromorphida of the Acritarcha Evitt 1963. More recent interpretation was made by Sun (1987) considering *Chuaria* as probable colonies of filamentous cyanobacteria comparable to the modern colonial cyanobacteria *Nostoc*. Steiner (1997) accepted Sun's opinion, but also proposed that the widely distributed and simply constructed

morphospecies *C. circularis* may have various biological affinities i.e. mainly prokaryotic colonies of eubacteria and chroococcal or filamentous cyanobacteria, but partly even eukaryotic algae.

In India, Jones (1909) reported carbonaceous discs from the Suket Shale of Rampura area, Neemuch district, Madhya Pradesh and related them to either *Obolella* or *C. circularis*. Chapman (1935) assigned the specimens to the two new genera and four new species *Protobolella jonesi*, *Fermoria minima*, *F. granulosa* and *F. capsella*. Sahni (1936) placed all of them in the synonymy of *F. minima*, but erected the new name *Vindhyanella* for one of the specimens figured as *Protobolella jonesi* by Chapman (1935, Plate 2, Figure 1). Maithy and Shukla (1977) suggested that the disc-like bodies are either imprints of acritarchs or algal colonies. Sahni (1977) considered the placement of *Fermoria* under *Chuaria* made by Ford and Breed (1973) an erroneous assignment. Maithy and Shukla (1984) agreed that morphologically these forms belong to *Chuaria* Walcott and compared them with the cryptarch genus *Orygmatosphaeridium*. Recently, Kumar (2001) studied the morphology of different carbonaceous fossils from the Suket Shale and considered *Chuaria* as a reproductive stage of a possibly cyst-like body of a Chlorophycean or Xanthophycean alga.

Molecular characterization of any Precambrian organic matter is difficult to carry out, because of its high thermal maturity. However, any structural investigation of organic matter of this age is essential in understanding evolution of Earth and life (Li et al., 2004). Pyrolysis-gas chromatographic study is herein reported for the first time on well defined organic material from the Proterozoic Vindhyan sediments of India. The pyrolytic degradation has been carried out in order to obtain information on the molecular composition of the organic matter, and its potential biological origin. Accordingly, this paper presents a comprehensive study including morphology, biostatistics, SEM and TEM images and molecular composition of *Chuaria* from the Suket Shale of the Lower Vindhyan, Semri Group.

### 6.2. Samples

The Vindhyan Supergroup represents a thick (up to 4500 m) succession of undeformed and slightly metamorphosed, Paleoproterozoic to Neoproterozoic sediments exposed in Rajasthan and Son Valley regions. The study area is situated in the less studied northwestern region of the Vindhyan Basin.

The Vindhyan Supergroup is two tiered and consists of the Lower Vindhyan Group (or the Semri Group) and the Upper Vindhyan Group. Vindhyan sedimentation took place largely in a shallow marine environment (Chanda and Bhattacharyya, 1982), but the depositional

environment fluctuated between offshore, deltaic, lagoonal, fluvial and even eolian settings (Bose et al., 2001).

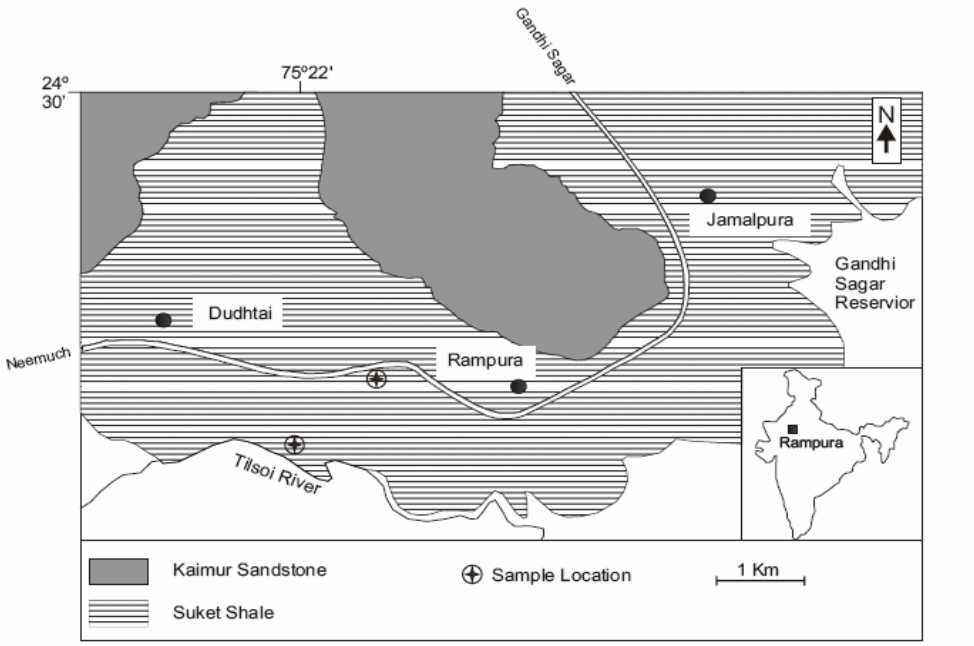


**Figure 6.1.** Geological map of the Rampura area, Neemuch district, Madhya Pradesh (after Kumar, 2001).

The Suket Shale occupies the low lying plains around Rampura (Fig. 6.1). The rocks are exposed in the Tilsoi River section, Nala cuttings and along the Rampura–Neemuch road section. The main lithologies of the Suket Shale are green shales, greyish yellow shales with subordinate occurrences of greyish black carbonaceous shales, siltstones and light brownish grey sandstones. The contact between Suket Shale and Kaimur Group is gradational. The Suket Shale is commonly correlated with the Rampur Shale in the Son valley (Sarkar et al., 2002) where it consists of greyish and carbonaceous shales intervened by siltstones/fine grained sandstones. The Suket Shale of the Rampura area has not been dated so far, however, its stratgraphical position can be inferred from a correlation with strata in the Son Valley area. Absolute ages for Vindhyan strata from the Son Valley are given by Rasmussen et al. (2002) who dated the tuff bands occurring at the base of the Rampur Shale and fixed an age of 1599±8 Ma by the U/Pb method. Sarangi et al. (2004) recently obtained an age of 1599±48 Ma for the overlying Rohtas Formation containing carbonaceous fossils (*Grypania*) by the Pb/Pb dating technique. On this basis the age of the Suket Shale can be estimated at roughly 1600 Ma. Samples for the present study have been

collected from comparably fresh well cuttings near the Tilsoi River section and are preserved at the China Research Center (Sekr. ACK 14) of Technical University Berlin.

## 6.3. Methods

### *6.3.1. Microscopy*

For reflected light, scanning electron microscope (SEM), transmission electron microscope (TEM) and micro- Fourier transform infrared (FTIR) spectroscopic analyses, specimens of *Chuaria* were extracted from the rock matrix using 40% HF acid (for three days). After treatment with HF the samples were neutralized using a 10 μm mesh filter. Well preserved individuals of *Chuaria* were picked from the organic residue by a pipette. Both, isolated specimens, and those preserved in situ on the rock surfaces were studied in reflected light under a Leitz-Wild-M3Z binocular microscope.

Specimens selected for SEM were mounted on a preparation stub and coated with a 20 nm layer of gold and investigated by a Hitachi S520 at TU Berlin. The wall thickness of specimens of *Chuaria circularis* was determined by measurement of transversal fractures under SEM or by measurement of embedded and sectioned individuals using light microscopy under high magnification. Extracted specimens for the TEM analysis were dehydrated using ethanol and embedded in Araldite CY 212 resin. The ultra-thin sections (thickness 70 nm) were cut perpendicular to the compressed surface of the specimens in an ULTRACUTE and placed on copper grids for study in a JEOL 200B TEM at TU Berlin.

For reflectance studies, whole rock fragments containing *Chuaria* as well as individuals of *Chuaria* isolated from the Suket Shale of India, the Visingsö Formation of Sweden and from the Liulaobei Formation of China were embedded in Araldite resin and polished by a standard coal petrographic technique (Mackowsky, 1982). The percentage of random reflectance was measured in oil immersion ($n_{oil}$=1.518) at a 546 nm wave length at 23ºC.

### *6.3.2. Pyrolysis-Gas Chromatography*

For pyrolysis, specimens of *Chuaria* were scratched off from the bedding planes of rock samples using a sharp scalpel and subsequently only the organic remains of *Chuaria* were handpicked under a stereomicroscope. Prior to chemical investigations, these organic walled fossils were cleaned several times with dichloromethane to remove free hydrocarbons.

Molecular characterisation of *Chuaria* was performed by open-system off-line pyrolysis method and pyrolysis products released during thermal degradation were first collected and studied at a later stage. Up to 1.0 mg of sample were heated in a flow of helium. Pyrolysis

products released over a temperature range <300°C (300°C held for 5 minutes) were vented. Products released over a temperature range from 300 to 600°C (50°C/min) were collected in a cryogenic trap (liquid nitrogen cooling) from which they were then liberated by ballistic heating. Gas chromatographic analysis was carried out using a 50m x 0.31mm fused silica column (HP-1; 0.5µm film thickness) programmed from 40°C to 300°C with a heating rate of 5°C per minute. The relative abundance of compounds was determined using Multichrom chromatography data system (VG DATA SYSTEMS).

*6.3.3. Micro-FTIR*

Micro-FTIR spectroscopic analyses were performed in transmission mode using a Nic-Plan microscope and a Protégé 460 FT-IR optical bench operated by the OMNIC® software. The microscope is equipped with an objective 15x/N.A. 0.58 with reflecting lenses of a Cassegrainian design and a Cassegrainian condenser. Two adjustable rectangular apertures allow to precisely define the size and shape of the measured area. The optical bench includes an Ever-Glo source, a KBr beamsplitter, and MCT-A detector which requires liquid-nitrogen cooling during data collection. Spectra were obtained of a defined area by co-adding up to 1024 scans with a spectral resolution of 4 $cm^{-1}$. The standard setting was 1024 scans/4 $cm^{-1}$ or 512 scans/4 $cm^{-1}$. The recorded spectral range was within 4000-650 $cm^{-1}$. Back ground spectra were collected after every sample. As the air in the system was not purged the spectra show the $CO_2$ band at 2360 $cm^{-1}$. All specimens were placed on a NaCl sample support (size 13 x 2 mm). This analysis was carried out at the school of Ocean and Earth Science, Southampton Oceanography Centre, University of Southampton, UK.

**6.4. Systematic Description**

**Genus:** *Chuaria* WALCOTT

**Species:** ***Chuaria circularis*** WALCOTT

(Plate 6.1 and Plate 6.2)

**Lectotype:** Ford and Breed, 1973; page 540; Figure 1; USNM 33800

**Synonymy:** for synonymy see Maithy and Shukla (1984), Steiner (1994), Talyzina (2000)

**Type locality:** Kwagunt Valley, Grand Canyon, Arizona, USA

**Investigated locality:** Rampura, Neemuch District, Madhya Pradesh, India

**Lithology:** black shales, greyish black shales, yellow shales

**Description:**

Circular to elliptical discs ranging in size from 0.25 mm to 4.75 mm are either preserved in the form of carbonised compressions on black/grey shale or imprints on weathered, yellow shale (Plate 6.1a, 6.1b, 6.1c). Discs may contain concentric and irregular wrinkles resulting from the compression of originally spherical bodies (Plate 6.1a). Rare three-dimensional specimens are occurring, probably due to infilling (Plate 6.1d). Few specimens occur as intergrown groups (Plate 6.1f). The surfaces of most compression have been deformed to a varying degree by sediment grains from the surrounding rock matrix during compaction (Plate 6.1b, 6.1e, 6.1g). Circular and irregular folds are also preserved in the specimen, isolated from rock matrix (Plate 6.1h). Isolated specimens show yellow to dark brown coloration in transmitted light or are opaque.

### 6.4.1. *Discussion*

Difficulties in interpreting the original primary morphology and biological assignment of *Chuaria circularis* are derived from the fact that numerous preservational artifacts and taphonomic alterations are incorporated within this simple fossil. The species *Chuaria circularis* is herein regarded as a form-taxon of very simple morphology, which may embrace similar remains of different biospecies. The characters of *Chuaria circularis* are partly overlapping with those of several species of large leiospherid acritarchs. Species differentiation based on the presence of such characters of acids resistance, opacity and compressional fold arrangement may be practical, but are arbitrary. Therefore, acid resistance, opacity and fold arrangement are not used in taxonomical sense herein. Walcott (1899) in his original report described this species as a brachiopod showing regular ring-like wrinkles. *Chuaria* was later considered as spheroidal or a hollow spheroid with a narrow flange (Ford and Breed, 1973). Duan (1982) believed that such concentric wrinkles are of inherent morphological features and may be diagnostic criterion and argued that the marginal flange described by Ford and Breed (1973) was originally a part of the ring-like wrinkles. Butterfield et al. (1994) used the presence of concentric wrinkles as diagnostic character. Specimens of *Chuaria circularis* from the Suket Shale occur with marginal wrinkles (Plate 6.1a), while others do not (Plate 6.1g). However, similarities in their size range, composition and other characteristics seem to indicate that the concentric wrinkles are only preservational alterations caused by slightly differing modes of compaction. Variable preservation with partial lack of the often typical concentric wrinkles is also reported from an early diagenetically mineralized (pyritized) assemblage of chuarids (Yuan et al., 2001).

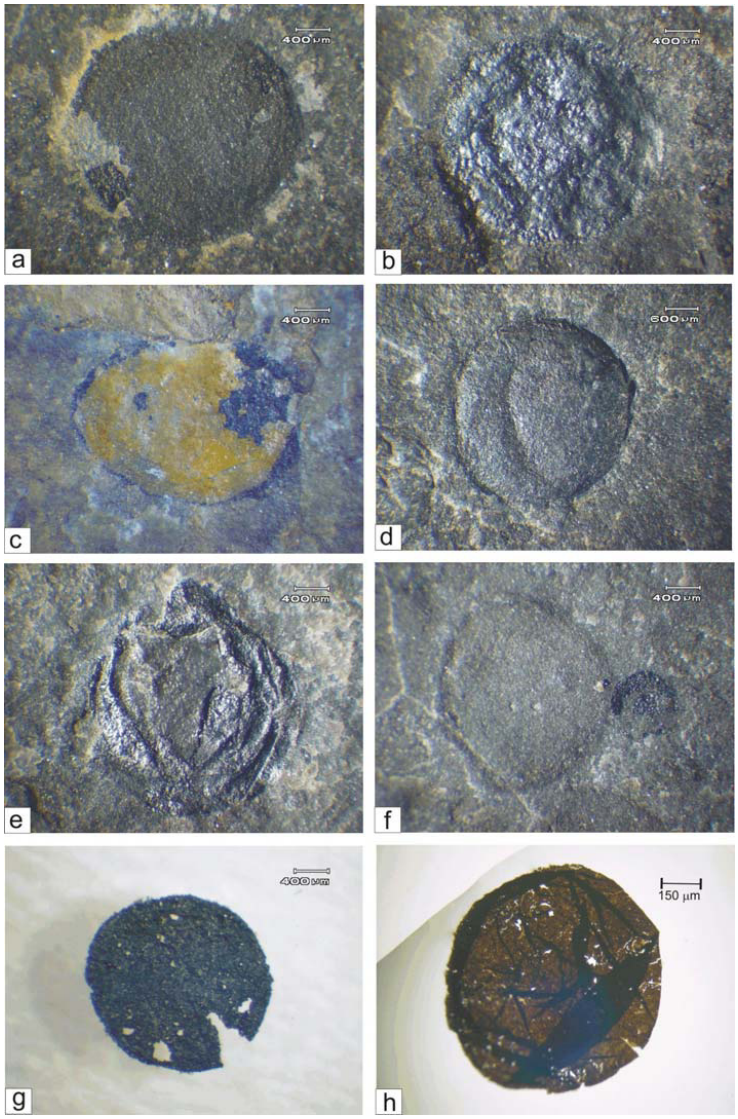


**Plate 6.1.**

(a) *C. circularis* with wrinkles at the boundary (Sample number $R_2$/10/1); (b) *C. circularis* with thick carbonaceous matter and imprints of sediment on top of it (Sample number $R_2$/4/2); (c) *C. circularis* showing elliptical shape, carbonaceous matter partially weathered out (Sample number $R_2$/4/3); (d) Three dimensionally preserved *C. circularis* (Sample number $R_2$/2/3); (e) *C. circularis* with strongly folded thick carbonaceous matter (Sample number $R_2$/5/2); (f) Attached individuals of *C. circularis* of different size and different thickness of preserved organic matter (Sample number $R_2$/3/2); (g) *C. circularis* after separation from rock matrix by HF. Note that the specimen shows a compactional crack structure (referred to as "opening structure" by other authors) and opaque, thick organic matter with sediment grain imprints. Opacity is correlated with a mostly large maximum diameter (ca. 200-4000 µm) and great wall thickness (> 1000 nm); (h) *C. circularis* after separation from rock matrix by HF. Note circular and irregular folds, resulting from compaction of relatively thin organic matter. Medium brown colour is correlated with medium maximum diameter (ca. 200-2000 µm) and a relatively thin wall thickness (ca. 350 nm). All samples are derived from the Suket Shale, Vindhyan Supergroup, Rampura, Madhya Pradesh, India. Specimens are deposited at the China Research Center (Sekr. ACK 14) of TU Berlin.

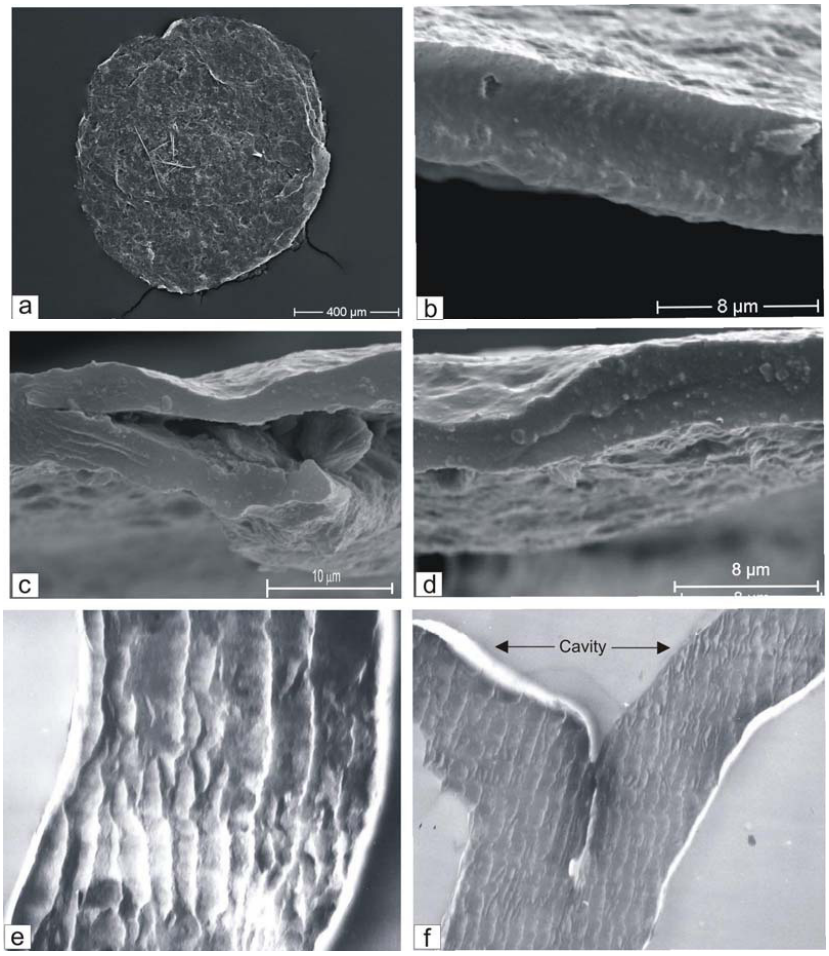


**Plate 6.2.**
(a) Scanning electron micrograph of *C. circularis*. Note that concentric wrinkles are not well developed, but sediment grain imprints are prominent; (b) Scanning electron micrograph of transversal fracture of a specimen of *C. circularis*, indicating massive single layer without a median split; (c) Scanning electron micrograph of transversal section of a specimen of *C. circularis* with folded layer; (d) Scanning electron micrograph of transversal section of a specimen of *C. circularis*, showing an irregular cavity within the wall, but no median line as it should be expected from the compaction of a central cavity of a vesicle; (e) Transmission electron micrograph of *C. circularis,* showing lamellar structure (magnification 30000x); (f) Transmission electron micrograph of *C. circularis,* showing cavity within the wall (magnification 25000x). All samples are derived from the Suket Shale, Vindhyan Supergroup, Rampura, Madhya Pradesh, India. Specimens are deposited at the China Research Center (Sekr. ACK 14) of TU Berlin.

The specimens of the present study also show irregular microfolds (Plate 6.1e) probably resulting from dewatering after deposition. Hofmann (1985a) also suggested that the folds and marks on carbonaceous megafossils are compactional artifacts. Overlapping of specimens is not common, even in dense accumulations. Therefore, Duan (1982) concluded that *Chuaria* was spherical in

shape. Compactional cracks have been postulated as excystment structures of eukaryotic megacysts (Yuan et al., 2001) or "opening-structure" for the release of spores on maturation of *Chuaria* (Kumar, 2001; Fig. 6j). However, similar cracks were produced by compaction experiments on modern spherical colonies of cyanobacteria (Steiner, 1994; Plate 1, Fig. 3). Similar structures found in the present study (Plate 6.1g) suggest a compressional origin, which is supported by the observation of Eisenack (1966) that cracks commonly occur in the younger stages rather than in mature specimens.

### 6.5. Colour

Butterfield et al. (1994) discussed opacity as an inherent character of *Chuaria* and postulated that opacity of these fossils from the Svanbergfjellet Formation is not a direct function of wall thickness, but rather dependent on histological characteristics. Therefore, translucency, wall thickness and colour of *C. circularis* are herein systematically studied. Specimens of the present study show colour variation from yellow via brown to black (opaque). Three major characters may be considered to determine the colour of any fossilised organic substance: (1) thermal maturity, (2) wall thickness and (3) type of the material. Specimens of the present study are collected from the same stratigraphic horizon and at the same locality but show a wide range of colours implying that thermal alteration could have played a little role only. Wall thickness of this fossil may be the reason for colour variation. To study the relationship between colour, wall thickness and size of *Chuaria circularis* a number of specimens was classified according to a subjective colour scale and their size and wall thickness were recorded (Fig. 6.2). Numerous specimens of each size class and colour group were measured. A systematic trend of increasing translucency and a presence of lighter colours with smaller maximum diameters of individuals of *C. circularis* was recognized. However, dark or opaque individuals occurred also in smaller size classes, although they were less abundant than individuals larger than 500 µm in diameter. Opacity occurred in Indian material from the Suket Shale at a total "wall" thickness of about 1 µm or more, while translucent individuals with brown colouration ranged from ca. 350 to 750 nm in total thickness (Fig. 6.2). The recorded range of total "wall" thickness from 0.3 to 23.85 µm, is quite large and contradicts an interpretation as vesicle or even cell walls of only one biological species. It is obvious that with increasing "wall" thickness the colour of *Chuaria* changes from yellow to brown to black (opaque). It has also been observed that large black (opaque) individuals of *Chuaria* became translucent (brown) in areas of corrosion.

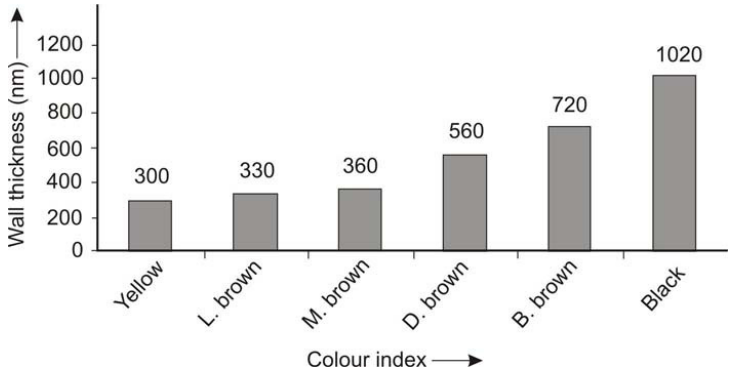


**Figure 6.2.** Variation of colour with total "wall" thickness of *Chuaria circularis*, Suket Shale, Vindhyan Supergroup, India.

Similar conclusions were also drawn by Steiner (1994) after detailed study of *C. circularis* from the Liulaobei Formation, North China. It can be concluded that opacity is a direct function of wall thickness and thus may not be an inherent property of *Chuaria*. Regional differences in opacity of organic matter of *Chuaria* may result from differing thermal history.

### 6.6. Biostatistics

Size statistic of *Chuaria circularis* from the Suket Shale reveals a variation from 0.25 mm to 4.75 mm and an unimodal size distribution with a mode in the size range of 2.25 mm to 2.75 mm (Fig. 6.3). In the scatter diagram (Fig. 6.4) the ratio between the longer and shorter diameter varies between 1 and 1.5. Both, smaller and larger forms exhibit almost identical morphological features. Gahre and Badve (1978) and Maithy and Shukla (1984) showed a size frequency distribution of *C. circualris* from the Suket Shale and concluded that large size specimens dominate in black shales whereas the smaller size are common in yellow shales. The present study, however, reveals equal occurrences of both, larger and smaller *Chuaria* specimens, within the black shales (Plate 6.1f).

The wall thickness ranges from 0.3 μm- 23.85 μm for examined specimens from the Suket Shale (Plate 6.2b-d). The original description of the type-species *Chuaria* Walcott from the Chuar Group (Wallcott, 1899) does not provide any data on the total "wall" thickness. However, Jux (1977) mentioned that "wall" thickness of *C. circularis* varies from 2-2.5 μm. Ford and Breed (1973) mentioned a "wall" thickness of 50-70 μm of *Chuaria* from the Visingsö Formation, but Amard (1992) argued that the original wall thickness ranges from 15-30 μm in these same samples. The wide range in thickness may be the result of either biodegradation or differential

compaction. Recently, Javaux et al. (2004) suggested that variations in wall thickness of the Proterozoic organic walled microfossils could be due to compaction.

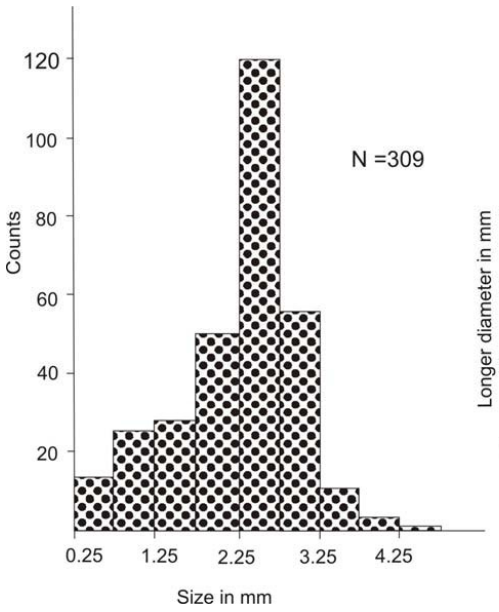


**Figure 6. 3.** Size histogram of *Chuaria circularis*, Suket Shale, Vindhyan Supergroup, India.

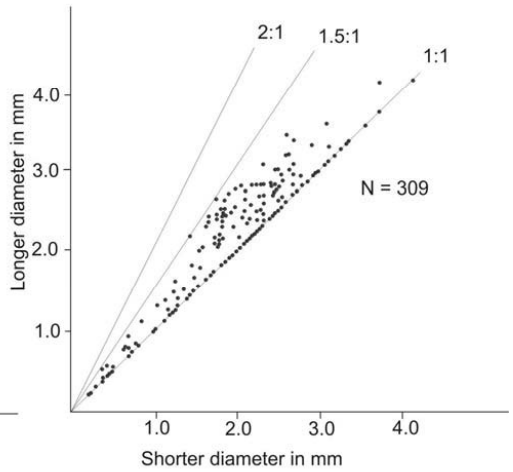


**Figure 6. 4.** Scatter diagram for longer dimension plotted against shorter dimension for *Chuaria circularis*, Suket Shale, Vindhyan Supergroup, India.

There is not much agreement on a potential size limitation as a diagnostic feature of *Chuaria*. Ford and Breed (1973) mentioned that *C. circularis* are flattened carbonaceous spheroids with wrinkles and cracks, but within a size limit of 500 to 5000 µm. Vidal (1974, 1976) did not agree with Ford and Breed (1973) in applying size limits and reported the size range of most of his specimens remain in the range of 0.09-0.2 mm and few up to 3 mm. Sun (1987) strongly recommended that *Chuaria* is typically characterized as macroscopic in size and mentioned that the size range should be taken as a practical, convenient criterion to distinguish *Chuaria* from various acritarch forms. But Steiner (1997) rejected that size limits are artificial in defining *C. circularis*. Kumar (2001) showed a bimodal distribution of *Chuaria* and on this basis he erected the new species as *C. vindhyansis* which is distinguished from *Chuaria circularis* by a smaller size. We do not agree with this interpretation, since both smaller and larger forms exhibit identical morphological features. In contrast to a biological interpretation, bimodality in size may indicate a sorting effect due to reworking if other characters do not differ.

### 6.7. Ultrastructure

SEM investigations reveal no special ornamentation on the surface of the specimens of *Chuaria circularis* except a few pits interpreted as impressions of sediment grains or resulting from biodegradation (Plate 6.2a). The "wall" of the compressed carbonaceous spheres of *Chuaria* is represented by a massive layer (plate 6.2b). At places small folds are randomly distributed on the wall surface (Plate 6.2c). Irregular cavities are found in particular regions of the massive layer ("wall") in some specimens (Plate 6.2d). Amard (1992) found that the wall exhibits a stepped row of horizontal dark and light lamellae and in some cases a column-like structure with perforations communicates between lamellae and concluded that number of lamellae is variable from one specimen to another depending on biological factors like juvenile or mature stage. Such structure has not yet been identified in SEM images of *Chuaria* from the Suket Shale of Rampura; and the structure has not been found in the specimens from the Chuar Group (Jux, 1977), Liulaobei Formation (Steiner, 1994) or the Visingsö Group (Steiner, 1994; Talyzina, 2000). According to SEM studies, the internal wall construction of *Chuaria* from the Suket Shale seems to be single layered (Plate 6.2b). The cavities within the solid organic body are observed in some specimens (Plate 6.2d). These cavities were either formed by dissolution of sediment, which had been incorporated within the wall before fossilization or by biodegradation.

The "zonal dark lamellae" of the topotype *C. circularis* reported by Jux (1977) using TEM and compared to those of Devonian *Tasmanites* and *Tapajonites* (Jux, 1977), are not comparable to the structures in *Chuaria* of the Suket Shales. Microtome sections in the present study show lamellar structures (Plate 6.2e, 6.2f). However, it is likely that these lamellar structures have formed during the sectioning process. Similar sectioning artifacts have also recently been described from organic microfossils of the Mesoproterozoic Roper Group of Australia (Javeaux et al., 2004; Figs. 3j, k). Jux (1977) observed in TEM ultrasections of *Chuaria* a "fine network of trabecular ultrastructure of the wall" at very high magnification. This ultrafine structure (the mesh of which is of the order of 0.001µm) is regarded by him as a fundamental feature of the topotype *C. circularis*. Amard (1992) also reported radial canals comparable to those reported by Jux (1977), but such ultrastructure has not been recorded in TEM ultrasections of *Chuaria* from the Suket Shale and also not been reported from the Cryogenian sequence of Australia (Arouri 2000). The SEM and TEM studies of specimens from the Liulaobei Formation in China (Steiner 1994) did not reveal any canal structures. Talyzina (2000) compared few cavities within the "wall" of *Chuaria* from the Visingsö Formation with "radial canal" structures reported by Jux (1977) and Amard (1992). The herein observed irregular cavities (Plate 6.2f) occur only locally,

probably caused by degradation. However, they are different from the cavities reported by Talyzina (2000) from *Chuaria* of the Visingsö Formation. TEM sections of leiosphaerids, which may be related to translucent specimens of *Chuaria circularis,* showed a similar ultrastructural construction as in *Chuaria* (Steiner, 1994; Javeaux et al., 2004). Porous inner zones of a compact layer may represent preservational artifacts, may be due to later degradation (compare Steiner, 1994; Javeaux et al., 2004). The interpretation of a fine-layered construction of wall in leiosphaerids and the existence of a trilaminar structure may be also due to preservational artifacts (see Javeaux et al., 2004).

### 6.8. Reflectance studies

A determination of thermal maturity of pre-Silurian sedimentary rocks from a routine application of petrographic techniques is somewhat limited due to absence of higher plant material.

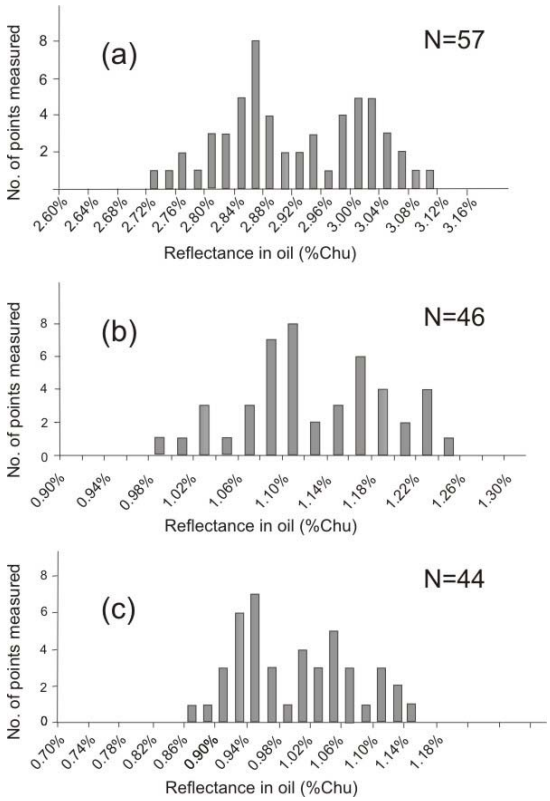


**Figure 6.5.** Composite histograms showing distribution of reflectance of *Chuaria* from (a) the Suket Shale, India (Sample number Ram 216); (b) the Visingsö Formation, Sweden (Sample number Mul 1); (c) the Liulaobei Formation, China (Sample number Llb 339b).

Incident light microscopy studies of marine fossils (e.g., chitinozoa, graptolites and scolecodonts) which are very common in Lower Paleozoic sedimentary rocks have been used for maturity studies in the last two decades (Bertrand and Héroux, 1987; Hoffknecht, 1991; Obermajer et al., 1996). But no initiative has been made until today for maturation studies of Precambrian sediments using reflectance studies of *Chuaria*. In the present study the reflectance of *Chuaria* was investigated as a means of determining the level of thermal maturity. Altogether 10 samples of *Chuaria* were measured from the Suket Shale. For comparison, *Chuaria* from the Visingsö Formation (Sweden) and from the Lilulaobei Formation (China) were also measured. The histograms of the reflectance studies of different samples are given in Figures 6.5a-c. The maximum value of reflectance of *Chuaria* ($ChuR_0$) from the Suket shale is 3.20% and the lowest value is 2.16%. The median values of $ChuR_0$ range from 2.34% to 2.90%. Reflectance of *Chuaria* from the Visingsö Formation ranges from 1.1 to 1.24% (Fig. 6.5b) and from 0.86% to 1.14% in the Lilulaobei Formation (Fig. 6.5c). *Chuaria* from different formations show different values of reflectance, which, in turn, probably indicate differences in their thermal maturity. The carbonaceous fossils from the Suket Shale show the highest maturity while that of the Liulaobei Formation is lowest and those of the Visingsö Formation are intermediate. Indian *Chuaria* samples and its host sediments have experienced a comparably high thermal overprinting as reflected from other black shale horizons of the Vindhyan Basin which are over matured (see Banerjee et al, this volume). Thermal maturity of organic remains depends on several factors during sedimentary basin evolution (Poelchau et al., 1997; Yalçin et al., 1997) and an analytical compilation of all these factors are beyond the scope of this paper. Here it is just concluded that reflectance studies of *Chuaria* might represent a time-temperature scale and tool to compare maturity of Precambrian sediments.

## 6.9. Molecular composition

### *6.9.1. Pyrolysis-Gas Chromatography*

The total ion chromatogram obtained by Pyrolysis-GC of the *Chuaria* from the Suket shale is shown in Figure 6.6. The pyrolysates are dominated by a bimodal distribution of *n*-alkene/*n*-alkane doublets ranging from $C_7$ to $C_{22}$ with maxima at $C_7$. *n*-Alkene/*n*-alkanes doublets are typical products of the algaenan biopolymer which occurs in the cell walls of various marine and fresh water algae (Hatcher and Clifford, 1997). Aromatic compounds like benzene, toluene, ethylbenzene have been detected. Pyrolytic studies of *Chuaria* from the Australian Centralian Superbasin were carried out by Arouri et al. (2000), however, no GC-amenable pyrolysates were produced and thus it was concluded by these authors that the samples were highly over mature. A

similar pattern is also reflected by the present pyrolytic studies of *Chuaria* as abundance of pyrolysates of this organic walled fossil is very low. But, any molecular investigation of this enigmatic fossil is essential to increase knowledge on its biological affinity. Pyrolytic degradation techniques for Precambrian kerogen are well known, but separation of indigenous molecular fossils from contaminants is sometimes difficult (see Brocks et al., 2003).

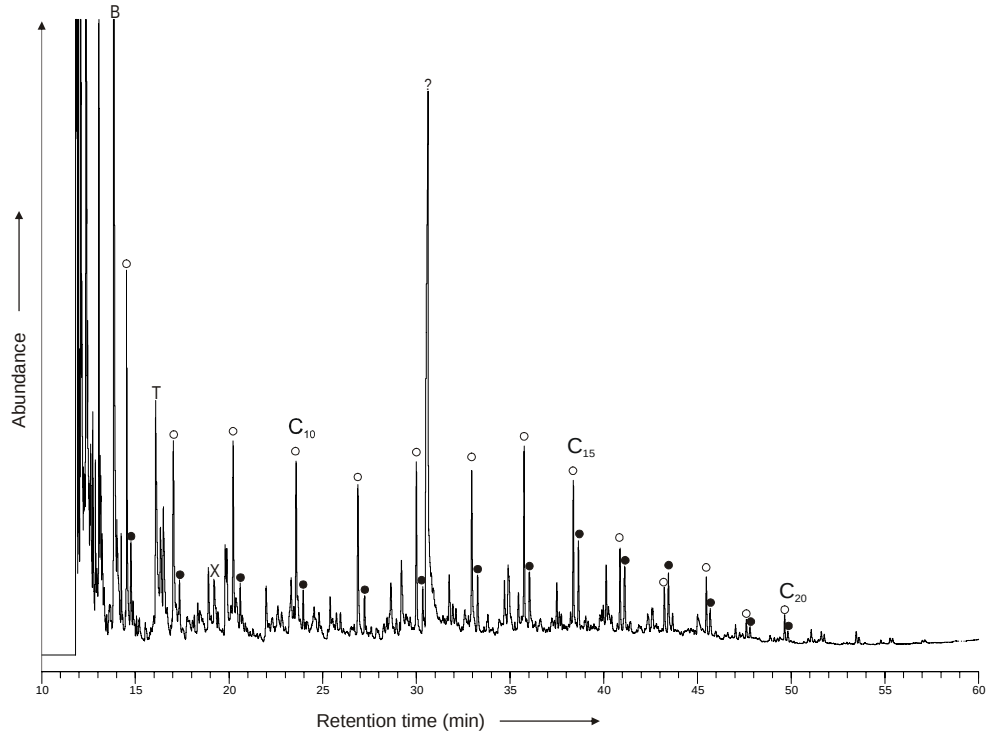


**Figure 6.6.** Total ion chromatogram resulting from Pyrolysis-GC of *Chuaria circularis*, Suket Shale, Vindhyan Supergroup, India. Each doublet corresponds to an alkene (○) and an alkane (●); selected C-numbers are indicated. B, T and X indicate benzene, toluene and ethyl benzene, respectively.

Prior to chemical investigation, the *Chuaria* samples were cleaned several times by dichloromethane, which minimizes the probability of presence of any contaminant. Recently, Grice et al. (2003) carried out Curie point pyrolysis of the fresh water alga *Botryococous braunii* from Miocene/Pliocene age and found a homologous series of *n*-alkene/*n*-alkane doublets. Similarly, pyrolysis of the marine alga *Tasmanites* from the Permian revealed *n*-alkene/*n*-alkane doublets with tricyclic hydrocarbons (Greenwood et al., 2000). Benzenes and alkylbenzenes were other pyrolysates detected in the pyrolysates. Low relative abundances of these aromatic compounds are also a common feature of algaenan (e.g. Derenne et al., 1992). The alkylated

aromatic products probably derive from biological precursors although pyrolysis-induced aromatisation processes can contribute to the abundance of simple aromatic hydrocarbons (see Larter and Horsfield 1993). Li et al., (2004) carried out pyrolysis of 1.2 Ga. old kerogen from the Hongshuizhuang Formation, North China and found that the pyrolytic products consist of benzene and naphthalene and that their alkylated homologs and *n*-alyphatic products occur in subordinate amounts suggesting that this kerogen was originated from Proterozoic cyanobacteria. A significant aliphatic moiety was detected from the Neoproterozoic acritarchs from South Australia and it was concluded that these acritarchs were Chlorophycean algae (Arouri et al., 1999). Very recently, Dutta et al (2006) carried out pyrolysis of handpicked prasinophycean algae (e.g., *Tasmanites*, *Leiosphaeridia*) from the Dadas Formation, SE-Turkey and observed predominance of *n*-aliphatic products. It is true that migration of aliphatic moieties from matrix to fossil is a topic of considerable debate in the field of organic geochemistry (see Stankiewicz et al., 2000; Versteegh et al., 2004; de Leeuw et al., 2006). At the present state of our knowledge, the predominance of *n*-aliphatic pyrolysates of *Chuaria* are consistent with a highly aliphatic nature and thus provide hints towards an algal affinity. These organic remains were probably very early eukaryotic algae which appeared during Early Mesoproterozoic time in the area of Indian Platform.

*6.9.2. Micro-FTIR*

A micro-FTIR spectrum from *Chuaria circularis* is shown in Figure 6.7. Spectral bands were assigned with reference to the literature (for example, Arouri et al., 1999; Yule et al., 2000; Marshall et al., 2005). The aliphaticity is indicated by prominent alkyl group bands between 2800-3000 and 1300-1500 $cm^{-1}$. The strong narrow absorption at 2920 is due to asymmetric stretching vibration of $CH_2$. The peak at 2847 $cm^{-1}$ represents symmetric stretching vibration of $CH_2$. The peak at 1465 $cm^{-1}$ assigned to $CH_2$ deformation. A subordinate absorption signal attributed to aromatic C=C stretching vibration (1560-1610 $cm^{-1}$) is peaking at 1597 $cm^{-1}$. The prominent absorption signals at 700-900 $cm^{-1}$ (peaking at 875 $cm^{-1}$, and 860 $cm^{-1}$) are due to aromatic CH out of plane deformation. A narrow, strong, band is centred at 1540 $cm^{-1}$ which could be a N-H deformational band. Presence of strong aliphatic bands suggests that the biomacromolecules of *Chuaria circularis* is of aliphatic nature and supports its algal affinity.

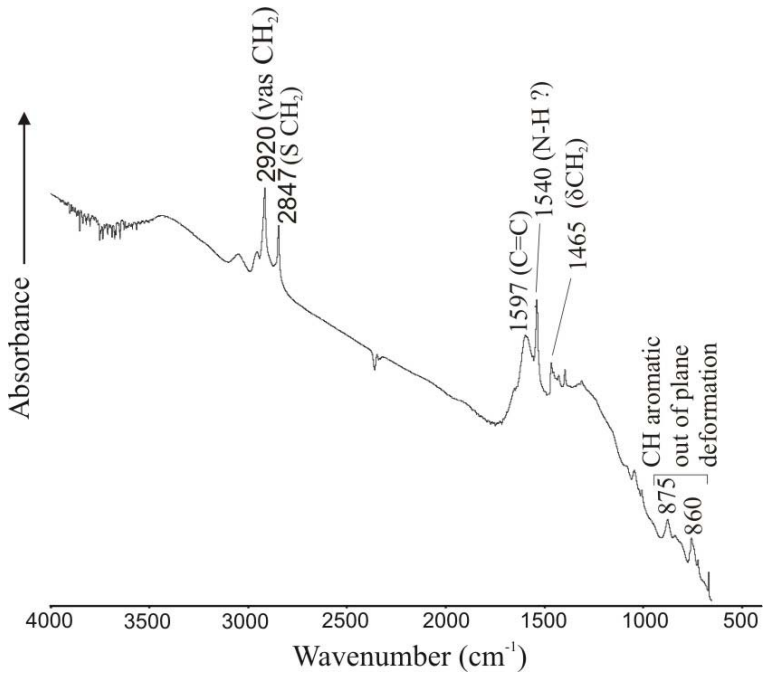


**Figure 6.7.** A micro-FTIR spectrum of *Chuaria circularis* from Suket Shale, Vindhyan Supergroup, India. Assignments of absorption bands and vibration modes (δ=deformation; ν=stretching; s=symmetric; as=asymmetric) are indicated in parentheses.

### 6.10. Age and geographical distribution

*Chuaria* has a wide geographical distribution and is recorded from United States, Canada, Russia, Australia, China, Kazakhstan, Spain, Namibia, Benin, Iran, Argentina, India, Antarctica, Sweden and Moldova/Ukraine (Fig. 6.8). Ford and Breed (1973) considered *Chuaria* as a potential index fossil for the time range of 1000 Ma to 570 Ma. But Hofmann and Chen (1981) and Du and Tian (1985) reported *Chuaria* from sedimentary sequences of Paleoproterozoic age. Recently, a *Chuaria–Tawuia* assemblage has also been found from the Paleoproterozoic Changzhougou Formation in the Yanshan Range, North China (Zhu et al., 2000). Vidal et al. (1993) discussed the significance of the time range of the *Chuaria–Tawuia* assemblage with emphasis on the 700-840 Ma interval, which generally predates the Varanger glacial event. A similar conclusion was also reached by Sun (1987) mentioning that *Chuaria* occurrences fall in the time range of 700-1000 Ma.

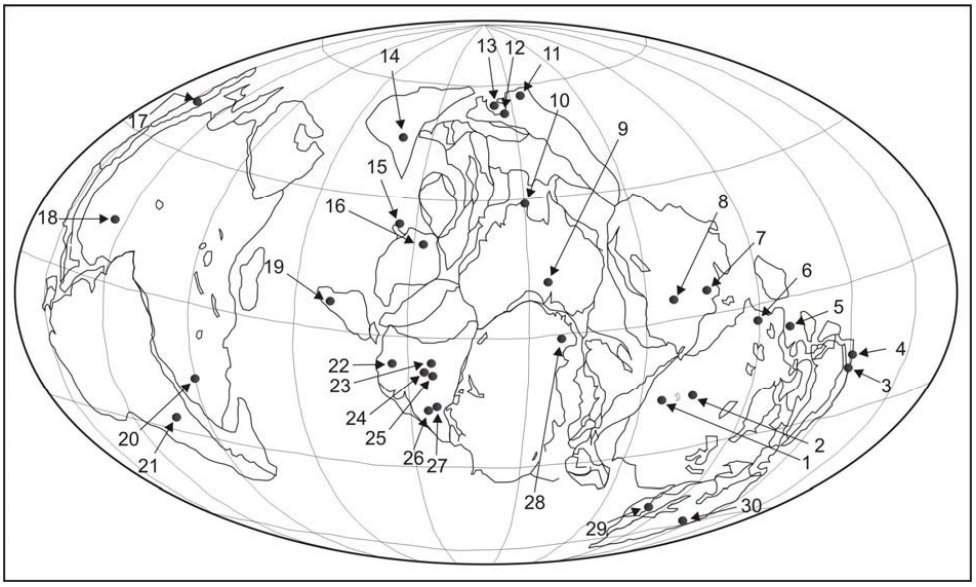


**Figure 6.8.** Distribution of the *Chuaria circularis* in a palaeogeographic reconstruction of Vendian age (Paleogeographic reconstruction modified after Kirschvink 1992) 1- Chuar Group, USA (Ford and Breed, 1973); 2- Uinta Mountain Group, Utah, USA (Hofmann, 1977); 3- Franklinsundet Group Kapp Lord Formation, Spitsbergen (Knoll, 1982); 4- Akademikerbreen Group, Svanbergfjellet Formation, Spitsbergen (Butterfield et al., 1994); 5- Shaler Supergroup, Wynniatt Formation, Victoria island, Canada (Hofmann and Rainbird, 1994); 6- Little Dal Group, Mackenzie Mountain, Canada (Hofmann, 1985b); 7- Debengdin, Khajpakh and Khatyspyt Formations, Yakutia (Vidal *et al* 1993); 8- Lachandin Formation, Uchur- Maja, Siberia (Pjatiletov, 1980); 9- Tent Hill Formation, Arcoona Quartzite, South Australia (Damssa and Knoll, 1986); 10- Wessel Group, Raiwalla Shale, Maningrida, Australia (Haines, 1998); 11- Liulaobei and Jiuliqiao Formations, Shouxian, China (Sun 1987); 12- Changlongshan Formation, Xinglong and Huailai, Hebei, China (Du and Tian, 1985); 13- Guotun, Diaoyutai, Nanfeng Formations, S. Liaoning, China (Chen, 1991); 14-Chichkan Series, Kazakhstan (Ogurtsova and Sergeev, 1989); 15- Shilu Group, Hainan island, China (Zhang et al., 1991); 16- Qingshuigou Formation, China (Dai and Peng, 1987); 17- Pusa Shale, Spain (Brasier et al., 1979); 18- Pendjari Formation, Benin and Burkina-Faso, West Africa (Amard, 1992); 19- Soltanieh Formation, Chapoghlu Shale, Elburz Mountain, Iran (Ford and Breed, 1973); 20- Nama Group, Namibia (Germs et al., 1986); 21- Sierra Bayas Formation, Argentina (Baldis et al., 1983); 22- Vindhyan Supergroup, Suket Shale, Rampura, India (Sahni, 1977; Kumar, 2001); 23- Vindhyan Supergroup, Rewa Formation, Jhiri Shale, India (Rai et al., 1997); 24- Vindhyan Supergroup, Bhander Limestone and Sirbu Shale, Maihar, India (Kumar and Srivastava, 1997); 25- Vindhyan Supergroup, Rohtas Formation, Katni, India (Rai and Gautam, 1998); 26- Bhima Group, Gangurthi Shale, South India (Suresh and Sundara Raju, 1983); 27- Kurnool Group, Owk Shale, Andhra Pradesh, India (Sharma and Shukla, 1999); 28- Robertson Bay Group, Northern Victoria Land, Antarctica (Cooper et al., 1982); 29- Visingsö Group, Sweden (Vidal, 1974); 30- Kanilov Formation, Podolia, Ukrain (Steiner, 1997).

However, Steiner (1994) reported *Chuaria* from the Early Cambrian (520-545 Ma) Yanjiahe Formation at Heziao and Jijiapo, Hubei Province, South China. Based on discoveries of fossils in an underlying unit, Amard (1997) also suggested an Early Cambrian age for *Chuaria* from the Pendjari Formation of West Africa. Therefore, the presently recorded stratigraphic range of

*Chuaria circularis* seems to range from the Paleoproterozoic to Early Cambrian. Accordingly, *Chuaria circularis* cannot be used as a biostratigraphic tool for global correlation of Proterozoic sedimentary sequences.

### 6.11. Conclusions

External surface features of *C. circularis* from the Suket Shale like wrinkles and "opening structures" are of taphonomic origin. Colour and/or opacity are not useful to define the genus because they depend on the wall thickness of the fossil. The investigated material of *C. circularis* from India shows neither radial pores/canals like those which are typical of *Tasmanites*, nor trabecular ultrastructures as observed by TEM in the topotype material of *C. circularis*. The cavities within the fossil wall occur only locally, and therefore have resulted either from previously incorporated sediments or by degradation of specific inner part of the fossil. The reflectance of *C. circularis* represents a useful tool for comparative maturity studies of Precambrian sediments. The gas chromatographic determination of pyrolysates from *C. circularis* suggests an eukaryotic algal affinity due to the predominance of *n*-alkene/*n*-alkane doublets. Micro-FTIR data are consistent with the pyrolytic studies emphasizing that biomacromolecules of the *C. circularis* investigated in the present study consist of aliphatic moiety and supports its algal affinity. Based on a review of the age and geographical distribution of *C. circularis*, it is concluded that *C. circularis* cannot be considered as an index fossil for the biostratigraphic subdivision of the Proterozoic.

### Acknowledgements

The Deutscher Akademischer Austauschdienst (DAAD) is acknowledged for providing a scholarship to SD during his stay at the Technical University Berlin. C. Hrtkopf-Fröder (Geologischer Dienst Nordrhein-Westfalen, Krefeld, Germany) is acknowledged for supporting with Micro-FTIR investigations. S. Das (IIT Bombay) is gratefully acknowledged for support with reflectance studies. We thank F. Leistner for assistance with PY-GC and J. Nissen and R. Liedtke for support with electron microscopy. SB is thankful to the Department of Earth Sciences, IIT Bombay for infrastructural facilities. Authors are thankful to N. Butterfield and M. Sharma for useful reviews of the earlier version of the manuscript.

**4.12. References**


Amard, B., 1992. Ultrastructure of *Chuaria* (Walcott) Vidal and Ford (Acritarcha) from the Late Proterozoic Pendjari Formation, Benin and Burkina- Faso, West Africa. Precambian Research 57, 121-133.

Amard, B., 1997. *Chuaria pendjariensis* n. sp. Acritarche du bassin des Volta, Benin et Burkina – Faso, Africa de l'Ouest: un taxon nouveau du Cambrien inférieur. C. R. Acad. Sci. Paris T324 (série Iia), 477-483.

Arouri, K., R., Greenwood, P.F., Walter, M.R., 1999. A possible chlorophycean affinity of some Neoproterozoic acritarchs. Organic Geochemistry 30, 1323-1337.

Arouri, K.R., Greenwood, P.F., Walter, M.R., 2000. Biological affinities of Neoproterozoic acritarchs from Australia: microscopic and chemical characterization. Organic Geochemistry 31, 75-89.

Baldis, E.D.P., Baldis, B.A, Cuomo, J., 1983. Los fosiles Precambricos de la formacion Sierras Bayas (Olavarria) y su importancia intercontinental. Asociación Geológica Argentina, Revista XXXVII, 73-83.

Bertrand, R., Héroux, Y., 1987. Chitinozoan, Graptolite and Scolecodont reflectance as an alternative to vitrinite and Pyrobitumen reflectance in Ordovician and Silurian strata, Anticosti island, Quebec, Canada. AAPG Bulletin 71, 951-957.

Bose, P.K., Sarkar, S., Chakraborty, S., Banerjee, S., 2001. Overview of the Meso- to Neoproterozoic evolution of the Vindhyan basin, Central India. Sed. Geol. 141, 395-419.

Brasier, M.D., Parejon, A., De San Jose, M.A., 1979. Discovery of an important fossiliferous Precambrian-Cambrian sequence in Spain. Estudios Geol. 35, 379-383.

Brocks, J.J., Love, G.D., Snape, C.E., Logan, G.A., Summons, R.E., Buick, R., 2003. Release of bound aromatic hydrocarbons from late Archean and Mesoproterozoic kerogens via hydropyrolysis. Geochimica et Cosmochimica Acta 67, 1521-1530.

Butterfield, N.J., Knoll, A.H., Swett, K., 1994. Paleobiology of the Neoproterozoic Svanbergfjellet Formation, Spitsbergen. Fossils and Strata 34, 1-84.

Chanda, S.K., Bhattacharyya, A., 1982. Vindhyan sedimentation and paleogeography: post-Auden developments; In: Valdiya, K.S., Bhatia, S.B., Gaur, V. K. (Eds.), Geology of Vindhyanchal (New Delhi: Hindustan Publishing Corporation), pp. 88-101.

Chapman, F., 1935. Primitive fossils, possibly Atrematous and Neotrematous brachiopoda from the Vindhyans of India. Rec. Geol. Surv. Ind. 69, 109-120.

Chen, M., 1991. Discussion on the stratigraphic significance of macrofossils from the Late Precambrian sequence in Southern Liaoning Province. Scienta Geologica Sinica 2, 120-128.

Cooper, R.A., Jago, J.B., Mackinnon, D.I., Shergold, J.H., Vidal, G., 1982. Late Precambrian and Cambrian fossils from Northern Victoria Land and their stratigraphic implications; In: Craddock, C. (Ed.), Antarctic Geoscience (The University of Wisconsin Press), pp. 629-633.

Dai, H., Peng, Y., 1987. Stratigraphic classification and biota characters of Late Presinian in Yunnan and discussion on its ages. Precambrian Geology (Geological Publishing House, Beijing), pp. 115-126.

Damassa, S.P., Knoll, A.H., 1986. Micropalaeontology of the late Proterozoic Arcoona Quartzite Member of the Tent Hill Formation, Stuart Shelf, South Australia. Alcheringa 10, 417-430.

de Leeuw, J.W., Versteegh, G.J.M. van Bergen, P.F., 2006. Biomacromolecules of algae and plants and their fossil analogues. Plant Ecology 182, 209-233.

Derenne, S., Largeau, C., Berkaloff, C., Rousseau, B., Wilheim, C., Hatcher, P., 1992. Non-hydrolysable macro-molecular constituents from outer walls of *Chlorella fusca* and *Nanochlorum eucaryotum*. Phytochemistry 31, 1923-1929.

Du, R., Tian, L., 1985. Algal macrofossils from the Qingbeikou System in the Yanshan Range of North China. Precambian Research 29, 5-14.

Duan, C., 1982. Late Precambrian algal megafossils *Chuaria* and *Tawuia* in some areas of eastern China. Alchering 6, 57-68.

Dutta, S., Greenwood, P.F., Brocke, R., Schaefer, R.G., Mann, U., 2006. New insights into the relationship between *Tasmanites* and tricyclic terpenoids. Organic Geochemistry 37, 117-127.

Eisenack, A., 1966. Über *Chuaria wimani* Brotzen. Neues Jahrbuch für Geologie und Paläontologie 1, 52-56.

Ford, T.D., Breed, W.J., 1973. The problematical Precambrian fossil *Chuaria*, Palaeontology 16, 535-550.

Germs, G.J.B., Knoll, A.H., Vidal, G., 1986. Latest Proterozoic microfossils from the Nama Group, Namibia (South West Africa). Precambian Research 32, 45-62.

Ghare, M.A., Badve, R.M., 1978. On *Chuaria circularis* Walcott from the Suket Shale of Rampura, Madhaya Pradesh; In: Rasheed, D.A. (Ed.), Proceedings of the Seventh Indian

Colloq. on Micropalaeontology and Stratigraphy (University of Madras, Madras), pp. 31-40.

Greenwood, P.F., Arouri, K.R., George, S.C., 2000. Tricyclic terpenoid composition of *Tasmanites* kerogen as determined by pyrolysis GC-MS. Geochimica et Cosmochimica Acta 64, 1249-1263.

Grice, K., Schouten, S., Blokker, P., Derenne, S., Largeau, C., Nissenbaum, A., Sinninghe Damsté, J.S., 2003. Structural and isotopic analysis of kerogens in sediments rich in free sulfurised *Botryococcus braunii* biomarkers, Organic Geochemistry 34, 471-482.

Hatcher, P.G., Clifford, D.J., 1997. The organic geochemistry of coal: from plant materials to coal. Organic Geochemistry 27, 251-274.

Haines, P.W., 1998. *Chuaria* Walcott, 1899 in the lower Wessel Group, Arafura Basin, northern Australia. Alcheringa 22, 1-8.

Hoffknecht, A., 1991. Mikropetrographische, organisch-geochemische, mikrothermometrische und mineralogische Untersuchungen zur Bestimmung der organischen Reife von Graptolithen-Periderm. Göttinger Arbeiten zur Geologie und Paläontologie 48, 1-98.

Hofmann, H.J., 1971. Precambrian fossils, pseudofossils and problematica in Canada. Bull. Geol. Surv. Canada 189, 1-146.

Hofmann, H.J., 1977. The problematic fossil *Chuaria* from the Late Precambrian Uinta mountain Group, Utah. Precambian Research 4, 1-11.

Hofmann, H.J., 1985a. Precambrian carbonaceous megafossils; In: Toomy D.F., Nitecki M.H. (Eds.), Paleoalgology: Contemporary Research and Applications (Berlin, Heidelberg: Springer-Verlag), pp. 20-33.

Hofmann, H.J., 1985b. The mid-Proterozoic Little Dal macrobiota, Mackenzie Mountains, northwest Canada. Palaeontology 28, 331-354.

Hofmann, H.J., 1992. Proterozoic carbonaceous films; In: Schopf J.W., Klein, C. (Eds.), The Proterozoc Biosphere- A Multidisciplinary Study (Cambridge University Press, Cambridge), pp. 349-357.

Hofmann, H.J., Chen, J., 1981. Carbonaceous megafossils from the Precambrian (1800 Ma) near Jixian Northern China, Can. J. Earth Sci. 18, 443-447.

Hofmann, H.J., Rainbird, R.H., 1994. Carbonaceous megafossils from the Neoproterozoic Shaler Supergroup of Arctic Canada. Palaeontology 37, 721-731.

Javaux, E.J., Knoll, A.H., Walter, M.R., 2004. TEM evidence for eukatytic diversity in mid-Proterozoic oceans. Geobiology 2, 121-132.

Jones, H.J., 1909. In: General Report, Rec. Geol. Surv. India 3**,** 66.

Jux, U., 1977. Über die Wandstrukuren sphaeromorpher Acritarchen: *Tasmanites* Newton, *Tapajonites* Sommer and Van Boekel, *Chuaria* Walcott. Palaeontographica Abt. B 160, 1-16.

Kirschvink, J.L., 1992. A Paleogeographic model for Vendian and Cambrian time. In: J.W., Klein, C. (Eds.), The Proterozoic Biosphere Schopf (Cambridge University Press), pp. 569-581.

Knoll, A.H., 1982. Microfossil-based biostratigraphy of the Precambrian Hecla Hoek sequence, Nordaustlandet, Svalbard. Geological Magazine 119, 269-279.

Kumar, S., 2001. Mesoproterozoic megafossil *Chuaria-Tawuia* association may represent parts of a multicellular plant, Vindhyan Supergroup, Central India. Precambian Research 106, 187-211.

Kumar, S., Srivastava, P., 1997. A note on the carbonaceous megafossils from the Neoproterozoic Bhander Group, Maihar area, Madhya Pradesh. J. Pal. Soc. India 42, 141-146.

Larter, S.R., Horsfield, B., 1993. Determination of structural components of kerogens by the use of analytical pyrolysis methods. In: Engel, M.H., Macko, S.A. (Eds.), Organic Geochemistry (New York: Plenum Press), pp. 271-288.

Li, C., Peng, P., Sheng, G., Fu, J., 2004. A study of a 1.2 Ga kerogen using Ru ion-catalyzed oxidation and pyrolysis-gas chromatography-mass spectrometry: structural features and possible source. Org. Geochem. 35, 531-541.

Mackowsky, M.T., 1982. Methods and tools of examination; In: Stach, E., Mackowsky, M .T., Taylor, G.H., Chandra, D., Teichmüller, R. (Eds.), Textbook of Coal Petrology (Gebrüder Borntraeger, Berlin), pp. 295-299.

Maithy, P.K., Shukla, M., 1977. Microbiota from the Suket Shale, Rampura, Vindhyan System, Madhya Pradesh. Palaeobotanist 23, 176-188.

Maithy, P.K., Shukla, M., 1984. Reappraisal of *Fermoria* and allied remains from the Suket Shale Formation, Rampura. Palaeobotanist 32, 146-152.

Marshall, C.P., Javaux, E.J., Knoll, A.H., Walter, M.R., 2005. Combined micro-Fourier transform infrared (FTIR) spectroscopy and micro-Raman spectroscopy of Proterozoic acritarchs: A new approach to Paleobiology. Precambrian Research 138, 208-224.

Obermajer, M., Fowler, M.G., Goodarzi, F., Snowdon, L.R., 1996. Assessing thermal maturity of Paleozoic rocks from reflectance of chitinozoa as constrained by geochemical indicators: an example from southern Ontario, Canada. Mar. Petrol. Geol. 13, 907-919.

Ogurtsova, R.N., Sergeev, V.N., 1989. The Megasphaeromorphids of the Tsitskaisk deposits of the Upper Precambrian of South Kazakhstan. Paleontologitscheskii Journal 2**,** 119-122 (in Russian).

Pjatiletov, V.G., 1980. New finds of microfossils of Navifusa in the Lachandin stage. Palaeontologitscheskii Journal 3, 143-145.

Poelchau, H.S., Baker, D.R., Hantchel, T., Horsfield, B., Wygrala, B., 1997. Basin simulation and the design of the conceptual basin model; In: Welte, D.H., Horsfield, B., Baker, D.R. (Eds.), Petroleum and Basin Evolution (Berlin, Heidelberg: Springer-Verlag), pp. 3-62.

Rai, V., Gautam, R., 1998. New occurrence of carbonaceous megafossils from the Meso-to Neoproterozoic horizons of the Vindhyan Supergroup, Kaimur-Katni areas, Madhya Pradesh, India. Geophytology 26, 13-25.

Rai, V., Shukla, M., Gautam, R., 1997. Discovery of carbonaceous megafossils (*Chuaria-Tawuia* assemblage) from the Neoproterozoic Vindhyan succession (Rewa Group), Allahabad-Rewa area, India. Current Science 73, 783-788.

Rasmussen, B., Bose, P.K., Sarkar, S., Banerjee, S., Fletcher, I.R., McNaughton, N.J., 2002. 1.6 Ga U-Pb zircon ages for the chorhat sandstone, Lower Vindhyan: possible implications for the early evolution of animals. Geology 30, 103-106.

Sahni, M.R., 1936. *Fermeria minima*: A revised classification of the organic remains from the Vindhyan of India. M. Rec. Geol. Surv. India. 458-468.

Sahni, M.R., 1977. Vindhyan palaeobiology, stratigraphy and depositional environments: a critical review. J. Pal. Soc. India 20, 289-304.

Sarangi, S., Gopalan, K., Kumar, S., 2004. Pb-Pb age of earliest megascopic, eukaryotic alga bearing Rohtas Formation, Vindhyan Supergroup, India: implications for Precambrian atmospheric oxygen evolution. Precambian Research 132, 107-121.

Sarkar, S., Banerjee, S., Chakraborty, S., Bose, P.K., 2002. Shelf storm flow dynamics: insight from the Mesoproterozoic Rampur Shale, Central India. Sedimentary Geology 147, 89-104.

Sharma, M., Shukla, M., 1999. Carbonaceous megaremains from the Neoproterozoic Owk Shales Formations of the Kurnool Group. Andhra Pradesh, India. Current Science 76, 1247-1251.

Stankiewicz, B.A., Briggs, D.E.G., Michels, R., Collinson, M.E., Flannery, M.B., Evershed, R.P., 2000. Alternative origin of aliphatic polymer in kerogen. Geology 28, 559-562.

Steiner, M., 1994. Die Neoproterozoischen Megaalgen Südchinas. Berliner Geowissenschaftliche Abhandlungen (E) 15,1-146.

Steiner, M., 1997. *Chuaria circularis* WALCOTT 1899-"Megasphaeromorph Acritarch" or Prokaryotic Colony ? In: Fatka, O., Servais,T. (Eds.), C. I. M. P. Acritarch in Praha Acta Univ. Carolinae Geol. 40, 645- 665.

Sun, W., 1987. Palaeontology and biostratigraphy of Late Precambrian macroscopic colonial algae: *Chuaria* and *Tawuia* Hofmann. Palaeontographica Abt. B 203, 109-134.

Suresh, R., Sundara Raju, T.P., 1983. Problematic *Chuaria*, from the Bhima Basin, South India. Precambian Research 23, 79-85.

Talyzina, M.N., 2000. Ultrastructure and morphology of *Chuaria circularis* (Walcott, 1899) Vidal and Ford (1985) from the Neoproterozoic Visingsö Group, Sweden. Precambian Research 102, 123-134.

Versteegh, G.J.M., Blokker, P., Wood, G., Collinson, M.E., Sinninghe Damsté, J.S., de Leeuw, J. W., 2004. Oxidative polymerization of unsaturated fatty acids as a preservation pathway for microalgal organic matter. Organic Geochemistry 35, 1129-1139.

Vidal, G., 1974. Late Precambrian microfossils from the basal sandstone unit of the Visingsö Beds, South Sweden. Geologica et Paleontologica 8, 1-14.

Vidal, G., 1976. Late Precambrian microfossils from the Visingsö Beds in Southern Sweden. Fossil and Strata 9, 1-57.

Vidal, G., Moczydlowska, M., Rudavskaya, V.A., 1993. Biostratigraphical implications of a *Chuaria-Tawuia* assemblage and associated acritarchs from the Neoproterozoic of Yakutia. Palaeontology 36, 387-402.

Walcott, C.D., 1899. Precambrian fossiliferous formations. Geol. Soc. Am. Bull. 19, 199-244.

White, D., 1928. Study of the fossil floras in the Grand Canyon; – Carnegie Inst. Washington, Yearbook 27, 389-390.

Yalçin, M.N., Littke, R., Sachsenhofer, R.F., 1997. Thermal history of sedimentary basins; In: Welte, D.H., Horsfield, B., Baker, D.R. (Eds.), Petroleum and Basin Evolution (Berlin, Heidelberg: Springer-Verlag), pp. 71-161.

Yuan, X., Xiao, S., Li, J., Yin, L., Cao, R., 2001. Pyritized chuaridis with excystment structures from the late Neoproterozoic Lantian formation in Anhui, South China. Precambrian Research 107, 253-263.

Yule, B.L., Roberts, S., Marshall, J.E.A., 2000. The thermal evolution of sporopollenin. Organic Geochemistry 31, 859-870.

Zhang, R., Feng, S., MA, G., XU, G., Yan, D., Li, Z., Jiang, D., WU, W., 1991. Discovery of *Chuaria-Tawuia* assemblage in Shilu Group, Hainan Island and its significance. Science in China (Series B) 33, 211-222.

Zhu, S., Sun, S., Huang, X., HE, Y., Zhu, G., Sun, L., Zhang, K., 2000. Discovery of carbonaceous compressions and their multicellur tissues from the Changzhougou Formation (1800 Ma) in the Yanshan range, North China. Chinese Science Bulletin 45, 841-847.

# CHAPTER 7

## Summary and Perspective

This study has revealed the molecular composition of extraordinarily well preserved, organic-walled microfossils (palynomorphs) from selected time windows of Proterozoic to Mesozoic time. Sedimentary rock samples were collected from 11 localities: Hazro area (SE Turkey), Ruhr Basin (Germany), Weilerbach (Germany), Zwickau (Germany), Alstätte Embayment (German-Dutch border), Wülfrath (Germany), Gotland (Sweden), Oklahoma (USA), Virginia (USA), Rampura (India) and Tasmania (Australia). All samples are of low thermal maturity (Rock Eval $T_{max}$ 418°C ($R_c$~0.40) - 444°C ($R_c$~0.75)), except sediments from Suket Shale (Rampura, India). Palynomorphs which are taxonomically well assigned by project collaborators have been handpicked. For the present investigations, various types of palynomorphs, for example, *Tasmanites*, *Leiosphaeridia*, chitinozoans, scolecodonts, megaspores and *Chuaria circularis* have been selected. An approach combining microscopy, Micro-Fourier transform infrared (FTIR) spectroscopy and pyrolysis-gas chromatography-mass spectrometry (Py-GC-MS) has been applied. Individual palynomorphs, and their pyrolysis products are given in the Table 7.1.

A chemical comparison between thick-walled (***Tasmanites***) and thin-walled (***Leiosphaeridia***) prasinophytes has been documented in **chapter 2**. The genus *Tasmanites* is characterised by radial canals, which are absent in the genus *Leiosphaeridia*. *Leiosphaeridia* are comparatively thin-walled and heavily folded. Extraordinarily well preserved, handpicked *Tasmanites* from Silurian–Devonain sedimentary sequence from SE Turkey (Fetlika-1 borehole), Oklahoma (USA) and Virginia (USA), and *Leiosphaeridia* from SE Turkey and from Virginia have been analysed using Curie point pyrolysis-gas chromatography-mass spectrometry to investigate their biomacromolecular structure (see chapter 2 and appendix). *Tasmanites* from Tasmania (Australia, Late Carboniferous/Early Permian) has also been analysed with same analytical protocol. Although *Tasmanites* and *Leiosphaeridia* are morphologically distinct, their overall chemical compositions are similar. The pyrolysates from both thick-walled and thin-walled prasinophytes are dominated by a series of *n*-$C_{6-22}$ alkene/alkane doublets which are typical of pyrolysis products of algaenan, the microbiological resistant algal biopolymer. Aromatic hydrocarbons such as alkylbenzenes and alkylphenanthrenes occur in minor concentration. *Tasmanites* are generally believed to be a

biological source of biomarker tricyclic terpenoids. The pyrolysates of the *Tasmanites* from Tasmania show a normal tricyclic terpenoid product distribution, but no traces of tricyclic terpenoids have been detected from the pyrolysates of *Tasmanites* from Turkey and USA. However, the pyrolysates of *Leiosphaeridia* from Turkey show the presence of monounsaturated and diunsaturated tricyclic terpenes as well as monoaromatic tricyclic terpanes. It is concluded that the inherent source-biomarker relationship between the *Tasmanites* and tricyclic terpenoids does not always exist. Furthermore, tricyclic terpenoid pyrolysates of the *Leiosphaeridia* from the Dadas Formation confirms that there are more than one biological source(s) of these biomarkers and they are not exclusively from or always diagnostic of *Tasmanites*. In the past, Leiosphaerids have been compared with alete spores and dinoflagellates other than prasinophycean green algae. A series of *n*-alkene/*n*-alkane doublets in the pyrolysates of *Leiosphaeridia* from Hazro area, SE Turkey and from Virginia clearly indicates that the biomacromolecules of *Leiosphaeridia* are of purely aliphatic nature which is the characteristic feature of an alga.

In **chapter 3**, the molecular composition of purely hand picked **chitinozoans** has been discussed. Chitinozoans are extensively used as biostratigraphic and palaeobiogeographical index fossils of Lower and Middle Paleozoic sequences. Chitinozoans also offer promising applications in the field of organic-petrography, for instance by measuring the reflectance of their vesicle wall thermal maturity of the host rock can be assessed. This is especially true for pre-Devonian sediments where the organic remains from higher plants are absent or very rare (see Obermajer et al., 1996 and references therein). Biomacromolecules of Chitinozoa consist of both aliphatic and aromatic moieties. A series of *n*-alkene/*n*-alkane doublets represents the aliphatic moiety. Alkylbenzenes, alkylnaphthalenes, alkylphenols and alkylphenanthrenes are the major aromatic compounds found in the pyrolysates of Chitinozoa. Aromatic compounds predominate over aliphatic compounds. 1,2,3,4-Tetramethylbenzene is the most abundant pyrolysates of Chitinozoa. Aryl isoprenoids are also present in the host sediment extract. Both, 1,2,3,4-tetramethylbenzene in the pyrolysates of Chitinozoan and aryl isoprenoids in the host sediment extract have been derived from same precursor diaromatic compound, but the biological precursor of those compounds is yet not clear. Presence of abundant alkylnaphthalenes in the pyrolysates of Chitinozoa and the host sediment extract suggests that chitinozoans are the biological precursor of alkylnaphthalenes and these compounds are not always diagnostic of higher plants. Micro-FTIR data are consistent with the pyrolytic studies emphasizing that biomacromolecules of the Chitinozoa investigated in the present study

consist of both aliphatic and aromatic components. No pyrolysis products diagnostic of chitin were detected in the present study. The compounds and their distribution pattern, which are found in the pyrolysates of Chitinozoa are not comparable to the compounds that are produced upon the pyrolysis of fossil arthropod cuticles consisting of degraded chitin biomacromolecules (for comparison see Stankiewicz et al. 1997). Therefore, it is evident that original macromolecules of Chitinozoa before fossilization were not made of chitin related compounds and hence, the incorporation of the word "chitin" into the name of these extinct organisms was not appropriate. Chitinozoans belong to a group of rare marine organisms that have substantial amount of 'lignin-like' macromolecular matter.

In **chapter 4**, the chemical composition of sporopollenin of fossil **megaspores** from the Cretaceous and from the Pennsylvanian has been discussed. Both spectroscopic and pyrolytic investigations demonstrate that the sporopollenin of the fossil spores consists of both aliphatic and aromatic moieties. The micro-FTIR spectra of the spore walls of all megaspores are characterised by aliphatic $CH_x$ (3000-2800 and 1460-1450 $cm^{-1}$) and $CH_3$ (1375 $cm^{-1}$) absorptions, aromatic C=C (1560-1610 $cm^{-1}$) and CH (3050 $cm^{-1}$ and 700-900 $cm^{-1}$) absorptions and various acid C=O group absorptions at 1740-1700 $cm^{-1}$. Alkylated benzenes and alkylphenols are the major aromatic compounds and a homologous series of *n*-alkenes/*n*-alkanes are present in the pyrolysates of all the fossil sporopollenin. Acetophenone is present in the pyrolysates of all three megaspores of Cretaceous age, but is absent in the pyrolysates of other spores from Pennsylvanian. The relative abundance of phenols compared to other compounds is higher in the Cretaceous megaspores than those from the Pennsylvanian. It is suggested that oxygenated aromatic compounds were selectively degraded during burial and diagenesis with increasing thermal maturation and time. The pyrolysates of *Paxillitriletes midas* contain aromatic compounds like cadalene, retene, dehydroabietin, simonellite and ferruginol which are generally believed to be the biomarkers of coniferous resins. More investigations are needed to reveal the relationship between these biomarkers and sporopollenin. The relative abundance of *n*-alkenes/*n*-alkanes pyrolysates of spores from the Pennsylvanian sediments is higher than those from the Cretaceous. As the megaspores from the Pennsylvanian are relatively older as well as thermally more mature than that of the Cretaceous samples, it is apparent that abundance of aliphatic moiety was selectively increased during burial and diagenesis with increasing thermal maturity and time.

**Table 7.1** Individual palynomorphs (handpicked), thermal maturity of their host rocks ($T_{max}$ from Rock Eval pyrolysis) and major, minor and specific biomarkers produced upon pyrolysis.

| **Taxon (origin)** | **Age** | **$T_{max}$ (°C)** | **Major compounds** | **Minor compounds** | **Specific biomarker(s)** |
|---|---|---|---|---|---|
| *Tasmanites* (Tasmania, Australia) | Late Carboniferous/ Early Permian | 444 | -*n*-alkene/*n*-alkane doublets ($C_6$-$C_{24}$) | -alkylbenzenes -alkylnaphthalenes | saturated ($C_{19}$-$C_{24}$), unsaturated ($C_{19}$-$C_{20}$) and aromatic ($C_{18}$-$C_{20}$) tricyclic terpenoids |
| *Tasmanites* (Hazro area, SE Turkey) | Late Silurian/Early Devonian | 430 | -*n*-alkene/*n*-alkane doublets ($C_6$-$C_{24}$) | -alkylbenzenes -alkylnaphthalenes | - |
| *Tasmanites* (Oklahoma, USA) | Late Devonian/ Early Carboniferous | 424 | -*n*-alkene/*n*-alkane doublets ($C_6$- $C_{24}$) | -alkylbenzenes -alkylnaphthalenes | - |
| Cf. *Tasmanites* (Virginia, USA) | Late Devonian | 439 | -*n*-alkene/*n*-alkane doublets ($C_6$-$C_{24}$) | -alkylbenzenes | - |
| *Leiosphaeridia* (Hazro area, SE Turkey) | Late Silurian/Early Devonian | 430 | -*n*-alkene/*n*-alkane doublets($C_6$-$C_{24}$) | -alkylbenzenes -alkylnaphthalenes | unsaturated ($C_{19}$-$C_{20}$) and aromatic ($C_{18}$-$C_{20}$) tricyclic terpenoids |
| Cf. *Leiosphaeridia* (Virginia, USA) | Late Devonian | 439 | -*n*-alkene/*n*-alkane doublets ($C_6$-$C_{24}$) | -alkylbenzenes -alkylnaphthalenes | - |
| Chitinozoa (Hazro area, SE Turkey) | Late Silurian | 430 | -alkylbenzenes -alkylnaphthalenes -*n*-alkene/*n*-alkane doublets ($C_6$-$C_{23}$) -alkylphenols -alkylphenanthrenes | -alkylphenanthrenes | 1,2,3,4-tetramethylbenzene |
| *Calamospora laevigata* (Saarland, Germany) | Pennsylvanian | 432 | -*n*-alkene/*n*-alkane doublets ($C_6$-$C_{25}$) -alkylbenzenes -alkylphenols -alkylnaphthalenes | - | - |

| | | | | | |
|---|---|---|---|---|---|
| *Laevigatisporites reinschii* (Ruhr Basin, Germany) | Pennsylvanian | 437 | -*n*-alkene/*n*-alkane doublets ($C_6$-$C_{27}$)<br>-alkylbenzenes<br>-alkylphenols<br>-alkylnaphthalenes | - | - |
| *Tuberculatisporites* sp. (Zwickau, Germany) | Pennsylvanian | 429 | -*n*-alkene/*n*-alkane doublets ($C_6$-$C_{24}$)<br>-alkylbenzenes<br>-alkylphenols<br>-alkylnaphthalenes | - | - |
| *Paxillitriletes midas* (Alstätte Embayment, German-Dutch border | Cretaceous | 419 | -*n*-alkylbenzene/*n*-alkenylbenzene doublets ($C_7$ -$C_{12}$)<br>-alkylphenols<br>-*n*-alkene/*n*-alkane doublets ($C_6$-$C_{18}$)<br>-acetophenone | -alkylnaphthalenes | cadalene, retene, dehydroabietane, simonellite, ferruginol |
| Megaspores (Wülfrath, Germany) | late Early to early Late Cretaceous | 422 | -alkylbenzenes<br>-alkylphenols<br>-*n*-alkene/*n*-alkane doublets ($C_6$-$C_{18}$)<br>-acetophenone | -alkylnaphthalenes | - |
| *Dijkstraisporites helios* (Wülfrath, Germany) | late Early to early Late Cretaceous | 418 | -alkylbenzenes<br>-alkylphenols<br>-*n*-alkene/*n*-alkane doublets ($C_6$-$C_{18}$)<br>-acetophenone | -alkylnaphthalenes | - |
| Scolecodont (Gotland, Sweden) | Silurian | 428 | -*n*-alkene/*n*-alkane doublets ($C_6$-$C_{15}$)<br>-alkylbenzenes<br>-alkylphenols | -alkylnaphthalenes | - |
| *Chuaria circularis* (Rampura, India) | Early Mesoproterozoic | - | -*n*-alkene/*n*-alkane doublets ($C_6$-$C_{22}$) | -alkylbenzenes | - |

In **chapter 5**, biomacromolecules of **scolecodonts** (Silurian in age) from Gotland, Sweden were investigated. The major pyrolysates from the scolecodonts include aromatic compounds such as alkylbenzenes, alkylnaphthalenes, alkylphenols and the aliphatic hydrocarbons are represented by a homologous series of *n*-alkenes and *n*-alkanes. Presence of predominant aromatic pyrolysates in scolecodonts may suggest that kerogen of marine origin enriched with zooclasts like scolecodonts can also yield aromatic pyrolysates which are commonly believed to be characteristic for type-III kerogen derived from terrestrial higher plants.

In **chapter 6**, the study on ***Chuaria circularis*** from the Early Mesoproterozoic Suket Shale of the Vindhyan Supergroup (Central India) using microscopy, spectroscopy and pyrolysis-gas chromatrogrphy is shown. Morphology and microscopic investigations provide little clues on the specific biological affinity of *Chuaria* as numerous preservational artifacts seem to be incorporated. The predominance of *n*-aliphatic pyrolysates of *Chuaria* from India suggests that the biomacomolecules of *C. circularis* are of aliphatic nature. Micro-FTIR data are consistent with the pyrolytic studies emphasizing that biomacromolecules of the *C. circularis* investigated in the present study consist of aliphatic moieties and support its algal affinity. It is concluded that *Chuaria circularis* was a probably very early eukaryotic algae which appeared during Early Mesoproterozoic time in the area of the Indian Platform.

According to the biomacromolecular composition, the investigated organic-walled micro fossils can be grouped as follows:

- As demonstrated by abundant alkenes/alkanes in pyrolysates, only algae posses a wall consisting of highly aliphatic biomacromolecules.
- Megaspores, chitinozoans and scolecodonts consist of both aliphatic and aromatic moieties.

It is concluded that kerogen of marine origin does also yield aromatic compounds including phenols upon pyrolysis. Conversely, aromatic compounds generated upon pyrolysis of kerogen may not always be associated to kerogen derived from terrestrial higher plants.

To extend our understanding on organic-geochemistry and paleobiology of organic-walled microfossils (palynomorphs), it is necessary to carry out more investigations on purely handpicked palynomorphs. Conventional extraction of lipid biomarker molecules can provide valuable information on ‘source rock’ characteristics, but correlation of biomarkers with specific microfossils taxa is difficult. Pyrolytic investigation of taxonomically well assigned

palynomorphs would certainly provide valuable information on source-biomarker relationship. The biological affinity of individual morphotypes of acritachs is still patchy. An approach combining microscopy, Fourier transform infrared spectroscopy and pyrolysis-gas chromatography-mass spectrometry can be used appropriately to understand the wall chemistry of individual morphotypes of acritarchs and may help us to understand the early evolution and diversification of the biosphere. Since the early 1970s, several attempts have been made to obtain pure dinoflagellate cyst fractions from the sediments (Combaz, 1971). Recently Versteegh et al. (2004) analysed monotypic assemblage of fossil dinoflagellate from the Eocene sediments of Pakistan. Their chemical analysis showed that macromolecles of those dinoflagellate were highly aliphatic consisting of ether-linked aliphatic carbon chains, notably with 16 and 18 carbon atoms and a predominantly $C_9$ mid chain functionality. They suggested that the microfossils had been formed post-mortem by oxidative polymerization of the fatty acids equivalents of the macromolecular building blocks, derived from cellular membranes and storage vesicles. Neoproterozoic acritarchs have been related to dinoflagellates (Arouri et al., 2000). This is in agreement with earlier studies, based on morphology (Butterfield and Rainbird, 1998), the fossil record of dinosteroids (Moldowan and Talyzina, 1998) and molecular phylogeny (Javaux et al., 2003) that the dinoflagellates originated in the Neoproterozoic. It is necessary to analyse purely handpicked and taxonomically well assigned fossil dinoflagellate cysts from Triassic and younger strata from different localities to get detailed insight into biomacromolecules of these palynomorphs and this may provide important clues on evolution of early eukaryotes. Furtheremore, wall chemistry of organic-walled microfossils provides clues to the biological relationship of Proterozoic and Paleozoic fossils (see Javaux and Marshal, 2006). The earliest fossil evidence for land plants is from the Ordovician (Servais and Paris, 2000) and consists of dispersed spores and phytodebris. The chemical composition of these organic remains may permit to understand the chemical and physiological adaptations which were needed for plants to survive in a new, hostile environment. A detailed chemical study on various organic-walled microfossils both from Proterozoic and Paleozoic is inevitable to understand the early evolutionary mechanisms and patterns and the early interactions between environment and life.

**References**


Arouri, K., Greenwood, P.F., Walter, M. R., 2000. Biological affinities of Neoproterozoic acritarchs from Australia: microscopic and chemical characterization. Organic Geochemistry 31, 75-89.

Butterfiled, N.J., Rainbird, R.H., 1998. Diverse organic-walled fossils, including 'possible dinoflagellates' from the early Neoproterozoic of arctic Canada. Geology 26, 963-966.

Combaz, A., 1971. Thermal degradation of sporopollenin and genesis of hydrocarbons. In Brocks, J. et al. (Eds.), Sporopollenin. Academic Press, London, pp. 621-653.

Javaux, E., Knoll, A.H., Walter, M., 2003. Recognizing and interpreting the fossils of early eukaryotes. Orig. Life Evol. Biosph. 33, 75-94.

Javaux, E.J., Marshal, C.P., 2006. A new approach in deciphering early protist paleobiology and evolution: Combined microscopy and microchemistry of single Proterozoic acritarchs. Review of Paleobotany and Palynology 139, 1-15.

Moldowan, J.M., Talyzina, N.M., 1998. Biogeochemical evidences for dinoflagellate ancestors in the early Cambrian. Science 281, 1168-1170.

Obermajer, M., Fowler, M.G., Goodarzi, F., Snowdon, L.R., 1996. Assessing thermal maturity of Paleozoic rocks from reflectance of chitinozoa as constrained by geochemical indicators: an example from southern Ontario, Canada. Marine and Petroleum Geology 13, 907-919.

Servais, T., Paris, F., 2000. Ordovician palynology: balance and future prospects at the beginning of the third millennium. Review of Paleobotany and Palynology 113, 1-14.

Stankiewicz, B.A., Briggs, D.E.G., Evershed, R.P., 1997. Chemical composition of Paleozoic and Mesozoic fossil invertebrate cuticles as revealed by pyrolysis-gas chromatography/mass spectrometry. Energy and Fuels 11, 515-521.

Versteegh, G.J.M., Blokker, P., Wood, G., Collinson, M.E., Sinninghe Damsté, J.S., de Leeuw, J.W., 2004. An example of oxidative polymerization of unsaturated fatty acids as a preservation pathway for dinoflagellate organic matter. Organic Geochemistry 35, 1129-1139.

# Appendix

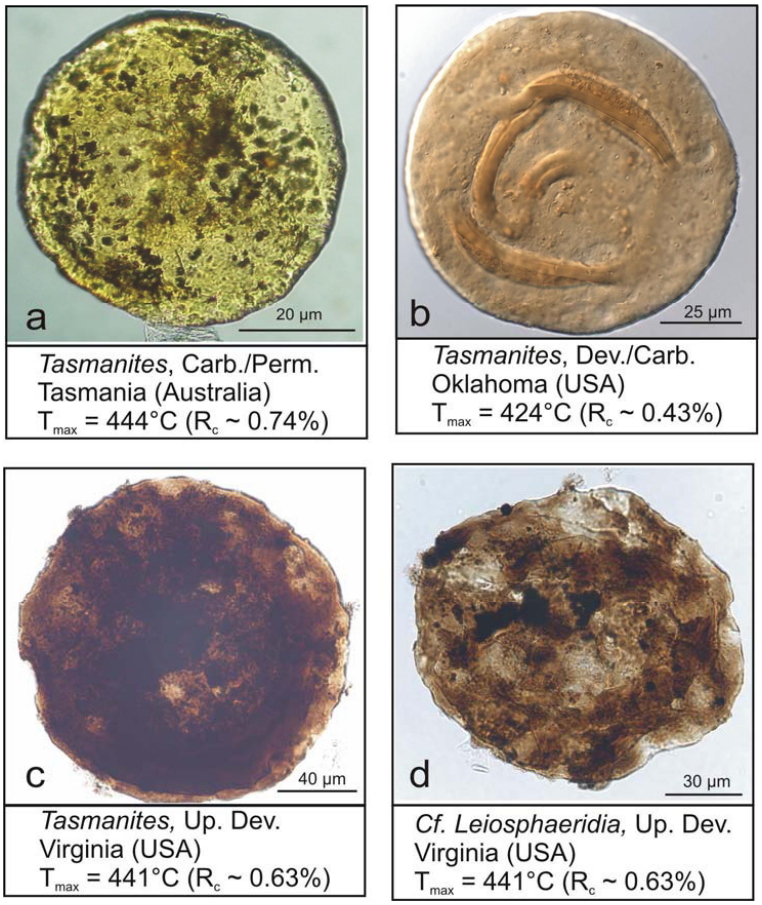


[Photo micrographs (b), (c) & (d) courtesy of C. Hartkopf-Fröder]

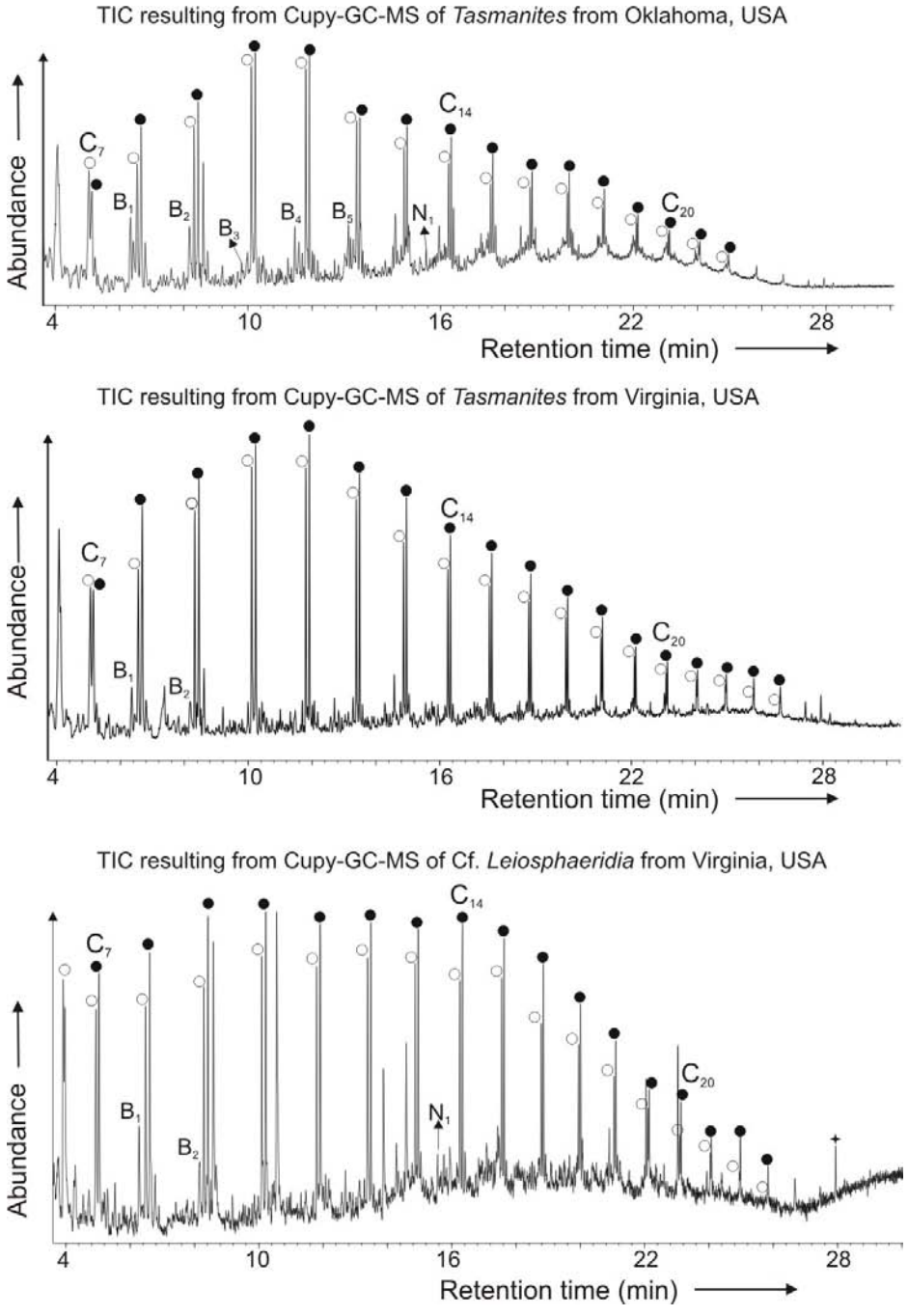
TIC resulting from Cupy-GC-MS of *Tasmanites* from Oklahoma, USA
Abundance
C7
B1
B2
B3
B4
B5
N1
C14
C20
4
10
16
22
28
Retention time (min)
TIC resulting from Cupy-GC-MS of *Tasmanites* from Virginia, USA
Abundance
C7
B1
B2
C14
C20
4
10
16
22
28
Retention time (min)
TIC resulting from Cupy-GC-MS of Cf. *Leiosphaeridia* from Virginia, USA
Abundance
C7
B1
B2
N1
C14
C20
4
10
16
22
28
Retention time (min)

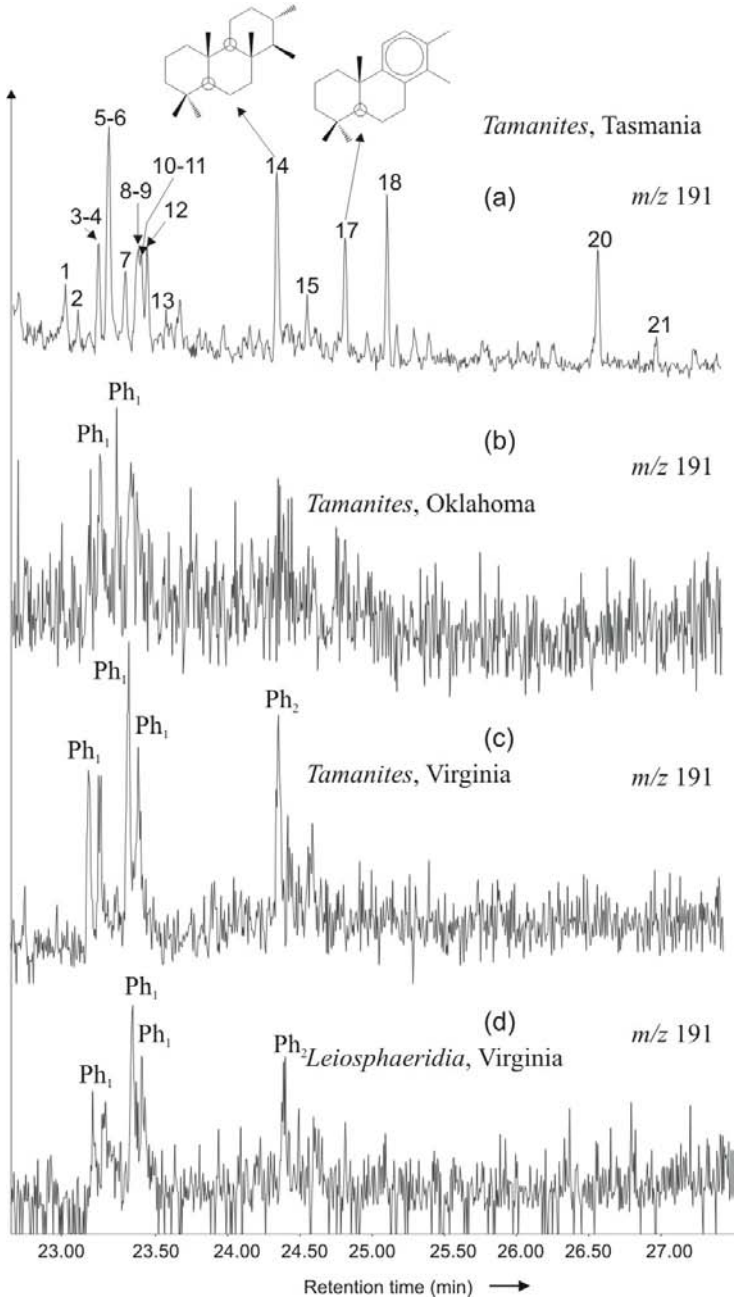


Partial mass chromatograms at *m/z* 191 from the Curie point pyrolysis-GC-MS analysis of (a) *Tasmanites* from Tasmanis; (b) *Tasmanites* from Olkahoma; (c) *Tasmanites* from Virginia and (d) Cf. *Leiosphaeridia* from Virginia. The assigned peaks are listed in Table 2.1; $Ph_1$ and $Ph_2$ indicate $C_1$ phenanthrene and $C_2$ phenanthrene, respectively.

## Publications

This thesis is based on the following publications:

**Chapter 2:** Dutta, S., Greenwood, P.F., Brocke, R., Schaefer, R.G., Mann, U., 2006. New insights into the relationship between *Tasmanites* and tricyclic terpenoids. Organic Geochemistry 37, 117-127.

**Chapter 3:** Dutta, S., Brocke, R., Hartkopf-Fröder, C., Littke, R., Wilkes, R., Mann, U., (submitted to 'Organic Geochemistry'). Highly aromatic character of biogeomacromolecules in Chitinozoa: a spectroscopic and pyrolytic study.

**Chapter 4:** Dutta, S., Hartkopf-Fröder, C., Greenwood, P.F., Littke, R., Wilkes, R., Mann, U., (in preparation). The molecular composition of sporopollenin from fossil megaspores as revealed by micro-FTIR and pyrolysis-GC-MS.

**Chapter 5:** Dutta, S., Hartkopf-Fröder, C., Littke, R., Wilkes, R., Mann, U., (in preparation) The molecular composition of Silurian scolecodonts (Gotland, Sweden) as revealed by pyrolysis-GC-MS.

**Chapter 6**: Dutta, S., Steiner, M., Banerjee S., Erdtmann, B.D., Jeevankumar, S., Mann, U., 2006. *Chuaria circularis* from the early Mesoproterozoic Suket Shale, Vindhyan Supergroup, Central India: Insights from light and electron microscopy and pyrolysis-gas chromatography. In: Ray, J.S., Chakraborty, C. (Eds.), Vindhyan Geology: Status and Perspectives. Journal of Earth System Science 115, 99-112.

Schriften des Forschungszentrums Jülich
Reihe Umwelt / Environment

1. **Energiemodelle in der Bundesrepublik Deutschland. Stand der Entwicklung**
   IKARUS-Workshop vom 24. bis 25. Januar 1996
   herausgegeben von S. Molt, U. Fahl (1997), 292 Seiten
   ISBN: 3-89336-205-3

2. **Ausbau erneuerbarer Energiequellen in der Stromwirtschaft**
   Ein Beitrag zum Klimaschutz
   Workshop am 19. Februar 1997, veranstaltet von der Forschungszentrum Jülich GmbH und der Deutschen Physikalischen Gesellschaft
   herausgegeben von J.-Fr. Hake, K. Schultze (1997), 138 Seiten
   ISBN: 3-89336-206-1

3. **Modellinstrumente für $CO_2$-Minderungsstrategien**
   IKARUS-Workshop vom 14. bis 15. April 1997
   herausgegeben von J.-Fr. Hake, P. Markewitz (1997), 284 Seiten
   ISBN: 3-89336-207-X

4. **IKARUS-Datenbank - Ein Informationssystem zur technischen, wirtschaftlichen und umweltrelevanten Bewertung von Energietechniken**
   IKARUS. Instrumente für Klimagas-Reduktionsstrategien
   Abschlußbericht Teilprojekt 2 „Datenbank“
   H.-J. Laue, K.-H. Weber, J. W. Tepel (1997), 90 Seiten
   ISBN: 3-89336-214-2

5. **Politikszenarien für den Klimaschutz**
   Untersuchungen im Auftrag des Umweltbundesamtes
   **Band 1. Szenarien und Maßnahmen zur Minderung von $CO_2$-Emissionen in Deutschland bis zum Jahre 2005**
   herausgegeben von G. Stein, B. Strobel (1997), 410 Seiten
   ISBN: 3-89336-215-0

6. **Politikszenarien für den Klimaschutz**
   Untersuchungen im Auftrag des Umweltbundesamtes
   **Band 2. Emissionsminderungsmaßnahmen für Treibhausgase, ausgenommen energiebedingtes $CO_2$**
   herausgegeben von G. Stein, B. Strobel (1997), 110 Seiten
   ISBN: 3-89336-216-9

7. **Modelle für die Analyse energiebedingter Klimagasreduktionsstrategien**
   IKARUS. Instrumente für Klimagas-Reduktionsstrategien
   Abschlußbericht Teilprojekt 1 „Modelle“
   P. Markewitz, R. Heckler, Ch. Holzapfel, W. Kuckshinrichs, D. Martinsen, M. Walbeck, J.-Fr. Hake (1998), VI, 276 Seiten
   ISBN: 3-89336-220-7

8. **Politikszenarien für den Klimaschutz**
   Untersuchungen im Auftrag des Umweltbundesamtes
   **Band 3. Methodik-Leitfaden für die Wirkungsabschätzung von Maßnahmen zur Emissionsminderung**
   herausgegeben von G. Stein, B. Strobel (1998), VIII, 95 Seiten
   ISBN: 3-89336-222-3

9. **Horizonte 2000**
   6. Wolfgang-Ostwald-Kolloquium der Kolloid-Gesellschaft
   3. Nachwuchstage der Kolloid- und Grenzflächenforschung
   Kurzfassungen der Vorträge und Poster
   zusammengestellt von F.-H. Haegel, H. Lewandowski, B. Krahl-Urban (1998), 150 Seiten
   ISBN: 3-89336-223-1

10. **Windenergieanlagen - Nutzung, Akzeptanz und Entsorgung**
    von M. Kleemann, F. van Erp, R. Kehrbaum (1998), 59 Seiten
    ISBN: 3-89336-224-X

11. **Policy Scenarios for Climate Protection**
    Study on Behalf of the Federal Environmental Agency
    **Volume 4. Methodological Guideline for Assessing the Impact of Measures for Emission Mitigation**
    edited by G. Stein, B. Strobel (1998), 103 pages
    ISBN: 3-89336-232-0

12. **Der Landschaftswasserhaushalt im Flußeinzugsgebiet der Elbe**
    Verfahren, Datengrundlagen und Bilanzgrößen
    Analyse von Wasserhaushalt, Verweilzeiten und Grundwassermilieu im Flußeinzugsgebiet der Elbe (Deutscher Teil). Abschlußbericht Teil 1.
    von R. Kunkel, F. Wendland (1998), 110 Seiten
    ISBN: 3-89336-233-9

13. **Das Nitratabbauvermögen im Grundwasser des Elbeeinzugsgebietes**
    Analyse von Wasserhaushalt, Verweilzeiten und Grundwassermilieu im Flußeinzugsgebiet der Elbe (Deutscher Teil). Abschlußbericht Teil 2.
    von F. Wendland, R. Kunkel (1999), 166 Seiten
    ISBN: 3-89336-236-3

14. **Treibhausgasminderung in Deutschland zwischen nationalen Zielen und internationalen Verpflichtungen**
    IKARUS-Workshop am 27.05.1998, Wissenschaftszentrum Bonn-Bad Godesberg. Proceedings
    herausgegeben von E. Läge, P. Schaumann, U. Fahl (1999), ii, VI, 146 Seiten
    ISBN: 3-89336-237-1

15. **Satellitenbildauswertung mit künstlichen Neuronalen Netzen zur Umweltüberwachung**
Vergleichende Bewertung konventioneller und Neuronaler Netzwerkalgorithmen und Entwicklung eines integrierten Verfahrens
von D. Klaus, M. J. Canty, A. Poth, M. Voß, I. Niemeyer und G. Stein (1999), VI, 160 Seiten
ISBN: 3-89336-242-8

16. **Volatile Organic Compounds in the Troposphere**
Proceedings of the Workshop on Volatile Organic Compounds in the Troposphere held in Jülich (Germany) from 27 – 31 October 1997
edited by R. Koppmann, D. H. Ehhalt (1999), 208 pages
ISBN: 3-89336-243-6

17. **$CO_2$-Reduktion und Beschäftigungseffekte im Wohnungssektor durch das $CO_2$-Minderungsprogramm der KfW**
Eine modellgestützte Wirkungsanalyse
von M. Kleemann, W. Kuckshinrichs, R. Heckler (1999), 29 Seiten
ISBN: 3-89336-244-4

18. **Symposium über die Nutzung der erneuerbaren Energiequellen Sonne und Wind auf Fischereischiffen und in Aquakulturbetrieben**
Symposium und Podiumsdiskussion, Izmir, Türkiye, 28.-30.05.1998. Konferenzbericht
herausgegeben von A. Özdamar, H.-G. Groehn, K. Ülgen (1999), IX, 245 Seiten
ISBN: 3-89336-247-9

19. **Das Weg-, Zeitverhalten des grundwasserbürtigen Abflusses im Elbeeinzugsgebiet**
Analyse von Wasserhaushalt, Verweilzeiten und Grundwassermilieu im Flußeinzugsgebiet der Elbe (Deutscher Teil). Abschlußbericht Teil 3.
von R. Kunkel, F. Wendland (1999), 122 Seiten
ISBN: 3-89336-249-5

20. **Politikszenarien für den Klimaschutz**
Untersuchungen im Auftrag des Umweltbundesamtes
**Band 5. Szenarien und Maßnahmen zur Minderung von $CO_2$-Emissionen in Deutschland bis 2020**
herausgegeben von G. Stein, B. Strobel (1999), XII, 201 Seiten
ISBN: 3-89336-251-7

21. **Klimaschutz durch energetische Sanierung von Gebäuden. Band 1**
von J.-F. Hake, M. Kleemann, G. Kolb (1999), 216 Seiten
ISBN: 3-89336-252-2

22. **Electroanalysis**
Abstracts of the 8th International Conference held from 11 to 15 June 2000 at the University of Bonn, Germany
edited by H. Emons, P. Ostapczuk (2000), ca. 300 pages
ISBN: 3-89336-261-4

23. **Die Entwicklung des Wärmemarktes für den Gebäudesektor bis 2050**
von M. Kleemann, R. Heckler, G. Kolb, M. Hille (2000), II, 94 Seiten
ISBN: 3-89336-262-2

24. **Grundlegende Entwicklungstendenzen im weltweiten Stoffstrom des Primäraluminiums**
von H.-G. Schwarz (2000), XIV, 127 Seiten
ISBN: 3-89336-264-9

25. **Klimawirkungsforschung auf dem Prüfstand**
Beiträge zur Formulierung eines Förderprogramms des BMBF
Tagungsband des Workshop „Klimaforschung“, Jülich, vom 02. bis 03.12.1999
von J.-Fr. Hake, W. Fischer (2000), 150 Seiten
ISBN: 3-89336-270-3

26. **Energiezukunft 2030**
Schlüsseltechnologien und Techniklinien
Beiträge zum IKARUS-Workshop 2000 am 2./3. Mai 2000
herausgegeben von U. Wagner, G. Stein (2000), 201 Seiten
ISBN: 3-89336-271-1

27. **Der globale Wasserkreislauf und seine Beeinflussung durch den Menschen**
Möglichkeiten zur Fernerkundungs-Detektion und -Verifikation
von D. Klaus und G. Stein (2000), 183 Seiten
ISBN: 3-89336-274-6

28. **Satelliten und nukleare Kontrolle**
Änderungsdetektion und objektorientierte, wissensbasierte Klassifikation von Multispektralaufnahmen zur Unterstützung der nuklearen Verifikation
von I. Niemeyer (2001), XIV, 206 Seiten
ISBN: 3-89336-281-9

29. **Das hydrologische Modellsystem J2000**
Beschreibung und Anwendung in großen Flußgebieten
von P. Krause (2001), XIV, 247 Seiten
ISBN: 3-89336-283-5

30. **Aufwands- und ergebnisrelevante Probleme der Sachbilanzierung**
von G. Fleischer, J.-Fr. Hake (2002), IV, 64 Blatt
ISBN: 3-89336-293-2

31. **Nachhaltiges Management metallischer Stoffströme**
Indikatoren und deren Anwendung
Workshop, 27.-28.06.2001 im Congresscentrum Rolduc, Kerkrade (NL)
herausgegeben von W. Kuckshinrichs, K.-L. Hüttner (2001), 216 Seiten
ISBN: 3-89336-296-7

32. **Ansätze zur Kopplung von Energie- und Wirtschaftsmodellen zur Bewertung zukünftiger Strategien**
IKARUS-Workshop am 28. Februar 2002, BMWi, Bonn. Proceedings
herausgegeben von S. Briem, U. Fahl (2003), IV, 184 Seiten
ISBN: 3-89336-321-1

33. **TRACE. Tree Rings in Archaeology, Climatology and Ecology**
Volume 1: Proceedings of the Dendrosymposium 2002,
April 11$^{th}$ – 13$^{th}$ 2002, Bonn/Jülich, Germany
edited by G. Schleser, M. Winiger, A. Bräuning et al., (2003), 135 pages, many partly coloured illustrations
ISBN: 3-89336-323-8

34. **Klimaschutz und Beschäftigung durch das KfW-Programm zur $CO_2$-Minderung und das KfW-$CO_2$-Gebäudesanierungsprogramm**
von M. Kleemann, R. Heckler, A. Kraft u. a., (2003), 53 Seiten
ISBN: 3-89336-326-2

35. **Klimaschutz und Klimapolitik: Herausforderungen und Chancen**
Beiträge aus der Forschung
herausgegeben von J.-Fr. Hake, K. L. Hüttner (2003), III, 231 Seiten
ISBN: 3-89336-327-0

36. **Umweltschutz und Arbeitsplätze, angestoßen durch die Tätigkeiten des Schornsteinfegerhandwerks**
Auswertung von Schornsteinfeger-Daten
von M. Kleemann, R. Heckler, B. Krüger (2003), VII, 66 Seiten
ISBN: 3-89336-328-9

37. **Die Grundwasserneubildung in Nordrhein-Westfalen**
von H. Bogena, R. Kunkel, T. Schöbel, H. P. Schrey, F. Wendland (2003), 148 Seiten
ISBN: 3-89336-329-7

38. **Dendro-Isotope und Jahrringbreiten als Klimaproxis der letzten 1200 Jahre im Karakorumgebirge/Pakistan**
von K. S. Treydte (2003), XII, 167 Seiten
ISBN: 3-89336-330-0

39. **Das IKARUS-Projekt: Energietechnische Perspektiven für Deutschland**
herausgegeben von P. Markewitz, G. Stein (2003), IV, 274 Seiten
ISBN: 3-89336-333-5

40. **Umweltverhalten von MTBE nach Grundwasserkontamination**
von V. Linnemann (2003), XIV, 179 Seiten
ISBN: 3-89336-339-4

41. **Climate Change Mitigation and Adaptation: Identifying Options for Developing Countries**
Proceedings of the Summer School on Climate Change, 7-17 September 2003, Bad Münstereifel, Germany
edited by K. L. Hüttner, J.-Fr. Hake, W. Fischer (2003), XVI, 341 pages
ISBN: 3-89336-341-6

42. **Mobilfunk und Gesundheit: Risikobewertung im wissenschaftlichen Dialog**
von P. M. Wiedemann, H. Schütz, A. T. Thalmann (2003), 111 Seiten
ISBN: 3-89336-343-2

43. **Chemical Ozone Loss in the Arctic Polar Stratosphere: An Analysis of Twelve Years of Satellite Observations**
by S. Tilmes (2004), V, 162 pages
ISBN: 3-89336-347-5

44. **TRACE. Tree Rings in Archaeology, Climatology and Ecology**
Volume 2: Proceedings of the Dendrosymposium 2003,
May 1$^{st}$ – 3$^{rd}$ 2003, Utrecht, The Netherlands
edited by E. Jansma, A. Bräuning, H. Gärtner, G. Schleser (2004), 174 pages
ISBN: 3-89336-349-1

45. **Vergleichende Risikobewertung: Konzepte, Probleme und Anwendungsmöglichkeiten**
von H. Schütz, P. M. Wiedemann, W. Hennings et al. (2004), 231 Seiten
ISBN: 3-89336-350-5

46. **Grundlagen für eine nachhaltige Bewirtschaftung von Grundwasserressourcen in der Metropolregion Hamburg**
von B. Tetzlaff, R. Kunkel, R. Taugs, F. Wendland (2004), 87 Seiten
ISBN: 3-89336-352-1

47. **Die natürliche, ubiquitär überprägte Grundwasserbeschaffenheit in Deutschland**
von R. Kunkel, H.-J. Voigt, F. Wendland, S. Hannappel (2004), 207 Seiten
ISBN: 3-89336-353-X

48. **Water and Sustainable Development**
edited by H. Bogena, J.-Fr. Hake, H. Vereecken (2004), 199 pages
ISBN: 3-89336-357-2

49. **Geo- and Biodynamic Evolution during Late Silurian / Early Devonian Time (Hazro Area, SE Turkey)**
by O. Kranendonck (2004), XV, 268 pages
ISBN: 3-89336-359-9

50. **Politikszenarien für den Umweltschutz**
Untersuchungen im Auftrag des Umweltbundesamtes
**Langfristszenarien und Handlungsempfehlungen ab 2012 (Politikszenarien III)**
herausgegeben von P. Markewitz u. H.-J. Ziesing (2004), XVIII, 502 Seiten
ISBN: 3-89336-370-X

51. **Die Sauerstoffisotopenverhältnisse des biogenen Opals lakustriner Sedimente als mögliches Paläothermometer**
von R. Moschen (2004), XV, 130 Seiten
ISBN: 3-89336-371-8

52. **MOSYRUR: Water balance analysis in the Rur basin**
von Heye Bogena, Michael Herbst, Jürgen-Friedrich Hake, Ralf Kunkel, Carsten Montzka, Thomas Pütz, Harry Vereecken, Frank Wendland (2005), 155 Seiten
ISBN: 3-89336-385-8

53. **TRACE. Tree Rings in Archaeology, Climatology and Ecology**
Volume 3: Proceedings of the Dendrosymposium 2004,
April 22$^{nd}$ – 24$^{th}$ 2004, Birmensdorf, Switzerland
edited by Holger Gärtner, Jan Esper, Gerhard H. Schleser (2005), 176 pages
ISBN: 3-89336-386-6

54. **Risikobewertung Mobilfunk: Ergebnisse eines wissenschaftlichen Dialogs**
herausgegeben von P. M. Wiedemann, H. Schütz, A. Spangenberg (2005), ca. 380 Seiten
ISBN: 3-89336-399-8

55. **Comparison of Different Soil Water Extraction Systems for the Prognoses of Solute Transport at the Field Scale using Numerical Simulations, Field and Lysimeter Experiments**
by L. Weihermüller (2005), ca. 170 pages
ISBN: 3-89336-402-1

56. **Effect of internal leaf structures on gas exchange of leaves**
by R. Pieruschka (2005), 120 pages
ISBN: 3-89336-403-X

57. **Temporal and Spatial Patterns of Growth and Photosynthesis in Leaves of Dicotyledonous Plants Under Long-Term CO2- and O3-Exposure**
by M. M. Christ (2005), 125 pages
ISBN: 3-89336-406-4

58. **Öffentliche Kommunikation über Klimawandel und Sturmflutrisiken Bedeutungskonstruktion durch Experten, Journalisten und Bürger**
von H. P. Peters, H. Heinrichs (2005), 231 Seiten, CD
ISBN: 3-89336-415-3

59. **Umsatz verschiedener Ernterückstände in einem Bodensäulenversuchssystem – Einfluss auf die organische Bodensubstanz und den Transport zweier Xenobiotika**
von N. Drewes (2005), 221 Seiten
ISBN: 3-89336-417-X

60. **Evaluierung der CO2-Minderungsmaßnahmen im Gebäudebereich**
von M. Kleemann, P. Hansen (2005), 84 Seiten
ISBN: 3-89336-419-6

61. **TRACE. Tree Rings in Archaeology, Climatology and Ecology**
Volume 4: Proceedings of the Dendrosymposium 2005,
April 21st – 23rd 2005, Fribourg, Switzerland
edited by Ingo Heinrich, Holger Gärtner, Michel Monbaron, Gerhard Schleser
(2006), 313 pages
ISBN: 3-89336-425-0

62. **Diffuse Nitrateinträge in die Grund- und Oberflächengewässer von Rhein und Ems**
Ist-Zustands- und Maßnahmenanalysen
von R. Kunkel, F. Wendland (2006), 130 Seiten
ISBN: 3-89336-437-4

63. **Abhängigkeit des Wurzelwachstums vom Lichtregime des Sprosses und deren Modifikation durch Nährstoffe sowie im Gravitropismus**
von Kerstin A. Nagel (2006), 119 Seiten
ISBN: 3-89336-443-9

64. **Chancen und Risiken zukünftiger netzgebundener Versorgung**
Ein multi-kriterielles Verfahren zur Bewertung von Zukunftsszenarien
von C. R. Karger, W. Hennings, T. Jäger (2006), 296 Seiten
ISBN: 3-89336-445-5

65. **Die Phosphatbelastung großer Flusseinzugsgebiete aus diffusen und punktuellen Quellen**
von B. Tetzlaff (2006), 287 Seiten
ISBN: 3-89336-447-1

66. **Fate of veterinary pharmaceuticals in soil: An experimental and numerical study on the mobility, sorption and transformation of sulfadiazine**
by A. Wehrhan (2006), XXII, 134 pages
ISBN: 3-89336-448-X

67. **Biomacromolecules of Fossil Algae, Spores and Zooclasts from Selected Time Windows of Proterozoic to Mesozoic Age as Revealed by Pyrolysis-Gas Chromatography-Mass Spectrometry – A Biogeochemical Study**
by S. Dutta (2006), XVI, 139 pages
ISBN: 3-89336-455-2

## Author

**Suryendu Dutta** studied Geology at the Jadavpur University, Kolkata, India and Geoexploration at the Indian Institute of Technology Bombay, Mumbai, India. After paleobiological studies under a DAAD scholarship programme at the Technical University of Berlin, Germany, he started to investigate biomacromolecules of organic-walled microfossils at Research Centre Jülich, ICG-V, Sedimentary Systems. This book represents his Ph.D. dissertation submitted to RWTH Aachen University in 2006.

## Biomacromolecules of organic-walled microfossils

Fossil algae, spores and zooclasts recorded crucial steps in the evolution and diversification of the biosphere. The investigation of biological affinities through identification of individual biomacromolecules of these organisms does not only clarify fundamental aspects of paleobiology, but also provides a basic understanding of the respective biogeodynamics, especially of their relationship with environment and climate.

Forschungszentrum Jülich
*in der Helmholtz-Gemeinschaft*

50 Jahre Zukunft

**Band/Volume 67**
**ISBN 3-89336-455-2**

**Umwelt**
**Environment**